

**Environmental Assessment of
Suncor Energy's Eastern Newfoundland Offshore Area
2D/3D/4D Seismic Program, 2014–2024
Addendum**

Prepared by



for



**August 2015
Project No. SA1233**

Environmental Assessment of Suncor Energy's Eastern Newfoundland Offshore Area 2D/3D/4D Seismic Program, 2014–2024 Addendum

Prepared by

LGL Limited
environmental research associates
388 Kenmount Road, Box 13248, Stn. A.
St. John's, NL A1B 4A5
Tel: 709-754-1992
jchristian@lgl.com
www.lgl.com

Prepared for

Suncor Energy
Suite 201, Scotia Centre
235 Water Street
St. John's, NL
A1C 1B6

August 2015
Project No. SA1233

Suggested format for citation:

Suncor Energy. 2015. Environmental Assessment of Suncor Energy's Eastern Newfoundland Offshore Area 2D/3D/4D Seismic Program, 2014–2024 Addendum. LGL Rep. SA1233. Rep. by LGL Limited, St. John's, NL, for Suncor Energy, St. John's, NL. 25 p.

TABLE OF CONTENTS

	Page
Table of Contents	ii
List of Figures	iii
List of Tables.....	iii
General Comments.....	1
Environment Canada – CWS	1
Fisheries and Oceans Canada (DFO)	1
FFAW	4
Specific Comments	5
Canada – Newfoundland and Labrador Offshore Petroleum Board.....	5
Environment Canada – CWS	9
Fisheries and Oceans Canada (DFO)	14
Department of National Defence (DND)	17
Fish, Food and Allied Workers (FFAW)	18
Literature Cited	23
List of Appendices	25
Appendix 1: Oceans Report (2012).	25

LIST OF FIGURES

	Page
Figure 1. Locations of the NL Shelves EBSAs, PBGB LOMA EBSAs, Bonavista Cod Box, and NAFO Coral/Sponge/Seamount Closure Areas Relative to the Suncor Project Area.....	3
Figure 2. Locations of Seabird Nesting Colonies at Important Bird Areas (IBAs) Relative to the Study Area.	10

LIST OF TABLES

	Page
Table 1. Corner Coordinates for Suncor's Study Area in the Eastern Newfoundland Offshore Area.....	5
Table 2. Corner Coordinates for Suncor's Project Area in the Eastern Newfoundland Offshore Area.....	6
Table 3. Numbers of Pairs of Marine Birds Nesting at Marine Bird Colonies in Eastern Newfoundland.....	11

GENERAL COMMENTS

Environment Canada – CWS

EC's previous comments on the scoping document and project description (submitted on 29 October 2013) are still applicable to the EA report.

***Response:** Carina Gjerdrum was contacted regarding the post-2009 seabird data. The data that were provided to LGL have not yet been analysed by Environment Canada. LGL reviewed the unprocessed data collected within the Study Area and concluded that they support the 2006-2009 seabird survey data analysed and published in Fifield et al. 2009. A cursory examination of the unprocessed post-2009 data indicated that no new seabird species were observed.*

Fisheries and Oceans Canada (DFO)

Section 1.1 Relevant Legislation and Regulatory Approvals, pg 2 - The proponent states in the environmental assessment report that the project will be guided by the “Statement of Canadian Practice with respect to the Mitigation of Seismic Sound in the Marine Environment” (SOCP). The requirements in the SOCP are minimum standards to be implemented during the planning and conduct of seismic programs. The proponent should be required to adhere to all relevant minimum mitigations outlined in the SOCP including the Planning Seismic Surveys, Safety Zone and Start-up, Shut-down of Air Source Array(s), Line Changes and Maintenance Shut-downs, Operations in Low Visibility and Additional Mitigative Measures and Modifications sections of the SOCP.

***Response:** Suncor will adhere to all relevant mitigations included in the “Statement of Canadian Practice with respect to the Mitigation of Seismic Sound in the Marine Environment” (SOCP).*

Section 4.3 Fisheries, pg 51 - The environmental assessment report quantifies the average landings of commercial species in the Project and Study Area in Newfoundland and Labrador from 2005-2010. Please note that some of the fisheries in the study area are managed by the Northwest Atlantic Fisheries Organization (NAFO) with landings in countries other than Canada that should be included in this report.

***Response:** Section 4.3.2 of the EA summarizes regional NAFO fisheries from 2005-2012, including the stocks and species managed by NAFO in the Study Area. The majority of landings were taken by Canadian vessels (77%), with the remaining portion taken by foreign vessels, including Cuba, Denmark (Greenland and mainland), Estonia, the Faroe Islands, the Federal Republic of Germany, France (St. Pierre et Miquelon), Iceland, Japan, Latvia, Lithuania, Norway, Poland, Portugal, Russia, Spain, Ukraine, the United Kingdom, and the United States of America.*

Section 4.3 Fisheries, pg 51 - Updated catch information since 2010, for all species is available from the DFO NL Commercial Fishery Landings Database and should be included in the environmental assessment report.

***Response:** The format of the 2011 and 2012 DFO NL Commercial Fishery Landings Database was changed by DFO such that individual catches are no longer georeferenced as they were for data from 2010 and earlier; rather, 2011/2012 catches are consolidated in 6 min x 6 min cells by latitude and longitude (see Section 4.3.1.1 of the EA for further details). The 2011/2012 data are presented as catch ranges within the cells, in accordance with quartile ranges calculated separately for each year. Currently, this new data format does not allow for detailed analyses nor direct comparisons between years, and can only be demonstrated as catch locations. Quartile catch ranges cannot currently be displayed owing to errors generated by multiple catch range data values within a given cell in the database. The 2011/2012 catch locations were presented in the EA (e.g., Figures 4.7, 4.12, 4.13, 4.18, 4.19, 4.23, 4.25, and 4.26).*

Section 4.3 Fisheries, pg 51 - There have been significant changes in a number of fisheries in recent years including:

- A decline in the landings of shrimp in recent years. Page 63 refers to a possible future decline in TAC for Northern shrimp which has now occurred. The TAC for 3L shrimp has declined from 30,000 t in 2010 to 19,200 in 2011, to 12,000 in 2012 to 8,600 in 2013 and to 4,300 t in 2014;
- The TAC for 3M Cod, primarily fished by other NAFO Contracting Parties and re-opened in 2010 and has increased to ~15,000 t.; and
- 3LN Redfish re-opened in 2010 with a TAC of 3,500 t and is now at 7,000 t.

***Response:** So noted.*

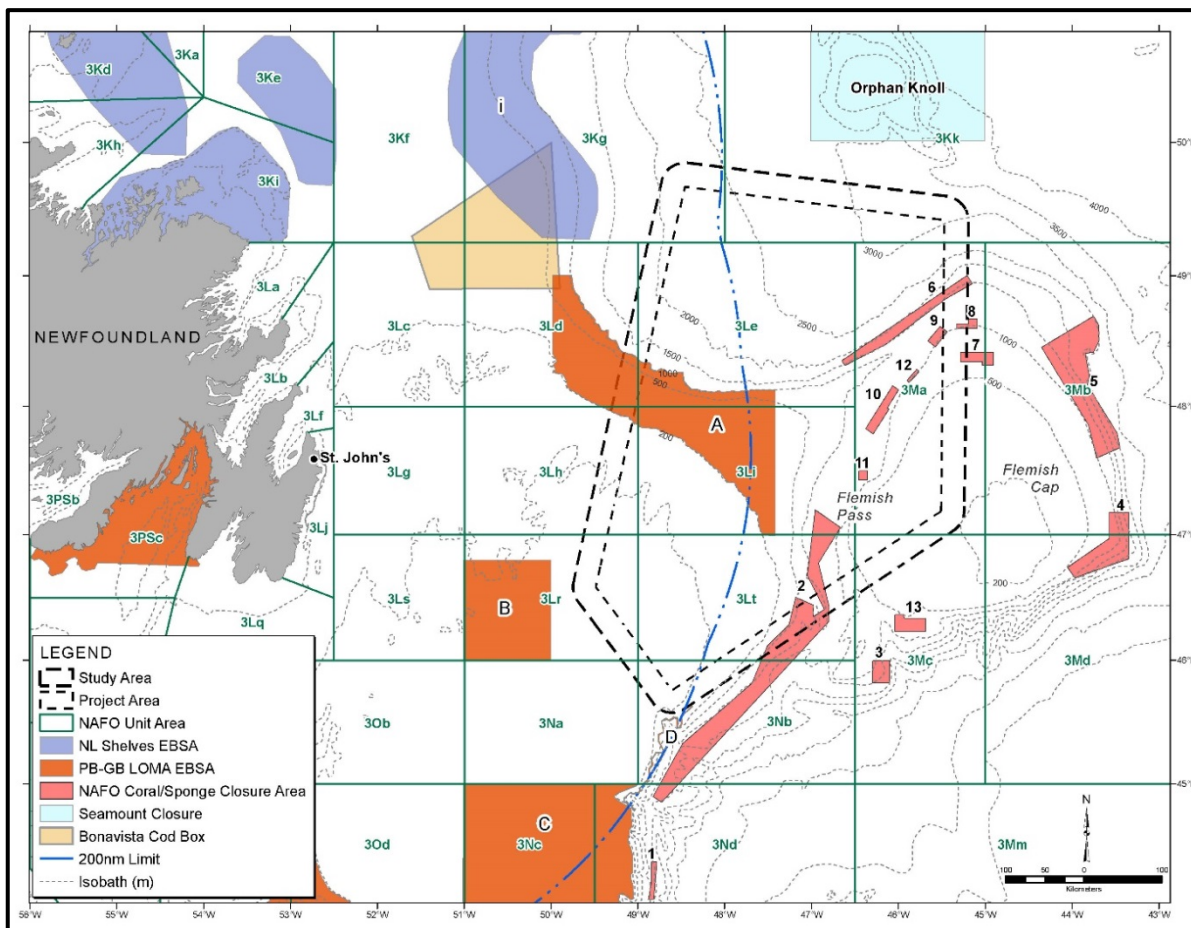
Section 4.3 Fisheries, pg 51 - A description of Bluefin Tuna fishery should be included. Historically, there has been significant catch of Bluefin tuna in portions of 3L (r).

***Response:** A summary of the biological background of bluefin tuna was provided in Section 4.2.4.2 of the EA; there were no commercial or RV survey catch records in the Study Area from 2005 to 2012 or 2007 to 2011, respectively. The Canadian bluefin tuna fishery uses rod-and reel gear or tended line, with a maximum of four lines per vessel and one hook per line (DFO 2014). The majority of the Canadian harvest is taken in a directed fishery; however, a small amount is taken as by-catch in the swordfish and other tuna fisheries (DFO 2014). The fishery usually begins with the migration of bluefin into Canadian waters in early July and continues until mid-November, with the majority of catches taken between late July and late September (DFO 2014). Owing to the highly migratory nature of bluefin tuna, this species is managed via international cooperation. Consistent with Canada's integrated fisheries management plan for bluefin tuna, Canada*

receives quotas from the International Commission for the Conservation of Atlantic Tunas (ICCAT), which are divided by fleet based on average historical landings (DFO 2014). Since 2002, the Canadian annual catches have been relatively stable at around 500 to 600 t (ICCAT 2012). The western Atlantic bluefin tuna stock has a TAC of 1,750 t for the 2014 to 2015 seasons, of which Canada's share will be ~483 t (DFO 2013a).

Section 4.7 Sensitive Areas, pg 124 - The boundaries of several areas closed to fishing for the protection of Vulnerable Marine Ecosystems were changed by NAFO in September 2013. The current boundaries of these areas should be reflected in the report. The NAFO website <http://www.nafo.int/data/frames/data.html> provides maps and the boundaries of closed areas.

Response: The updated boundaries of areas closed to bottom fishing are presented in the following figure (Figure 1):



Source: DFO (2013b) and NAFO website (2014).

Note: NL Shelves EBSA: Orphan Spur (i); PBGB LOMA EBSA: Northeast Shelf and Slope (A), Virgin Rocks (B), Southeast Shoal and Tail of the Banks (C), Lilly Canyon-Carson Canyon (D).

Figure 1. Locations of the NL Shelves EBSAs, PBGB LOMA EBSAs, Bonavista Cod Box, and NAFO Coral/Sponge/Seamount Closure Areas Relative to the Suncor Project Area.

FFAW

The spatial coverage that this Environmental Assessment involves prime harvesting areas for three major species of the Newfoundland and Labrador fishing industry. It is important that full consideration of potential impacts on other ocean users is given by the Canada-Newfoundland and Labrador Offshore Petroleum Board.

In the context of avoidance of fishing grounds and areas in which the Industry-DFO Collaborative Post-Season Trap Survey for Snow Crab, the FFAW would reiterate as we have done with other projects, there should be no seismic activity in vicinity of either active fishing grounds or survey locations. With the lack of scientific evidence showing that seismic activity does not have an impact on the biological strata.

***Response:** Suncor commits to maintain regular communication with DFO, the FFAW, independent fishers, and managers of other key corporate fisheries in the area throughout survey operations. Seismic surveys will be scheduled, to the extent possible, to reduce potential for impact or interference with DFO science surveys or fishing activities.*

FFAW Reply to Response

Fisheries are managed under the precautionary approach, the purpose being to ensure long-term sustainability. It is with respect to said precaution that FFAW-Unifor strongly opposes pursuing seismic activity on important active fishing grounds.

Although the personal communication from the DFO Scientist is not construed as official acceptance, it does indicate support for the FFAW-Unifor position in a precautionary context. As previously stated in various submissions by FFAW-Unifor to the C-NLOPB, the Post-Season Trap Survey for Snow Crab Stations are considered active fishing grounds until surveyed.

***Response to FFAW Reply:** Suncor acknowledges that the Industry-DFO Collaborative Post-Season Trap Survey for Snow Crab is considered to be part of active fishing grounds until surveyed. Suncor will ensure that planned mitigation measures to minimize potential interactions with the fishing industry as outlined in the environmental assessment are maintained during all active fishing periods.*

SPECIFIC COMMENTS

Canada – Newfoundland and Labrador Offshore Petroleum Board

Section 2.2 Spatial and Temporal Boundaries, pg 5 - Please confirm that equipment deployment and data acquisition will only occur within the Project Area and not the Study Area.

***Response:** Under normal operating conditions, Suncor commits to restrict equipment deployment and data acquisition to only the Project Area. It is important to note that during any seismic survey, weather conditions (i.e., hurricanes or tropical storms) may require suspension of survey activities and navigation of the vessel outside the Project or Study Areas for safety reasons. When possible, equipment will be recovered. However, depending on the situation and circumstances, and to ensure the safety of personnel and the vessel, retrieval of streamers may or may not be possible prior to navigating outside the Project or Study Areas. In such circumstances, the C-NLOPB would be notified of the intent to respond to these conditions to ensure safety.*

Section 2.2 Spatial and Temporal Boundaries, pg 5 - Only four coordinates are provided for a five-sided Study Area. The fifth coordinate is required.

***Response:** The corner coordinates for the Study Area are as follows (Table 1):*

Table 1. Corner Coordinates for Suncor’s Study Area in the Eastern Newfoundland Offshore Area.

Vertex	WGS84		NAD83, UTM Zone 22N	
	Latitude	Longitude	Easting	Northing
1	49.82258	-48.60473	672285	5521657
2	49.55187	-45.28750	913083	5504503
3	47.09298	-45.28109	933976	5231386
4	45.58096	-48.65033	683308	5050176
5	46.54150	-49.73987	596618	5154986

Section 2.2 Spatial and Temporal Boundaries, pg 5 - The coordinates for the Project Area should be provided.

***Response:** The corner coordinates for the Project Area are as follows (Table 2):*

Table 2. Corner Coordinates for Suncor’s Project Area in the Eastern Newfoundland Offshore Area.

Vertex	WGS84		NAD83, UTM Zone 22N	
	Latitude	Longitude	Easting	Northing
1	49.66986	-48.45822	683396	5505028
2	49.41799	-45.47109	900907	5488635
3	47.18375	-45.50815	916039	5240231
4	45.75859	-48.60932	685918	5070005
5	46.58501	-49.48670	615936	5160162

Section 2.2 Spatial and Temporal Boundaries, pg 5 - Details on the 2014 program should be provided if the decision is made to proceed with a seismic survey in 2014.

Response: Suncor will not be conducting a seismic program in 2015.

Section 3.0 Physical Environment, pg 13 - The Oceans (2012) report should be provided.

Response: Suncor provides a copy of the Ocean (2012) report in Appendix 1.

Section 4.3.1.1 Data Sets, pg 52 - Unit Areas 3Kgk, 3Ldehirt, 3Mac and 3Nab? It appears to the reader that this is an attempt to contract multiple Unit Areas. It is awkward and requires expansion, if this is the case.

Response: The above nomenclature is a common method used to list multiple NAFO Unit Areas within multiple NAFO Divisions. Expanded in full, this list would be as follows: 3Kg, 3Kk, 3Ld, 3Le, 3Lh, 3Li, 3Lr, 3Lt, 3Ma, 3Mc, 3Na, and 3Nb.

Section 4.7.1 Integrated Management Areas, Figure 4.43, pg 125 - The “Southeast Shoal and Tail of the Banks EBSA” has not been included on the figure although included in the list below the figure.

Response: The Southeast Shoal and Tail of the Banks EBSA is present on Figure 4.43. As indicated in the figure footnote, this EBSA is identified as “C” on the figure; it is the orange-coloured region near the bottom of the figure, within NAFO Unit Areas 3Nc and 3Nd.

Section 5.6.1.1 Underwater Sound, subsection Invertebrate Fisheries, 1st para, pg 146 - Anecdotal information requires multiple observations (in these cases it would require multiple fish harvesters observing the same events). If it is only a single report from a fish harvester, which it appears to be, then the “anecdotal” needs to be removed and the observation by each fish harvester needs to be properly described as a single observation.

Response: *Noted. In the future, ‘anecdotal’ will not be used as an adjective if the observation is made by a single fisher.*

Section 5.6.2 Fisheries VEC, pg 154 - VSP Programs and Wellsite Surveys d). Section 5.2 of the Guidelines state that “Guidance on the reporting and investigation of incidents is provided in the C-NLOPB/CNSOPB Guideline for the Reporting and Investigation of Incidents”.

Response: *In the EA, the section of text to which this comment refers was quoted verbatim from Appendix 2 of the C-NLOPB Geophysical, Geological, Environmental and Geotechnical Program Guidelines (C-NLOPB 2012a). Edit this text to the following:*

d) Procedures must be in place on the survey vessel(s) to ensure that any incidents of contact with fishing gear are clearly detected and documented (e.g., time, location of contact, loss of contact, and description of any identifying markings observed on affected gear). As per Section 5.0 of the C-NLOPB/CNSOPB Guideline for the Reporting and Investigation of Incidents (C-NLOPB 2012b), any incident should be reported immediately to the 24-hour answering service at (709) 778-1400 or to the C-NLOPB Duty Officer.

Consequently, all C-NLOPB (2012) citations within the EA must be edited to C-NLOPB (2012a).

Section 5.6.2.1 Sound, Fisheries Liaison Officer (FLO), line 2, pg 156 - “when necessary Suncor will have an on-board fisheries industry liaison officer”. The commitment is made in Section 2.3.5 to have a FLO onboard the seismic vessel.

Response: *The use of FLOs will be done in a manner consistent with the Geophysical, Geological, Environmental and Geotechnical Program Guidelines and the One Ocean Risk Management Matrix Guidelines for the Utilization of Fisheries Liaison Officers and Fisheries Guide Vessels for the Fishing and Petroleum Industries of Newfoundland and Labrador.*

Section 5.6.2.2 Vessel Presence (including towed seismic equipment), line 6, pg 158 - Although specific survey areas have not been identified in the EA Report, it is worth noting that any future survey areas should be planned to include adequate space within the Project Area to accommodate vessel turning.

Response: *Under normal operating conditions, Suncor commits to conduct all vessel turning within the Project Area. See Suncor response under “Section 2.2 Spatial and Temporal Boundaries” for additional information.*

Section 5.6.2.2 Vessel Presence (including towed seismic equipment), Avoidance, 2nd para, line 4, pg 159 - A copy of this “route analysis” should be provided to the C-NLOPB.

***Response:** In preparation for a seismic program, Suncor will engage fishing interests (e.g., FFAW, Association of Seafood Producers, etc.), One Ocean and DFO regarding planned operations to understand potential conflicts. Operations will be planned to avoid active fixed gear fishing areas to the extent possible. During the program, the use of a SPOC and FLO will help to minimize conflict. At the time of the program, Suncor can meet with the C-NLOPB to discuss the planned operations and activities to avoid conflict with fishing interest.*

Section 5.6.4.3 Effects of Presence of Vessels, 1st para, pg 179 - Is the reference to “...standby or picket vessel and support vessel.” supposed to be a reference to vessels that the Fisheries Liaison Officer (FLO) will be on? If so, then the reference to the vessels “possibly” being present is not correct. The commitment to the use of a FLO in the EA Report, as mitigation, implies that a second vessel will be in the area at all times. This requires clarification.

***Response:** The use of FLOs will be done in a manner consistent with the Geophysical, Geological, Environmental and Geotechnical Program Guidelines and the One Ocean Risk Management Matrix Guidelines for the Utilization of Fisheries Liaison Officers and Fisheries Guide Vessels for the Fishing and Petroleum Industries of Newfoundland and Labrador. Under normal operating conditions the FLO is present on the seismic vessel.*

Section 5.7 Cumulative Effects, pg 185 - “... in the Regional Area (as ~~pre~~[per] the C-NLOPB public registry...”

***Response:** So noted. Edit text to “Potential offshore oil and gas industry activities in the Regional Area (as per the C-NLOPB public registry, www.cnlopb.nl.ca) include:”*

Section 5.8 Mitigations and Follow-up, last para, pg 188 - The raw observational data shall also be submitted, in addition to the monitoring report.

***Response:** Suncor will submit said raw observational data in addition to the monitoring report.*

Section 6.0 Literature Cited, pg 190 - Personal Communications referenced throughout the report should be included in Section 6.0.

***Response:** Add the following text to Section 6.0:*

Personal Communications

Chidley, G. n.d. Pers. comm. Newfoundland fisherman.

Lawson, J. 2013. Pers. comm. Fisheries and Oceans Canada, St. John's, NL.

Payne, J. n.d. Pers. comm. Fisheries and Oceans Canada, St. John's, NL.

Sheppard, G. 2013. Pers. comm. Fisheries and Oceans Canada, St. John's, NL.

Thorne, H. n.d. Pers. comm. Newfoundland fisherman.

Environment Canada – CWS

EC-01: Section 2.3.8 Seismic Streamers, pg 8 - We recommend that solid streamers be used, in order to eliminate risk of fluids leaking into the environment.

Response: *Suncor will consider using solid streamers during its seismic program.*

EC-02: Section 2.3.9.2 Helicopter, pg 8 - Helicopters and other aircraft should keep well away from breeding colonies, as aircraft can cause severe disturbance to seabird and waterbird colonies, and there is a serious risk of collision with flying birds. In general, maintain a distance of at least 300 m from seabird and waterbird colonies. See Environment Canada's guidelines to avoid disturbance to seabird and waterbird colonies in Canada for further information, found at <http://www.ec.gc.ca/paom-itmb/default.asp?lang=En&n=E3167D46-1>.

Response: *The Witless Bay Ecological Reserve is the closest such site to the Study Area, and provincial regulations state that aircraft are not permitted to fly lower than 300 m, take off, or land within the reserve from 1 April to 1 September (NL Canada 2014). Any helicopters or other aircraft employed by Suncor will maintain a flight path with a distance of at least 300 m from seabird and waterbird colonies, and will not land or take off in breeding colony areas.*

EC-03: Section 4.4.3 Breeding Seabirds in Eastern Newfoundland, pg 90 - The Terra Nova National Park Important Bird Area (NF017) should be added to this section and to Figure 4.39. See <http://ibacanada.com/site.jsp?siteID=NF017&lang=EN> for further details.

Response: *Terra Nova National Park and Mistaken Point have been added to the following IBA figure (Figure 2) (replaces Figure 4.39 in the EA), and the number of marine birds nesting at marine bird colonies in eastern Newfoundland has been updated in the table below (Table 3) (replaces Table 4.8 in the EA).*

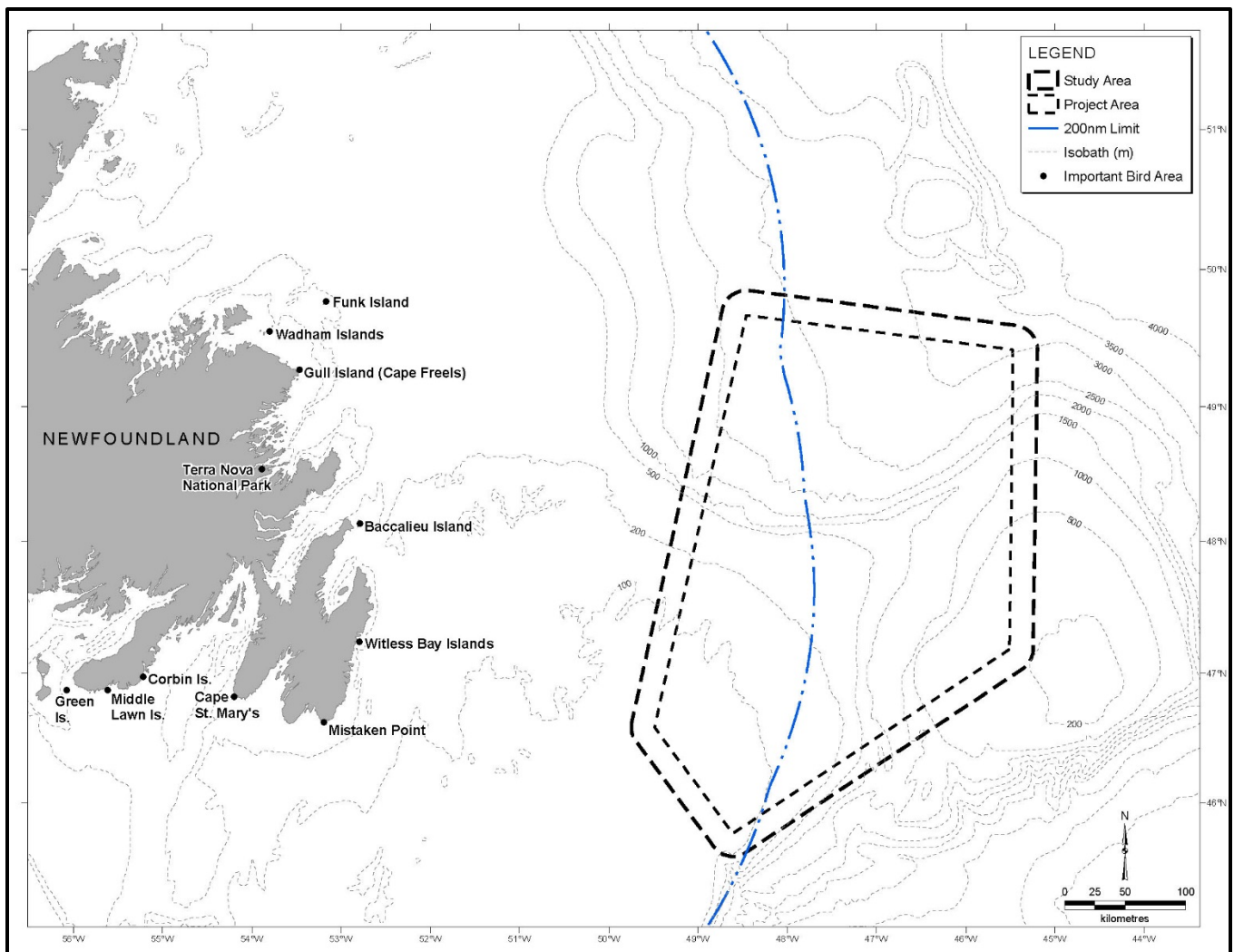


Figure 2. Locations of Seabird Nesting Colonies at Important Bird Areas (IBAs) Relative to the Study Area.

Table 3. Numbers of Pairs of Marine Birds Nesting at Marine Bird Colonies in Eastern Newfoundland.

Species	Wadham Islands	Funk Island	Cape Freels and Cabot Island	Baccalieu Island	Witless Bay Islands	Mistaken Point	Cape St. Mary's	Middle Lawn Island	Corbin Island	Green Island	Terra Nova National Park
Northern Fulmar	-	13 ^a	-	-	13 ^a	-	Present ^a	-	-	-	-
Manx Shearwater	-	-	-	-	-	-	-	7 ^c	-	-	-
Leach's Storm-Petrel	6000 ^a	-	250 ^b	3,336,000 ^b	314,020 ^a	-	-	13,879 ^d	100,000 ^b	103,833 ^b	-
Northern Gannet		6,075 ^a		2,564 ^a	-	-	14,789 ^a	-	-	-	-
Herring Gull	-	150 ^a	-	46 ^a	2,045 ^a	-	Present ^b	20 ^b	5,000 ^b	Present ^b	-
Great Black-backed Gull	Present ^b	75 ^a	-	2 ^a	15 ^a	-	Present ^b	6 ^b	25 ^b	-	-
Black-legged Kittiwake	-	100 ^a	-	5,096 ^a	13,950 ^a	4,750 ^a	10,000 ^b	-	50 ^b	-	-
Arctic and Common Terns	376 ^b	-	250 ^b	-	-	-	-	-	-	Present ^b	1,000 ^e
Common Murre	-	470,000 ^a	2,600 ^b	1,440 ^a	268,660 ^a	100 ^b	15,484 ^a	-	-	-	-
Thick-billed Murre		250 ^a	-	73 ^a	240 ^a	-	1,000 ^b	-	-	-	-
Razorbill	30 ^a	200 ^a	25 ^b	406 ^a	846 ^a	Present ^b	100 ^b	-	-	-	-
Black Guillemot	25 ^a	1 ^b	-	113 ^a	20 ^a	Present ^b	Present ^b	-	-	-	-
Atlantic Puffin	7,140 ^a	2,000 ^a	20 ^b	45,300 ^a	324,650 ^a	40 ^b	-	-	-	-	-
TOTALS	13,571	478,864	3,145	3,390,634	924,459	4,890	41,373	13,912	105,075	103,833	1,000

Sources: ^a EC-CWS, unpubl.data; ^b Cairns et al. (1989); ^c Fraser et al. (2013); ^d Robertson and Elliot (2002); ^e <http://ibacanada.com>

EC-04: Section 4.4.4 Seasonal Occurrence and Abundance, pg 92 - The latest seabird data cited in this document are from 2009. EC-CWS has data that is more recent than 2009. Please contact EC-CWS Biologist Carina Gjerdrum at carina.gjerdrum@ec.gc.ca for updated information.

***Response:** Carina Gjerdrum was contacted regarding the post-2009 seabird data. The data that were provided to LGL have not yet been analysed by Environment Canada. LGL reviewed the unprocessed data collected within the Study Area and concluded that they support the 2006-2009 seabird survey data analysed and published in Fifield et al. 2009. A cursory examination of the unprocessed post-2009 data indicated that no new seabird species were observed.*

EC-05: Section 5.6.3 Seabird VEC, pg 161 - The potential interaction of seabirds with light during times of poor visibility should be discussed in this section. Additionally, the potential for migratory birds to strand on the ship should be discussed.

***Response:** Attraction to Lights on Ships:*

Birds that spend most of their lives at sea are often influenced by artificial light (Montevecchi et al. 1999; Montevecchi 2006). Birds are more strongly attracted to lights at sea during fog and drizzle conditions. Moisture droplets in the air refract light increasing illumination creating a glow around vessels at seas. In Newfoundland waters, the Leach's Storm-Petrel is the species most often found stranded on the decks of offshore vessels after being attracted to lights at night (Moulton et al. 2005, 2006; Abgrall et al. 2008a, 2008b, 2009). Occasionally, other Newfoundland seabirds e.g., Great Shearwater, Northern Fulmar, Thick-billed Murre and Dovekie have been found stranded on vessels in Newfoundland waters at night, presumably attracted to lights on ships. Visibility during nights when storm-petrels stranded on seismic vessels off Newfoundland and Labrador was usually reduced due to fog, rain or overcast sky. This has been documented among other seabird species (Telfer et al. 1987; Black 2005). On a Grand Banks seismic vessel, tens of birds in one night can be considered a "large scale stranding". The largest single stranding event observed by LGL biologists on seismic vessels was 46 birds, all of which were released alive (LGL Limited, unpublished data).

Birds may be attracted to light because of a preference for bioluminescent prey (Imber 1975) or because the red component of lights disrupt their magnetic orientation (Poot et al. 2008). Many seabirds have great difficulty becoming airborne from flat surfaces. Once on a hard surface, stranded seabirds tend to crawl into corners or under objects such as machinery to hide. Here they may die from exposure, dehydration or starvation over hours or days. A stranded seabird's plumage is prone to oiling from residual oil that may be present in varying degrees on the ship's decks. The open ended structure of the stern of a typical seismic ship allows entry of seabirds to several decks. These decks are lighted to various degrees, sometimes brightly. This is unavoidable as seismic surveying is conducted around the clock and adequate lighting is required for

safe work practices. Mitigation measures to rescue stranded storm-petrels on board the seismic vessel will be the responsibility of the MMO. The MMO will conduct daily searches of the ship and the ship's crew will also be notified to contact the MMO if a bird is found. Procedures developed by the CWS and Petro-Canada (now Suncor) will be used to handle the birds and gently release them (Williams and Chardine, n.d.). Other vessels, while working on the Project will be made aware of the potential problem of storm-petrels stranding on their vessels. Each vessel will have a copy of the manual developed by CWS and Suncor on proper procedure and handling of stranded storm-petrels (Williams and Chardine, n.d.). Suncor acknowledges that a CWS Bird Handling Permit will be required. Project personnel will also be made aware of bird attraction to the lights on offshore structures. Mitigation and monitoring for stranded birds will reduce any effects of attraction to lights to a low to medium magnitude, over a geographic extent of 1-10 km², and for a duration of <1 month to 1 to 12 months (Table 5.8 in the EA). Thus, effects are predicted to be not significant (Table 5.9 in the EA). A report documenting each stranded bird including the date, global position and the general condition of the feathers when found, and if releasable, the condition upon release, will be completed and delivered to the CWS by the end of the calendar year.

EC-06: Section 5.6.3.2 Effects of Aircraft Overflights, pg 163 - See EC-02.

Response: See response for comment EC-02. Helicopters or other aircraft will not operate within 300 m of seabird breeding colonies. The residual effect of helicopters on seabirds is expected to be negligible to low and not significant.

EC-07: Section 5.6.3.3 Effects of Accidental Releases, pg 163 - Even a small spill could have significant impacts on migratory bird populations if the spill happened to coincide with a particularly large flock of seabirds or sea ducks during a peak migratory period. The report should include references and a discussion of at least the two following relevant studies:

- O'Hara and Morandin (2010) Effects of sheens associated with offshore oil and gas development on the feather microstructure of pelagic seabirds. *Marine Oil Pollution* 60: 672-678. This study investigates the effects of very low concentrations of oil-forming sheens affecting the microstructure of feather in seabirds.
- Burger, A. (1993) Estimating the mortality of seabirds following oil spills: effects of spill volume. *Marine Pollution Bulletin* 26:140-143. This study shows that spill size does not necessarily correlate with mortality estimates.

Response: Small amounts of oil on the surface of the ocean have the potential to impact large numbers of seabirds. As little as 10 mL of oil can result in lethally reduced thermoregulation in seabirds (O'Hara and Morandin 2010). Repeated exposure to even a thin oil sheen can result in an accumulation of oil on a bird. A statistical analysis of 45 oil spills showed there is no consistent relationship between the volume of oil spilled and

seabird mortality (Burger 1993). Other factors such as the density of seabirds in the affected area, wind velocity and direction, and wave action may have a greater bearing on the resultant mortality.

EC-08: Section 5.6.3.4 Effects summary, pg 164 - See EC-05.

***Response:** The effects of seismic sounds, aircraft overflights, artificial lighting and accidental releases of hydrocarbons on sea associated birds were assessed. Diving seabirds are more likely to be affected by underwater seismic sounds than are birds that remain at or near the surface of the water. However, there are no specific data on the levels of low-frequency underwater sound that are adverse to waterbirds, or that cause temporary hearing impairment. The ramp-up period for the airguns will help to displace birds from the immediate program area. Aircraft overflights are expected to be infrequent and potential effects temporary. Deck lighting can be minimized (if it is safe and practical to do so) to reduce the likelihood of stranding. Mitigation and monitoring for stranded birds will reduce any effects of attraction to lights. Accidental releases are of low probability and limited to the volume of material stored onboard the vessels in the worst-case scenario. No significant residual effects on the Seabird VEC are predicted.*

EC-09: Section 5.8 Mitigations and Follow-up, pg 188 - The seabird data collection protocols are properly cited as: Gjerdrum, C., D.A. Fifield, and S.I. Wilhelm. 2012.

Eastern Canada Seabirds at Sea (ECSAS) standardized protocol for pelagic seabird surveys from moving and stationary platforms. Canadian Wildlife Service Technical Report Series No. 515. Atlantic Region. vi + 37 pp.

***Response:** So noted. Update all Gjerdrum et al. (2011) citations within the EA to Gjerdrum et al. (2012).*

Fisheries and Oceans Canada (DFO)

Section 4.6 Table 4.13, pg 117 - It is the “Atlantic and Northern Gulf of St. Lawrence” population or DU of White Hake that is recommended as Threatened.

***Response:** So noted. Add “(Atlantic and Northern Gulf of St. Lawrence population)” to White Hake in the Common Name column of Table 4.13.*

Section 4.6, pg 118 - DFO emphasizes the importance of complying with relevant regulations pertaining to SARA Recovery Strategies and Action Plan including the identification of critical habitat during the life of the project.

Response: Suncor will refer to the Species at Risk Public Registry to monitor for Species at Risk Act updates throughout the life of the project, and will comply with relevant regulations pertaining to SARA Recovery Strategies and Action Plans.

Section 4.6.1 Fishes, Subsection White Shark, pg 118 - For White Shark, the second sentence should read “*captured in inshore waters as well as offshore waters over the continental shelves...*”. Reference to offshore waters is missing.

Response: So noted. Edit text to “*The white shark is widely distributed in sub-polar to tropical seas of both hemispheres, but it is most frequently observed and captured in inshore waters as well as offshore waters over the continental shelves of the Northwest Atlantic, Mediterranean Sea, southern Africa, southern Australia, New Zealand, and the eastern North Pacific.*”

Section 4.6.1 Fishes, Subsections Northern and Spotted Wolffish, pg 119-120 - Future EA updates should include recently published papers on Northern Wolffish and Spotted Wolffish (see Simpson *et al.* 2011, 2013).

Response: In recent years there has been no major change in the distribution of northern and spotted wolffish, with the highest concentrations on the northeast Newfoundland and Labrador shelves (Simpson *et al.* 2011, 2012) (see Figure 4.37 in the EA). Significant declines in indices of relative abundance and area occupied by these species occurred through the 1980s and early 1990s (Simpson *et al.* 2011, 2012), and further into the early 2000s (see Section 4.6.1.1 in the EA). However, some signs of recovery have been detected in the Newfoundland and Labrador region in the last decade, with wolffish starting to return to several historical areas and displaying similar distribution patterns to those observed during periods of high abundance (Simpson *et al.* 2011, 2012). Reported wolffish landings declined considerably through the 1980s and early 1990s (namely in NAFO Divisions 2J3KL), increased in the early 2000s, and then abruptly declined as a result of their listing on Schedule 1 of SARA in 2003 (see Section 4.6.1.1 in the EA) and the subsequent mandatory release of northern and spotted wolffish in Canadian waters (Simpson *et al.* 2011, 2013). While the impacts of wolffish removals by commercial fisheries (as bycatch and discards; unreported) in recent years are unknown, the upward trends in survey abundance suggest that fishing mortality is not currently a main factor driving population dynamics (Simpson *et al.* 2011). Although overall depth ranges are similar for these two species, northern wolffish are known to inhabit somewhat deeper waters than spotted wolffish (see Figure 4.37 and Section 4.6.1.1 in the EA). Habitat associations have been partially driven by temperature preferences, with wolffish tending to occupy the warmest waters, and depth distribution is likely related to water mass thermal characteristics (Simpson *et al.* 2011).

Table 4.13, pg 116 - The title of this table should be revised to read “SARA-listed and COSEWIC-assessed Marine Species that May Occur in the Study Area” as species are assessed by COSEWIC, not listed. Also, the row containing Atlantic Cod listed on Schedule 3 of SARA should be removed from the table.

Response: *Edit the title of Table 4.13 to read “SARA-listed and COSEWIC-assessed Marine Species that May Occur in the Study Area”.*

The paragraph preceding Table 4.13 in the EA described the reasoning for the inclusion of Schedules 2 and 3-listed species in Table 4.13, with emphasis on legal implications. Provisions of SARA, which came into force in June 2004, prohibit harming or harassing listed endangered and threatened species or damaging or destroying their critical habitat, without specifying Schedules. As such, these provisions – which must be adhered to by Suncor – are applicable to all marine mammal and fish species listed on SARA Schedules 1, 2 and 3, and it is therefore not necessary to remove these species from Table 4.13.

Section 5.6.5 Species at Risk (SAR) VEC, pg 180 - The document, “Recovery Strategy for Northern Wolffish (*Anarhichas denticulatus*) and Spotted Wolffish (*Anarhichas minor*), and Management Plan for Atlantic Wolffish (*Anarhichas lupus*) in Canada” should have been considered during the effects assessment in this section.

Response: *The draft version of the document, “Recovery Strategy for Northern Wolffish (*Anarhichas denticulatus*) and Spotted Wolffish (*Anarhichas minor*), and Management Plan for Atlantic Wolffish (*Anarhichas lupus*) in Canada” was completed in 2007, and the final version was approved in 2008. This document was cited as Kulka et al. (2007) by Simpson et al. (2011, 2013) (see above comment); however, it was cited as Kulka et al. (2008) in the EA (in reference to the final version). In keeping with Simpson et al. (2011, 2013), the following response cites this reference as Kulka et al. (2007).*

Note that Kulka et al. (2007) was cited in Section 4.2.4.2 and Section 4.6. As indicated in Kulka et al. (2007), one of the recommended recovery actions is to identify and mitigate impacts of human activities on wolffishes. These human activities include oil and gas activities. The seismic survey-related mitigations that apply to the Fish and Fish Habitat VEC (see Section 5.6.1 of the EA) also apply to the three wolffish species. Considering the typical deep-dwelling habits of these fishes and the fact that they do not have swim bladders, potential significant effects of exposure to airgun sound (key activity with most potential to cause effect) on the wolffishes are unlikely. Not having a swim bladder means that wolffishes rely primarily on the detection of particle motion rather than sound pressure. The particle motion component of sound attenuates much more quickly than the sound pressure component so wolffishes on or near the sea bottom should not be affected by the airgun discharges.

Department of National Defence (DND)

Section 5.6.2, Subsection Communications, pg 156 - On October 28, 2013, DND replied to the draft scoping document with the following:

“A search of the DND unexploded ordnance (UXO) records was conducted to determine the possible presence of UXO within the study area. DND records indicate that there are two wreck sites within the survey area. The sites are two submarines that were sunk during World War II:

- U-658 (46.5333W, 50.0089N); and
- U-520 (49.8333W, 47.7834N).

Given DND’s understanding of the survey activities to be conducted, the associated UXO risk is assessed as low. Nonetheless, due to the inherent dangers associated with UXO and the fact that the Atlantic Ocean was exposed to many naval engagements during WWII, should any suspected UXO be encountered during the course of the proponent’s operations, the UXO should not be disturbed/manipulated. The proponent should mark the location and immediately inform the Coast Guard. Additional information is available in the Annual Edition - Notices to Mariners. Section F, No. 37.

In the event of activities which may have contact with the seabed (such as drilling or mooring), it is strongly advised that operational aids, such as remote operated vehicles, be used to conduct seabed surveys in order to prevent unintentional contact with harmful UXO items that may have gone unreported or undetected.

Further information regarding UXO is available at our website at www.uxocanada.forces.gc.ca.

DND is likely to be operating in the vicinity of the study area in a non-interference manner during the project timeframe; thus, there is potential for interaction with naval operations in areas where seismic activities will occur. DND is to be kept informed of dates and locations of seismic activities.”

Information regarding UXO data should have been included in the EA document and Suncor’s activities assessed against the data at that time.

Response: *The presence of two sunken submarines in the Study Area is noted. If undocumented UXO is discovered within the Project Area during the seismic program, positions will be marked and the Coast Guard will be contacted. Suncor will communicate with DND prior to the commencement of any seismic surveying to ensure that there is not any conflict between the seismic operation and any potential DND operations.*

Fish, Food and Allied Workers (FFAW)

Section 4.3.3.1 1986 to 2010 Catch Trends, pg 54 - It is suggested that the demise of the groundfish fisheries was purely a result from exhaustive fishing effort. This is not a complete description, as there is strong science suggesting that a significant change of the environmental regime, which substantially impacted the recruitment and survivability of many of the groundfish species.

***Response:** All fish have physiological limits within which they can survive, such as sea temperatures and salinities (Rose 2005). Frank et al. (1990) analyzed the effects of changes in oceanographic conditions induced by a global increase in atmospheric CO₂, and their models predicted a general warming and freshening of the continental shelf waters, leading to shifts in the geographic distribution of important commercial groundfish stocks, earlier arrival times and later departures for highly migratory large pelagics, and – in combination with increased water column stratification – decreased organic material reaching the seabed. Rose (2005) inferred that capelin (*Mallotus villosus*) and herring (*Clupea harengus*) react strongly and quickly to climate change, owing to their physiological limits and potential for fast population growth; this was verified through the examination of historical data from Icelandic and Greenland waters, which warmed considerably during 1920 to 1940, resulting in capelin, herring, cod (*Gadus morhua*), and other species shifting north very quickly.*

FFAW Reply to Response

The response does not address the reviewer's comment. Rather it appears that the response is a replacement of the original paragraph without relating it to the scientific knowledge of the local context.

***Response to FFAW Reply:** Suncor acknowledges that factors other than overfishing may have contributed to the collapse of several groundfish stocks in the early 1990s. Changes in environmental aspects, such as water temperature, may have affected the groundfish stocks. Suncor's prior response emphasized the physiological limits of fishes, including some pelagic species which serve as important prey for many groundfish species. A distributional shift by prey species could also affect the predatory groundfish species.*

Section 4.3.7 Industry and DFO Science Surveys, pg 87 - It appears that the Industry-DFO Collaborative Post-Season Trap Survey for Snow Crab is a new project with a limited scope. In fact this survey has been ongoing for over a decade and involves the sampling of approximately 1,000 locations by almost 100 fishing vessels. In 2013 the Industry-DFO Collaborative Post-Season Trap Survey for Snow Crab, the locations in NAFO region 3L were completed between September 4th and September 25th. This survey provides significant input into the scientific advice of DFO when it comes to the establishment of quotas and recruitment estimates.

Response: *Future EAs will avoid text that implies that the Industry-DFO Collaborative Post-Season Trap Survey for Snow Crab is a relatively new project, and will instead indicate the appropriate time frame referenced in the comment above.*

FFAW Reply to Response

The current Environmental Assessment should also avoid said text as reference in the response. The comment was made in context of the current Environmental Assessment; hence the correction should apply to the current document.

Response to FFAW Reply: *Suncor acknowledges that the Industry-DFO Collaborative Post-Season Trap Survey for Snow Crab is not a new project; rather it has been conducted annually since 2003.*

Section 5.6.2.2 Vessel Presence, pg 158 - Further in the context of avoidance it is worth to note that the Environmental Assessment suggests that “other vessels must give way” to the seismic vessel, the FFAW is inclined to suggest this to be inappropriate language in this context. In Section 5.6.2.1 under *Avoidance*, it suggests “potential effects of seismic sound on fishery catch success **can be** mitigated by avoiding heavily fished areas ...” (emphasis added), it is the perspective of this reviewer that **should be** mitigated by avoidance.

Response: *The need for the vessel with greater maneuverability to adjust its course in favour of a vessel with limited maneuverability is long established in Maritime Law and navigational practice as reflected by Rule 18 of the Collision Regulations pursuant to the Canada Shipping Act. However, in preparation for a seismic program, Suncor will engage fishing interests (e.g., FFAW, Association of Seafood Producers, etc.), One Ocean and DFO regarding planned operations to understand potential conflicts. Operations will be planned to avoid active fixed gear fishing areas to the extent possible. During the program, the use of a SPOC and FLO will help to minimize conflict. Suncor also recognizes that there may be situations where both the fishing vessel and the seismic survey vessels have limited maneuverability due to towed gear. In this situation proactive interaction with the fishing industry using the picket vessel and the FLO is essential.*

Section 5.6.2.2 Vessel Presence, pg 159 - It is indicated that for previous Newfoundland & Labrador surveys there has been a temporal and spatial separation plan; the FFAW would feel inclined for the proponent to indicate said occurrences. In the context of the surveys estimating the biological abundance, for the FFAW Science there is no such concept of adequate “quiet time” – the FFAW is unsure what is being implied and would like to reiterate that there be no activity in the areas of the Industry-DFO Collaborative Post-Season Trap Survey for Snow Crab.

Response: *See Response below to Section 5.7 Cumulative Effects, pg 184.*

Section 5.7 Cumulative Effects, pg 184 - The FFAW reviewer is only aware of the implementation of spatial separation of about 20 nautical miles having been discussed in the context of any recent programs in Newfoundland & Labrador. The suggested acceptance of a 7 day window is something that has only been seen in the context of the DFO multi-species trawl survey. The FFAW therefore reiterates the concern that exposure to seismic activity can have an effect on harvested species. Any impact on surveys and/or stock assessments would have a lasting impact for harvesters. Although the proponent suggests that there would be no significant cumulative effects on the commercial fisheries from the seismic program (page 184), the FFAW is obliged to again state that any impact on either harvesting or fisheries science should be recognized as unacceptable in Newfoundland & Labrador waters.

Combined Response to comments on Section 5.6.2.2 Vessel Presence, pg 159 & Section 5.7 Cumulative Effects, pg 184:

Suncor recognizes and understands the FFAW concerns noted above. Suncor is aware that the issue of a spatial separation, nominally 20 nautical miles, has come up in its own and other operators' discussions with FFAW representatives. In addition, the EA notes on page 159 the context in which the "quiet time" approach was implemented in the context of a DFO research survey. As the FFAW is aware, there are also other circumstances under which the oil/seismic survey industry has practiced temporal and spatial avoidance of active fisheries (e.g., during joint Statoil and Husky surveys in 2008 when significant parts of the survey areas were not surveyed due to the intensity of fishing activity in those areas).

Suncor has reviewed its conclusion with respect to cumulative effects in this context and considers that it remains valid in light of current scientific research with respect to the behavioural responses of commercial fish species to seismic surveys.

As noted in the EA and this Addendum, Suncor, in preparation for a seismic program, will engage fishing interests (e.g., FFAW, Association of Seafood Producers, etc.), One Ocean and DFO regarding planned operations to understand potential conflicts and to minimize the interaction between commercial fish harvesting activities and survey operations, both spatially and temporally. Operations will be planned to avoid active fixed gear fishing areas to the extent possible. During the program, the use of a SPOC and FLO will help to minimize conflict.

The Proponent contacted DFO regarding temporal and/or spatial separation between seismic activity and the Industry-DFO Collaborative Post-Season Trap Survey for Snow Crab. Avoidance measures previously voiced by the FFAW (e.g., maintaining a distance of ~20 nm from crab survey stations prior to their sampling) may be viewed as a precautionary measure; however, there is currently no indication of official acceptance of avoidance protocols by DFO (E. Dawe, DFO, NL, pers. comm., 2014).

Research activities are contributing valuable scientific knowledge on the subject matter, which may be used to establish future guidance. Christian et al. (2003) investigated the potential behavioural effects of exposure to sound from seismic airguns on snow crabs using two methods: (1) telemetry; and (2) remote camera monitoring.

In the telemetry study, eight animals were equipped with ultrasonic tags, released, and monitored for multiple days prior to exposure and after exposure. Received SPL and SEL were ~191 dB re 1 μ Pa_{0-p} and <130 dB re 1 μ Pa_{2-s}, respectively. The crabs were exposed to 200 discharges from a fixed source over a 33-min period. None of the tagged animals left the immediate area after exposure. Five animals were captured in the snow crab commercial fishery the following year, one at the release location, one 35 km from the release location, and three at intermediate distances from the release location.

The other study approach used by Christian et al. (2003) involved monitoring snow crabs with a remote video camera during their exposure to sound from a seismic source. The caged animals were placed on the ocean bottom at a depth of 50 m. Received SPL and SEL were ~202 dB re 1 μ Pa_{0-p} and 150 dB re 1 μ Pa_{2-s}, respectively. The crabs were also exposed to 200 discharges over a 33-min period. They did not exhibit any overt startle response during the exposure period.

ESRF is in the process of finalizing a report on the effects of sound energy on lobster feeding in a laboratory setting. This study will assess the general and histological pathology and serum biochemistry of lobsters exposed to the levels of sound energy typically generated by an air gun both immediately after exposure and six months later.

In 2015 ESRF, through Fisheries and Oceans Canada, will initiate a three-year field study aimed at evaluation of the behaviour of snow crab in response to a typical seismic air gun array. In addition, in 2015 will sponsor a second three-year study to characterize the ambient underwater soundscape over a broad area of the east coast offshore as a basis for improving modelling of the propagation and intensity of sound energy generated by seismic surveys.

Section 5.7 Cumulative Effects, pg 185 - It would be worthwhile for the proponent to update as questions and comments on the Environmental Assessment are being reviewed.

Response: *Suncor will strive to ensure that this section is as up to date as possible with respect to known expected activities in the Study Area and will address any changes to the cumulative assessment in response to reviewer's comments as necessary.*

Section 5.7 Cumulative Effects, pg 185, second last paragraph - This may hold true historically, but in recent years there has been an increase in the Seismic Programs operating in Newfoundland and Labrador waters in a given year.

Response: *It is unclear what types of geophysical programs the reviewer is including in Seismic Programs. The text as written on page 185 (second last paragraph) is accurate in that it refers specifically to 2D or 3D seismic programs. The C-NLOPB maintains a geophysical activity summary, currently ranging from 1996 to 2013 (http://www.cnlopb.nl.ca/exp_stat.shtml), which indicates that from 2009 to 2013 there were zero to three 2D or 3D seismic surveys in a given year. If the reviewer is including wellsite and geohazard surveys (which periodically use small airgun arrays—typically four airguns for geohazard surveys for short duration programs) in addition to 2D and 3D seismic surveys in Seismic Programs, then in recent years, the number of programs which are employing airgun arrays in Newfoundland and Labrador waters have been variable, with two to seven wellsite surveys and zero to two geohazard surveys in a given year from 2009 to 2013.*

LITERATURE CITED

- Black, A. 2005. Light induced seabird mortality on vessels operating in the Southern Ocean: incidents and mitigation measures. *Antarctic Science* 17:67-68.
- Burger, A. 1993. Estimating the mortality of seabirds following oil spills: Effects of spill volume. *Mar. Poll. Bull.* 26: 140-143.
- Cairns, D.K., W.A. Montevecchi, and W. Threlfall. 1989. Researcher's guide to Newfoundland seabird colonies. Second edition. Memorial University of Newfoundland Occasional Papers in Biology, No. 14. 43 p.
- C-NLOPB (Canada-Newfoundland and Labrador Offshore Petroleum Board). 2012a. Canada-Newfoundland and Labrador Offshore Petroleum Board: Geophysical, geological, environmental and geotechnical program guidelines, January 2012.
- C-NLOPB. 2012b. Canada-Newfoundland and Labrador Offshore Petroleum Board: Incident reporting and investigation guidelines, November 2012.
- DFO (Fisheries and Oceans Canada). 2013a. International Commission for the Conservation of Atlantic Tunas. Available at <http://www.dfo-mpo.gc.ca/international/tuna-thon/iccat-cicta-eng.htm>.
- DFO. 2013b. Identification of additional ecologically and biologically significant areas (EBSAs) within the Newfoundland and Labrador shelves bioregion. *Can. Sci. Avis. Sec. Sci. Rep.* 2013/048.
- DFO. 2014. Bluefin tuna management in Atlantic Canada. Available at <http://www.dfo-mpo.gc.ca/international/tuna-thon/bluefin-mgt-gestion-rouge-eng.htm>.
- Frank, K.T., R.I. Perry, and K.F. Drinkwater. 1990. Predicted response of northwest Atlantic invertebrate and fish stocks to CO₂-induced climate change. *Trans. Amer. Fish. Soc.* 119: 353-365.
- Fraser, G.S., J. Russell, G.J. Robertson, R. Bryant and D.A. Fifield. 2013. Prospects for the Manx Shearwater colony on Middle Island, Newfoundland, Canada. *Marine Ornithology* 41: 137-140.
- ICCAT (International Commission for the Conservation of Atlantic Tunas). 2012. Report of the 2012 Atlantic bluefin tuna stock assessment session (Madrid, Spain – September 4 to 11, 2012). Doc. No. SCI-033/2012.
- Imber, M. J. 1975. Behaviour of petrels in relation to the moon and artificial lights. *Notornis* 22:302-306.
- Kulka, D., C. Hood, and J. Huntington. 2007. Recovery strategy for Northern Wolffish (*Anarhichas denticulatus*) and Spotted Wolffish (*Anarhichas minor*), and management plan for Atlantic Wolffish (*Anarhichas lupus*) in Canada. Fisheries and Oceans Canada: Newfoundland and Labrador Region. St. John's, NL. X + 103 p.
- Montevecchi, W. A. 2006. Influences of artificial light on marine birds. p. 94-113 In: C. Rich and T. Longcore (editors), *Ecological Consequences of Artificial Night Lighting*, Island Press, Washington, D.C. 478 p.
- Montevecchi, W.A., F.K. Wiese, G. Davoren, A.W. Diamond, F. Huettmann and J. Linke. 1999. Seabird attraction to offshore platforms and seabird monitoring from support vessels and other ships: Literature review and monitoring designs. Prepared for Canadian Association of Petroleum Producers by Memorial University of Newfoundland, St. John's, Newfoundland and University of New Brunswick, Saint John. New Brunswick. 35 p.
- NAFO (Northwest Atlantic Fisheries Organization) website. 2014. NAFO website. Available at <http://www.nafo.int/about/frames/about.html>.
- NL (Newfoundland and Labrador) Canada. 2014. Rules and regulations: Witless Bay Ecological Reserve. Department of Environment and Conservation. Available at http://www.env.gov.nl.ca/env/parks/wer/r_wbe/rules.html.
- O'Hara, P.D. and L.A. Morandin. 2010. Effects of sheens associated with offshore oil and gas development on the feather microstructure of pelagic seabirds. *Mar. Oil Poll.* 60: 672-678.

- Poot, H., B.J. Ens, H. de Vries, M.A.H. Donners, M.R. Wernand, and J.M. Marquenic. 2008. Green light for nocturnally migrating birds. *Ecology and Society*, 13(2): 47.
Available at <http://www.ecologyandsociety.org/vol13/iss/art47/>.
- Robertson, G.J. and R.D. Elliot. 2002. Changes in seabird populations breeding on Small Island, Wadham Islands, Newfoundland. Canadian Wildlife Service, Atlantic Region, Technical Report Series No. 381.
- Rose, G.A. 2005. On distributional responses of north Atlantic fish to climate change. *ICES J. Mar. Sci.* 62(7): 1360-1374.
- Simpson, M.R., L.G.S. Mello, C.M. Miri, and M. Treble. 2011. A pre-COSEWIC assessment of three species of wolffish (*Anarhichas denticulatus*, *A. minor*, and *A. lupus*) in Canadian waters of the northwest Atlantic Ocean. DFO Can. Sci. Advis. Sec. Res. Doc. 2011/122. iv + 69 p.
- Simpson, M.R., D. Chabot, K. Hedges, J. Simon, C.M. Miri, and L.G.S. Mello. 2013. An update on the biology, population status, distribution, and landings of wolffish (*Anarhichas denticulatus*, *A. minor*, and *A. lupus*) in the Canadian Atlantic and Arctic Oceans. DFO Can. Sci. Advis. Sec. Res. Doc. 2013/089. v + 82 p.
- Telfer, T. C., J. L. Sincock, G. V. Byrd and J. R. Reed. 1987. Attraction of Hawaiian seabirds to lights: conservation efforts and effects of moon phase. *Wildlife Society Bulletin* 15:406-413.

LIST OF APPENDICES

Appendix 1: Oceans Report (2012).

Appendix 1

Physical Environment of the Western Geco Seismic area in Orphan Basin, Flemish Pass and the North-east Grand Banks

**Submitted To:
LGL
388 Kenmount Road
St. John's, NL**

**Submitted By;
Oceans Ltd.
85 LeMarchant Road
St. John's, NL
A1C 2H1**

February 2012

Table of Contents

1.0	Introduction.....	8
2.0	Climatology.....	10
2.1	General Description of Weather Systems	10
2.2	Data Sources	12
2.2.1	ICOADS.....	14
2.2.2	MSC50	15
2.2.3	Platform Observations	15
2.2.4	National Hurricane Centre Best-Track Dataset	16
2.3	Wind.....	16
2.3.1	Region 1	16
2.3.2	Region 3	26
2.3.3	Tropical Systems.....	31
2.4	Waves.....	35
2.4.1	Region 1	36
2.4.2	Region 2	43
2.4.3	Region 3	50
2.5	Weather Variables.....	56
2.5.1	Temperature	56
2.5.2	Visibility	62
2.5.3	Precipitation	65
2.5.4	Sea Spray Vessel Icing.....	69
3.0	Wind and Wave Extreme Value Analysis	73
3.1.1	Extreme Value Estimates for Winds from the Gumbel Distribution.....	73
3.1.2	Extreme Value Estimates for Waves from a Gumbel Distribution.....	76
3.1.3	Joint Probability of Extreme Wave Heights and Spectral Peak Periods...	78
4.0	Oceanography	82
4.1	Major Currents in the Study Area	82
4.2	Currents in the Project Area.....	90
4.2.1	Northern Section of the Study Area.....	90
4.2.2	Southern Section of the Study Area.....	99
4.3	Water Mass Structure.....	107
4.4	Water Properties in the Project Area	118
5.0	Sea Ice and Icebergs.....	138
5.1	Sea Ice	138
5.1.1	30-Year Median Ice Concentration.....	139
5.1.2	30-Year Frequency of Presence of Sea Ice	139
5.2	Icebergs	Error! Bookmark not defined.

Table of Figures

Figure 1.1 The Study area.....	8
Figure 2.1 Location of the Climate Data Sources.....	13
Figure 2.2 Annual Wind Rose for MSC50 Grid Point 14845 located near 48.9°N; 47.8°W. 1954 – 2010	18
Figure 2.3 Annual Percentage Frequency of Wind Speeds for MSC50 Grid Point 14845 located near 48.9°N; 47.8°W. 1954 – 2010	18
Figure 2.4 Percentage Exceedance of 10 m wind speed at Grid Point 14845 located near 48.9°N; 47.8°W. 1954 – 2010.....	19
Figure 2.5 Annual Wind Rose for MSC50 Grid Point 13912 located near 48.3°N; 46.3°W. 1954 – 2010	23
Figure 2.6 Annual Percentage Frequency of Wind Speeds for MSC50 Grid Point 14845 located near 48.9°N; 47.8°W. 1954 – 2010	23
Figure 2.7 Percentage Exceedance of 10 m wind speed at Grid Point 13912 located near 48.3°N; 46.3°W. 1954 – 2010.....	24
Figure 2.8 Annual Wind Rose for MSC50 Grid Point 11423 located near 46.9°N; 48.1°W. 1954 – 2010	27
Figure 2.9 Annual Percentage Frequency of Wind Speeds for MSC50 Grid Point 11423 located near 46.9°N; 48.1°W. 1954 – 2010	28
Figure 2.10 Percentage Exceedance of 10 m wind speed at Grid Point 11423 located near 46.9°N; 48.1°W. 1954 – 2010.....	29
Figure 2.11 5-Year Average of the number of Tropical Storms which formed in the Atlantic Basin since 1961	33
Figure 2.12 Storm Tracks of Tropical Systems Passing within 200 nm of 48.0°N, 47.5°W	35
Figure 2.13 Annual Wave Rose for MSC50 Grid Point 14845 located near 48.9°N; 47.8°W. 1954 – 2010	37
Figure 2.14 Annual Percentage Frequency of Wave Height for MSC50 Grid Point 14845 located near 48.9°N; 47.8°W. 1954 – 2010	38
Figure 2.15 Percentage Exceedance of Significant Wave Height at Grid Point 14845 located near 48.9°N; 47.8°W. 1954 – 2010	40
Figure 2.16 Percentage of Occurrence of Peak Wave Period at Spectrum at Grid Point 14845 located near 48.9°N; 47.8°W. 1954 – 2010	42
Figure 2.17 Annual Wave Rose for MSC50 Grid Point 13912 located near 48.3°N; 46.3°W. 1954 – 2010	44
Figure 2.18 Annual Percentage Frequency of Wave Height for MSC50 Grid Point 13912 located near 48.3°N; 46.3°W. 1954 – 2010	44
Figure 2.19 Percentage Exceedance of Significant Wave Height at Grid Point 13912 located near 48.3°N; 46.3°W. 1954 – 2010	47
Figure 2.20 Percentage of Occurrence of Peak Wave Period at Spectrum at Grid Point 13912 located near 48.3°N; 46.3°W. 1954 – 2010	49
Figure 2.21 Annual Wave Rose for MSC50 Grid Point 11423 located near 46.9°N; 48.1°W. 1954 – 2010	51
Figure 2.22 Annual Percentage Frequency of Wave Height for MSC50 Grid Point 11423 located near 46.9°N; 48.1°W. 1954 – 2010	51

Figure 2.23 Percentage Exceedance of Significant Wave Height at Grid Point 11423 located near 46.9°N; 48.1°W. 1954 – 2010	53
Figure 2.24 Percentage of Occurrence of Peak Wave Period at Spectrum at Grid Point 11423 located near 46.9°N; 48.1°W. 1954 – 2010	55
Figure 2.25 Monthly Mean Air and Sea Surface Temperature for ICOADS Region 1....	58
Figure 2.26 Monthly Mean Air and Sea Surface Temperature for ICOADS Region 2....	60
Figure 2.27 Monthly Mean Air and Sea Surface Temperature for ICOADS Region 3....	62
Figure 2.28 Monthly and Annual Percentage Occurrence of Visibility in Region 1	63
Figure 2.29 Monthly and Annual Percentage Occurrence of Visibility in Region 2.....	64
Figure 2.30 Monthly and Annual Percentage Occurrence of Visibility in Region 3.....	65
Figure 2.31 Percentage Frequency of Potential Spray Icing Conditions in Region 1	70
Figure 2.32 Percentage Frequency of Potential Spray Icing Conditions in Region 2	71
Figure 2.33 Percentage Frequency of Potential Spray Icing Conditions in Region 3	72
Figure 3.1 Environmental Contour Plot for Grid Point 14845 located near 48.9°N; 47.8°W. 1954 – 2010	80
Figure 3.2 Environmental Contour Plot for Grid Point 13912 located near 48.3°N; 46.3°W. 1954 – 2010	80
Figure 3.3 Environmental Contour Plot for Grid Point 11423 located near 46.9°N; 48.1°W. 1954 – 2010	81
Figure 4.1 Major ocean circulation features in the Northeast Atlantic	83
Figure 4.2 The major circulation features around the Flemish Cap and Sackville Spur ..	84
Figure 4.3 Computed Currents from Drifting Buoy Data.....	85
Figure 4.4 Composite Map of Mean Near-Surface Currents	86
Figure 4.5 Model-Derived Depth-Averaged Currents	88
Figure 4.6 Modeled Currents at 30 m below the Surface (left) and 20 m above the Seabed (right) in May (above) and November (below).....	89
Figure 4.7 Mooring location in the northern section of the study area.....	91
Figure 4.8 Progressive vector diagrams of currents in Orphan Basin	93
Figure 4.9 Progressive vector diagrams for the currents on the northeast Newfoundland Shelf at 143 m and 293 m	96
Figure 4.10 Progressive vector diagrams for the currents on the Sackville Spur at 467 m and 767 m.....	97
Figure 4.11 Progressive vector diagram of currents in northern Flemish Pass	98
Figure 4.12 Location of current moorings in Flemish Pass	99
Figure 4.13 Current at the western side of Flemish Pass	101
Figure 4.14 Progressive vector diagram of currents at Terra Nova.....	103
Figure 4.15 Annual progressive vector diagrams for depths of 20 m, 64 m, and 112 m at White Rose.....	106
Figure 4.16 Average Spatial Distribution of Temperature and Salinity at 20 m in January and July	109
Figure 4.17 Average Spatial Distribution of Temperatures and Salinity at 75 m in January and July	110
Figure 4.18 Average near bottom temperature during spring from all available data for the decade 1991-2000	111
Figure 4.19 Bottom temperature and salinity maps derived for the trawl-mounted CTD data.....	112

Figure 4.20 Hydrographic contours across the Flemish Cap section during July 2011 .	113
Figure 4.21 Hydrographic contours along the Flemish Cap Section during November 2011	114
Figure 4.22 Hydrographic contours across the Bonavista section during May 2011	115
Figure 4.23 Hydrographic contours across the Bonavista section during July 2011	116
Figure 4.24 Hydrographic contours across the Bonavista section during November 2011	117
Figure 4.25 Seasonal T-S plots for Orphan Basin	123
Figure 4.26 Seasonal T-S plots for northern Flemish Pass and Sackville Spur.....	128
Figure 4.27 Seasonal T-S diagrams for sub-area 3 at depths less than 100 m.....	131
Figure 4.28 Seasonal T-S diagrams for sub-area 3 at depths from 100 m – 200 m.....	134
Figure 4.29. Seasonal T-S diagrams for sub-area 3 at water depths from 200 m to 500 m	137
Figure 5.1 30-Year Frequency of Presence of Sea Ice within the Project Area (March 05)	139
Figure 5.2 30-Year Frequency of Presence of Sea Ice within the Project Area (March 12)	141
Figure 5.3 30-Year Frequency of Presence of Sea Ice within the Project Area for the week of March 19	142
Figure 5.4 Iceberg Sightings within the Project Area.....	143
Figure 5.5 Iceberg sightings within Region 1 from 1974 - 2009.....	144
Figure 5.6 Iceberg Size by month within Region 1	145
Figure 5.7 Iceberg sightings within Region 2 from 1974 – 2009	146
Figure 5.8 Iceberg Size by month within Region 2	147
Figure 5.9 Iceberg sightings within Region 3 from 1974 - 2009.....	148
Figure 5.10 Iceberg Size by month within Region 3	149

Table of Tables

Table 2.1 Locations of MANMAR observations.....	15
Table 2.2 Locations of wave observations.....	15
Table 2.3 Mean Wind Speed (m/s) Statistics for Region 1.....	17
Table 2.4 Maximum Wind Speed (m/s) Statistics for Region 1	20
Table 2.5 Monthly Maximum 10m Wind Speed by Direction (m/s) speed at Grid Point 14845 located near 48.9°N; 47.8°W. 1954 – 2010	20
Table 2.6 Percentage occurrence of Wind Direction by month speed at Grid Point 14845 located near 48.9°N; 47.8°W. 1954 – 2010	21
Table 2.7 Mean Wind Speed (m/s) Statistics for Region 2.....	22
Table 2.8 Maximum Wind Speed (m/s) Statistics for Region 2	25
Table 2.9 Monthly Maximum 10m Wind Speed by Direction (m/s) speed at Grid Point 13912 located near 48.3°N; 46.3°W. 1954 – 2010	25
Table 2.10 Percentage occurrence of Wind Direction by month at Grid Point 13912 located near 48.3°N; 46.3°W. 1954 – 2010	26
Table 2.11 Mean Wind Speed Statistics in Region 3.....	26
Table 2.12 Maximum Wind Speed (m/s) Statistics in Region 3	30
Table 2.13 Monthly Maximum 10m Wind Speed by Direction (m/s) at Grid Point 11423 located near 46.9°N; 48.1°W. 1954 – 2010	31
Table 2.14 Percentage occurrence of Wind Direction by month at Grid Point 11423 located near 46.9°N; 48.1°W. 1954 – 2010	31
Table 2.15 Tropical Systems Passing within 370 km of 48.0°N, 47.5°W (1960 to 2010)	34
Table 2.16 Combined Significant Wave Height Statistics (m).....	39
Table 2.17 Percentage Occurrence of Peak Spectral Period of the Total Spectrum at Grid Point 14845 located near 48.9°N; 47.8°W. 1954 – 2010.....	41
Table 2.18 Percent Frequency of Occurrence of Significant Combined Wave Height and Peak Spectral Period at Grid Point 14845 located near 48.9°N; 47.8°W. 1954 – 2010 ...	43
Table 2.19 Combined Significant Wave Height Statistics (m).....	45
Table 2.20 Maximum Combined Significant Wave Height Statistics (m)	46
Table 2.21 Percentage Occurrence of Peak Spectral Period of the Total Spectrum at Grid Point 13912 located near 48.3°N; 46.3°W. 1954 – 2010.....	48
Table 2.22 Percent Frequency of Occurrence of Significant Combined Wave Height and Peak Spectral Period at Grid Point 13912 located near 48.3°N; 46.3°W. 1954 – 2010 ...	50
Table 2.23 Combined Significant Wave Height Statistics (m).....	52
Table 2.24 Maximum Combined Significant Wave Height Statistics (m)	52
Table 2.25 Percentage Occurrence of Peak Spectral Period of the Total Spectrum at Grid Point 11423 located near 46.9°N; 48.1°W. 1954 – 2010.....	54
Table 2.26 Percent Frequency of Occurrence of Significant Combined Wave Height and Peak Spectral Period at Grid Point 11423 located near 46.9°N; 48.1°W. 1954 – 2010 ...	56
Table 2.27 ICOADS Region 1 Air Temperature Statistics.....	57
Table 2.28 ICOADS Region 1 Sea Surface Temperature Statistics	57
Table 2.29 ICOADS Region 2 Air Temperature Statistics.....	59
Table 2.30 ICOADS Region 2 Sea Surface Temperature Statistics	59
Table 2.31 ICOADS Region 3 Air Temperature Statistics.....	61
Table 2.32 ICOADS Region 3 Sea Surface Temperature Statistics	61

Table 2.33 Percentage Frequency (%) Distribution of Precipitation in Region 1	67
Table 2.34 Percentage Frequency (%) Distribution of Precipitation in Region 2	68
Table 2.35 Percentage Frequency (%) Distribution of Precipitation in Region 3	69
Table 3.1 Number of Storms Providing Best Fit for Extreme Value Analysis of Winds and Waves	73
Table 3.2 1-hr Extreme Wind Speed Estimates (m/s) for Return Periods of 1, 10, 25, 50 and 100 Years	74
Table 3.3 10-minute Extreme Wind Speed (m/s) Estimates for Return Periods of 1, 10, 25, 50 and 100 Years	74
Table 3.4 1-minute Extreme Wind Speed (m/s) Estimates for Return Periods of 1, 10, 25, 50 and 100 Years	75
Table 3.5 Extreme Significant Wave Height Estimates for Return Periods of 1, 10, 25, 50 and 100 Years	76
Table 3.6 Extreme Maximum Wave Height Estimates for Return Periods of 1, 10, 25, 50 and 100 Years	77
Table 3.7 Extreme Associated Peak Period Estimates for Return Periods of 1, 10, 25, 50 and 100 Years	77
Table 3.8 Annual Extreme Significant Wave Estimates and Spectral Peak Periods for Return Periods of 1, 10, 25, 50 and 100 Years	79
Table 4.1 Current meter data for the northern section of the study area	90
Table 4.2 Current statistics data for the northern section of the study area.....	92
Table 4.3 Current Statistics for the western side of Flemish Pass	100
Table 4.4 Near-surface currents at Terra Nova.....	104
Table 4.5 Mid-depth currents at Terra Nova	104
Table 4.6 Near-bottom currents at Terra Nova.....	104
Table 4.7 Near-surface currents at White Rose	106
Table 4.8 Mid-depth currents at White Rose.....	107
Table 4.9 Near bottom currents at White Rose.....	107
Table 4.10 Monthly temperature and salinity statistics for the surface water in Orphan Basin from historical CTD data	119
Table 4.11 Monthly temperature and salinity data for a depth of 50 m in Orphan Basin from historical CTD data	119
Table 4.12 Monthly temperature and salinity data for a depth of 100 m in Orphan Basin from historical CTD data	120
Table 4.13 Monthly temperature and salinity data for a depth of 200 m in Orphan Basin from historical data	121
Table 4.14 Monthly temperature and salinity data for a depth of 300 to 900 m in Orphan Basin from historical CTD data	121
Table 4.15 Monthly temperature and salinity data for a depth of 1000 to 3000 m in Orphan Basin from historical CTD data	122
Table 4.16 Monthly temperature and salinity statistics for the surface water in northern Flemish Pass and the Sackville Spur	124
Table 4.17 Monthly temperature and salinity data for a depth of 50 m in northern Flemish Pass and Sackville Spur	125
Table 4.18 Monthly temperature and salinity data for a depth of 100 m in northern Flemish Pass and Sackville Spur	125

Table 4.19 Monthly temperature and salinity data for a depth of 200 m in northern Flemish Pass and Sackville Spur	126
Table 4.20 Monthly temperature and salinity data for a depth of 300 to 900 m in northern Flemish Pass and Sackville Spur	127
Table 4.21 Monthly temperature and salinity data for a depth of 1000 to 3000 m in northern Flemish Pass and Sackville Spur	127
Table 4.22. Monthly temperature and salinity statistics for the surface water from historical CTD data for a water depth < 100 m on the Grand Banks.....	129
Table 4.23 Monthly temperatures and salinity statistics at 75 m depth from historical CTD data for a water depth of < 100 m on the Grand Banks	130
Table 4.24 Monthly temperature and salinity statistics for the surface water from historical CTD data for a water depth between 100 m and 200m	132
Table 4.25 Monthly temperature and salinity statistic for 75 m depth from historical CTD data for water depth between 100 m and 200 m	133
Table 4.26. Monthly temperature and salinity statistics for the surface water from historical CTD data for water depth between 200 m and 500 m	135
Table 4.27. Monthly temperature and salinity statistics for 75 m depth from historical CTD data for water depth between 200 m and 500 m	136
Table 5.1 Classifications of Sea Ice.....	138
Table 5.2 Iceberg Size by month within Region 1.....	144
Table 5.3 Iceberg Size by month within Region 2.....	146
Table 5.4 Iceberg Size by month within Region 3.....	148

1.0 Introduction

The purpose of this report is to provide a description of the physical environment of Orphan Basin, northeast Grand Banks and Flemish Pass. The most prominent features in the study area are the Grand Banks, the Sackville Spur, and Flemish Pass. The study area is shown in Figure 1.1.

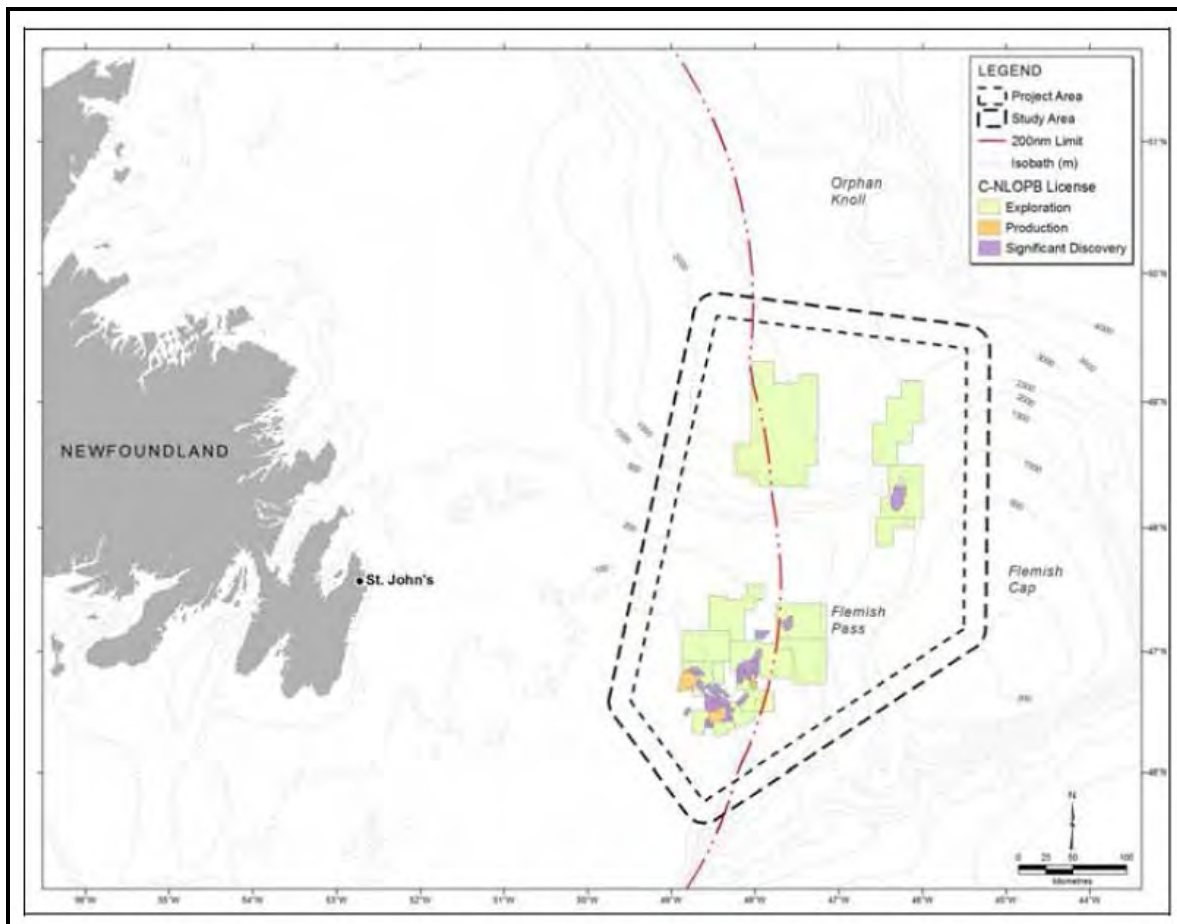


Figure 1.1 The Study area

The wind and wave climatology of the project area was prepared from the MCS50 hindcast data set prepared by Oceanweather Inc. for Environment Canada. The climate analysis was carried out using three grid points to represent the project area. The grid points are Grid Point 14854 at 48.9°N; 47.4°W, Grid Point 13912 at 48.3°N; 46.3°W, and Grid Point 11423 at 46.9°N; 48.1°W. One grid point was selected in Southern Orphan Basin, one on the Grand Banks north of White Rose, and one in Flemish Pass. The International Comprehensive Ocean-Atmosphere Data Set (ICOADS) was used for information on air temperature, sea surface temperature, and visibility.

The physical oceanography section consists of a description of the currents and the water properties in the area. The current data base consists of moored current data from

exploration drilling sites from Terra Nova and White Rose fields, and data from the Bedford Institute of Oceanography archive. A general description of currents is presented for the area using information from published literature and models as well as statistics of mean velocities and monthly mean and maximum current speeds from current measurements. The water properties are described using published literature, hydrographic contours from data collected by Fisheries and Oceans Canada, statistics of temperature and salinity data, and T-S diagrams from data archived at the Bedford Institute of Oceanography.

2.0 Climatology

2.1 General Description of Weather Systems

The study area experiences weather conditions typical of a marine environment with the surrounding waters having a moderating effect on temperature. In general, marine climates experience cooler summers and milder winters than continental climates and have a much smaller annual temperature range. Furthermore, a marine climate tends to be fairly humid, resulting in reduced visibilities, low cloud heights, and receives significant amounts of precipitation.

The climate of the study area is very dynamic, being largely governed by the passage of high and low pressure circulation systems. These circulation systems are embedded in, and steered by, the prevailing westerly flow that typifies the upper levels of the atmosphere in the mid-latitudes, which arises because of the normal tropical to polar temperature gradient. The mean strength of the westerly flow is a function of the intensity of this gradient, and as a consequence is considerably stronger in the winter months than during the summer months, due to an increase in the south to north temperature gradient. [Meteorological convention defines seasons by quarters; e.g., winter is December, January, February, etc.]

At any given time, the upper level flow is a wave-like pattern of large and small amplitude ridges and troughs. These ridges and troughs tend to act as a steering mechanism for surface features and therefore their positions in the upper atmosphere determine the weather at the earth's surface. Upper ridges tend to support areas of high pressure at the surface, while upper troughs lend support to low pressure developments. The amplitude of the upper flow pattern tends to be higher in winter than summer, which is conducive to the development of more intense storm systems.

During the winter months, an upper level trough tends to lie over Central Canada and an upper ridge over the North Atlantic resulting in three main storm tracks affecting the region: one from the Great Lakes Basin, one from Cape Hatteras, North Carolina and one from the Gulf of Mexico. These storm tracks, on average, bring eight low pressure systems per month over the area. The intensity of these systems ranges from relatively weak features to major winter storms. Recent studies (Archer and Caldeira, 2008) have shown that there exists a poleward shift of the jet stream, and consequently storm tracks, at a rate of 0.17 to 0.19 degrees/decade in the northern hemisphere. This shift has been related to an increase in the equator-to-pole temperature gradient. McCabe (2001) obtained similar results, finding that there has been a decrease in mid-latitude cyclone frequency and an increase in high-latitude cyclone frequency. In addition, McCabe found that storm intensity has increased in both the high and mid-latitudes.

In the case where the upper level long wave trough lies well west of the region, the main storm track will lie through the Gulf of St. Lawrence or Newfoundland. Under this regime, an east to south-east flow ahead of a warm front associated with a low will give way to winds from the south in the warm sector of the system. Typically, the periods of southerly winds and mild conditions will be of relatively long duration and, in general, the incidence of extended storm conditions is likely to be relatively infrequent. Strong frictional effects in the stable flow from the south results in a marked shear in the surface

boundary layer and relatively lower winds at the sea surface. As a consequence, local wind wave development tends to be inhibited under such conditions. Precipitation types are more likely to be in the form of rain or drizzle, with relatively infrequent periods of continuous snow, although periods of snow showers prevail in the unstable air in the wake of cold fronts associated with the lows. Visibility will be reduced at times in frontal and advection fogs, in snow, and in snow shower activity.

At other times, with the upper long wave trough further to the east, the main storm track may lie through or to the east of the Grand Banks. With the lows passing closer to the site and frequent high potential for storm development, the incidence of strong gale and storm conditions is greater. Longer bouts of cold, west to northwest winds behind cold fronts occur more frequently, and because the flow is colder than the surface water temperatures, the surface layer is unstable. The shear in the boundary layer is lower, resulting in relatively higher wind speeds near the surface and, consequently, relatively higher sea state conditions. With cold air and sea surface temperatures coupled with high winds, the potential for freezing spray will occur quite frequently. In this synoptic situation, a greater incidence of precipitation in the form of snow is likely to occur. Freezing precipitation, either as rain or drizzle, occurs rather infrequently on the Grand Banks. Visibility will be reduced in frontal and advection fogs and, relatively more frequently, by snow.

Frequently, intense low pressure systems become ‘captured’ and slow down or stall off the coast of Newfoundland and Labrador. This may result in an extended period of little change in conditions that may range, depending on the position, overall intensity and size of the system, from the relatively benign to heavy weather conditions.

By summer, the main storm tracks have moved further north than in winter. Low-pressure systems are less frequent and much weaker. With increasing solar radiation during spring, there is a general warming of the atmosphere that is relatively greater at higher latitudes. This decreases the north-south temperature contrast, lowers the kinetic energy of the westerly flow aloft and decreases the potential energy available for storm development. Concurrently, there is a northward shift of the main band of westerly winds at upper levels and a marked development of the Bermuda-Azores sub-tropical high-pressure area to the south. This warm-core high-pressure cell extends from the surface through the entire troposphere. The main track of the weaker low-pressure systems typically lies through the Labrador region and tends to be oriented from the west-southwest to the east-northeast.

With low pressure systems normally passing to the north of the region in combination with the northwest shoulder of the sub-tropical high to the south, the prevailing flow across the Grand Banks is from the southwest during the summer season. Wind speed is lower during the summer and the incidence of gale or storm force winds relatively infrequent. There is also a corresponding decrease in significant wave heights.

The prevailing south-westerly flow during the late spring and early summer tends to be moist and it is relatively warmer than the underlying surface waters on the Grand Banks.

Rapidly deepening storms are a problem south of Newfoundland in the vicinity of the warm water of the Gulf Stream. Sometimes these explosively deepening oceanic cyclones develop into a “weather bomb”; defined as a storm that undergoes central

pressure falls greater than 24 mb over 24 hours. Hurricane force winds near the center, the outbreak of convective clouds to the north and east of the center during the explosive stage, and the presence of a clear area near the center in its mature stage (Rogers and Bosart 1986) are typical of weather bombs. After development, these systems will either move across Newfoundland or near the southeast coast producing gale to storm force winds from the southwest to south over the area.

In addition to extratropical cyclones, tropical cyclones often retain their tropical characteristics as they enter the study area. Tropical cyclones account for the strongest sustained surface winds observed anywhere on earth. The hurricane season in the North Atlantic basin normally extends from June through November, although tropical storm systems occasionally occur outside this period. Once formed, a tropical storm or hurricane will maintain its energy as long as a sufficient supply of warm, moist air is available. Tropical storms and hurricanes obtain their energy from the latent heat of vapourization that is released during the condensation process. These systems typically move east to west over the warm water of the tropics; however, some of these systems turn northward and make their way towards Newfoundland. Since the capacity of the air to hold water vapour is dependent on temperature, as the hurricanes move northward over the colder ocean waters, they begin to lose their tropical characteristics. By the time these weakening cyclones reach Newfoundland, they are usually embedded into a mid-latitude low and their tropical characteristics are usually lost.

A significant number of tropical cyclones which move into the midlatitudes transition into extratropical cyclones. On average, 46% of tropical cyclones which formed in the Atlantic transition into extratropical cyclones. During this transformation, the system loses tropical characteristics and becomes more extratropical in nature. These systems frequently produce large waves, gale to hurricane force winds and intense rainfall. The likelihood that a tropical cyclone will transition increases toward the second half of the tropical season; with October having the highest probability of transition. In the Atlantic, extratropical transition occurs at lower altitudes in the early and late hurricane season and at higher latitudes during the peak of the season (Hart and Evans, 2001).

2.2 Data Sources

The data sources to describe the climatology of the Project Area came from four main sources: the International Comprehensive Ocean-Atmosphere Data Set (ICOADS), rig observations, the MSC50 North Atlantic wind and wave climatology database and the National Hurricane Centre's best-track dataset. The locations of the climate data sources are presented in Figure 2.1

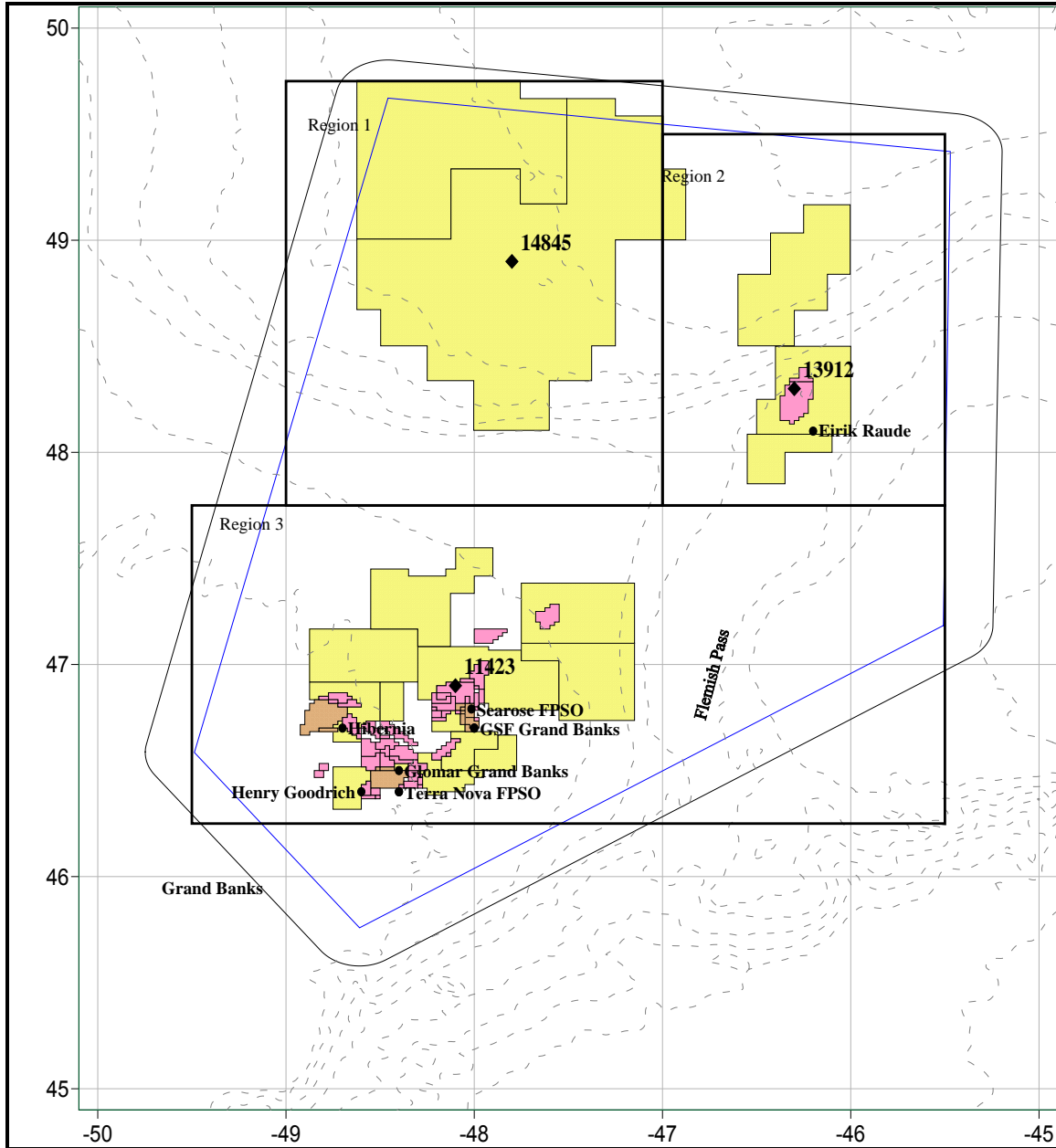


Figure 2.1 Location of the Climate Data Sources

It should be noted that wind speeds from the MSC50 and ICOADS data sets are not directly comparable to each other due to their sampling period and the heights at which they were measured. Wind speed is dependent on height since the wind speed increases at increasing heights above sea level. Methods to reduce wind speeds from anemometer level to 10 m have proven ineffective due to atmospheric stability issues. Winds in the ICOADS data set were either estimated or measured by anemometers at various heights above sea level.

Winds speeds from each of the data sources have different averaging periods. The MSC50 winds are 1-hour averages while the ICOADS and MANMAR winds are 10-

minute average winds. For consistency, the MSC50 wind speeds have been adjusted to 10-minute wind speeds. The adjustment factor to convert from 1-hour mean values to 10-minute mean values is usually taken as 1.06 (U.S. Geological Survey, 1979).

2.2.1 ICOADS

Air temperature, sea surface temperature and visibility statistics for the area were compiled using data from the International Comprehensive Ocean-Atmosphere Data Set (ICOADS). A subset of global marine surface observations from ships, drilling rigs, and buoys for three separate regions within the project area was generated for the period from January 1980 to December 2010. The regions are defined as Region 1 from 47.75°N to 49.75°N, and 47.0°W to 49.0°W; Region 2 from 47.75°N to 49.50°N, and 45.50°W to 47.00°W; and Region 3 from 46.25°N to 47.75°N, and 45.50°W to 49.50°W.

The ICOADS data set has certain inherent limitations in that the observations are not spatially or temporally consistent. In addition, the data set is somewhat prone to observation and coding errors, resulting in some erroneous observations within the data set. The errors were minimized by using an outlier trimming level of 5.5 standard deviations for wind speed, and 3.5 standard deviations for air temperature and sea surface temperatures. In an attempt not to exclude valid observations from the data set, any data greater than 4.5 standard deviations for wind speed and 2.8 standard deviations for air and sea surface temperature were flagged and subsequently analyzed for consistency with other data within the same region and same time. Despite this analysis however valid observations may still have been excluded from the data set. Conversely, invalid data which fell within the limits of the quality control analysis may have been included in the data set.

While the ship-based reports have been quality controlled to the extent possible, they are likely to contain some observation errors, in addition to position report errors, particularly for the older reports. As well, the data set is known to contain a 'fair weather bias', which arises for the following reasons: ship's captains may choose to avoid areas of heavy weather, and since the reporting program is voluntary, fewer observations are likely to be taken under adverse weather and sea state conditions. This bias is more likely to be present during the winter season and over temperate and northern seas where vessel traffic is light.

Kent et al. (1993) demonstrated various systematic inconsistencies in the meteorological observations from voluntary observing ships. These inconsistencies were mostly dependent on the method of estimation used. Sea surface temperature data from engine intake thermometers were found to be biased high by an average of 0.3°C. The dewpoint temperatures from fixed thermometer screens were biased high compared to psychrometer readings. The magnitude of the bias was of the order of 1°C and varied with dewpoint temperature. Wind speeds from anemometers were biased high compared to visual winds by about two knots for winds up to about 25 knots. It was unknown whether visual winds or anemometer winds were more accurate. Compared to daytime values, visual winds at night were underestimated by about 1 m/sec at 15 m/sec and 5 m/sec at 25 m/sec.

2.2.2 MSC50

Wind and wave climate statistics for the area were extracted from the MSC50 North Atlantic wind and wave climatology database compiled by Oceanweather Inc under contract to Environment Canada. The MSC50 database consists of continuous wind and wave hindcast data in 1-hour time steps from January 1954 to December 2005, on a 0.1° latitude by 0.1° longitude grid. Winds from the MSC50 data set are 1-hour averages of the effective neutral wind at a height of 10 m (Harris, 2007). Three grid points were chosen to represent conditions within the project area; grid point 14845, located at 48.9°N 47.8°W, grid point 13912, located at 48.3°N 46.3°W and grid point 11423, located at 46.9°N 48.1°W. Wave heights and periods in the MSC50 data base are computed using a Pierson Moskowitz spectrum.

2.2.3 Platform Observations

Wind statistics were compiled using MANMAR data from several offshore platforms located in the region. The location, period of observation and anemometer height for each of these stations is presented in Table 2.1. Note: The Glomar Grand Banks and the GSF Grand Banks are the same platform under different names at the time of the observations.

Table 2.1 Locations of MANMAR observations

	Latitude	Longitude	Anemometer Height	Period
Searose FPSO	46.8°N	48.0°W	42	Aug 02, 2007 – Sep 30, 2011
Terra Nova FPSO	46.4°N	48.4°W	50	Aug 12, 2007 - Sep 30, 2011
Glomar Grand Banks	46.5°N	48.4°W	82.5	Dec 31, 1998 - Jul 02, 2000
GSF Grand Banks	46.7°N	48.0°W	82.5	Aug 01, 2007 - Sep 30, 2011
Henry Goodrich	46.4°N	48.6°W	95	Feb 23, 2000 - Sep 30, 2011
Hibernia	46.7°N	48.7°W	139	Jan 01, 1999 - Sep 30, 2011
Eirik Raude	48.1°N	46.2°W	82.5	Feb 08, 2003 – Apr 27, 2003

Wave statistics were also compiled from wave data obtained from the Integrated Science Data Management (ISDM) website and MANMAR data. The location, period and observation type for each of these stations is presented in Table 2.2.

Table 2.2 Locations of wave observations

	Latitude	Longitude	Format	Period
Terra Nova	46.4°N	48.4°W	Datawell Waverider	July 13, 1999 – Sept 30, 2009
Ocean Ranger	46.5°N	48.4°W	Datawell Waverider	Dec 04, 1980 – Feb 09, 1982
Hibernia	46.8°N	48.7°W	WRIPS Buoy	Sept 15, 1986 – Jan 08, 1988
Hibernia	46.7°N	48.7°W	MANMAR	Jan 01, 1998 - Dec 31, 2008
Husky	46.8°N	48.0°W	Triaxis Buoy	Oct 06, 2003 – Aug 18, 2007
Eirik Raude	48.2°N	46.3°W	Datawell Waverider	Mar 04, 2003 – Apr 12, 2003

2.2.4 National Hurricane Centre Best-Track Dataset

Tropical cyclone climatology statistics were calculated from the National Hurricane Centre's best-track dataset (Neumann et al. 1993; Jarvinen et al. 1984). This dataset provides positions and intensities at 6-hour intervals for every Atlantic tropical cyclone since 1886. In this report, a subset of the NHC data set consisting of all storms of tropical origin from 1960 to 2010 which have tracked within 370 km of 48.0°N; 47.5°W was used. This subset was obtained from the National Oceanic and Atmospheric Administration's Coastal Services Center Historical Hurricane Tracks website.

2.3 Wind

The Project area experiences predominately southwest to west flow throughout the year. There is a strong annual cycle in the wind direction. West to northwest winds which are prevalent during the winter months begin to shift counter-clockwise during March and April resulting in a predominant southwest wind by the summer months. As autumn approaches, the tropical-to-polar temperature gradient strengthens and the winds shift slightly, becoming predominately westerly again by late fall and into winter. Low pressure systems crossing the area are more intense during the winter months. As a result, mean wind speeds tend to peak during this season.

In addition to mid-latitude low pressure systems crossing the Grand Banks, tropical cyclones often move northward out of the influence of the warm waters south of the Gulf Stream, passing near the Island of Newfoundland. Once the cyclones move over colder waters they lose their source of latent heat energy and often begin to transform into a fast-moving and rapidly developing extratropical cyclone producing large waves and sometimes hurricane force winds.

2.3.1 Region 1

Mean wind speeds in Region 1 at Grid Point 14845 in the MSC50 data set as well as the ICOADS data set reach their peak during the month of January (Table 2.3). Grid Point 14845 had mean wind speeds in January of 11.9 m/s and the ICOADS dataset recorded the highest mean wind speed of 12.7 m/s during January month. There are no MANMAR observations available within Region 1 for comparison.

Table 2.3 Mean Wind Speed (m/s) Statistics for Region 1

	MSC50 Grid Point 14845	ICOADS
January	11.9	12.7
February	11.6	11.0
March	10.5	10.5
April	8.9	9.2
May	7.7	7.8
June	6.9	7.4
July	6.5	6.7
August	6.8	7.5
September	8.1	7.8
October	9.5	9.7
November	10.4	10.6
December	11.4	11.4

A wind rose of the annual wind speed and a histogram of the wind speed frequency for Grid Points 14845 is presented in Figure 2.2 and Figure 2.3, respectively. Monthly wind roses along with histograms of the frequency distributions of wind speeds can be found in Appendix 1. There is a marked increase in the occurrence of winds from the west to northwest in the winter months as opposed to the summer months, which is consistent with the wind climatology of the area.

The percentage exceedance of wind speeds at Grid Point 14845 is presented in Figure 2.4.

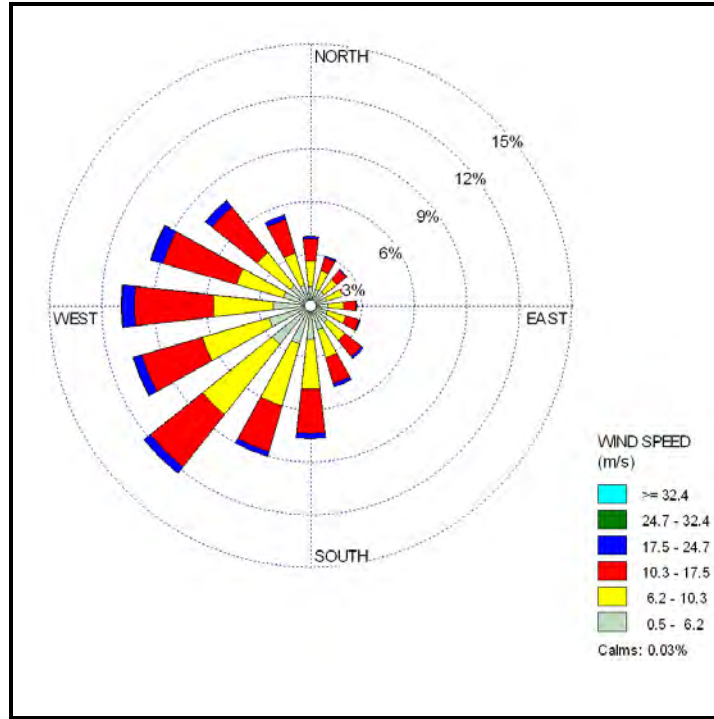


Figure 2.2 Annual Wind Rose for MSC50 Grid Point 14845 located near 48.9°N; 47.8°W. 1954 – 2010

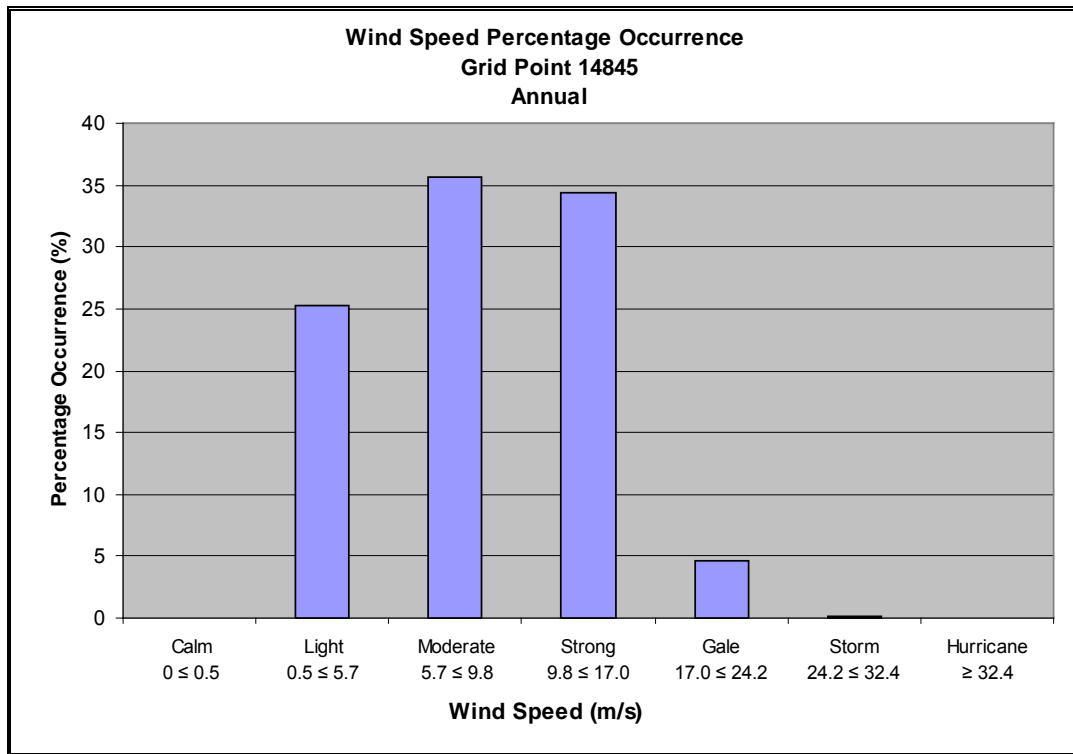


Figure 2.3 Annual Percentage Frequency of Wind Speeds for MSC50 Grid Point 14845 located near 48.9°N; 47.8°W. 1954 – 2010

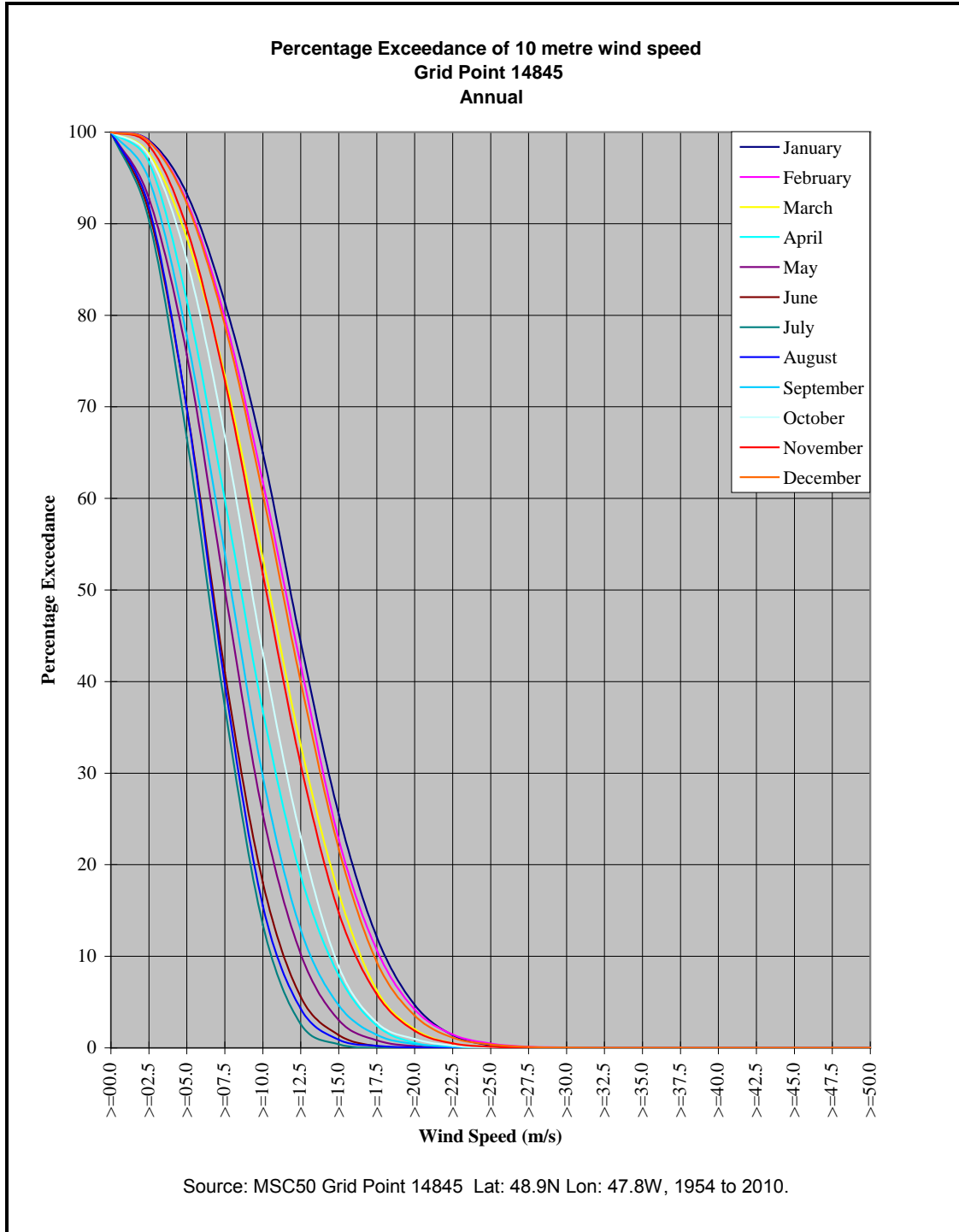


Figure 2.4 Percentage Exceedance of 10 m wind speed at Grid Point 14845 located near 48.9°N; 47.8°W. 1954 – 2010

A table of monthly maximum wind speeds for both data sets is presented in Table 2.4. Rapidly deepening storm systems known as weather bombs frequently cross the region. These storm systems typically develop in the warm waters of Cape Hatteras and move

northeast across the project area. The highest measured wind speed in the ICOADS data set was measured by the German Trawler Junge Garde as it took part in the World Meteorological Organization's Voluntary Observing Ship program on December 19, 1985. This wind speed occurred as a 985 mb low pressure moved west across Newfoundland and deepened to 959 mb over the region 12 hours later.

Table 2.4 Maximum Wind Speed (m/s) Statistics for Region 1

	MSC50 Grid Point 14845	ICOADS
January	28.1	39.6
February	32.3	37.0
March	30.1	30.9
April	24.6	28.3
May	25.5	24.2
June	23.8	26.2
July	17.7	23.1
August	24.5	30.4
September	28.6	28.3
October	31.3	26.8
November	27.6	34.4
December	30.5	47.8

The maximum monthly wind speeds by direction from the MSC50 data set are presented in Table 2.5 the percentage occurrence of wind direction by month is presented in Table 2.6.

Table 2.5 Monthly Maximum 10m Wind Speed by Direction (m/s) speed at Grid Point 14845 located near 48.9°N; 47.8°W. 1954 – 2010

	Direction								All Directions	
Month	NE	E	SE	S	SW	W	NW	N	Min	Max
January	22.0	23.4	24.5	24.8	27.0	28.1	26.8	26.3	22.0	28.1
February	24.1	24.0	28.2	27.7	26.6	32.3	29.8	23.4	23.4	32.3
March	21.5	24.2	23.4	23.3	26.7	29.8	30.1	23.0	21.5	30.1
April	21.1	23.4	21.7	21.7	23.1	23.1	23.4	24.6	21.1	24.6
May	21.7	17.3	18.2	19.9	21.6	20.4	25.5	21.8	17.3	25.5
June	17.0	17.7	21.6	18.5	19.1	19.5	23.8	17.3	17.0	23.8
July	14.3	15.6	16.8	17.7	17.7	16.5	16.6	15.8	14.3	17.7
August	18.7	19.6	19.9	18.8	19.3	18.9	22.4	24.5	18.7	24.5
September	19.8	18.9	28.6	26.3	26.7	26.1	24.9	20.9	18.9	28.6
October	19.8	22.7	23.4	22.8	31.3	26.6	27.1	25.4	19.8	31.3
November	22.4	24.5	23.4	24.7	27.6	27.3	25.8	26.0	22.4	27.6
December	23.9	23.2	24.7	24.1	26.5	29.4	30.5	27.0	23.2	30.5
Annual	24.1	24.5	28.6	27.7	31.3	32.3	30.5	27.0		

Table 2.6 Percentage occurrence of Wind Direction by month speed at Grid Point 14845 located near 48.9°N; 47.8°W. 1954 – 2010

	Direction							
Month	NE	E	SE	S	SW	W	NW	N
January	4.8	4.8	7.8	10.4	18.6	30.1	16.8	6.8
February	5.1	6.1	8.1	10.8	16.1	27.5	17.7	8.5
March	8.0	7.4	7.3	11.5	17.4	21.2	16.8	10.4
April	7.9	8.7	9.5	13.3	17.7	16.6	15.7	10.6
May	7.9	7.3	9.3	16.1	19.8	15.8	13.1	10.7
June	4.8	5.4	7.4	17.7	30.4	15.0	11.3	8.0
July	2.9	3.7	7.1	21.7	37.3	15.3	8.1	4.0
August	4.4	3.8	7.0	18.3	32.8	16.3	11.2	6.2
September	4.8	4.4	5.5	14.3	24.0	21.6	16.7	8.6
October	4.7	4.7	6.8	12.4	19.2	23.2	20.4	8.6
November	4.5	5.0	7.6	13.5	19.5	23.5	19.1	7.3
December	4.6	5.6	7.2	12.4	17.6	26.5	18.0	8.3
Annual	5.4	5.6	7.6	14.4	22.5	21.0	15.4	8.2

Region 2

Mean wind speeds in Region 2 at Grid Point 13912 in the MSC50 data set as well as the ICOADS data set peak during the month of January (Table 2.7). Grid Point 13912 had a mean wind speed in January of 12.0 m/s while the ICOADS dataset recorded the highest mean wind speed of 12.5 m/s during January month. Observations from the Eirik Raude were available from February to April 2003. Statistics from this platform are presented because the period covers a severe storm event which occurred on February 11, 2003, as well as a second event which occurred on March 08, 2003. Due to these two storms, and the data set only covering a period of 3 months, mean statistics are higher than that of the other two data sets.

Table 2.7 Mean Wind Speed (m/s) Statistics for Region 2

	MSC50 Grid Point 13912	ICOADS	Eirik Raude
January	12.0	12.5	
February	11.6	11.6	17.5
March	10.5	10.7	13.1
April	8.8	8.4	12.0
May	7.6	7.8	
June	6.9	7.3	
July	6.4	7.0	
August	6.7	7.5	
September	8.1	8.2	
October	9.5	9.4	
November	10.3	10.7	
December	11.4	11.1	

A wind rose of the annual wind speed and a histogram of the wind speed frequency for Grid Points 13912 is presented in Figure 2.5 and Figure 2.6. Monthly wind roses along with histograms of the frequency distributions of wind speeds can be found in Appendix 2. There is a marked increase in the occurrence of winds from the west to northwest in the winter months as opposed to the summer months, which is consistent with the wind climatology of the area.

The percentage exceedance of wind speeds at Grid Point 13912 is presented in Figure 2.7.

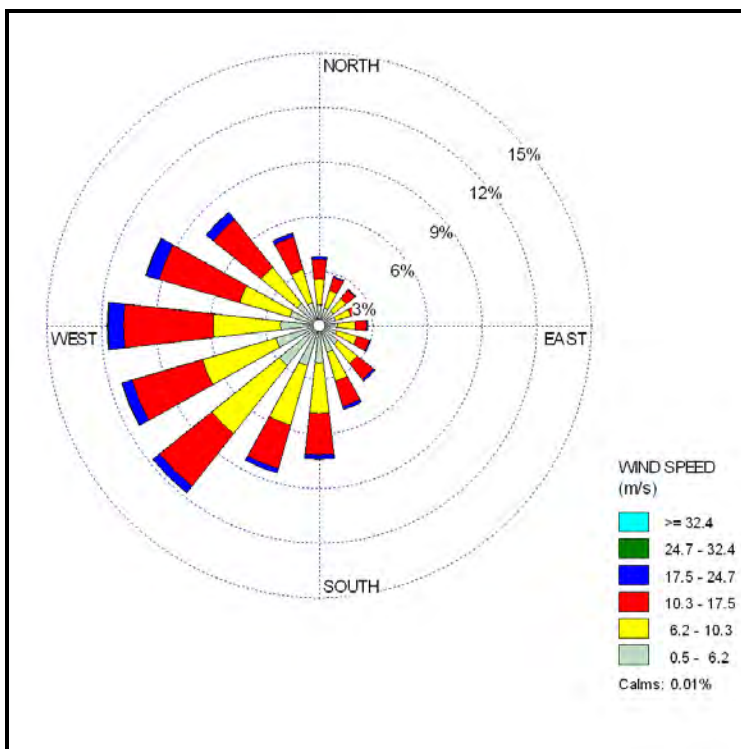


Figure 2.5 Annual Wind Rose for MSC50 Grid Point 13912 located near 48.3°N; 46.3°W. 1954 – 2010

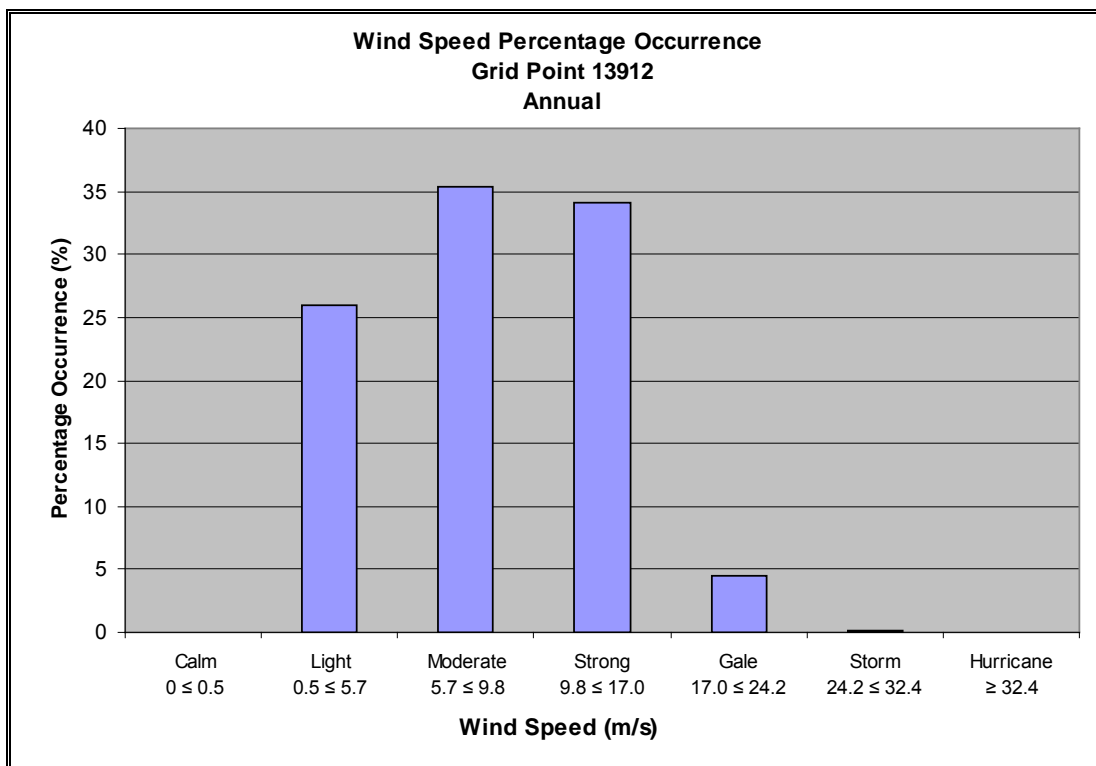


Figure 2.6 Annual Percentage Frequency of Wind Speeds for MSC50 Grid Point 14845 located near 48.9°N; 47.8°W. 1954 – 2010

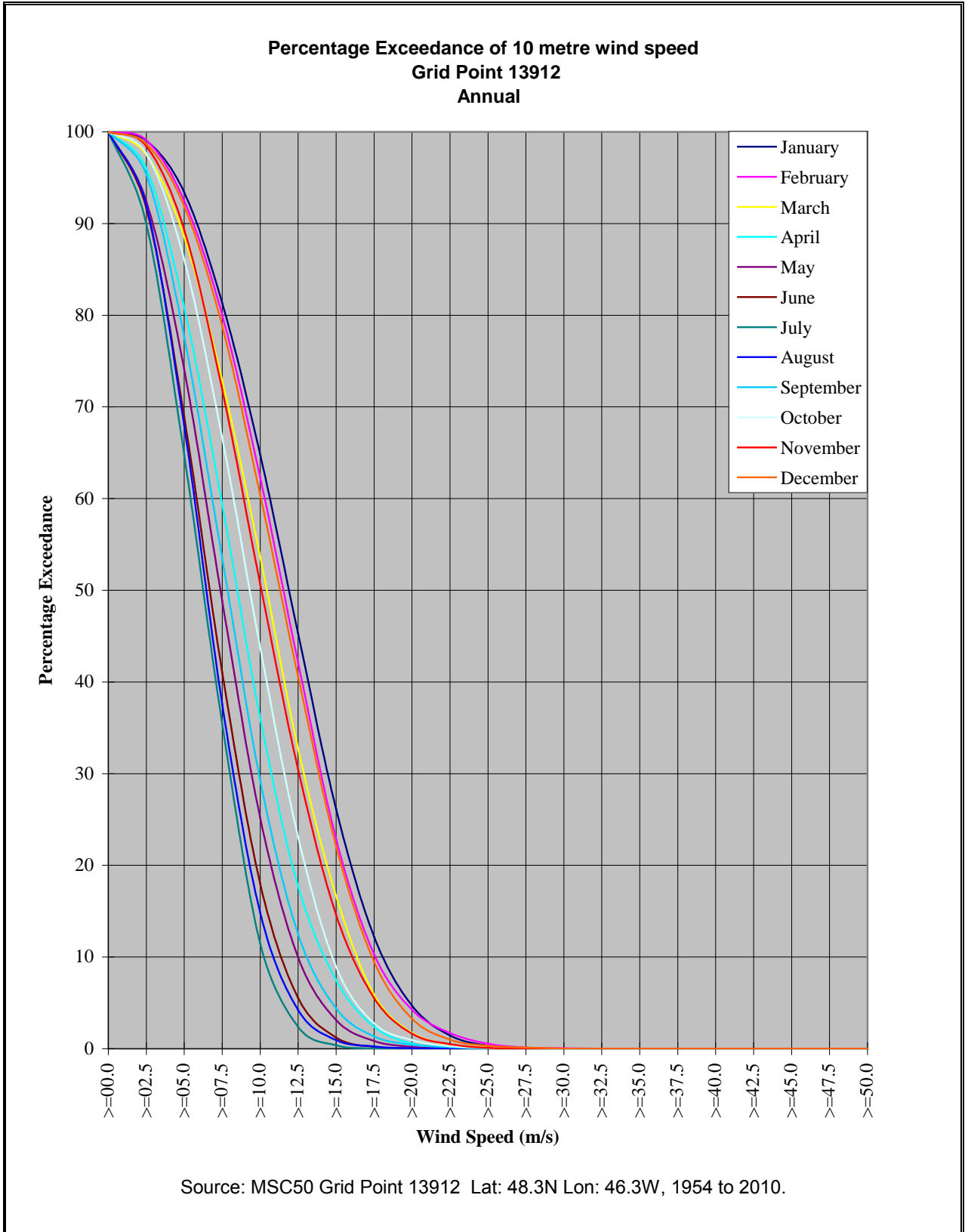


Figure 2.7 Percentage Exceedance of 10 m wind speed at Grid Point 13912 located near 48.3°N; 46.3°W. 1954 – 2010

Maximum wind speed statistics are presented from the Eirik Raude platform while at Mizzen L-11. This platform was in the region during an extreme wind event which occurred on February 11, 2003. During this event, the Eirik Raude recorded a mean 10-minute wind speed of 43.2 m/s (Table 2.8). A similar, although somewhat weaker system passed through the project area on March 08, 2003. Mean wind speeds recorded by the Eirik Raude during this event peaked at 33.4 m/s.

The maximum monthly wind speeds by direction from the MSC50 data set are presented in Table 2.9 and the percentage occurrence of wind direction by month is presented in Table 2.10.

Table 2.8 Maximum Wind Speed (m/s) Statistics for Region 2

	MSC50 Grid Point 13912	ICOADS	Eirik Raude
January	29.6	32.4	
February	31.1	33.4	43.2
March	30.7	29.8	33.4
April	25.7	24.0	23.2
May	25.4	24.7	
June	23.1	22.1	
July	19.9	20.6	
August	28.4	26.8	
September	28.7	28.8	
October	27.8	25.7	
November	27.0	23.7	
December	31.0	27.3	

Table 2.9 Monthly Maximum 10m Wind Speed by Direction (m/s) speed at Grid Point 13912 located near 48.3°N; 46.3°W. 1954 – 2010

Month	Direction								All Directions	
	NE	E	SE	S	SW	W	NW	N	Min	Max
January	21.0	21.4	23.5	26.5	27.0	29.6	27.9	24.4	21.0	29.6
February	25.9	24.3	25.5	31.1	30.8	31.0	27.6	23.0	23.0	31.1
March	21.2	23.2	23.9	23.5	26.3	30.7	29.3	21.7	21.2	30.7
April	23.8	21.6	23.8	25.7	25.1	23.5	24.8	23.1	21.6	25.7
May	20.9	17.8	16.4	20.3	21.3	20.8	25.4	21.0	16.4	25.4
June	15.4	15.8	19.8	18.9	19.1	22.7	23.1	17.5	15.4	23.1
July	14.6	14.1	18.3	19.9	16.7	18.1	16.3	14.6	14.1	19.9
August	22.0	18.5	22.1	28.4	24.2	22.3	23.0	24.8	18.5	28.4
September	16.9	18.9	28.7	27.0	27.5	25.7	23.9	19.8	16.9	28.7
October	20.1	21.8	25.5	27.8	25.9	26.8	27.8	26.4	20.1	27.8
November	20.5	20.9	25.4	25.3	26.2	27.0	26.0	24.4	20.5	27.0
December	21.6	22.3	23.7	24.2	30.1	29.8	31.0	25.6	21.6	31.0
Annual	25.9	24.3	28.7	31.1	30.8	31.0	31.0	26.4		

Table 2.10 Percentage occurrence of Wind Direction by month at Grid Point 13912 located near 48.3°N; 46.3°W. 1954 – 2010

	Direction							
Month	NE	E	SE	S	SW	W	NW	N
January	4.5	4.4	7.8	10.7	18.2	31.0	16.9	6.5
February	5.1	6.2	7.9	11.2	16.2	28.7	17.0	7.8
March	7.3	7.8	7.6	11.3	17.0	22.7	16.5	9.8
April	7.2	8.5	9.9	13.1	17.3	18.2	16.0	9.8
May	7.6	7.6	8.8	14.9	19.5	17.8	13.8	10.0
June	4.4	5.3	7.0	16.5	30.5	16.8	11.8	7.6
July	2.8	3.3	7.0	19.7	37.2	17.3	8.4	4.2
August	4.3	3.7	6.7	17.5	31.1	18.5	11.7	6.5
September	4.6	4.2	5.8	13.9	22.7	22.6	17.6	8.6
October	4.4	4.6	6.9	12.1	18.2	24.4	20.9	8.5
November	4.2	4.8	8.0	13.4	18.8	23.6	19.7	7.5
December	4.3	5.4	7.1	12.5	17.3	27.3	18.3	7.6
Annual	5.0	5.5	7.5	13.9	22.0	22.4	15.7	7.9

2.3.2 Region 3

Wind speed typically increases with increasing heights above sea level. Statistics provided in Table 2.11 are presented in order of increasing height, with the MSC50 data set being the lowest and the Hibernia Platform data set being the highest. The anemometer heights for each platform are found in Table 2.1. Statistics for each anemometer level are presented to give a better idea of winds at varying levels above sea level.

Table 2.11 Mean Wind Speed Statistics in Region 3

	MSC50 Grid Point 11423	ICOADS	Searose FPSO	Terra Nova FPSO	Glomar Grand Banks	GSF Grand Banks	Henry Goodrich	Hibernia
January	11.1	13.9	12.8	13.8	12.9	13.2	15.5	16.1
February	10.9	13.2	12.1	13.6	11.9	12.8	15.4	15.6
March	9.9	12.1	11.0	12.2	11.9	12.1	14.0	14.5
April	8.3	11.1	10.3	11.6	11.4	12.0	13.0	13.6
May	7.0	10.2	8.9	10.5	9.7	10.9	11.8	12.2
June	6.5	10.2	8.6	9.8	9.4	9.8	11.6	11.7
July	6.1	9.7	8.4	9.6	9.5	9.6	11.0	11.4
August	6.4	9.0	10.3	9.2	8.4	8.8	9.7	10.6
September	7.5	10.1	10.7	10.5	10.3	9.7	10.8	11.7
October	8.8	11.6	12.5	11.7	12.8	10.2	12.3	13.3
November	9.6	12.2	12.7	12.3	11.0	11.5	13.0	13.7
December	10.7	13.8	13.9	14.5	12.6	13.4	14.7	15.9

A wind rose of the annual wind speed for Grid Points 11423 is presented in Figure 2.8 and the associated histogram of the wind speed frequency in Figure 2.9. Monthly wind roses along with histograms of the frequency distributions of wind speeds can be found in Appendix 3.

Wind speeds are much lower in the summer than in winter. The percentage exceedance of wind speeds at grid point 11423 is presented in Figure 2.10.

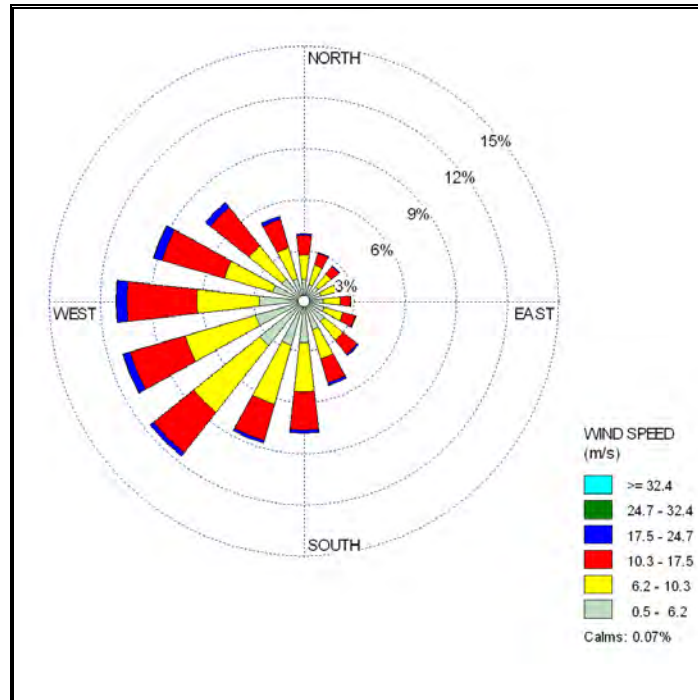


Figure 2.8 Annual Wind Rose for MSC50 Grid Point 11423 located near 46.9°N; 48.1°W. 1954 – 2010

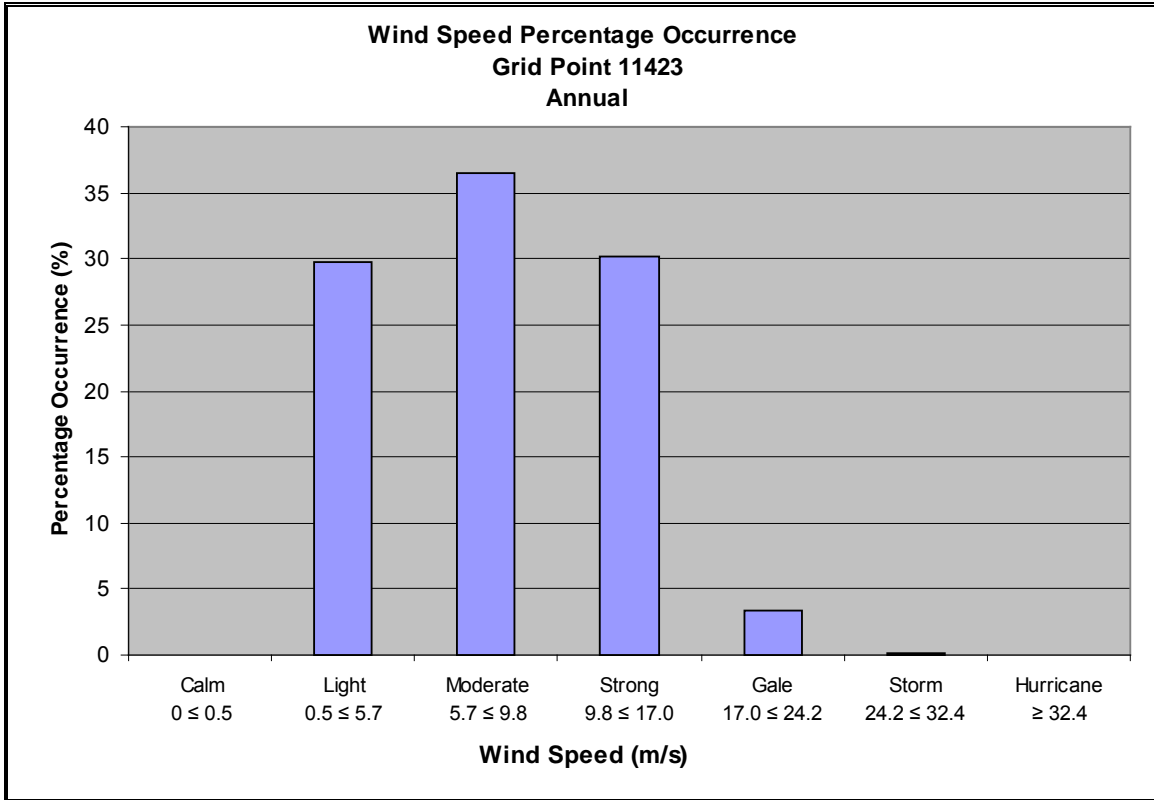


Figure 2.9 Annual Percentage Frequency of Wind Speeds for MSC50 Grid Point 11423 located near 46.9°N; 48.1°W. 1954 – 2010

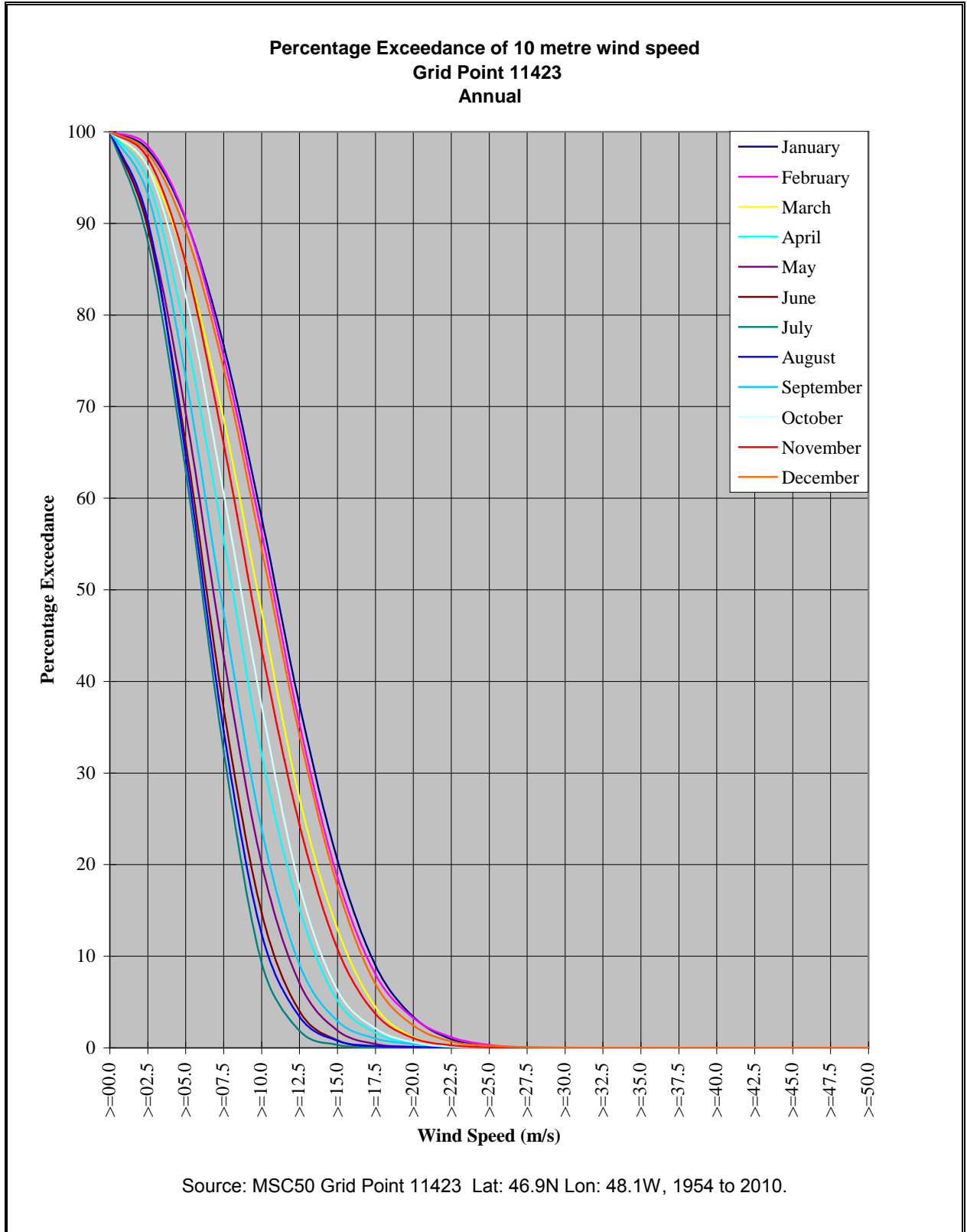


Figure 2.10 Percentage Exceedance of 10 m wind speed at Grid Point 11423 located near 46.9°N; 48.1°W. 1954 – 2010

A table of monthly maximum wind speeds for each of the data sets is presented in Table 2.12. Rapidly deepening storm systems known as weather bombs frequently cross the Grand Banks. These storm systems typically develop in the warm waters of Cape Hatteras and move northeast across the Grand Banks. Wind speeds of 49.4 m/s and 52.5 m/s from the southwest were recorded by the Hibernia Platform and the Henry Goodrich anemometers, respectively, as this system passed. During this storm, a low pressure developing off Cape Hatteras on February 10th, 2003 rapidly deepened to 949 mb as it tracked northeast across the Avalon Peninsula around 18Z on February 11th, 2003. A wind speed of 43.7 m/s was recorded by the Sea Rose FPSO at 00Z and 03Z on October 15, 2009. This occurred as another storm, following a similar track to the February 10th storm passed over the area. During this event, the low pressure deepened from 1002 mb at 00Z October 14th, to 963 mb as it passed northeast of the Avalon on October 15th.

The maximum monthly wind speeds by direction from the MSC50 data set are presented in Table 2.13 and the percentage occurrence of wind direction by month is presented in Table 2.14.

Table 2.12 Maximum Wind Speed (m/s) Statistics in Region 3

	MSC50 Grid Point 11423	ICOADS	Searose FPSO	Terra Nova FPSO	Glomar Grand Banks	GSF Grand Banks	Henry Goodrich	Hibernia
January	29.2	43.7	25.7	31.9	30.9	37.6	44.2	43.2
February	31.5	49.9	29.8	34.0	26.8	31.4	52.5	49.4
March	30.2	38.0	23.7	29.8	23.7	28.8	32.9	37.6
April	24.9	35.0	24.7	26.8	26.8	33.4	35.0	37.6
May	22.8	33.9	21.6	25.2	22.1	25.7	32.9	32.4
June	23.8	31.9	18.5	24.2	21.1	27.3	31.4	35.5
July	18.5	29.3	18.0	23.2	20.1	25.2	28.3	31.9
August	29.0	36.0	33.4	29.8	25.7	26.2	30.9	41.2
September	25.8	43.2	30.9	34.5	29.3	27.8	35.0	43.2
October	26.9	44.8	43.7	31.9	32.9	30.9	33.4	44.8
November	27.7	36.0	25.2	28.3	25.7	25.2	37.6	38.1
December	30.5	42.2	24.7	37.6	27.3	29.3	39.6	39.1

Table 2.13 Monthly Maximum 10m Wind Speed by Direction (m/s) at Grid Point 11423 located near 46.9°N; 48.1°W. 1954 – 2010

Month	Direction								All Directions	
	NE	E	SE	S	SW	W	NW	N	Min	Max
January	20.5	23.5	24.3	25.8	29.2	27.4	27.2	25.3	20.5	29.2
February	23.1	22.2	26.1	30.8	30.4	30.0	31.5	24.1	22.2	31.5
March	21.9	25.2	23.0	22.2	25.1	28.6	30.2	24.4	21.9	30.2
April	22.0	20.4	21.9	24.9	24.3	23.4	23.8	24.0	20.4	24.9
May	16.9	17.4	17.9	19.8	20.4	19.6	22.8	19.3	16.9	22.8
June	16.1	16.9	21.2	17.9	18.3	21.7	23.8	15.4	15.4	23.8
July	14.4	15.1	18.5	17.5	17.1	16.3	17.5	15.4	14.4	18.5
August	17.0	18.9	26.1	27.3	28.5	22.5	29.0	23.5	17.0	29.0
September	20.5	20.7	24.5	24.8	25.8	23.8	21.6	20.7	20.5	25.8
October	21.3	21.1	23.9	26.5	26.2	26.9	25.7	22.9	21.1	26.9
November	21.2	22.8	24.3	27.7	22.3	25.8	27.7	25.8	21.2	27.7
December	21.3	22.9	25.9	23.5	28.7	28.4	30.5	25.2	21.3	30.5
Annual	23.1	25.2	26.1	30.8	30.4	30.0	31.5	25.8		

Table 2.14 Percentage occurrence of Wind Direction by month at Grid Point 11423 located near 46.9°N; 48.1°W. 1954 – 2010

Month	Direction							
	NE	E	SE	S	SW	W	NW	N
January	4.4	5.0	7.8	11.6	17.8	29.1	17.4	6.8
February	5.4	6.1	8.5	11.6	15.5	26.8	17.9	8.3
March	7.5	7.2	7.8	11.9	16.6	21.7	16.4	10.8
April	7.6	9.1	9.9	12.8	17.8	18.0	14.7	10.1
May	7.8	7.3	9.3	15.3	20.6	17.1	13.0	9.6
June	4.9	5.5	7.7	17.0	30.8	16.8	9.8	7.5
July	2.7	3.6	6.8	21.7	38.3	16.2	6.8	4.0
August	4.6	4.2	8.2	18.4	30.6	18.2	9.1	6.8
September	5.7	4.6	6.7	14.6	22.2	21.3	15.6	9.3
October	4.8	5.2	7.3	13.2	18.5	22.6	19.3	9.2
November	5.1	5.4	9.0	14.3	17.5	21.7	18.9	8.2
December	4.3	5.5	8.3	12.7	16.3	26.6	18.2	8.2
Annual	5.4	5.7	8.1	14.6	21.9	21.3	14.8	8.2

2.3.3 Tropical Systems

The hurricane season in the North Atlantic basin normally extends from June through November, although tropical storm systems occasionally occur outside this period. While the strongest winds typically occur during the winter months and are associated with mid-latitude low pressure systems, storm force winds may occur at any time of the year as a result of tropical systems. Once formed, a tropical storm or hurricane will maintain its energy as long as a sufficient supply of warm, moist air is available. Tropical storms and hurricanes obtain their energy from the latent heat of vapourization that is released during the condensation process. These systems typically move east to

west over the warm water of the tropics. However, some of these systems turn northward and make their way towards Newfoundland and the project area. Since the capacity of the air to hold water vapour is dependent on temperature, the hurricanes begin to lose their tropical characteristics as they move northward over the colder ocean waters. By the time these weakening cyclones reach Newfoundland, they are usually embedded into a mid-latitude low and their tropical characteristics are usually lost.

There has been a significant increase in the number of Hurricanes that have developed within the Atlantic Basin during the last 15 years. Figure 2.11 shows the 5-year average of tropical storms which have developed within the Atlantic Basin since 1961. This increase in activity has been attributed to naturally occurring cycles in tropical climate patterns near the equator called the tropical multi-decadal signal (Bell and Chelliah 2006). As a result of the increase in tropical activity in the Atlantic Basin, there has also been an increase in tropical storms or their remnants entering the Canadian Hurricane Centre Response zone. There is little change in the 5-year trend for hurricanes coming within the project area. It should be noted that the unusually high number of tropical storms in 2005 may be skewing the results for the 2000 – 2005 season.

A significant number of tropical cyclones which move into the midlatitudes transform into extratropical cyclones. On average, 46% of tropical cyclones which formed in the Atlantic transformed into extratropical cyclones. During this transformation, the system loses tropical characteristics and becomes more extratropical in nature resulting in an increase in the area which produces large waves, gale to hurricane force winds and intense rainfall. The likelihood that a tropical cyclone will transform increases toward the second half of the tropical season, with October having the highest probability of transition. In the Atlantic, extratropical transition occurs at lower latitudes in the early and late hurricane season and at higher latitudes during the peak of the season (Hart and Evans, 2001).

On occasion, these systems still maintain their tropical characteristics when they reach Newfoundland. Seven Category 1 and one Category 2 hurricane crossed the region during this time period. The most intense of these storms was Hurricane Gladys which crossed at 12Z on October 03, 1975 with maximum sustained wind speeds of 43.7 m/s and a central pressure of 960 mb. Hurricane Gladys underwent extratropical transition over the next several hours and move northeast of the area as an extratropical storm with wind speeds of 38.6 m/s.

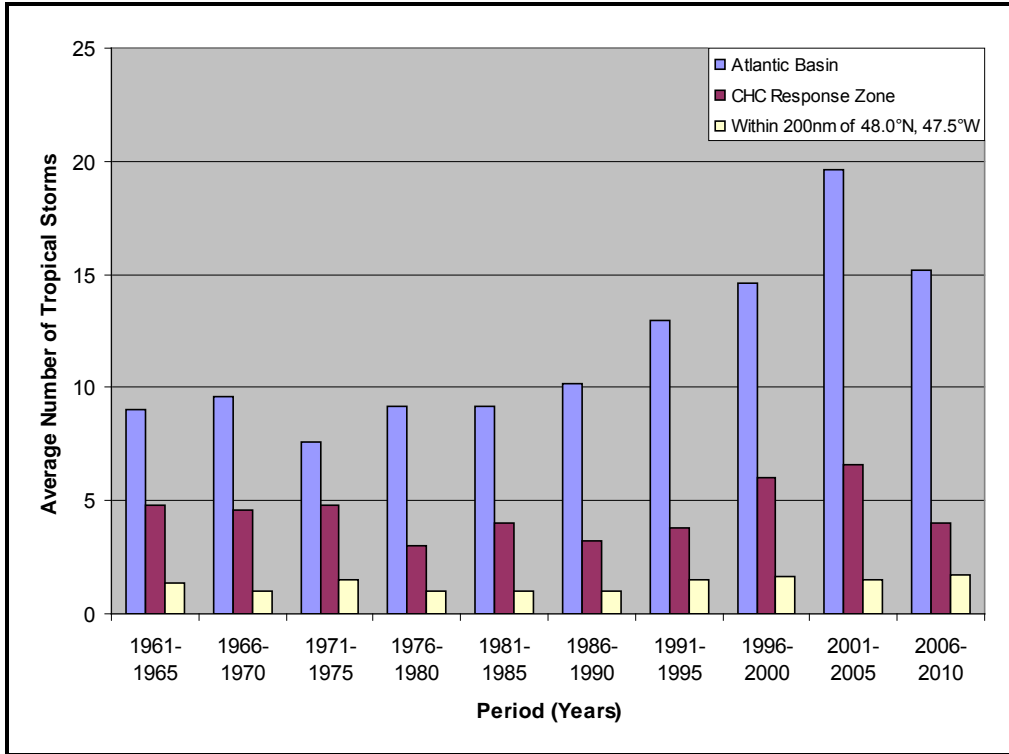


Figure 2.11 5-Year Average of the number of Tropical Storms which formed in the Atlantic Basin since 1961

Since 1960, 40 tropical systems have passed within 370 km of 48.0°N; 47.5°W. The names are given in Table 2.15 and the tracks over the project area are shown in Figure 2.12. It should be noted that the values in the table are the maximum 1-minute mean winds speeds occurring within the tropical system at the 10-m reference level as it passed within 200 nm of the location.

Table 2.15 Tropical Systems Passing within 370 km of 48.0°N, 47.5°W (1960 to 2010)

Year	Month	Day	Hour	Name	Latitude	Longitude	Wind (m/s)	Pressure	Category
1962	10	22	1800	Ella	49.0	-50.0	30.9	N/A	Extratropical
1963	8	28	0000	Beulah	45.8	-48.3	33.4	N/A	Category 1
1963	10	13	0000	Flora	47.0	-45.0	5.1	N/A	Extratropical
1964	9	4	1800	Cleo	46.9	-49.8	36.0	N/A	Category 1
1967	9	4	1200	Arlene	46.6	-46.0	30.9	N/A	Extratropical
1969	8	13	0000	Blanche	47.1	-49.0	25.7	N/A	Extratropical
1971	7	7	1800	Arlene	46.5	-53.0	23.1	N/A	Extratropical
1971	8	6	1200	Unnamed	55.7	-43.8	36.0	974	Category 1
1973	10	28	0600	Gilda	47.5	-51.5	28.3	968	Extratropical
1974	7	20	0600	Subtrop 2	46.7	-48.0	20.6	N/A	Extratropical
1975	7	4	0600	Amy	44.5	-51.6	25.7	986	Tropical Storm
1975	10	3	1200	Gladys	46.6	-50.6	43.7	960	Category 2
1976	8	24	0000	Candice	45.9	-48.7	33.4	N/A	Category 1
1977	9	30	0000	Dorothy	47.0	-51.0	41.2	995	Extratropical
1978	9	5	0600	Ella	47.2	-50.2	12.9	975	Category 1
1979	8	6	0600	Unnamed	48.2	-50.6	34.5	N/A	Tropical Depression
1980	9	8	1200	Georges	45.6	-51.1	38.6	993	Category 1
1982	9	19	1200	Debby	48.5	-47.1	36.0	987	Category 1
1984	9	2	1200	Cesar	46.0	-50.4	28.3	994	Tropical Storm
1990	9	3	0000	Gustav	46.0	-46.5	28.3	993	Tropical Storm
1992	10	26	1800	Frances	46.0	-46.9	33.4	988	Tropcail Storm
1995	7	21	0000	Chantal	47.7	-45.2	25.7	1001	Extratropical
1995	8	22	1800	Felix	49.0	-46.0	41.2	985	Extratropical
1998	9	6	1800	Earl	49.5	-50.0	28.3	966	Extratropical
1999	9	19	0600	Floyd	48.5	-52.5	18.0	994	Extratropical
1999	10	19	1200	Irene	48.0	-48.0	28.3	968	Extratropical
2000	9	25	1200	Helene	44.0	-55.5	23.1	988	Tropical Storm
2001	8	29	0000	Dean	47.0	-48.5	30.9	999	Extratropical
2001	9	20	0000	Gabrielle	48.5	-48.5	30.9	988	Extratropical
2003	10	7	1800	Kate	47.5	-47.2	30.9	980	Tropical Storm
2004	9	2	0000	Gaston	47.0	-50.0	23.1	997	Extratropical
2005	7	30	1800	Franklin	46.4	-48.8	23.1	1006	Extratropical
2005	9	12	0600	Ophelia	49.0	-48.8	23.1	1001	Extratropical
2006	6	16	1800	Alberto	49.3	-51.5	20.6	990	Extratropical
2006	9	14	0600	Florence	48.6	-48.3	20.6	967	Extratropical
2006	10	3	0600	Isaac	48.6	-49.0	23.1	998	Extratropical
2006	6	18	0600	Not-Named	48.6	-52.9	18.0	1004	Tropical Storm
2007	8	1	0000	Chantal	49.0	-49.5	30.9	988	Extratropical
2008	10	1	1800	Laura	47.5	-46.3	20.6	995	Extratropical
2009	8	24	1200	Bill	49.2	-47.2	30.9	980	Extratropical

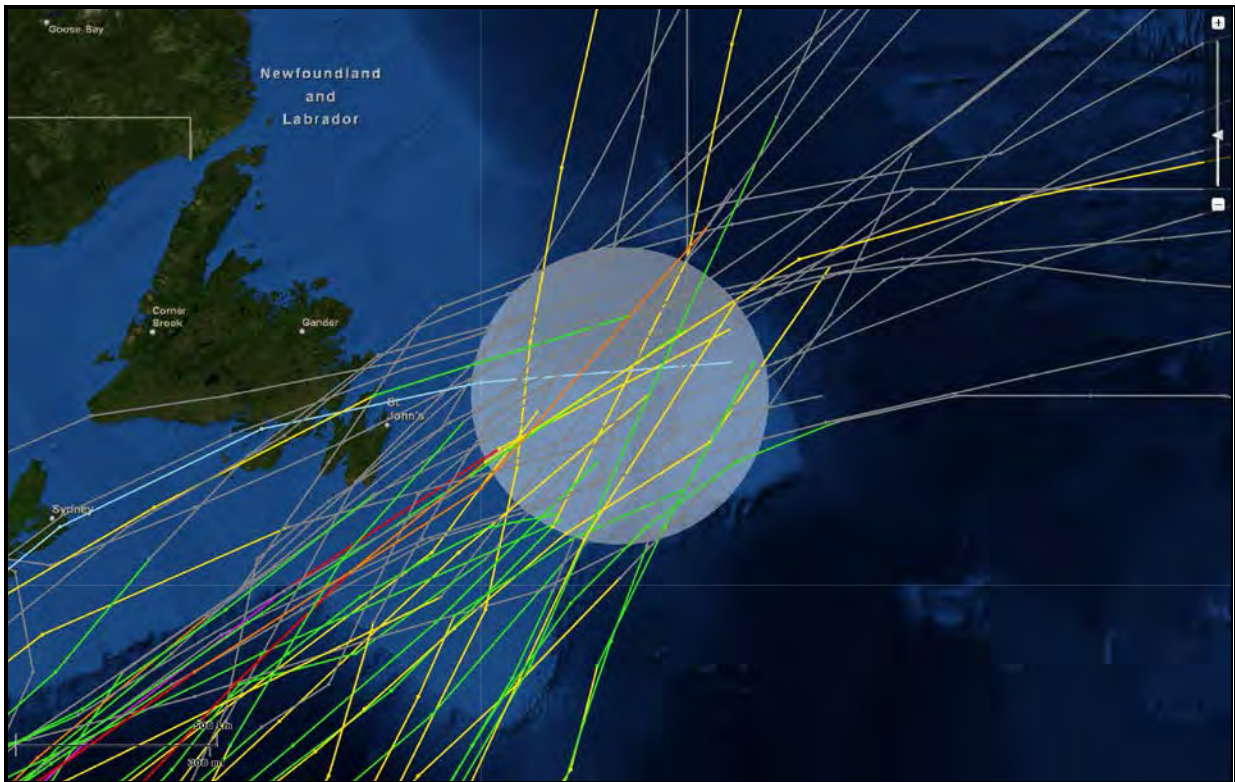


Figure 2.12 Storm Tracks of Tropical Systems Passing within 370 km of 48.0°N, 47.5°W

2.4 Waves

The main parameters for describing wave conditions are the significant wave height, the maximum wave height, the peak spectral period, and the characteristic period. The significant wave height is defined as the average height of the 1/3 highest waves, and its value roughly approximates the characteristic height observed visually. The maximum height is the greatest vertical distance between a wave crest and adjacent trough. The spectral peak period is the period of the waves with the largest energy levels, and the characteristic period is the period of the 1/3 highest waves. The characteristic period is the wave period reported in ship observations, and the spectral period is reported in the MSC50 data set.

A sea state may be composed of the wind wave alone, swell alone, or the wind wave in combinations with one or more swell groups. A swell is a wave system not produced by the local wind blowing at the time of observation and may have been generated within the local weather system, or from within distant weather systems. The former situation typically arises when a front, trough, or ridge crosses the point of concern, resulting in a marked shift in wind direction. Swells generated in this manner are usually of low period. Swells generated by distant weather systems may propagate in the direction of the winds that originally formed to the vicinity of the observation area. These swells may

travel for thousands of miles before dying away. As the swell advances, its crest becomes rounded and its surface smooth. As a result of the latter process, swell energy may propagate through a point from more than one direction at a particular time.

The wave climate of the Grand Banks is dominated by extra-tropical storms, primarily during October through March, however severe storms may, on occasion, occur outside these months. Storms of tropical origin may occur during the early summer and early winter, but most often from late August through October. Hurricanes are usually reduced to tropical storm strength or evolve into extra-tropical storms by the time they reach the area, however they are still capable of producing storm force winds and high waves.

During autumn and winter, the dominate direction of the combined significant wave height is from the west. This corresponds with a higher frequency of occurrence of the wind wave during these months, suggesting that during the late fall and winter, the wind wave is the main contributor to the combined significant wave height. During the months of March and April, the wind wave remains predominately westerly, while the swell begins to back to southerly, resulting in the vector mean direction of the combined significant wave heights backing to south-westerly. A mean south-westerly direction for the combined significant wave heights during the summer months is a result of a mainly south-westerly wind wave and a south-westerly swell. As winter approaches again, during the months of September and October, the wind wave will veer to the west and become the more dominant component of the combined significant wave height. This will result in the frequency of occurrence of the combined significant wave heights veering to westerly once again.

Prior to 1962, mean monthly ice statistics were used when calculating the wave heights in the MSC50 data. As a result, if the mean monthly ice coverage for a particular grid point is greater than 50% for a particular month, the whole month (from the 1st to the 31st) gets “iced out”; meaning that no forecast wave data has been generated for that month. This sometimes results in gaps in the wave data. Since 1962, weekly ice data supplied by the Canadian Ice Service was used which allowed the MSC50 hindcast to better represent the changing ice conditions (Swail et al., 2006).

2.4.1 Region 1

The annual wave rose from the MSC50 grid point 14845 is presented in Figure 2.13. The wave rose shows that the majority of wave energy is from a south to southwest direction, and accounts for 32.2% of the waves. Waves were “iced out” for 0.67% of the time at grid point 14845 over the data record.

The annual percentage frequency of significant wave heights is presented in Figure 2.14. These figures show that the majority of significant wave heights lie between 1.0 and 3.0 m. There is a gradual decrease in frequency of wave heights above 3.0 m and only a small percentage of the wave heights exceed 7.0. Monthly wave rose histograms of frequency distributions of wave heights can be found in Appendix 4.

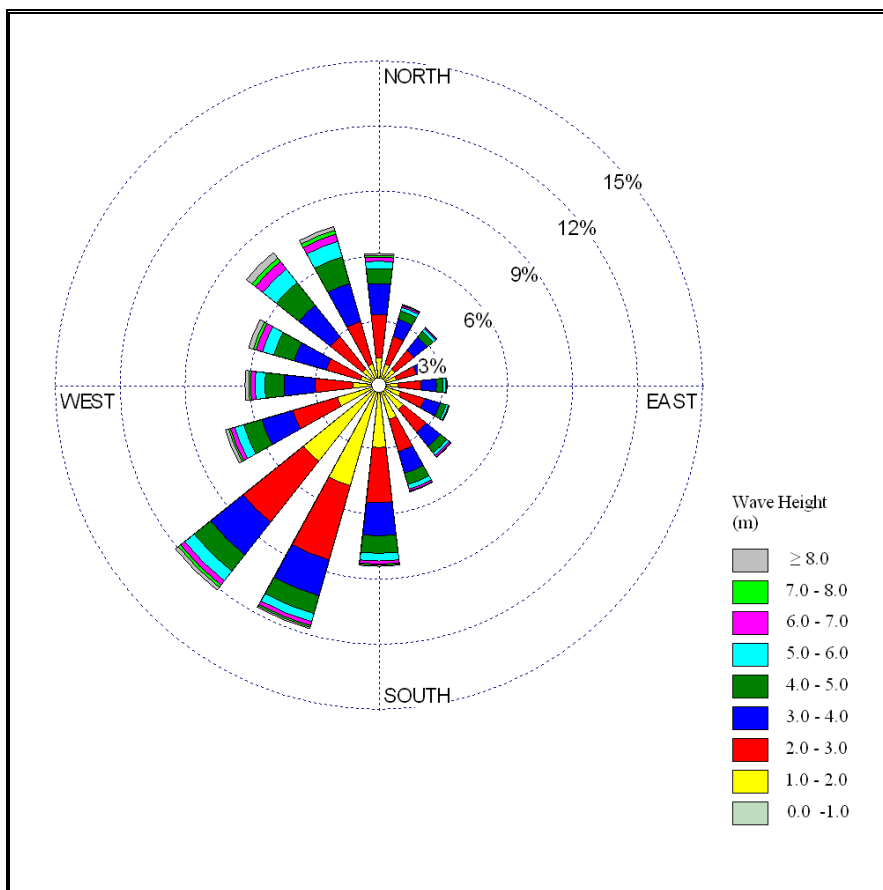


Figure 2.13 Annual Wave Rose for MSC50 Grid Point 14845 located near 48.9°N; 47.8°W. 1954 – 2010

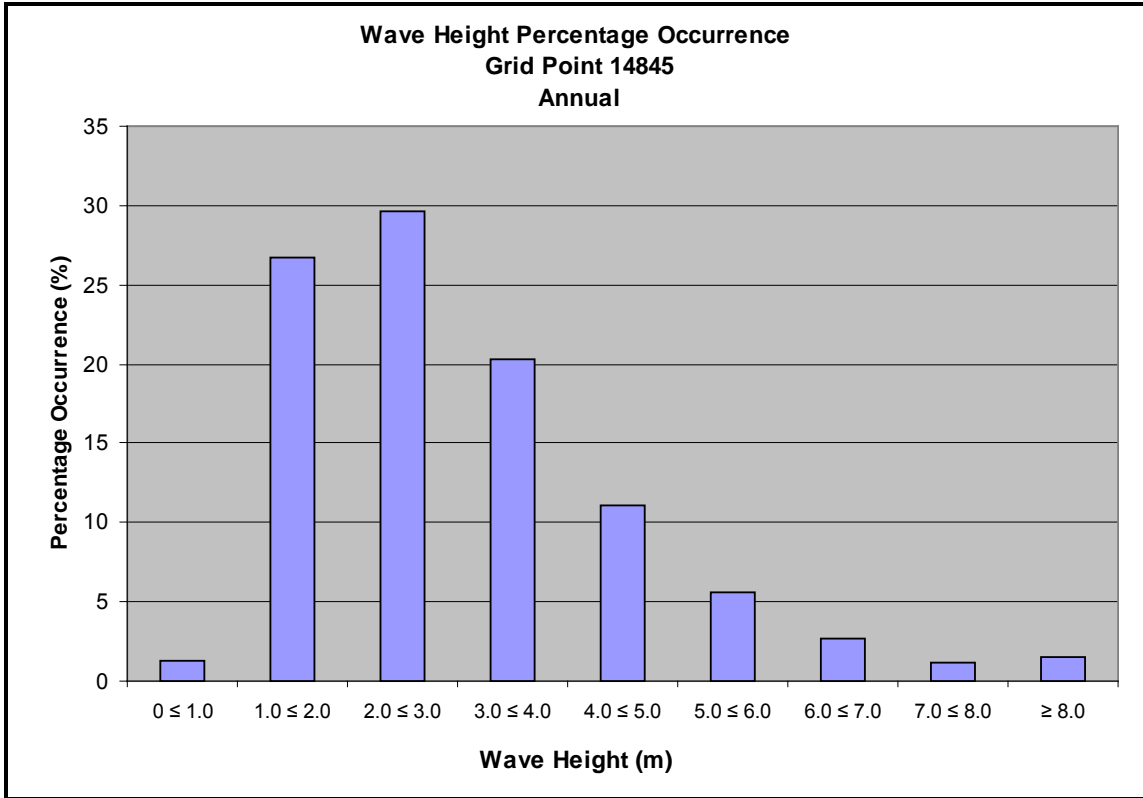


Figure 2.14 Annual Percentage Frequency of Wave Height for MSC50 Grid Point 14845 located near 48.9°N; 47.8°W. 1954 – 2010

Significant wave height statistics from Grid Point 14845 are presented in Table 2.16. Numerous errors were present within the ICOADS dataset and have not been used in the wave analysis.

Significant wave heights on the Grand Banks peak during the winter months with Grid Point 14845 having a mean monthly significant wave height of 4.4 m in January. The lowest significant wave heights occur in the summer with July month having a mean monthly significant wave height of only 1.8 m.

Combined significant wave heights of 10.0 m or higher occurred in each month with the exception of July and August, with the highest waves occurring during the month of December (Table 2.16). While maximum significant wave heights tend to peak during the winter months, a tropical system could pass through the area and produce wave heights during any month.

Table 2.16 Combined Significant Wave Height Statistics (m)

	Mean	Max
January	4.4	14.1
February	4.0	13.8
March	3.3	11.6
April	2.9	11.0
May	2.4	11.6
June	2.0	10.2
July	1.8	6.3
August	1.9	7.4
September	2.6	12.5
October	3.2	12.3
November	3.6	13.0
December	4.2	14.7

Figure 2.15 shows percentage exceedance of significant wave heights for Grid Points 14845. Percentage exceedance curves for the months of January through April show that the curves do not reach 100% because of the presence of ice during these months.

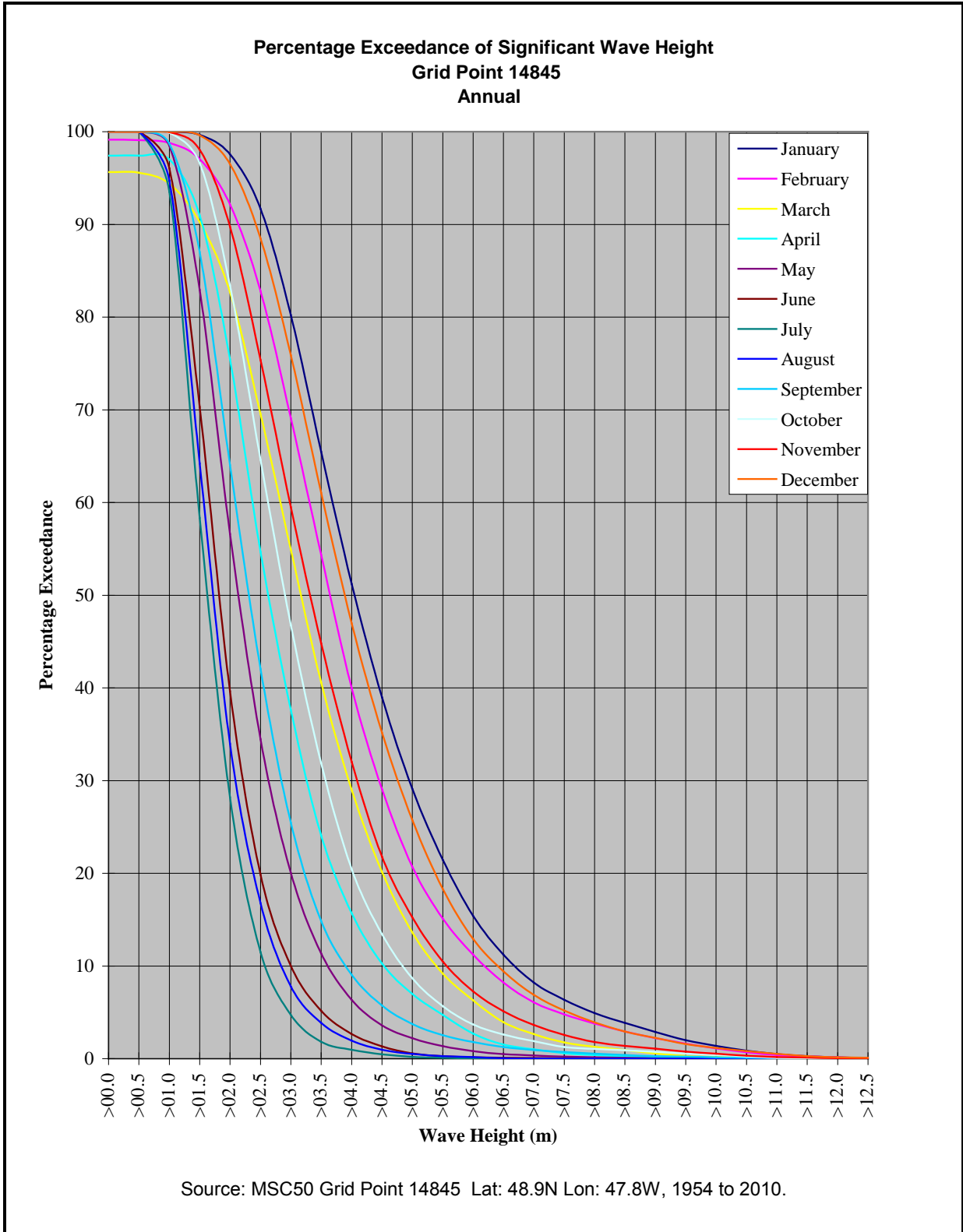


Figure 2.15 Percentage Exceedance of Significant Wave Height at Grid Point 14845 located near 48.9°N; 47.8°W. 1954 – 2010

The spectral peak period of waves vary with season with the most common period varying from 7 seconds during summer to 11 seconds in winter. Annually, the most common peak spectral period is 9 seconds, occurring 19.1% of the time at Grid Point 14845. The percentage occurrence of spectral peak period for each month at both grid points is shown in Table 2.17 with the highest percentage for each month highlighted.

Table 2.17 Percentage Occurrence of Peak Spectral Period of the Total Spectrum at Grid Point 14845 located near 48.9°N; 47.8°W. 1954 – 2010

Peak Spectral Period (seconds)																
Month	1	2	3	4	5	6	7	8	9	10	11	12	13	14	15	16
January	0.0	0.0	0.0	0.0	0.2	1.3	4.9	9.1	16.2	17.7	21.0	12.2	10.7	5.7	0.7	0.2
February	0.0	0.0	0.0	0.2	1.1	3.0	8.6	11.0	16.3	15.7	18.7	11.2	8.1	5.1	0.8	0.3
March	0.0	0.0	0.1	0.8	2.3	5.0	9.7	10.7	16.4	15.2	17.3	10.8	6.4	4.6	0.3	0.4
April	0.0	0.0	0.0	0.1	1.6	4.8	11.2	13.3	22.7	18.5	14.5	6.9	3.9	2.1	0.1	0.1
May	0.0	0.0	0.0	0.2	2.4	7.7	18.6	20.0	24.9	14.2	6.6	4.0	1.2	0.3	0.0	0.0
June	0.0	0.0	0.0	0.3	4.1	10.8	26.3	22.2	20.7	9.7	2.3	1.2	1.9	0.3	0.1	0.1
July	0.0	0.0	0.0	0.4	5.0	15.0	34.2	20.0	14.4	6.2	1.3	0.7	1.8	0.2	0.2	0.3
August	0.0	0.0	0.0	0.5	5.3	14.7	31.2	19.8	15.5	5.8	2.4	2.1	1.9	0.5	0.1	0.2
September	0.0	0.0	0.0	0.1	1.8	6.6	18.4	19.2	21.7	10.2	8.6	7.1	4.1	1.5	0.3	0.3
October	0.0	0.0	0.0	0.0	0.7	3.5	10.8	16.8	23.9	15.3	13.2	7.9	5.1	2.1	0.4	0.3
November	0.0	0.0	0.0	0.0	0.5	2.7	8.4	15.1	20.0	18.0	16.4	9.0	6.8	2.8	0.3	0.2
December	0.0	0.0	0.0	0.0	0.1	1.1	5.1	9.5	16.3	19.9	20.3	12.9	9.1	4.8	0.5	0.3
Winter	0.0	0.0	0.0	0.1	0.5	1.8	6.2	9.9	16.3	17.8	20.0	12.1	9.3	5.2	0.6	0.3
Spring	0.0	0.0	0.0	0.4	2.1	5.8	13.1	14.7	21.4	16.0	12.8	7.2	3.9	2.4	0.2	0.2
Summer	0.0	0.0	0.0	0.4	4.8	13.5	30.6	20.7	16.9	7.3	2.0	1.3	1.9	0.4	0.1	0.2
Autumn	0.0	0.0	0.0	0.1	1.0	4.3	12.5	17.0	21.9	14.5	12.7	8.0	5.3	2.1	0.3	0.3
Annual	0.0	0.0	0.0	0.2	2.1	6.4	15.6	15.6	19.1	13.9	11.9	7.2	5.1	2.5	0.3	0.2

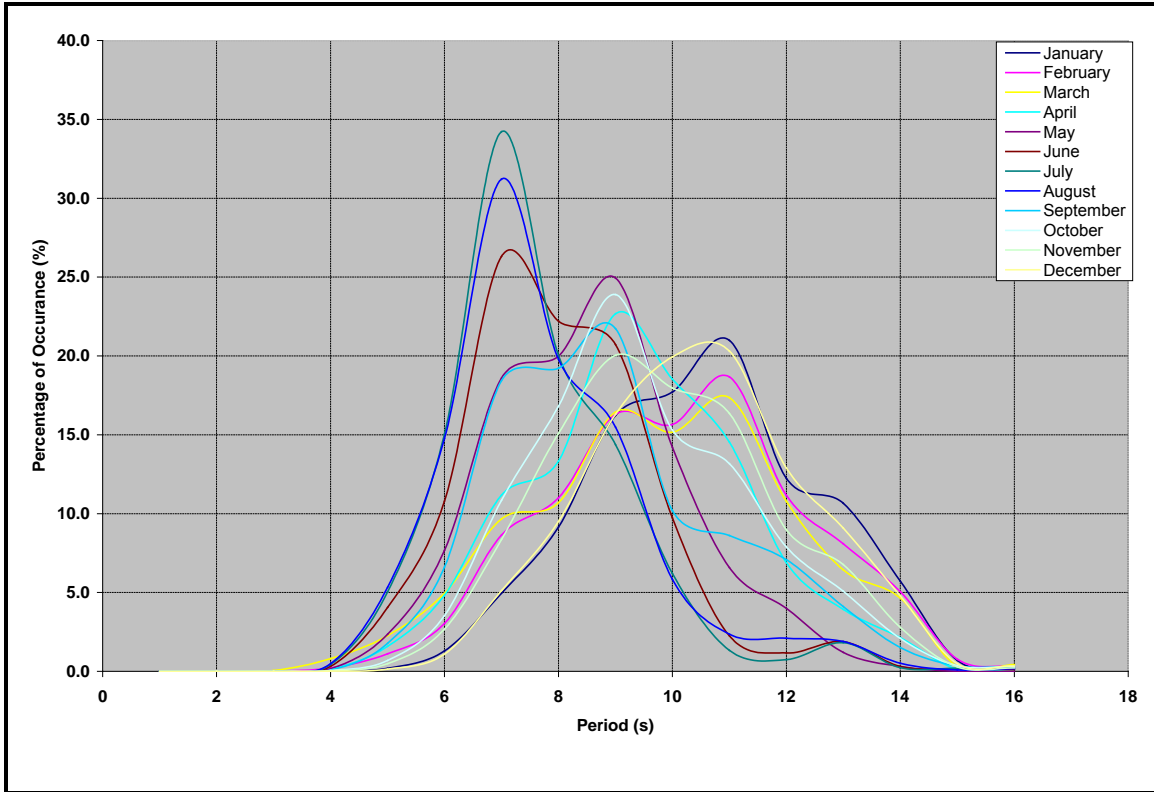


Figure 2.16 Percentage of Occurrence of Peak Wave Period at Spectrum at Grid Point 14845 located near 48.9°N; 47.8°W. 1954 – 2010

A scatter diagram of the significant wave height versus spectral peak period is presented in Table 2.18. From this table it can be seen that the most common wave at grid points 14845 is 2 m with a spectral peak period of 9 seconds. Note that wave heights in these tables have been rounded to the nearest whole number. Therefore, the 1 m wave bin would include all waves from 0.51 m to 1.50 m.

Table 2.18 Percent Frequency of Occurrence of Significant Combined Wave Height and Peak Spectral Period at Grid Point 14845 located near 48.9°N; 47.8°W. 1954 – 2010

		Wave Height (m)														Total
		<1	1	2	3	4	5	6	7	8	9	10	11	12	13	
Period (s)	0	0.65														0.65
	1	0.00														0.00
	2															0.00
	3	0.00	0.01													0.01
	4	0.00	0.19	0.03	0.00											0.23
	5		1.12	0.93	0.03											2.08
	6	0.00	1.56	4.32	0.44	0.02	0.00									6.35
	7		4.18	6.73	4.30	0.38	0.01									15.60
	8		2.77	5.00	4.96	2.58	0.18	0.00								15.50
	9	0.00	1.84	6.96	4.27	4.29	1.49	0.10	0.00							18.96
	10		0.77	3.95	3.23	2.38	2.45	0.88	0.08	0.00	0.00					13.75
	11	0.00	0.19	1.84	3.80	2.13	1.52	1.50	0.65	0.09	0.02	0.00				11.73
	12	0.00	0.14	1.39	1.81	1.25	0.67	0.54	0.58	0.43	0.22	0.04	0.00			7.07
	13		0.25	0.64	1.06	1.09	0.67	0.39	0.23	0.20	0.23	0.19	0.07	0.00		5.03
	14	0.00	0.05	0.14	0.33	0.61	0.51	0.30	0.14	0.07	0.07	0.09	0.10	0.05	0.00	2.47
	15		0.02	0.03	0.03	0.04	0.07	0.05	0.03	0.01	0.00	0.00	0.01	0.01	0.01	0.31
	16		0.04	0.03	0.05	0.05	0.04	0.01	0.00	0.00	0.00		0.00	0.00	0.00	0.23
	17		0.01	0.01	0.01	0.00	0.00									0.04
18			0.00	0.00											0.00	

Note: The incidence of 0 wave height and <1 wave period is due to the presence of sea ice.

2.4.2 Region 2

The annual wave rose from the MSC50 grid point 13912 is presented in Figure 2.17. The wave rose shows that the majority of wave energy comes from the south-southwest to west-southwest, and accounts for 33.5% of the waves. Waves were “iced out” for 0.25% of the time at grid point 13912 over the data record.

The annual percentage frequency of significant wave heights is presented in Figure 2.18. These figures show that the majority of significant wave heights lie between 1.0 and 3.0 m. There is a gradual decrease in frequency of wave heights above 3.0 m and only a small percentage of the wave heights exceed 7.0 m. Monthly wave rose histograms of frequency distributions of wave heights can be found in Appendix 5.

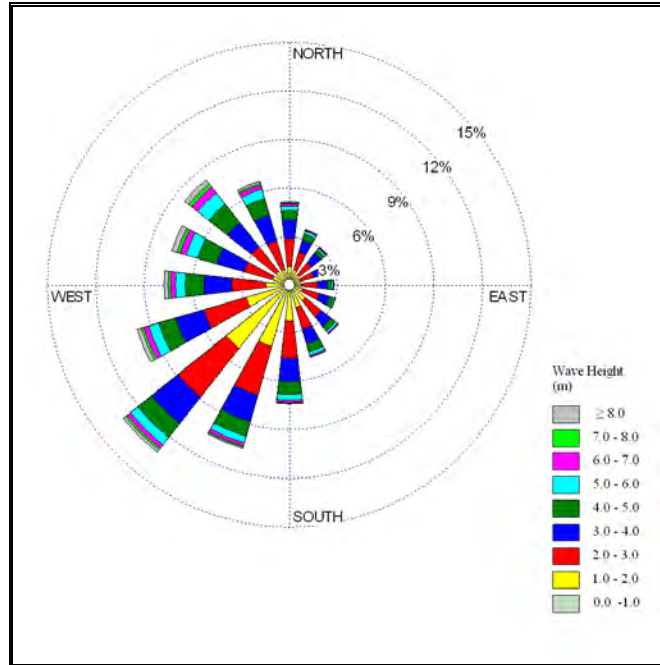


Figure 2.17 Annual Wave Rose for MSC50 Grid Point 13912 located near 48.3°N; 46.3°W. 1954 – 2010

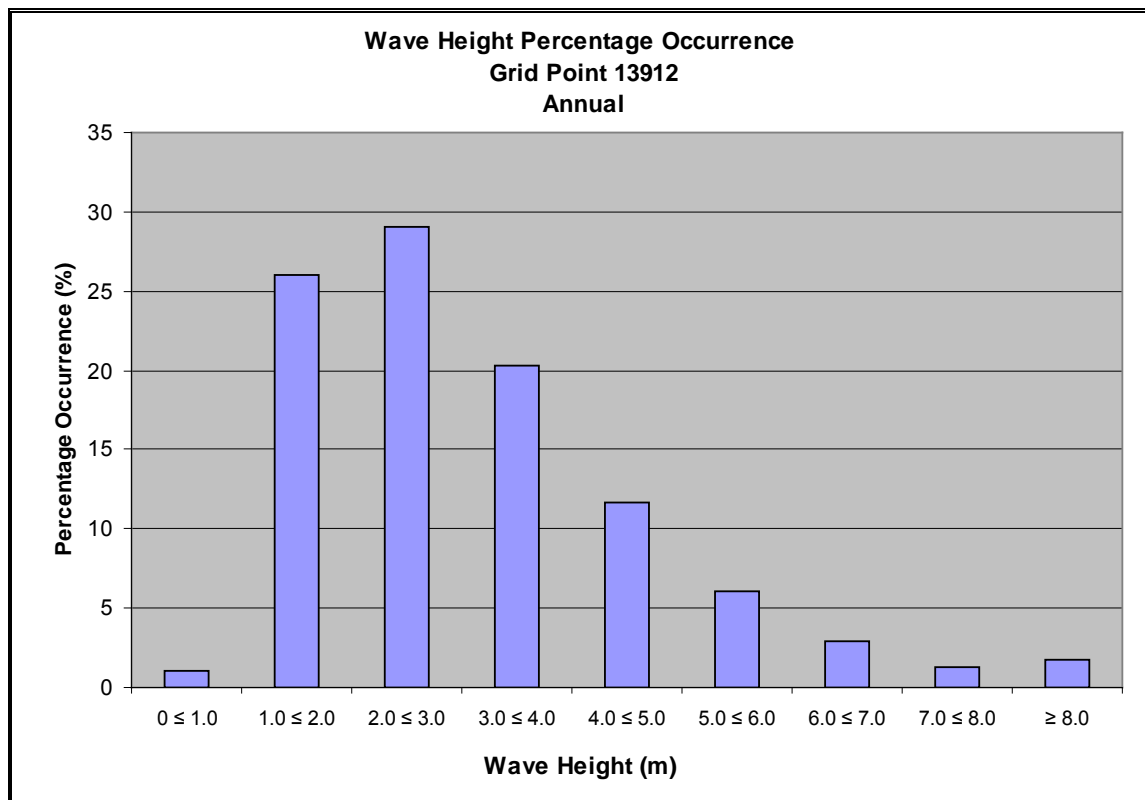


Figure 2.18 Annual Percentage Frequency of Wave Height for MSC50 Grid Point 13912 located near 48.3°N; 46.3°W. 1954 – 2010

Significant wave height statistics from Grid Point 13912 are presented in Table 2.19 below. Numerous errors were present within the ICOADS dataset and have not been used in the wave analysis. A wave rider was present at Mizzen L-11 in support of the Eirik Raude from March 04, 2003 to April 12, 2003. Statistics are presented from this buoy for comparison with the MSC50 data set.

Significant wave heights on the Grand Banks peak during the winter months with Grid Point 13912 having a mean monthly significant wave height of 4.6 m in January. The lowest significant wave heights occur in the summer with July having a mean monthly significant wave height of only 1.8 m.

Table 2.19 Combined Significant Wave Height Statistics (m)

	MSC50 Grid Point 13912	Eirik Raude
January	4.6	
February	4.2	
March	3.6	2.9
April	3.0	2.7
May	2.4	
June	2.0	
July	1.8	
August	1.9	
September	2.6	
October	3.2	
November	3.6	
December	4.3	

Combined significant wave heights of 10.0 m or higher occurred in each month with the exception of July and August, with the highest waves occurring during the month of December (Table 2.20). While maximum significant wave heights tend to peak during the winter months, a tropical system could pass through the area and produce wave heights during any month.

Table 2.20 Maximum Combined Significant Wave Height Statistics (m)

	MSC50 Grid Point 13912	Eirik Raude
January	14.2	
February	15.3	
March	13.1	4.3
April	11.0	3.9
May	11.7	
June	10.5	
July	7.1	
August	8.2	
September	13.3	
October	12.5	
November	13.2	
December	15.3	

Figure 2.19 shows percentage exceedance of significant wave heights for Grid Points 13912. Percentage exceedance curves for the months of January through April show that the curves do not reach 100% because of the presence of ice during these months.

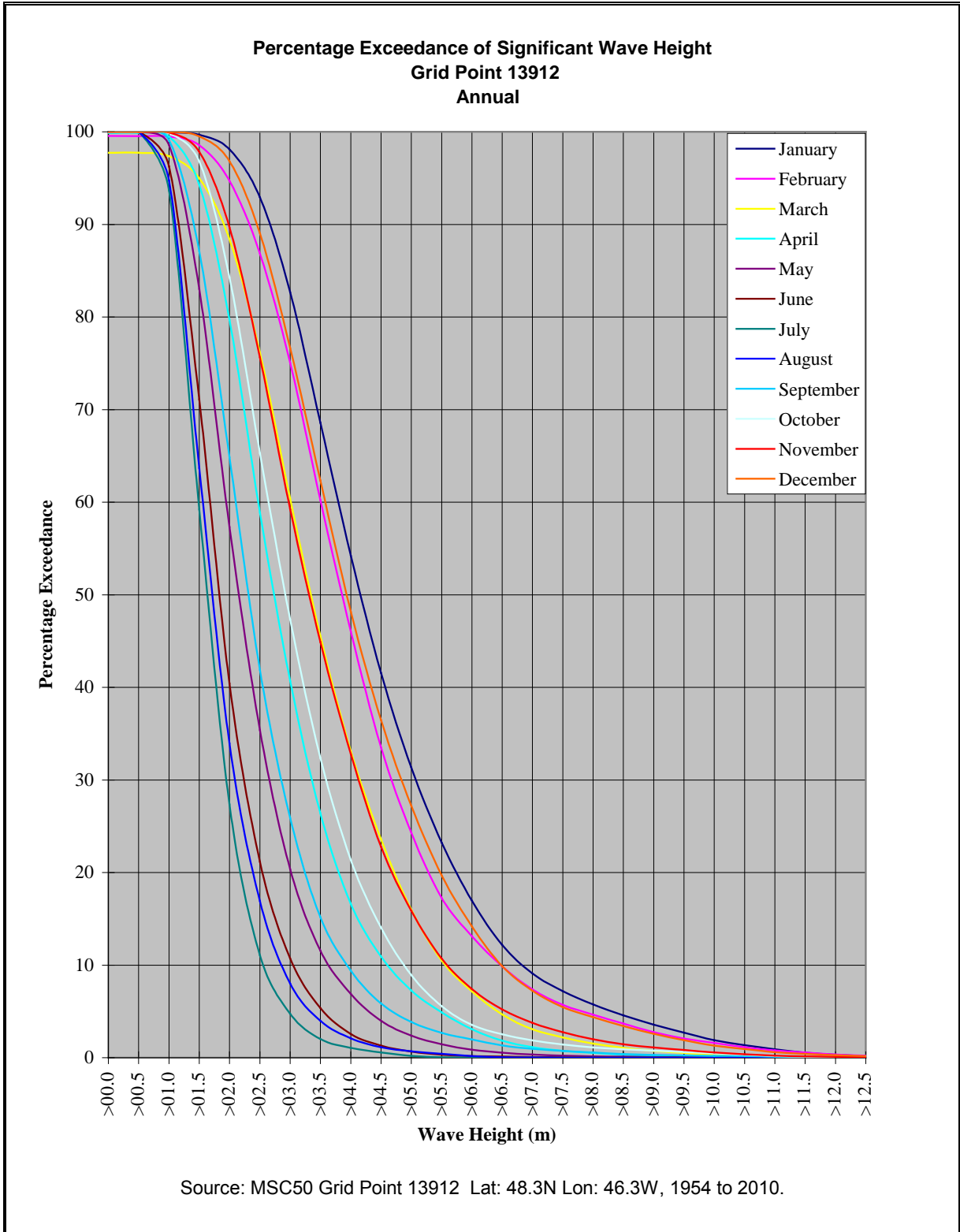


Figure 2.19 Percentage Exceedance of Significant Wave Height at Grid Point 13912 located near 48.3°N; 46.3°W. 1954 – 2010

The spectral peak period of waves vary with season with the most common period varying from 7 seconds during summer to 11 seconds in winter. Annually, the most common peak spectral period is 9 seconds, occurring 18.7% of the time at Grid Point 13912. The percentage occurrence of spectral peak period for each month at both grid points is shown in Table 2.21 with the highest percentage for each month highlighted.

Table 2.21 Percentage Occurrence of Peak Spectral Period of the Total Spectrum at Grid Point 13912 located near 48.3°N; 46.3°W. 1954 – 2010

Peak Spectral Period (seconds)																
Month	1	2	3	4	5	6	7	8	9	10	11	12	13	14	15	16
January	0.0	0.0	0.0	0.0	0.1	0.6	3.6	7.9	14.4	19.6	21.7	13.1	11.7	6.0	0.9	0.3
February	0.0	0.0	0.0	0.1	0.4	1.7	5.5	10.3	15.8	18.3	19.9	12.1	9.3	5.3	0.9	0.3
March	0.0	0.0	0.0	0.1	0.7	2.7	8.2	11.2	16.9	17.7	18.9	11.5	6.7	4.6	0.4	0.4
April	0.0	0.0	0.0	0.1	0.8	3.6	10.4	13.7	22.6	19.5	15.3	7.4	4.0	2.4	0.2	0.1
May	0.0	0.0	0.0	0.1	2.0	6.1	18.5	20.9	24.9	15.2	6.7	3.8	1.4	0.4	0.0	0.0
June	0.0	0.0	0.0	0.3	3.5	9.6	25.8	24.4	21.1	9.3	2.5	1.5	1.6	0.3	0.1	0.1
July	0.0	0.0	0.0	0.3	4.1	14.1	32.5	21.8	15.8	6.5	1.2	0.8	2.1	0.3	0.1	0.3
August	0.0	0.0	0.0	0.3	4.4	12.3	31.8	22.3	15.5	6.0	2.6	2.3	1.7	0.5	0.1	0.1
September	0.0	0.0	0.0	0.1	1.4	5.4	18.3	20.9	20.6	10.6	9.0	6.9	4.2	1.8	0.4	0.3
October	0.0	0.0	0.0	0.0	0.6	3.0	10.3	16.8	22.8	17.5	12.9	8.2	4.8	2.3	0.4	0.2
November	0.0	0.0	0.0	0.0	0.4	2.2	7.8	13.6	19.0	20.3	16.1	9.5	7.1	3.3	0.4	0.2
December	0.0	0.0	0.0	0.0	0.1	0.9	4.6	8.8	14.5	21.4	20.4	13.8	9.6	4.9	0.7	0.3
Winter	0.0	0.0	0.0	0.0	0.2	1.1	4.6	9.0	14.9	19.8	20.7	13.0	10.2	5.4	0.8	0.3
Spring	0.0	0.0	0.0	0.1	1.2	4.1	12.4	15.3	21.4	17.4	13.6	7.6	4.0	2.5	0.2	0.2
Summer	0.0	0.0	0.0	0.3	4.0	12.0	30.0	22.8	17.5	7.3	2.1	1.5	1.8	0.4	0.1	0.1
Autumn	0.0	0.0	0.0	0.0	0.8	3.6	12.1	17.1	20.8	16.2	12.7	8.2	5.4	2.5	0.4	0.2
Annual	0.0	0.0	0.0	0.1	1.5	5.2	14.8	16.1	18.7	15.2	12.3	7.6	5.3	2.7	0.4	0.2

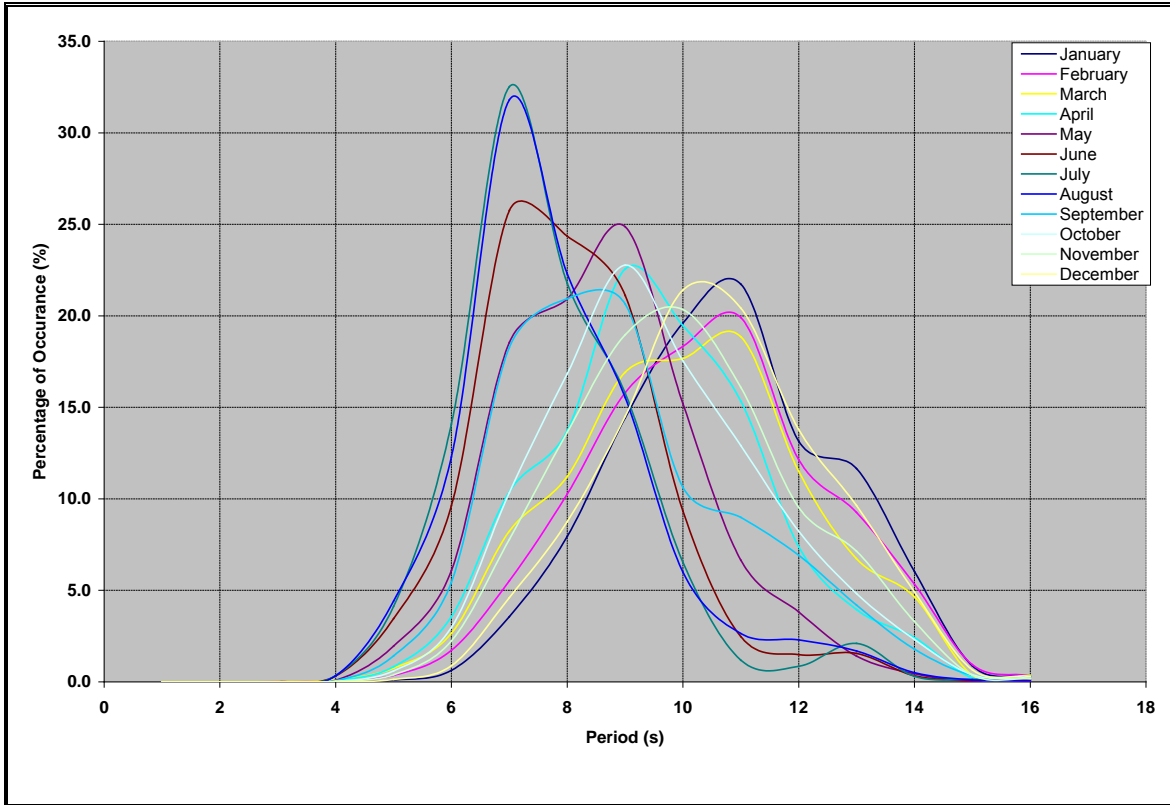


Figure 2.20 Percentage of Occurrence of Peak Wave Period at Spectrum at Grid Point 13912 located near 48.3°N; 46.3°W. 1954 – 2010

A scatter diagram of the significant wave height versus spectral peak period is presented in Table 2.22. From this table it can be seen that the most common wave at grid points 13912 is 2 m with a peak spectral period of 9 seconds. Note that wave heights in these tables have been rounded to the nearest whole number. Therefore, the 1 m wave bin would include all waves from 0.51 m to 1.50 m.

Table 2.22 Percent Frequency of Occurrence of Significant Combined Wave Height and Peak Spectral Period at Grid Point 13912 located near 48.3°N; 46.3°W. 1954 – 2010

		Wave Height (m)														Total
		<1	1	2	3	4	5	6	7	8	9	10	11	12	13	
Period (s)	0	0.24														0.24
	1															0.00
	2															0.00
	3	0.00	0.00													0.00
	4	0.00	0.10	0.02												0.12
	5		0.85	0.67	0.03	0.00										1.55
	6		1.38	3.44	0.36	0.01	0.00									5.20
	7		4.38	6.43	3.68	0.31	0.01									14.81
	8		3.02	5.60	4.94	2.32	0.16	0.00								16.04
	9	0.00	1.65	7.10	4.21	4.14	1.41	0.09	0.00							18.61
	10	0.00	0.65	3.98	4.03	2.80	2.73	0.86	0.06	0.00	0.00					15.10
	11	0.00	0.17	1.86	3.81	2.38	1.71	1.58	0.57	0.09	0.00	0.00				12.18
	12		0.16	1.35	1.79	1.38	0.85	0.66	0.71	0.44	0.18	0.03	0.00			7.54
	13		0.24	0.65	1.01	1.03	0.71	0.47	0.30	0.27	0.31	0.25	0.07	0.01		5.31
	14		0.04	0.12	0.41	0.70	0.52	0.30	0.14	0.07	0.07	0.10	0.13	0.06	0.01	2.67
	15		0.01	0.03	0.03	0.04	0.08	0.06	0.03	0.01	0.00	0.01	0.01	0.03	0.03	0.37
	16		0.03	0.03	0.04	0.05	0.04	0.01	0.01	0.00	0.00	0.00		0.00	0.01	0.20
	17		0.01	0.01	0.01	0.00	0.01	0.00								0.04
18				0.00											0.00	

Note: The incidence of 0 wave height and <1 wave period is due to the presence of sea ice.

2.4.3 Region 3

The annual wave rose from the MSC50 grid point 11423 is presented in Figure 2.21. The wave rose shows that the majority of wave energy comes from the south-southwest to west-southwest, and accounts for 35.8% of the waves. Waves were “iced out” for 2.04% of the time at grid point 11423 over the record.

The annual percentage frequency of significant wave heights is presented in Figure 2.22. These figures show that the majority of significant wave heights lie between 1.0 and 3.0 m. There is a gradual decrease in frequency of wave heights above 3.0 m and only a small percentage of the wave heights exceed 7.0 m. Monthly wave rose histograms of frequency distributions of wave heights can be found in Appendix 6.

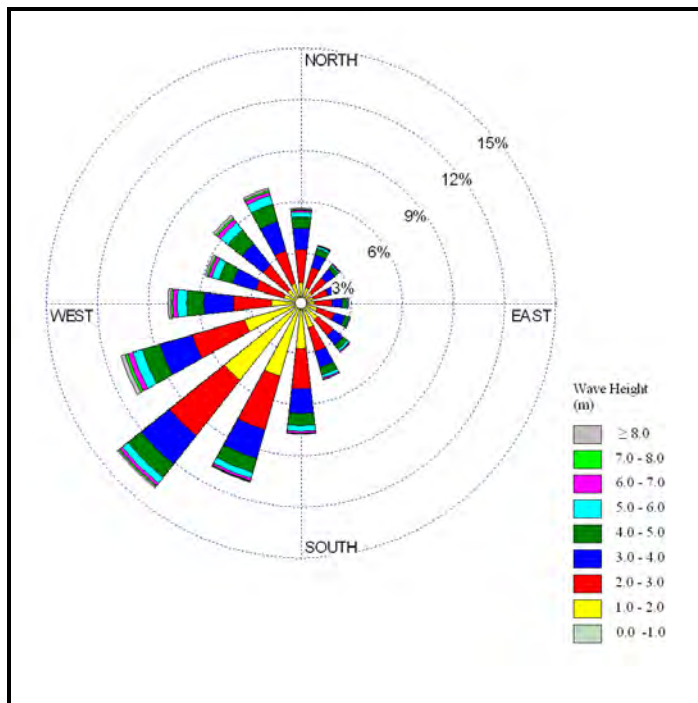


Figure 2.21 Annual Wave Rose for MSC50 Grid Point 11423 located near 46.9°N; 48.1°W. 1954 – 2010

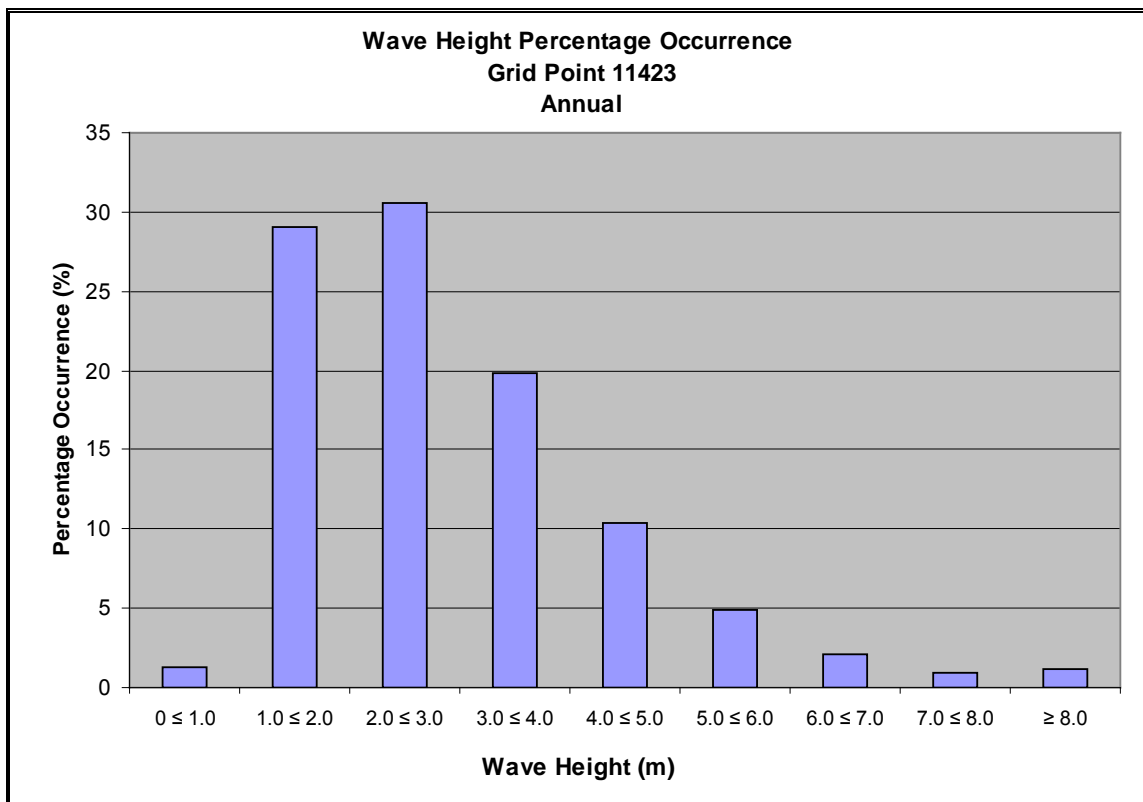


Figure 2.22 Annual Percentage Frequency of Wave Height for MSC50 Grid Point 11423 located near 46.9°N; 48.1°W. 1954 – 2010

Significant wave height statistics from a number of sources on the Grand Banks are presented below. Significant wave heights on the Grand Banks peak during the winter months with the wave heights from all data sources peaking in January. The lowest significant wave heights occur in the summer with July having the lowest mean monthly significant wave height of 1.7 m at grid point 11423 (Table 2.23).

Table 2.23 Combined Significant Wave Height Statistics (m)

	MSC50 Grid Point 11423	Terra Nova FPSO	Ocean Ranger	Hibernia WRIPS	Hibernia MANMAR	White Rose
January	4.1	4.1	5.2	5.8	4.0	4.9
February	3.7	3.8	4.4	5.9	3.7	4.5
March	3.1	3.4	4.7	3.6	3.2	4.3
April	2.6	2.6	3.7	1.8	2.5	2.7
May	2.2	2.2	1.7		2.1	2.6
June	1.9	1.8	1.5		1.9	2.6
July	1.7	1.5	1.8		1.6	2.4
August	1.8	1.8	1.8	1.9	1.8	2.3
September	2.4	2.3	3.8	2.6	2.3	2.8
October	3.0	3.0	3.0	2.6	3.0	3.8
November	3.4	3.1	4.8	3.4	3.0	3.8
December	4.0	3.7	4.6	4.3	3.7	4.2

Combined significant wave heights of 10.0 m or more occurred in each month between September and June in the MSC50 data set, with the highest waves occurring during the month of February (Table 2.24). The highest combined significant wave heights of 14.7 m and 12.0 m in the Terra Nova and Hibernia datasets, respectively, occurred during the February 11, 2003 storm event mentioned previously.

Table 2.24 Maximum Combined Significant Wave Height Statistics (m)

	MSC50 Grid Point 11423	Terra Nova FPSO	Ocean Ranger	Hibernia WRIPS	Hibernia MANMAR	White Rose
January	13.0	12.5	10.6	7.0	11.5	12.2
February	15.0	14.7	8.3	5.9	12.0	11.9
March	11.1	9.7	7.2	8.0	9.4	12.8
April	10.8	8.6	7.8	2.1	7.6	11.0
May	10.4	6.4	3.8		6.6	10.9
June	10.1	6.5	3.0		6.7	9.2
July	6.2	4.1	4.2		5.0	8.5
August	9.1	8.0	3.3	5.1	8.0	9.3
September	12.2	10.5	8.4	5.7	9.5	11.1
October	12.2	10.6	5.8	5.2	11.0	12.2
November	11.6	10.2	7.0	9.2	9.7	11.2
December	13.8	11.7	8.1	7.7	10.0	11.1

While maximum significant wave heights tend to peak during the winter months, a tropical system could pass through the area and produce high wave heights during any month.

Figure 2.23 shows percentage exceedance of significant wave heights for Grid Points 11423. Percentage exceedance curves for the months of January through April show that the curves do not reach 100% because of the presence of ice during these months.

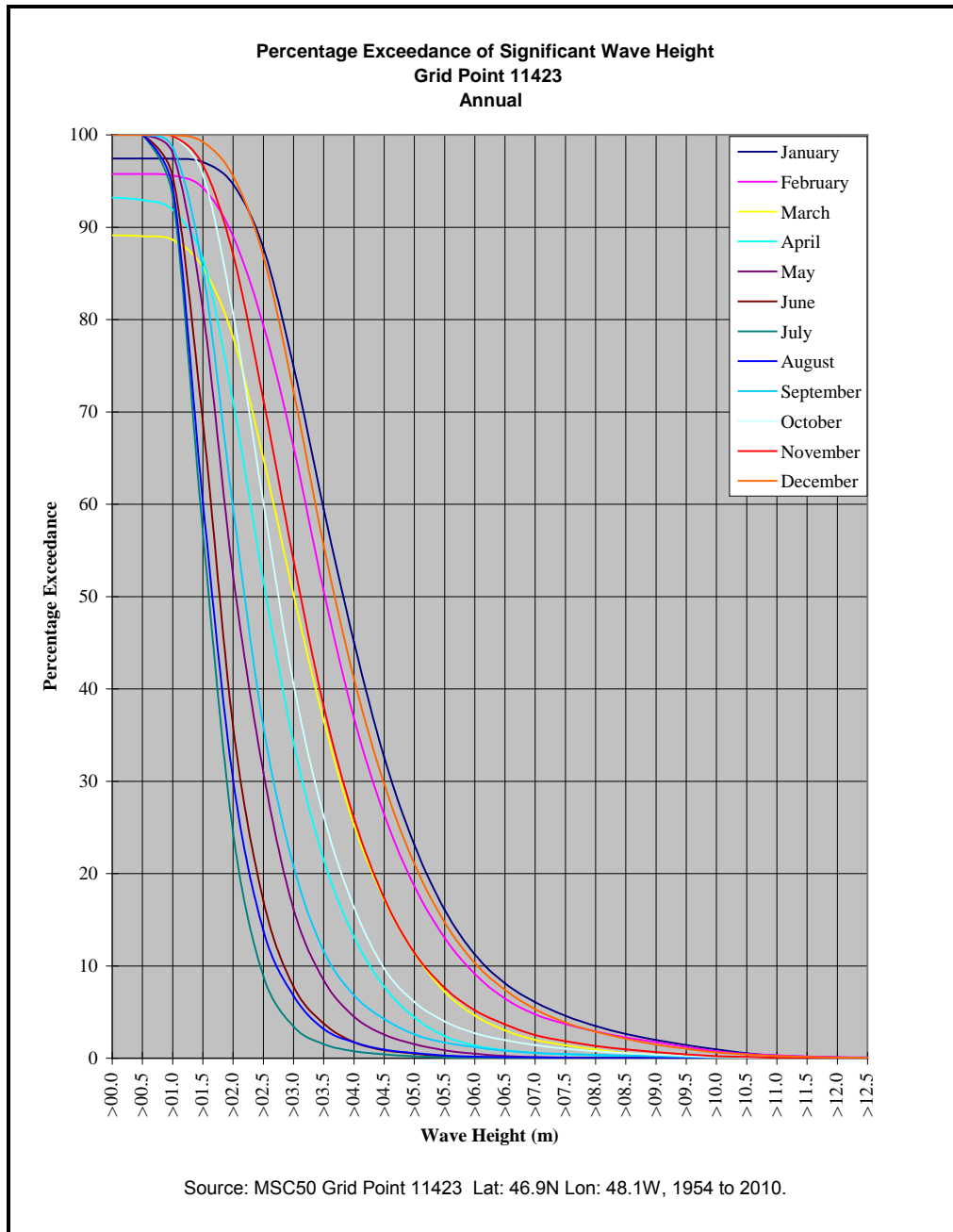


Figure 2.23 Percentage Exceedance of Significant Wave Height at Grid Point 11423 located near 46.9°N; 48.1°W. 1954 – 2010

The spectral peak period of waves vary with season with the most common period varying from 7 seconds during summer to 11 seconds in winter. Annually, the most common peak spectral period is 9 seconds, occurring 18.3% of the time at Grid Point 13912. The percentage occurrence of spectral peak period for each month is shown in Table 2.1 with the highest percentage for each month highlighted.

Table 2.25 Percentage Occurrence of Peak Spectral Period of the Total Spectrum at Grid Point 11423 located near 46.9°N; 48.1°W. 1954 – 2010

Peak Spectral Period (seconds)																
Month	1	2	3	4	5	6	7	8	9	10	11	12	13	14	15	16
January	0.0	0.0	0.0	0.0	0.2	1.1	4.6	8.8	14.6	18.6	22.0	12.7	11.6	5.1	0.6	0.1
February	0.0	0.0	0.0	0.1	0.6	2.3	6.8	10.1	15.8	18.2	19.6	12.8	8.6	4.2	0.8	0.3
March	0.0	0.0	0.0	0.2	1.2	3.1	8.3	11.4	17.4	18.8	17.8	11.7	6.0	3.8	0.2	0.3
April	0.0	0.0	0.0	0.2	1.1	4.0	9.1	14.9	23.5	20.5	14.1	7.5	3.2	1.6	0.2	0.1
May	0.0	0.0	0.0	0.1	1.5	7.2	15.6	25.2	23.2	14.9	6.2	4.4	1.4	0.4	0.0	0.0
June	0.0	0.0	0.0	0.3	3.6	10.5	24.3	27.4	19.7	8.8	2.2	1.4	1.5	0.2	0.0	0.0
July	0.0	0.0	0.0	0.3	4.2	14.5	29.2	27.8	13.8	5.7	1.4	0.7	1.8	0.2	0.1	0.2
August	0.0	0.0	0.0	0.4	4.8	12.9	28.8	26.2	14.4	5.6	2.7	2.1	1.6	0.4	0.1	0.1
September	0.0	0.0	0.0	0.1	1.8	6.3	17.1	21.5	20.4	10.5	8.4	7.3	4.5	1.3	0.4	0.3
October	0.0	0.0	0.0	0.0	0.8	3.5	10.7	17.7	22.2	16.4	12.1	9.0	5.3	1.9	0.3	0.2
November	0.0	0.0	0.0	0.1	0.5	2.6	8.1	12.6	19.5	20.5	15.9	9.7	7.5	2.7	0.3	0.2
December	0.0	0.0	0.0	0.0	0.2	1.2	4.6	9.1	15.4	21.1	20.7	12.9	10.0	3.9	0.5	0.2
Winter	0.0	0.0	0.0	0.0	0.3	1.6	5.3	9.3	15.3	19.3	20.8	12.8	10.0	4.4	0.6	0.2
Spring	0.0	0.0	0.0	0.2	1.3	4.7	11.0	17.2	21.3	18.0	12.7	7.9	3.5	1.9	0.1	0.1
Summer	0.0	0.0	0.0	0.3	4.2	12.6	27.4	27.1	16.0	6.7	2.1	1.4	1.6	0.3	0.1	0.1
Autumn	0.0	0.0	0.0	0.1	1.0	4.2	12.0	17.3	20.7	15.8	12.2	8.7	5.8	2.0	0.3	0.2
Annual	0.0	0.0	0.0	0.2	1.7	5.8	13.9	17.7	18.3	15.0	11.9	7.7	5.2	2.1	0.3	0.2

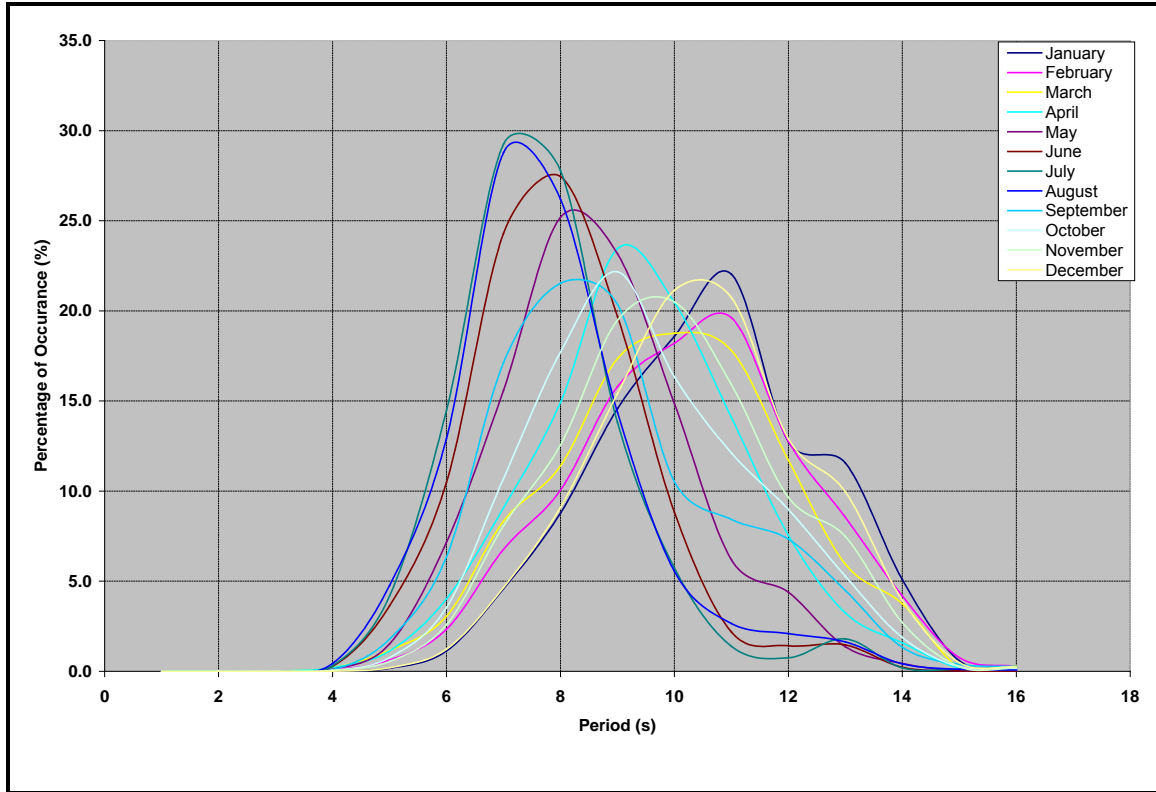


Figure 2.24 Percentage of Occurrence of Peak Wave Period at Spectrum at Grid Point 11423 located near 46.9°N; 48.1°W. 1954 – 2010

A scatter diagram of the significant wave height versus spectral peak period is presented in Table 2.26. From this table it can be seen that the most common wave at grid points 11423 is 2 m with a peak spectral period of 9 seconds. Note that wave heights in these tables have been rounded to the nearest whole number. Therefore, the 1 m wave bin would include all waves from 0.51 m to 1.50 m.

Table 2.26 Percent Frequency of Occurrence of Significant Combined Wave Height and Peak Spectral Period at Grid Point 11423 located near 46.9°N; 48.1°W. 1954 – 2010

		Wave Height (m)															Total
		<1	1	2	3	4	5	6	7	8	9	10	11	12	13		
Period (s)	0	2.02															2.02
	1	0.00															0.00
	2	0.00															0.00
	3	0.00	0.00														0.00
	4	0.00	0.12	0.03													0.15
	5	0.00	0.94	0.72	0.03	0.00											1.70
	6	0.00	1.55	3.78	0.38	0.02											5.73
	7	0.00	4.18	5.88	3.46	0.28	0.01										13.81
	8	0.01	4.39	6.44	4.51	2.02	0.15	0.00									17.52
	9	0.01	1.53	7.80	3.93	3.45	1.11	0.07	0.00	0.00							17.91
	10	0.00	0.62	4.42	4.19	2.47	2.19	0.60	0.05	0.00							14.54
	11	0.00	0.18	1.95	4.08	2.27	1.38	1.17	0.43	0.07	0.00						11.53
	12	0.00	0.21	1.41	2.13	1.46	0.72	0.53	0.48	0.33	0.15	0.03	0.00				7.44
	13	0.00	0.23	0.69	1.13	1.22	0.70	0.34	0.20	0.19	0.20	0.16	0.03	0.00			5.09
	14	0.00	0.04	0.13	0.38	0.58	0.42	0.18	0.08	0.05	0.04	0.07	0.06	0.03	0.00		2.07
	15		0.01	0.02	0.04	0.06	0.07	0.03	0.01	0.01	0.00	0.00	0.01	0.00	0.01		0.28
	16		0.02	0.02	0.03	0.04	0.02	0.01	0.00	0.00	0.00			0.00	0.00		0.15
	17		0.01	0.02	0.01	0.00	0.00	0.00	0.00								0.04
	18		0.00		0.00		0.00	0.00									0.00

Note: The incidence of 0 wave height and <1 wave period is due to the presence of sea ice.

2.5 Weather Variables

2.5.1 Temperature

The moderating influence of the ocean serves to limit both the diurnal and the annual temperature variation on the Grand Banks. Diurnal temperature variations due to the day/night cycles are very small. Short-term, random temperature changes are due mainly to a change of air mass following a warm or cold frontal passage. In general, air mass temperature contrasts across frontal zones are greater during the winter than during the summer season.

Air and sea surface temperatures for the each region were extracted from the ICOADS data set.

Region 1

A plot of monthly mean air temperature and sea surface temperature for Region 1 is presented in Figure 2.25. Temperature statistics are presented in Table 2.27 and show that the atmosphere is coldest in March with a mean monthly air temperature of 4.5°C, and warmest in August with a mean monthly air temperature of 10.8°C. Similarly, sea surface temperature (Table 2.28) is warmest in August with a mean monthly temperature of 11.3°C and coldest in March with a mean monthly temperature of 3.7°C. The mean sea surface temperature is cooler than the mean air temperature from October to June,

with the greatest difference occurring in the month of January. From July to September, sea surface temperatures are warmer than the mean air temperature.

Monthly mean daily maximum and minimum temperature statistics are also presented for the ICOADS data set. Mean temperatures for each month are the mean of all temperatures recorded at the site during that month. The maximum and minimum temperatures are the highest and lowest temperatures respectively, recorded during the month over the entire data set. The mean daily maximum is the average of all daily maximum temperatures recorded during the specified month, and the mean daily minimum is the average of all minimum temperatures recorded during the specified month.

Table 2.27 ICOADS Region 1 Air Temperature Statistics

	Mean	Maximum	Minimum	Standard Deviation	Mean Daily Maximum	Mean Daily Minimum
January	5.0	9.5	-12.0	7.6	0.8	-1.1
February	4.6	11.5	-13.0	6.8	0.6	-1.2
March	4.5	13.0	-9.6	5.6	1.7	0.0
April	4.7	11.0	-5.3	5.0	3.0	1.6
May	5.0	13.0	-4.6	3.6	5.0	3.5
June	6.6	17.0	0.2	2.8	7.3	6.0
July	8.6	19.0	0.0	3.4	10.6	9.7
August	10.8	20.0	5.5	3.9	13.5	12.4
September	10.0	22.1	-0.2	3.8	12.2	10.9
October	8.8	18.5	-1.0	3.4	8.7	7.4
November	7.0	16.0	-6.1	4.8	5.3	3.8
December	6.1	15.0	-10.2	5.5	3.1	1.7

Table 2.28 ICOADS Region 1 Sea Surface Temperature Statistics

	Mean	Maximum	Minimum	Standard Deviation	Mean Daily Maximum	Mean Daily Minimum
January	4.1	10.0	-2.0	6.5	2.9	1.7
February	3.8	12.0	-2.0	5.8	2.3	1.2
March	3.7	10.0	-2.0	4.5	2.2	1.0
April	3.9	12.0	-2.0	4.3	2.6	1.5
May	4.4	11.0	-2.0	3.1	3.9	2.7
June	6.5	16.1	-0.5	2.5	6.2	5.1
July	8.9	17.4	0.4	2.9	9.4	8.7
August	11.3	18.0	5.0	3.4	12.4	11.4
September	10.4	19.0	3.0	3.4	11.7	10.7
October	8.7	15.2	0.0	2.9	8.7	7.6
November	6.8	16.0	-1.2	4.3	6.1	4.9
December	5.6	12.0	-2.0	4.5	4.4	3.4

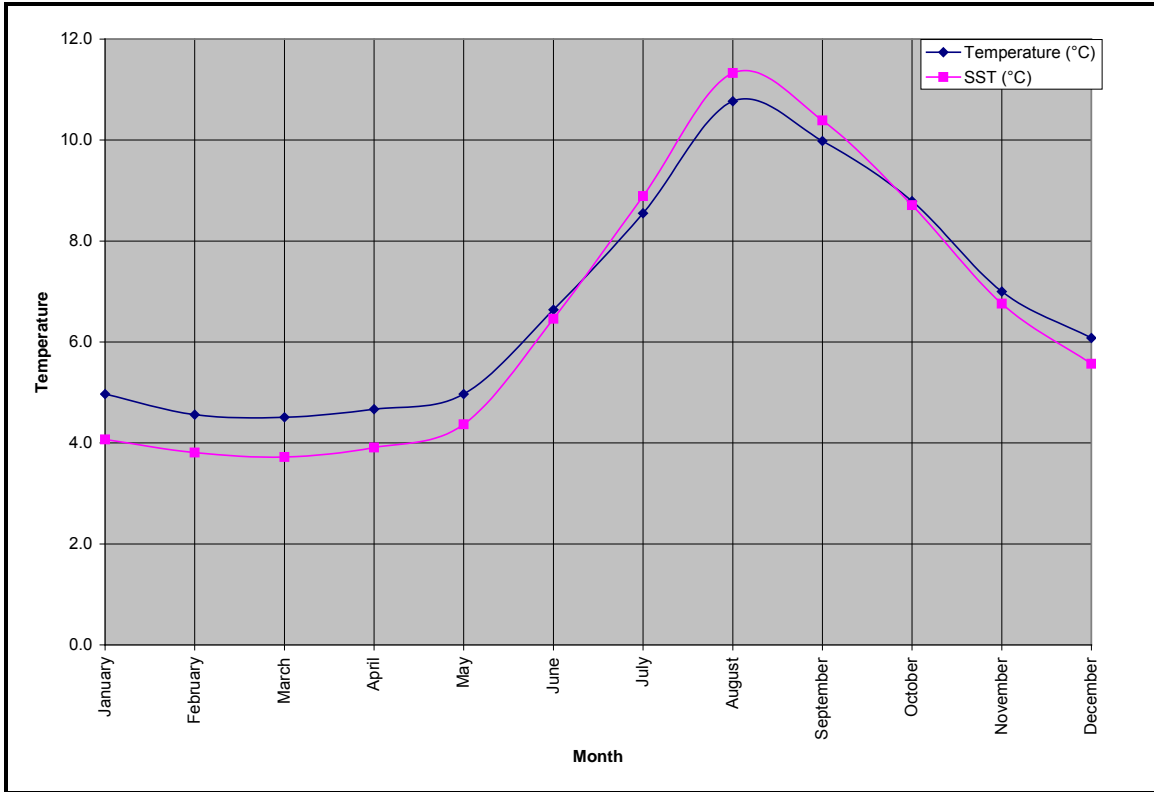


Figure 2.25 Monthly Mean Air and Sea Surface Temperature for ICOADS Region 1

(Source: ICOADS Data set (1980-2010))

Region 2

A plot of monthly mean air temperature and sea surface temperature for Region 2 is presented in Figure 2.26. Temperature statistics presented in Table 2.29 and show that the atmosphere is coldest in February with a mean monthly air temperature of 3.1°C, and warmest in August with a mean monthly air temperature of 11.5°C. Similarly sea surface temperature is warmest in August with a mean monthly temperature of 11.8°C and coldest in February with mean monthly temperatures of 3.1°C (Table 2.30). The mean sea surface temperature is cooler than the mean air temperature from October to June, with the greatest difference occurring in the month of May. From July to September, sea surface temperatures are warmer than the mean air temperature.

Monthly mean daily maximum and minimum temperature statistics are also presented for the ICOADS data set. Mean temperatures for each month are the mean of all temperatures recorded at the site during that month. The maximum and minimum temperatures are the highest and lowest temperatures, respectively, recorded during the month over the entire data set. The mean daily maximum is the average of all daily maximum temperatures recorded during the specified month, while the mean daily minimum is the average of all minimum temperatures recorded during the specified month.

Table 2.29 ICOADS Region 2 Air Temperature Statistics

	Mean	Maximum	Minimum	Standard Deviation	Mean Daily Maximum	Mean Daily Minimum
January	3.9	10.5	-12.0	8.2	1.7	0.2
February	3.1	10.2	-12.0	7.4	1.2	-0.8
March	3.7	11.5	-9.0	7.5	2.8	0.8
April	3.8	14.0	-6.0	6.8	4.6	2.3
May	5.2	16.3	-6.8	7.8	6.1	4.1
June	6.7	16.5	-0.1	3.9	8.0	6.5
July	9.3	21.0	0.0	2.9	10.8	9.7
August	11.5	19.0	6.0	3.2	13.5	12.6
September	11.3	23.0	6.5	3.2	12.5	11.6
October	9.4	16.0	1.0	2.8	9.4	8.5
November	7.4	14.0	-2.0	8.9	6.3	5.5
December	5.8	12.5	-7.0	12.1	4.0	2.9

Table 2.30 ICOADS Region 2 Sea Surface Temperature Statistics

	Mean	Maximum	Minimum	Standard Deviation	Mean Daily Maximum	Mean Daily Minimum
January	4.0	11.7	-2.0	5.6	4.0	3.1
February	2.9	14.4	-2.0	5.8	3.2	2.1
March	3.3	13.0	-2.0	5.4	3.2	2.1
April	3.3	13.0	-2.0	5.2	3.7	2.3
May	4.7	13.6	-1.2	5.6	5.2	3.8
June	6.6	14.0	0.6	3.0	6.9	5.6
July	9.2	16.6	0.0	2.6	9.5	8.4
August	11.8	18.3	5.0	2.7	12.5	11.7
September	11.6	19.0	5.2	2.7	12.2	11.2
October	9.9	18.0	-1.0	2.5	9.8	8.9
November	7.2	14.0	0.0	6.0	7.3	6.3
December	5.6	12.0	0.0	8.0	5.6	4.7

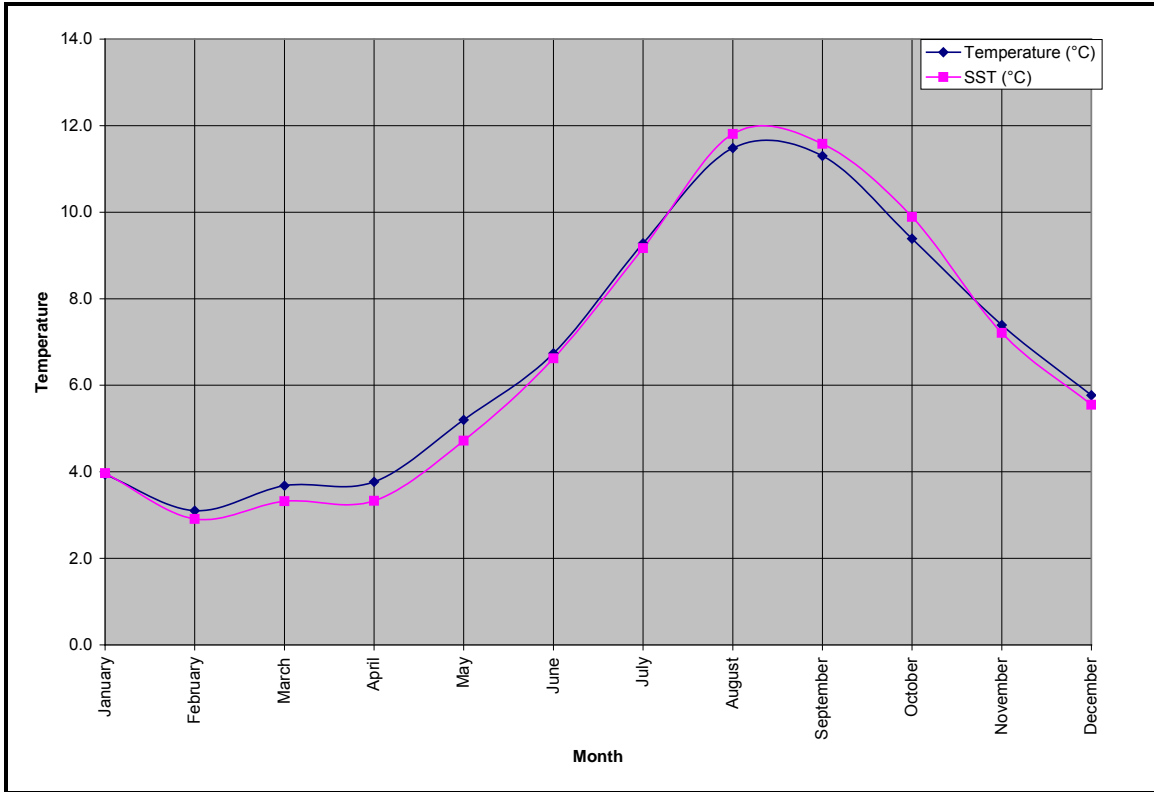


Figure 2.26 Monthly Mean Air and Sea Surface Temperature for ICOADS Region 2

(Source: ICOADS Data set (1980-2010))

Region 3

A plot of monthly mean air temperature and sea surface temperature for Region 3 is presented in Figure 2.26. Temperature statistics presented in Table 2.31 show that the atmosphere is coldest in February with a mean monthly air temperature of -0.3°C , and warmest in August with a mean monthly air temperature of 14.2°C . Similarly sea surface temperature is warmest in August with a mean monthly temperature of 13.6°C and coldest in February with mean monthly temperatures of 0.8°C . The mean sea surface temperature is cooler than the mean air temperature from October to June, with the greatest difference occurring in the month of January. From July to September, sea surface temperatures are warmer than the mean air temperature.

Monthly mean daily maximum and minimum temperature statistics are also presented for the ICOADS data set. Mean temperatures for each month are the mean of all temperatures recorded at the site during that month. The maximum and minimum temperatures are the highest and lowest temperatures respectively, recorded during the month over the entire data set. The mean daily maximum is the average of all daily maximum temperatures recorded during the specified month, while the mean daily minimum is the average of all minimum temperatures recorded during the specified month.

Table 2.31 ICOADS Region 3 Air Temperature Statistics

	Mean	Maximum	Minimum	Standard Deviation	Mean Daily Maximum	Mean Daily Minimum
January	0.2	12.0	-13.8	3.2	3.3	3.3
February	-0.3	10.5	-13.1	3.2	2.8	2.8
March	0.7	12.8	-17.3	3.0	3.8	3.8
April	2.3	13.0	-7.0	2.5	5.1	5.1
May	4.3	14.2	-4.0	2.4	6.8	6.8
June	7.1	21.0	-1.2	2.5	9.7	9.7
July	11.8	23.4	0.0	2.6	14.0	14.0
August	14.2	23.5	4.2	2.3	16.4	16.4
September	12.6	21.0	4.2	2.5	14.9	14.9
October	8.9	18.0	-1.0	3.0	11.3	11.3
November	5.2	16.0	-4.6	3.1	7.9	7.9
December	2.2	12.8	-13.5	3.3	4.8	4.8

Table 2.32 ICOADS Region 3 Sea Surface Temperature Statistics

	Mean	Maximum	Minimum	Standard Deviation	Mean Daily Maximum	Mean Daily Minimum
January	1.3	10.5	-2.0	1.7	3.5	0.2
February	0.8	10.0	-2.0	1.6	3.0	-0.3
March	0.9	11.8	-2.0	1.8	3.4	-0.2
April	1.3	11.0	-2.0	1.6	3.4	0.3
May	3.2	12.0	-2.0	1.8	4.9	1.8
June	6.0	16.0	-0.5	1.9	7.5	4.4
July	10.4	20.0	0.0	2.5	11.5	8.2
August	13.6	21.8	5.0	2.1	14.8	11.8
September	12.7	20.0	1.1	2.1	14.0	10.7
October	9.3	18.3	0.0	2.6	11.0	7.3
November	5.7	15.0	-1.9	2.5	8.0	4.1
December	2.9	13.0	-2.0	2.1	5.0	1.7

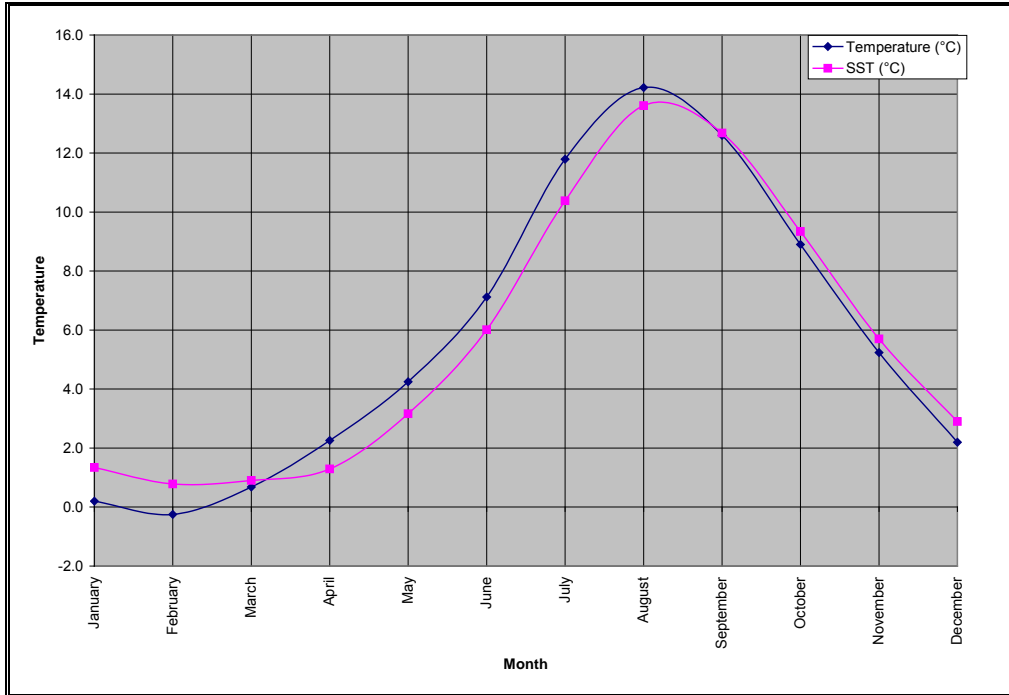


Figure 2.27 Monthly Mean Air and Sea Surface Temperature for ICOADS Region 3

(Source: ICOADS Data set (1980-2010))

2.5.2 Visibility

Visibility is defined as the greatest distance at which objects of suitable dimensions can be seen and identified. Horizontal visibility may be reduced by any of the following phenomena, either alone or in combination:

- Fog
- Mist
- Haze
- Smoke
- Liquid Precipitation (e.g., drizzle)
- Freezing Precipitation (e.g., freezing rain)
- Frozen Precipitation (e.g., snow)
- Blowing Snow

During the winter months, the main obstruction is snow; however, mist and fog may also reduce visibilities at times. As spring approaches, the amount of visibility reduction attributed to snow decreases. As the air temperature increases, so does the occurrence of advection fog. Advection fog forms when warm moist air moves over cooler waters. By April, the sea surface temperature south of Newfoundland is cooler than the surrounding air. As warm moist air from the south moves over the colder sea surface, the air cools and its ability to hold moisture decreases. The air will continue to cool until it becomes saturated and the moisture condenses to form fog. The presence of advection fog increases from April through July. The month of July has the highest percentage of obscuration to visibility, most of which is in the form of advection fog, although frontal fog can also contribute to the

reduction in visibility. In August the temperature difference between the air and the sea begins to narrow and by September, the air temperature begins to fall below the sea surface temperature. As the air temperature drops, the occurrence of fog decreases. Reduction in visibility during autumn and winter is relatively low and is mainly attributed to the passage of low-pressure systems. Fog is the main cause of the reduced visibilities in autumn and snow is the main cause of reduced visibilities in the winter. September and October have the lowest occurrence of reduced visibility since the air temperature has, on average, decreased below the sea surface temperature and it is not yet cold enough for snow.

Fog also occurs in the Jean d'Arc Basin as relatively warm rain falls through cooler air beneath a frontal surface. Typically, the base of the cloud layer lowers as the air becomes saturated and condensation occurs. If the cloud base reaches the surface, frontal fog occurs. Most frequently, frontal fog occurs ahead of a warm front associated with a frontal disturbance. As the front moves through, clearing of the fog may occur but frequently, frontal fog gives way to advection fog in the warm sector of a low pressure system. Typically, fog clears as drier air is advected into the region from continental source regions to the west.

Region 1

A plot of the frequency distribution of visibility for Region 1 from the ICOADS data set is presented in Figure 2.28. This figure shows that obstructions to vision can occur in any month. Annually, 39.0% of the observations had reduced visibilities.

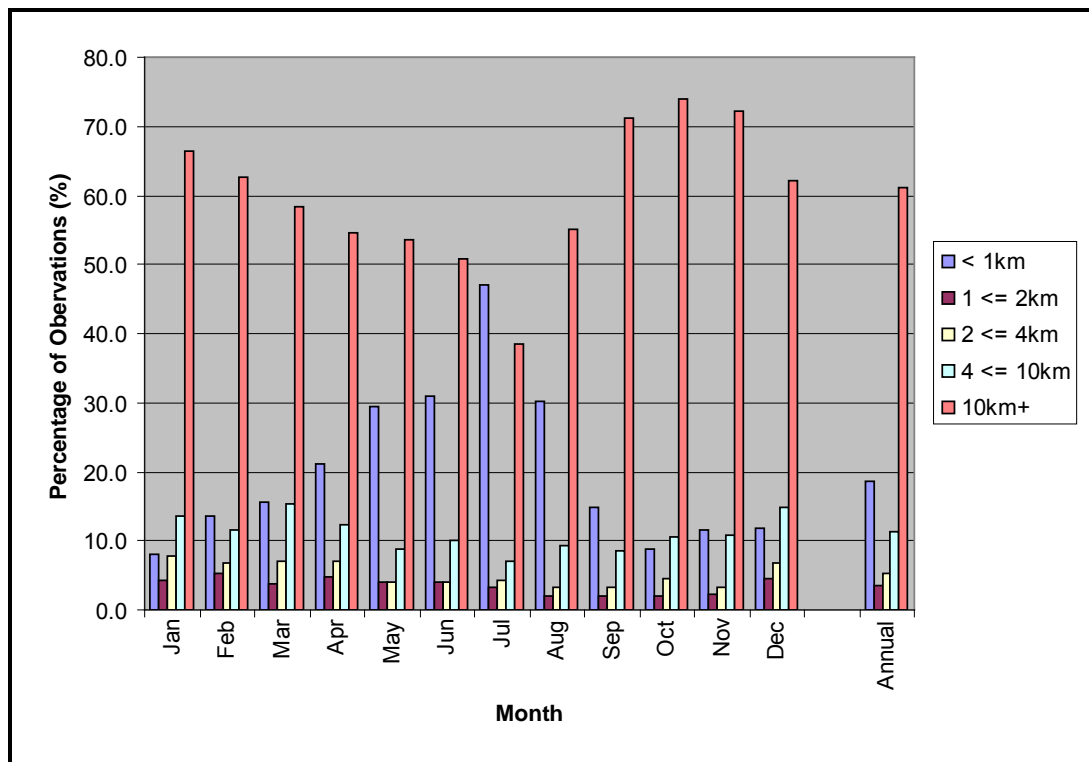


Figure 2.28 Monthly and Annual Percentage Occurrence of Visibility in Region 1

(Source: ICOADS Data set (1980-2010))

Region 2

A plot of the frequency distribution of visibility for Region 2 from the ICOADS data set is presented in Figure 2.29. This figure shows that obstructions to vision can occur in any month. Annually, 38.9% of the observations had reduced visibilities.

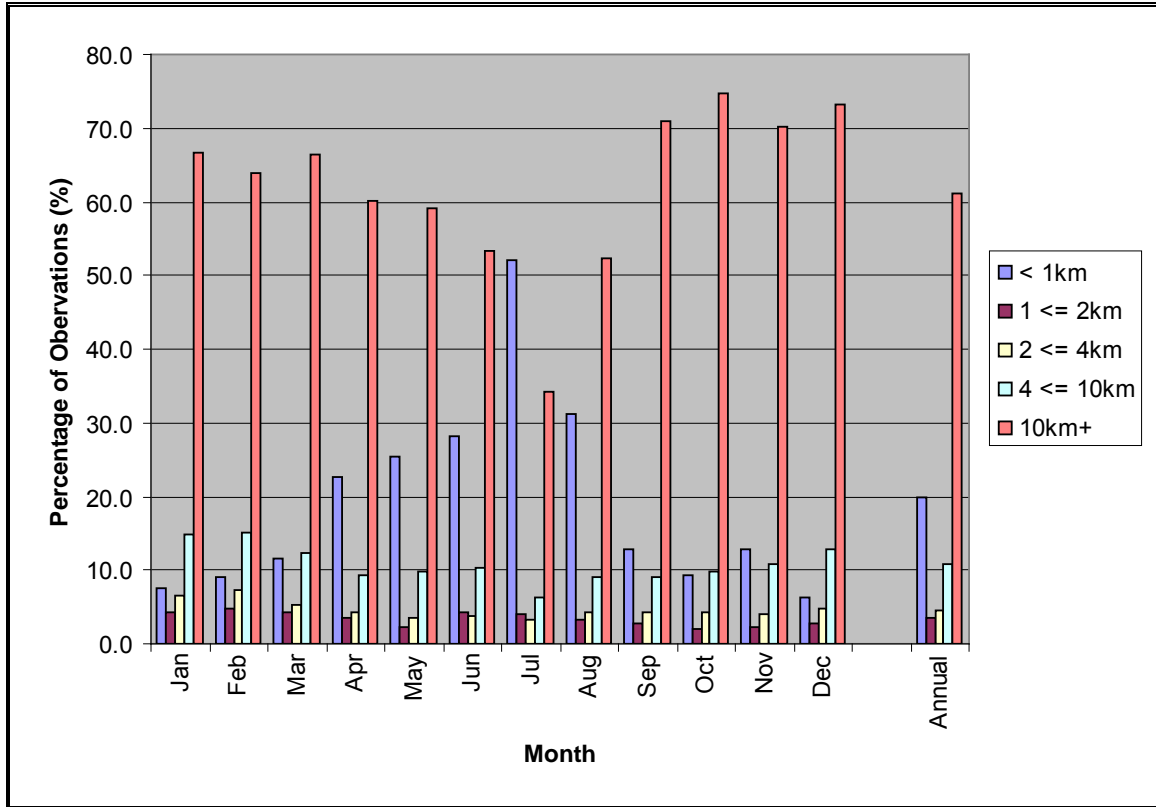


Figure 2.29 Monthly and Annual Percentage Occurrence of Visibility in Region 2

(Source: ICOADS Data set (1980-2010))

Region 3

A plot of the frequency distribution of visibility for Region 3 from the ICOADS data set is presented in Figure 2.30. This figure shows that obstructions to vision can occur in any month. Annually, 37.9% of the observations had reduced visibilities.

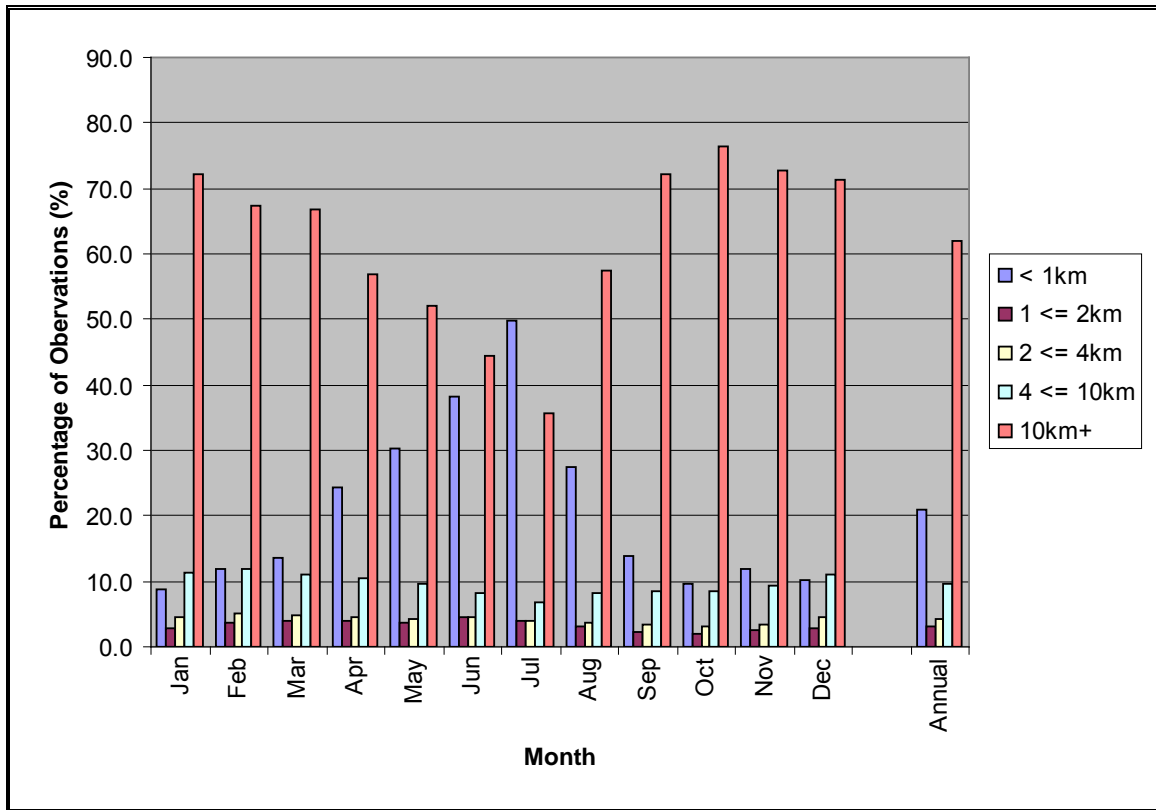


Figure 2.30 Monthly and Annual Percentage Occurrence of Visibility in Region 3

(Source: ICOADS Data set (1980-2010))

2.5.3 Precipitation

Precipitation can come in three forms and are classified as liquid, freezing or frozen. Included in the three classifications are:

- (1) Liquid Precipitation
 - Drizzle
 - Rain
- (2) Freezing Precipitation
 - Freezing Drizzle
 - Freezing Rain
- (3) Frozen Precipitation
 - Snow
 - Snow Pellets

- Snow Grains
- Ice Pellets
- Hail
- Ice Crystals

The frequency of precipitation type for each region was calculated using data from the ICOADS data set, with each occurrence counting as one event. Precipitation statistics for these regions may be low due a fair weather bias. That is, ships tend to either avoid regions of inclement weather, or simply do not report during these events.

Region 1

The frequency of precipitation type (Table 2.33) shows that annually, precipitation occurs 25.6% of the time within Region 1. Winter has the highest frequency of precipitation with 39.9% of the observations reporting precipitation. Snow accounts for the majority of precipitation during the winter months, accounting for 61.4% of the occurrences of winter precipitation. Summer has the lowest frequency of precipitation with a total frequency of occurrence of 11.8%. Snow has been reported in every month; however this is may be due to coding error rather than the actual presence of snow.

The percentage of occurrences of freezing precipitation data was also calculated from the ICOADS data set. Freezing precipitation occurs when rain or drizzle aloft enters negative air temperatures near the surface and becomes super-cooled so that the droplets freeze upon impact with the surface. This situation typically arises ahead of a warm front extending from low pressure systems passing west of the area. The frequency of freezing precipitation was slightly higher in the winter months than during the spring. No freezing precipitation occurred during summer and autumn.

Thunderstorms occur relatively infrequently over the study area though they may occur in any month of the year. Autumn has the least number of thunderstorms occurring only 0.04% of the time while winter has the highest frequency of thunder storms with 0.12%. It should be noted that hail only occurs in the presence of severe thunderstorms, yet in Table 2.33, the frequency of hail is higher than the frequency of thunderstorms during the months of January. This may be due to observer inexperience, classifying what should be ice pellets (formed through entirely different atmospheric processes) as hail or mistyping what should have been “Thunderstorm without Hail – Code 95” as “Thunderstorm with Hail – Code 96” in the original Manmar data.

Table 2.33 Percentage Frequency (%) Distribution of Precipitation in Region 1

(Source: ICOADS Data set (1980-2010))

	Rain / Drizzle	Freezing Rain / Drizzle	Rain / Snow Mixed	Snow	Thunder storm	Hail	Total
January	12.5	0.4	3.4	27.7	0.1	0.2	44.2
February	11.0	0.2	1.0	25.2	0.0	0.0	37.4
March	12.7	0.1	3.0	16.0	0.0	0.0	31.8
April	10.9	0.0	0.5	7.4	0.2	0.1	19.1
May	14.2	0.0	0.6	4.7	0.1	0.1	19.7
June	9.9	0.0	0.2	0.7	0.0	0.0	10.7
July	9.4	0.0	0.0	0.6	0.0	0.0	10.0
August	13.1	0.0	0.1	0.4	0.1	0.0	13.8
September	15.2	0.0	0.0	0.1	0.0	0.0	15.4
October	20.8	0.0	0.1	1.1	0.0	0.0	22.1
November	16.6	0.0	1.4	7.7	0.1	0.1	26.0
December	14.1	0.5	2.5	19.2	0.4	0.1	36.8
Winter	12.4	0.4	2.4	24.5	0.1	0.1	39.9
Spring	12.7	0.0	1.3	9.3	0.1	0.1	23.5
Summer	11.1	0.0	0.1	0.6	0.1	0.0	11.8
Autumn	17.5	0.0	0.6	3.2	0.0	0.0	21.4
Total	13.4	0.1	1.2	10.7	0.1	0.1	25.6

Region 2

The frequency of precipitation type (Table 2.34) shows that annually, precipitation occurs 21.8% of the time within Region 2. Winter has the highest frequency of precipitation with 33.4% of the observations reporting precipitation. Snow accounts for the majority of precipitation during the winter months, accounting for 55.7% of the occurrences of winter precipitation. Summer has the lowest frequency of precipitation with a total frequency of occurrence of 14.3%. Snow has been reported in every month; however this is may be due to coding error rather than the actual presence of snow.

The percentage of occurrences of freezing precipitation data was also calculated from the ICOADS data set. Freezing precipitation occurs when rain or drizzle aloft enters negative air temperatures near the surface and becomes super-cooled so that the droplets freeze upon impact with the surface. This situation typically arises ahead of a warm front extending from low pressure systems passing west of the area. The frequency of freezing precipitation was slightly higher in the winter months than during the spring. No freezing precipitation occurred during summer and autumn.

Thunderstorms occur relatively infrequently over the study area though they may occur in any month of the year. Spring has the least number of thunderstorms occurring only 0.05% of the time while summer has the highest frequency of thunder storms with 0.26%. It should be noted that hail only occurs in the presence of severe thunderstorms, yet in Table 2.34, the frequency of hail is higher than the frequency of thunderstorms during the months of November - January. This may be due to observer inexperience, classifying what should be ice pellets (formed through entirely different atmospheric processes) as

hail or mistyping what should have been “Thunderstorm without Hail – Code 95” as “Thunderstorm with Hail – Code 96” in the original Manmar data.

Table 2.34 Percentage Frequency (%) Distribution of Precipitation in Region 2

(Source: ICOADS Data set (1980-2010))

	Rain / Drizzle	Freezing Rain / Drizzle	Rain / Snow Mixed	Snow	Thunder storm	Hail	Total
January	12.3	0.1	1.7	20.8	0.1	0.3	35.4
February	11.6	0.2	1.5	20.5	0.1	0.0	34.0
March	11.2	0.1	1.0	14.2	0.1	0.0	26.5
April	9.9	0.1	0.4	6.0	0.0	0.1	16.5
May	13.5	0.0	0.2	2.2	0.1	0.0	15.9
June	14.9	0.0	0.0	0.2	0.1	0.0	15.3
July	12.2	0.0	0.0	0.1	0.4	0.0	12.7
August	14.5	0.0	0.0	0.1	0.3	0.1	15.1
September	21.1	0.0	0.0	0.6	0.2	0.0	21.8
October	19.7	0.0	0.0	0.6	0.2	0.0	20.6
November	17.9	0.0	1.6	3.6	0.2	0.8	24.2
December	14.6	0.0	2.5	11.5	0.2	0.4	29.3
Winter	12.5	0.1	1.8	18.6	0.1	0.2	33.4
Spring	11.3	0.1	0.5	7.4	0.1	0.0	19.3
Summer	13.8	0.0	0.0	0.2	0.3	0.0	14.3
Autumn	19.6	0.0	0.5	1.6	0.2	0.3	22.2
Total	13.4	0.1	0.7	7.3	0.1	0.1	21.8

Region 3

The frequency of precipitation type (Table 2.35) shows that annually, precipitation occurs 21.6% of the time within Region 3. Winter has the highest frequency of precipitation with 34.0% of the observations reporting precipitation. Snow accounts for the majority of precipitation during the winter months, accounting for 57.7% of the occurrences of winter precipitation. Summer has the lowest frequency of precipitation with a total frequency of occurrence of 12.5%. Snow has been reported in each month from September to May; however this is may be due to coding error rather than the actual presence of snow.

The percentage of occurrences of freezing precipitation data was also calculated from the ICOADS data set. Freezing precipitation occurs when rain or drizzle aloft enters negative air temperatures near the surface and becomes super-cooled so that the droplets freeze upon impact with the surface. This situation typically arises ahead of a warm front extending from low pressure systems passing west of the area. The frequency of freezing precipitation was slightly higher in the winter months than during the spring. No freezing precipitation occurred during summer and autumn.

Thunderstorms occur relatively infrequently over the study area though they may occur in any month of the year. Spring has the least number of thunderstorms occurring only

0.03% of the time while summer has the highest frequency of thunder storms with 0.11%. It should be noted that hail only occurs in the presence of severe thunderstorms, yet in Table 2.35, the frequency of hail is higher than the frequency of thunderstorms for several months. This may be due to observer inexperience, classifying what should be ice pellets (formed through entirely different atmospheric processes) as hail or mistyping what should have been “Thunderstorm without Hail – Code 95” as “Thunderstorm with Hail – Code 96” in the original Manmar data.

Table 2.35 Percentage Frequency (%) Distribution of Precipitation in Region 3

(Source: ICOADS Data set (1980-2010))

	Rain / Drizzle	Freezing Rain / Drizzle	Rain / Snow Mixed	Snow	Thunder storm	Hail	Total
January	13.0	0.5	0.7	22.5	0.0	0.2	36.9
February	10.7	0.7	0.4	21.5	0.0	0.1	33.3
March	11.8	0.8	0.3	13.4	0.0	0.1	26.4
April	12.6	0.2	0.2	4.7	0.1	0.0	17.7
May	13.9	0.0	0.1	1.0	0.0	0.0	15.0
June	13.0	0.0	0.0	0.0	0.1	0.0	13.1
July	10.5	0.0	0.0	0.0	0.1	0.0	10.7
August	13.5	0.0	0.0	0.0	0.2	0.0	13.7
September	15.0	0.0	0.0	0.1	0.1	0.0	15.2
October	20.2	0.0	0.1	1.0	0.1	0.1	21.5
November	19.2	0.0	0.4	5.7	0.0	0.2	25.5
December	15.7	0.1	0.6	14.9	0.0	0.3	31.6
Winter	13.2	0.4	0.6	19.6	0.0	0.2	34.0
Spring	12.8	0.3	0.2	6.2	0.0	0.0	19.6
Summer	12.3	0.0	0.0	0.0	0.1	0.0	12.5
Autumn	18.1	0.0	0.2	2.2	0.1	0.1	20.7
Total	14.0	0.2	0.2	7.0	0.1	0.1	21.6

2.5.4 Sea Spray Vessel Icing

Sea spray icing can accumulate on vessels and shore structures when air temperatures are below the freezing temperature of water and there is potential for spray generation. In addition to air temperature, icing severity depends on water temperature, wave conditions, and wind. A review of the sea spray icing hazard is provided by Minsk (1977). The frequency of potential icing conditions and its severity was estimated from the algorithm proposed by Overland et al. (1986) and subsequently updated by Overland (1990). The algorithm generates an icing predictor based on air temperature, wind speed, and sea surface temperature which was empirically related to observed icing rates of fishing vessels in the Gulf of Alaska. This method will provide conservative estimates of icing severity in the study region as winter sea surface temperatures are colder and wave conditions are lower in the study area compared to the Gulf of Alaska where the algorithm was calibrated (Makkonen et al., 1991). Potential icing rates were computed

using wind speed, air and sea surface temperature observations from the ICOADS data set.

Region 1

Potential sea spray icing conditions start within the project area during the month of November with a frequency of icing potential of 1.2%. As temperatures cool throughout the winter, the frequency of icing potential increases to a maximum of 37.2% of the time in January. Extreme sea spray icing conditions were calculated to occur 2.9% of the time during January. Icing potential decreases rapidly after February in response to warming air and sea surface temperatures, and by June the frequency of icing conditions is 0.0%. A graph of the percentage occurrence of sea spray icing potential is presented in Figure 2.31.

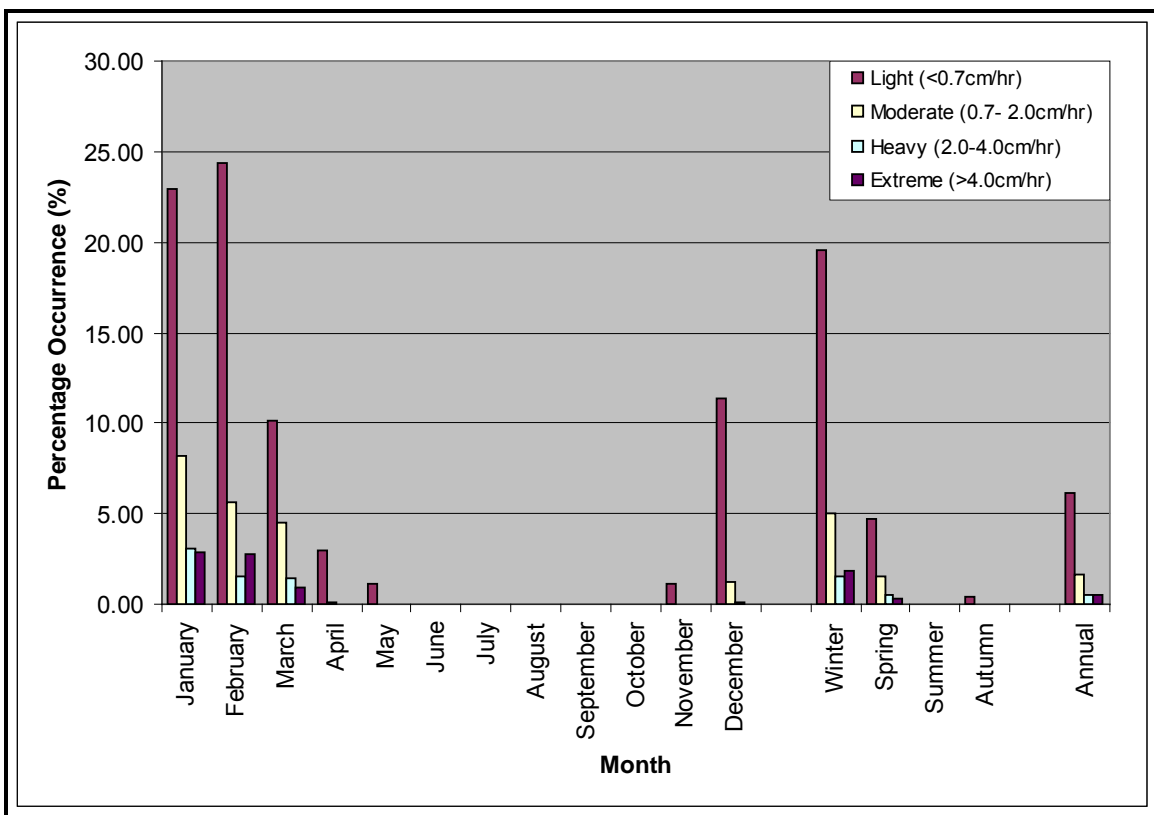


Figure 2.31 Percentage Frequency of Potential Spray Icing Conditions in Region 1

(Source: ICOADS Data set (1980-2010))

Region 2

Potential sea spray icing conditions start within the project area during the month of November with a frequency of icing potential of just 0.2%. As temperatures cool throughout the winter, the frequency of icing potential increases to a maximum of 26.1% of the time in February. Extreme sea spray icing conditions were calculated to occur 0.6% of the time during January. Icing potential decreases rapidly after February in response to warming air and sea surface temperatures, and by June the frequency of icing conditions is 0.0%. A graph of the percentage occurrence of sea spray icing potential is presented in Figure 2.32.

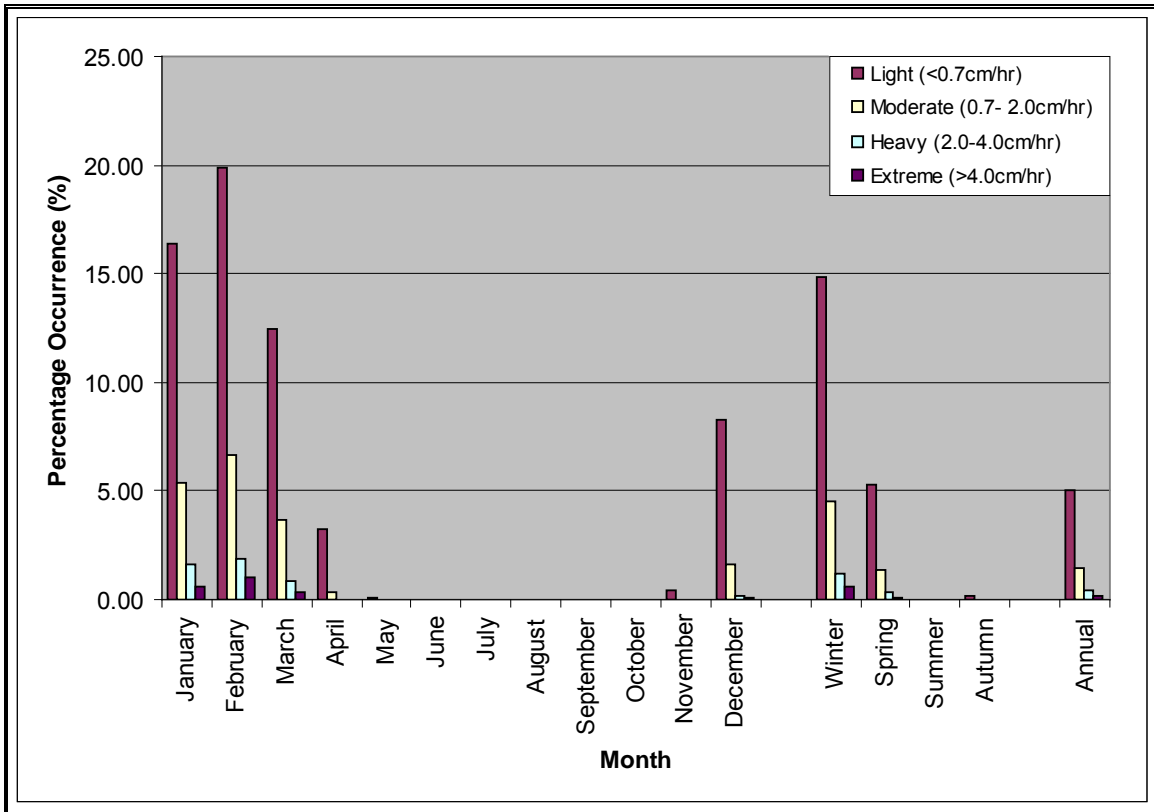


Figure 2.32 Percentage Frequency of Potential Spray Icing Conditions in Region 2

(Source: ICOADS Data set (1980-2010))

Region 3

Potential sea spray icing conditions start within the project area during the month of November with a frequency of icing potential of just 0.4%. As temperatures cool throughout the winter, the frequency of icing potential increases to a maximum of 28.7% of the time in February. Extreme sea spray icing conditions were calculated to occur 0.9% of the time during February. Icing potential decreases rapidly after February in response to warming air and sea surface temperatures, and by June the frequency of icing conditions is 0.0%. A graph of the percentage occurrence of sea spray icing potential is presented in Figure 2.33.

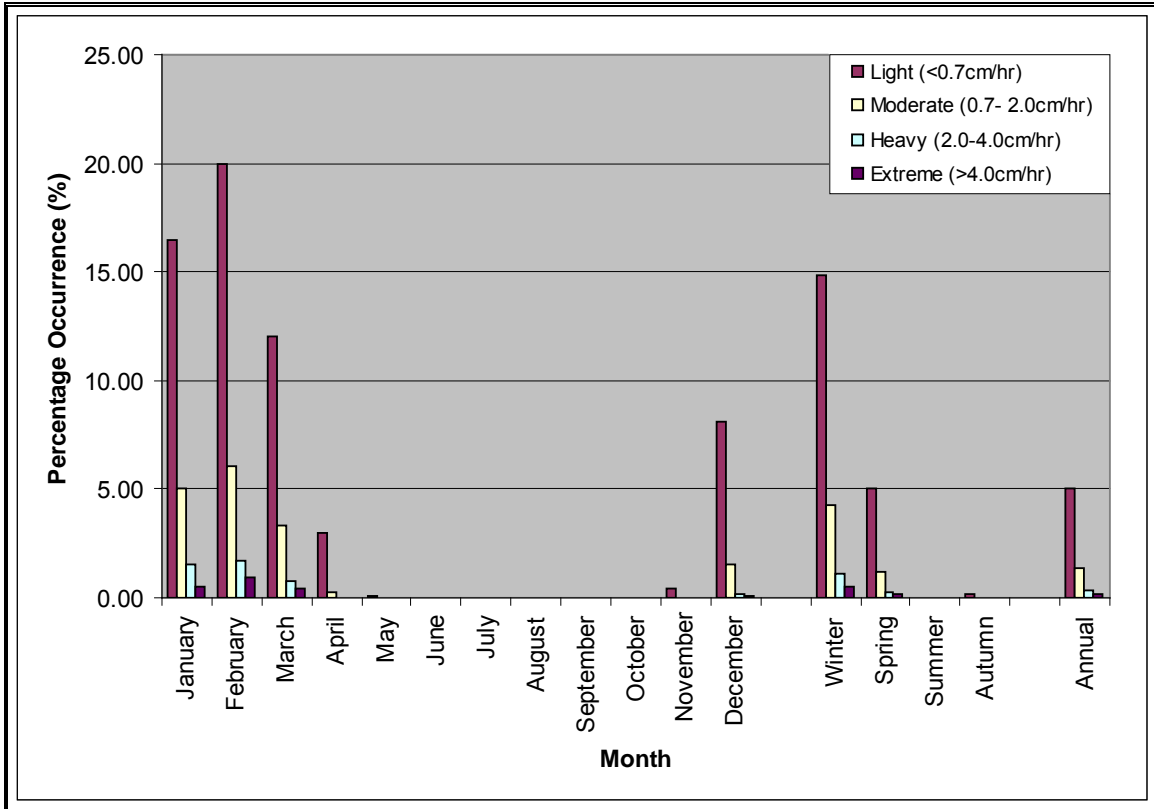


Figure 2.33 Percentage Frequency of Potential Spray Icing Conditions in Region 3

(Source: ICOADS Data set (1980-2010))

3.0 Wind and Wave Extreme Value Analysis

An analysis of extreme wind and waves was performed using the same three MSC50 grid points as the wind and wave analysis in the previous section. This data set was determined to be the most representative of the available datasets, as it provides a continuous 57-year period of hourly data for the study area. The extreme values for wind and waves were calculated using the peak-over-threshold method, and after considering four different distributions, the Gumbel distribution was chosen to be the most representative as it provided the best fit to the data.

Since extreme values can vary depending on how well the data fits the distribution, a sensitivity analysis was carried out to determine the number storms to use. The number of storms determined to provide the best fit annually and monthly for each grid point is presented in Table 3.1.

Table 3.1 Number of Storms Providing Best Fit for Extreme Value Analysis of Winds and Waves

		Annually	Monthly
Grid Point 14845	Wind	265	66
	Wave	181	58
Grid Point 13912	Wind	314	84
	Wave	192	79
Grid Point 11423	Wind	259	107
	Wave	251	76

3.1.1 Extreme Value Estimates for Winds from the Gumbel Distribution

The extreme value estimates for wind were calculated using Oceanweather's Osmosis software program for the return periods of 1-year, 10-years, 25-years, 50-years and 100-years. The calculated annual and monthly values for 1-hour, 10-minutes and 1-minute are presented in Table 3.2 to Table 3.4. The analysis used hourly mean wind values for the reference height of 10 m above sea level. These values were converted to 10-minute and 1-minute wind values using a constant ration of 1.06 and 1.22, respectively (U.S. Geological Survey 1979). The annual 100-year extreme 1-hour wind speed was determined to be 32.8 m/s for grid point 14845, 33.1 m/s for grid point 13912 and 32.3 m/s for grid point 11423. Monthly, the highest 100-year extreme winds occurred during the month of February.

Table 3.2 1-hr Extreme Wind Speed Estimates (m/s) for Return Periods of 1, 10, 25, 50 and 100 Years

	Grid Point #14845					Grid Point #13912					Grid Point #11423				
Month	1	10	25	50	100	1	10	25	50	100	1	10	25	50	100
January	23.3	26.8	27.8	28.6	29.3	23.3	27.1	28.4	29.3	30.3	22.8	26.5	27.8	28.8	29.7
February	22.5	28.1	29.8	31.1	32.4	23.0	28.0	29.6	30.9	32.1	22.4	27.2	28.9	30.2	31.5
March	20.9	25.9	27.4	28.6	29.7	20.8	20.6	27.2	28.4	29.6	20.5	24.9	26.5	27.7	28.8
April	18.6	22.4	23.6	24.4	25.3	18.7	22.5	23.8	24.8	25.7	18.2	22.5	24.0	25.2	26.3
May	16.1	21.0	22.5	23.6	24.7	16.5	20.9	22.4	23.5	24.6	15.7	19.7	21.1	22.1	23.2
June	14.8	19.0	20.2	21.2	22.1	15.1	18.8	20.1	21.0	21.9	14.7	18.4	19.8	20.8	21.8
July	13.5	16.6	17.6	18.3	19.0	13.6	16.8	17.8	18.6	19.4	13.5	16.7	17.9	18.7	19.6
August	14.2	19.4	21.0	22.1	23.3	14.4	20.7	22.9	24.5	26.0	14.7	21.1	23.3	25.0	26.7
September	17.3	23.3	25.1	26.5	27.9	17.7	24.0	26.2	27.8	29.4	17.2	22.6	24.6	26.0	27.4
October	18.3	25.0	27.0	28.5	30.0	19.0	24.4	26.3	27.7	29.0	18.6	23.5	25.3	26.6	27.9
November	20.3	25.0	26.4	27.8	28.5	20.5	24.8	26.3	27.3	28.4	20.0	24.4	25.9	27.1	28.2
December	22.2	27.6	29.2	30.4	31.6	22.4	27.6	29.3	30.6	31.8	22.0	26.5	28.1	29.3	30.4
Annual	26.0	29.5	30.8	31.8	32.8	25.9	29.6	31.0	32.1	33.1	25.3	28.9	30.2	31.2	32.3

Table 3.3 10-minute Extreme Wind Speed (m/s) Estimates for Return Periods of 1, 10, 25, 50 and 100 Years

	Grid Point #14845					Grid Point #13912					Grid Point #11423				
Month	1	10	25	50	100	1	10	25	50	100	1	10	25	50	100
January	24.7	28.4	29.5	30.3	31.1	24.7	28.7	30.1	31.1	32.1	24.1	28.0	29.4	30.5	31.5
February	23.9	29.8	31.6	33.0	34.3	24.4	29.6	31.4	32.7	34.0	23.8	28.9	30.7	32.0	33.4
March	22.1	27.4	29.1	30.3	31.5	22.1	21.8	28.8	30.1	31.4	21.7	26.4	28.1	29.3	30.5
April	19.8	23.8	25.0	25.9	26.8	19.8	23.9	25.2	26.3	27.3	19.2	23.8	25.5	26.7	27.9
May	17.1	22.3	23.8	25.0	26.2	17.5	22.1	23.7	24.9	26.1	16.6	20.8	22.3	23.5	24.6
June	15.7	20.1	21.4	22.4	23.4	16.0	19.9	21.3	22.3	23.3	15.5	19.5	21.0	22.0	23.1
July	14.3	17.6	18.6	19.4	20.1	14.4	17.8	18.9	19.8	20.6	14.3	17.7	18.9	19.9	20.8

August	15. 0	20. 5	22. 2	23. 5	24. 7	15. 2	22. 0	24. 2	25. 9	27. 6	15. 6	22. 3	24. 7	26. 5	28. 3
Septem ber	18. 3	24. 7	26. 6	28. 1	29. 5	18. 7	25. 5	27. 8	29. 5	31. 2	18. 2	24. 0	26. 0	27. 5	29. 1
October	19. 4	26. 4	28. 6	30. 2	31. 8	20. 1	25. 9	27. 9	29. 3	30. 8	19. 7	24. 9	26. 8	28. 2	29. 6
Novemb er	21. 5	26. 5	28. 0	29. 4	30. 3	21. 8	26. 3	27. 8	29. 0	30. 1	21. 2	25. 8	27. 5	28. 7	29. 9
Decemb er	23. 6	29. 2	30. 9	32. 2	33. 5	23. 8	29. 2	31. 0	32. 4	33. 8	23. 3	28. 0	29. 7	31. 0	32. 3
Annual	27. 5	31. 2	32. 6	33. 7	34. 8	27. 5	31. 4	32. 8	34. 0	35. 1	26. 8	30. 6	32. 0	33. 1	34. 2

Table 3.4 1-minute Extreme Wind Speed (m/s) Estimates for Return Periods of 1, 10, 25, 50 and 100 Years

	Grid Point #14845					Grid Point #13912					Grid Point #11423				
Month	1	10	25	50	100	1	10	25	50	100	1	10	25	50	100
January	28. 5	32. 6	33. 9	34. 9	35. 8	28. 4	33. 1	34. 6	35. 8	37. 0	27. 8	32. 3	33. 9	35. 1	36. 3
Februar y	27. 5	34. 3	36. 4	37. 9	39. 5	28. 1	34. 1	36. 2	37. 7	39. 2	27. 3	33. 2	35. 3	36. 9	38. 4
March	25. 4	31. 6	33. 4	34. 8	36. 2	25. 4	25. 1	33. 2	34. 6	36. 1	25. 0	30. 4	32. 3	33. 7	35. 2
April	22. 7	27. 3	28. 7	29. 8	30. 8	22. 8	27. 5	29. 0	30. 2	31. 4	22. 2	27. 4	29. 3	30. 7	32. 1
May	19. 7	25. 6	27. 4	28. 8	30. 1	20. 1	25. 5	27. 3	28. 7	30. 0	19. 1	24. 0	25. 7	27. 0	28. 3
June	18. 1	23. 1	24. 7	25. 8	27. 0	18. 4	23. 0	24. 5	25. 6	26. 8	17. 9	22. 5	24. 1	25. 4	26. 6
July	16. 5	20. 3	21. 4	22. 3	23. 2	16. 6	20. 5	21. 8	22. 7	23. 7	16. 5	20. 4	21. 8	22. 9	23. 9
August	17. 3	23. 6	25. 6	27. 0	28. 4	17. 5	25. 3	27. 9	29. 8	31. 8	17. 9	25. 7	28. 4	30. 5	32. 5
Septem ber	21. 1	28. 4	30. 7	32. 3	34. 0	21. 6	29. 3	32. 0	33. 9	35. 9	21. 0	27. 6	30. 0	31. 7	33. 5
October	22. 3	30. 4	32. 9	34. 8	36. 6	23. 1	29. 8	32. 1	33. 7	35. 4	22. 7	28. 7	30. 9	32. 5	34. 1
Novemb er	24. 8	30. 5	32. 2	33. 9	34. 8	25. 0	30. 3	32. 0	33. 4	34. 7	24. 4	29. 7	31. 6	33. 0	34. 4
Decemb er	27. 1	33. 6	35. 6	37. 1	38. 6	27. 4	33. 6	35. 7	37. 3	38. 8	26. 8	32. 3	34. 2	35. 7	37. 1
Annual	31. 7	35. 9	37. 6	38. 8	40. 0	31. 6	36. 1	37. 8	39. 1	40. 4	30. 9	35. 2	36. 9	38. 1	39. 4

3.1.2 Extreme Value Estimates for Waves from a Gumbel Distribution

The annual and monthly extreme value estimates for significant wave height for return periods of 1-year, 10-years, 25-years, 50-years and 100-years are given in Table 3.5. The annual 100-year extreme significant wave height was 14.9 m at grid point 14845, 16.0 metres at grid point 13912 and 15.0 m at grid point 11423. A storm with a return period of 100 years means that the calculated significant wave height will occur once every 100 years, averaged over a long period of time.

Table 3.5 Extreme Significant Wave Height Estimates for Return Periods of 1, 10, 25, 50 and 100 Years

	Grid Point #14845					Grid Point #13912					Grid Point #11423				
Month	1	10	25	50	100	1	10	25	50	100	1	10	25	50	100
January	9.2	12.1	12.9	13.5	14.0	10.1	12.8	13.7	14.4	15.0	9.2	12.0	12.9	13.5	14.2
February	8.5	12.1	13.0	13.7	14.4	9.4	13.0	14.2	15.0	15.9	8.5	12.2	13.4	14.3	15.2
March	6.8	10.1	10.9	11.6	12.2	7.8	10.5	11.4	12.1	12.8	7.1	10.0	11.0	11.7	12.4
April	5.7	9.0	9.9	10.5	11.1	6.4	9.2	10.0	10.7	11.4	5.7	8.6	9.6	10.3	11.0
May	4.2	8.1	9.1	9.9	10.6	5.1	8.1	9.1	9.9	10.6	4.6	7.2	8.1	8.7	9.4
June	3.4	6.5	7.3	7.9	8.5	4.1	6.5	7.3	7.9	8.5	3.8	6.1	6.9	7.4	8.0
July	3.1	5.2	5.8	6.2	6.6	3.3	5.4	6.0	6.4	6.8	3.4	5.3	5.9	6.3	6.8
August	3.5	6.2	6.9	7.4	7.9	4.1	6.5	7.2	7.8	8.4	3.8	6.7	7.7	8.4	9.1
September	4.5	10.1	11.5	12.6	13.6	5.8	10.3	11.7	12.8	13.9	5.3	9.3	10.6	11.6	12.5
October	5.7	10.8	12.2	13.1	14.1	6.7	11.1	12.5	13.6	14.6	6.3	10.0	11.2	12.1	13.0
November	7.2	11.3	12.4	13.1	13.9	8.1	11.5	12.6	13.4	14.2	7.4	10.5	11.5	12.3	13.0
December	9.0	12.5	13.5	14.2	14.9	9.7	12.9	14.0	14.8	15.6	8.9	11.7	12.7	13.4	14.1
Annual	11.3	13.2	13.9	14.4	14.9	11.8	14.0	14.8	15.4	16.0	10.8	13.0	13.8	14.4	15.0

The maximum individual wave heights were calculated within Oceanweather's OSMOSIS software by evaluating the Borgman integral (Borgman 1973), which was derived from a Raleigh distribution function. The variant of this equation used in the software has the following form (Forristall, 1978):

$$\Pr\{H > h\} = \exp\left[-1.08311\left(\frac{h^2}{8M_0}\right)^{1.063}\right]; \quad T = \frac{M_0}{M_1}$$

where h is the significant wave height, T is the wave period, and M_0 and M_1 are the first and second spectral moments of the total spectrum. The associated peak periods are calculated by plotting the peak periods of the chosen storm peak values versus the corresponding significant wave heights. This plot is fitted to a power function ($y = ax^b$), and the resulting equation is used to calculate the peak periods associated with the extreme values of significant wave height. The maximum individual wave heights and extreme associated peak periods are presented in Table 3.6 and Table 3.7. Maximum individual wave heights and the extreme associated peak periods peak during the month

of December at grid point 14845, and the month of February at grid point 13912 and grid point 11423.

Table 3.6 Extreme Maximum Wave Height Estimates for Return Periods of 1, 10, 25, 50 and 100 Years

	Grid Point #14845					Grid Point #13912					Grid Point #11423				
Month	1	10	25	50	100	1	10	25	50	100	1	10	25	50	100
January	16.9	22.6	24.1	25.3	26.4	18.8	24.0	25.7	27.0	28.3	17.0	22.0	23.6	24.8	26.0
February	15.8	22.4	24.2	25.4	26.7	17.5	24.1	26.2	27.9	29.5	15.8	22.6	24.8	26.5	28.1
March	12.5	19.1	20.8	22.1	23.4	14.5	19.7	21.4	22.7	24.0	13.4	18.7	20.4	21.7	23.0
April	10.6	16.5	18.0	19.2	20.3	12.1	17.1	18.7	20.0	21.2	10.7	15.9	17.7	18.9	20.2
May	7.5	15.6	17.7	19.2	20.7	9.9	15.7	17.7	19.1	20.5	8.7	14.0	15.7	17.0	18.3
June	6.6	12.0	13.4	14.4	15.4	7.9	12.1	13.5	14.5	15.6	7.4	11.6	13.0	14.0	15.0
July	5.9	9.9	10.9	11.7	12.4	7.0	10.0	11.1	11.8	12.6	6.5	9.9	11.0	11.8	12.6
August	6.7	11.5	12.7	13.6	14.5	7.8	12.2	13.7	14.7	15.8	7.2	12.3	14.0	15.3	16.6
September	8.7	18.4	20.9	22.8	24.6	10.9	18.6	21.2	23.1	25.0	10.0	17.0	19.2	20.9	22.6
October	10.5	20.0	22.5	24.3	26.1	12.8	20.5	23.1	25.0	26.9	11.8	18.5	20.7	22.4	24.0
November	13.5	21.0	22.9	24.3	25.7	15.0	21.2	23.2	24.7	26.2	13.8	19.5	21.3	22.7	24.0
December	16.6	23.1	24.9	26.3	27.6	18.0	23.9	25.8	27.3	28.7	16.3	21.7	23.5	24.8	26.1
Annual	20.9	24.4	25.7	26.6	27.6	21.8	25.7	27.2	28.3	29.4	20.0	23.9	25.3	26.5	27.6

Table 3.7 Extreme Associated Peak Period Estimates for Return Periods of 1, 10, 25, 50 and 100 Years

	Grid Point #14845					Grid Point #13912					Grid Point #11423				
Month	1	10	25	50	100	1	10	25	50	100	1	10	25	50	100
January	12.8	14.5	14.9	15.2	15.5	13.4	14.9	15.3	15.7	16.0	12.8	14.4	14.9	15.3	15.6
February	11.9	14.6	15.3	15.7	16.2	12.7	14.9	15.6	16.1	16.5	12.4	14.3	14.9	15.3	15.7
March	11.7	13.1	13.5	13.7	13.9	12.1	13.3	13.7	14.0	14.2	11.8	13.2	13.6	13.9	14.2
April	10.6	13.1	13.6	14.0	14.4	11.4	12.9	13.3	13.6	13.9	10.7	12.3	12.8	13.1	13.4
May	9.3	12.3	12.9	13.4	13.8	10.2	12.3	12.9	13.3	13.7	9.9	12.0	12.6	13.0	13.4
June	8.6	11.1	11.6	11.9	12.3	9.2	11.2	11.7	12.1	12.5	8.8	10.9	11.5	11.9	12.3
July	7.9	10.4	10.9	11.3	11.7	8.3	10.6	11.1	11.6	12.0	8.5	10.6	11.2	11.6	12.0
August	9.1	10.1	11.1	11.1	11.1	9.4	11.1	11.1	12.1	12.1	9.0	11.1	12.1	13.1	13.1

		9	3	6	8		3	9	3	6		8	6	2	7
September	9.9	13.6	14.3	14.8	15.3	11.1	13.8	14.6	15.1	15.6	10.9	13.2	13.9	14.3	14.7
October	11.3	13.6	14.1	14.4	14.7	11.8	14.0	14.5	15.0	15.3	11.4	13.4	14.0	14.4	14.8
November	11.6	13.8	14.3	14.6	15.0	12.3	13.9	14.4	14.7	15.1	12.1	13.4	13.8	14.0	14.3
December	12.6	14.5	14.9	15.3	15.6	13.2	14.9	15.4	15.7	16.1	12.8	14.3	14.7	15.1	15.4
Annual	13.9	15.0	15.3	15.6	15.9	14.3	15.5	15.9	16.3	16.6	13.7	14.9	15.3	15.6	15.9

3.1.3 Joint Probability of Extreme Wave Heights and Spectral Peak Periods

The extreme analysis was carried out on the 3-hourly data set. For comparison purposes with the previous report and since the equations involved in the methodology were originally developed for 6-hourly data, a 6-hourly data set was also analyzed. In order to examine the period ranges of storm events, an environmental contour plot was produced showing the probability of the joint occurrence of significant wave heights and the spectral peak periods using the methodology of Winterstein et al. (1993). The wave heights were fitted to a Weibull distribution and the peak periods to a lognormal distribution. The wave data was divided into bins of 1 m for significant wave heights and 1 second for peak periods. Since the lower wave values were having too much of an impact on the wave extremes, the wave heights below 2 m were modeled separately in a Weibull distribution. The two Weibull curves were combined near 2 m, the point where both functions had the same probability.

Three-parameter Weibull distributions were used with a scaling parameter α , shape parameter β , and location parameter γ . The three parameters were solved by using a least square method, the maximum log likelihood, and the method of moments. The following equation was minimized to get the coefficients:

$$LS(\alpha, \beta, \gamma) := \sum_{i=0}^{13} \left[\ln(-\ln(1 - FP_i)) - \beta \cdot \ln \left[\frac{(h_i - \gamma)}{\alpha} \right] \right]^2$$

where h_i is the endpoint of the height bin (0.5, 1.5, ...) and FP_i is the cumulative probability of the height bin. Using a minimizing function the three parameters α , β and γ were calculated.

A lognormal distribution was fitted to the spectral peak periods in each wave height bin. The coefficient of the lognormal distribution was then calculated. Using the coefficients and the two distribution functions, the joint wave height and period combinations were calculated for the various return periods.

Contour plots for each grid point depicting the joint wave height and period combinations values for return periods of 1-year, 10-years, 25-years, 50-years and 100-years is

presented in Figure 3.1 through Figure 3.3. The annual values for the significant wave height estimates and the associated spectral peak periods for each grid point are given in Table 3.8. The extreme wave height for all return periods was higher using the Weibull Distribution when compared to the Gumbel Distribution. The 100-year extreme significant wave heights for grid point 14845, 13912 and 11423 were 16.7 m, 17.5 m, and 16.3 m, respectively.

Table 3.8 Annual Extreme Significant Wave Estimates and Spectral Peak Periods for Return Periods of 1, 10, 25, 50 and 100 Years

Grid Point	Return Period (years)	Significant Wave Height (m)	Spectral Peak Period Median Value (s)
14845	1	12.2	14.5
	10	14.5	15.7
	25	15.4	16.2
	50	16.1	16.5
	100	16.7	16.9
13912	1	12.7	14.9
	10	15.1	16.2
	25	16.1	16.7
	50	16.8	17.1
	100	17.5	17.5
11423	1	11.7	14.2
	10	14.0	15.5
	25	14.9	15.9
	50	15.6	16.3
	100	16.3	16.6

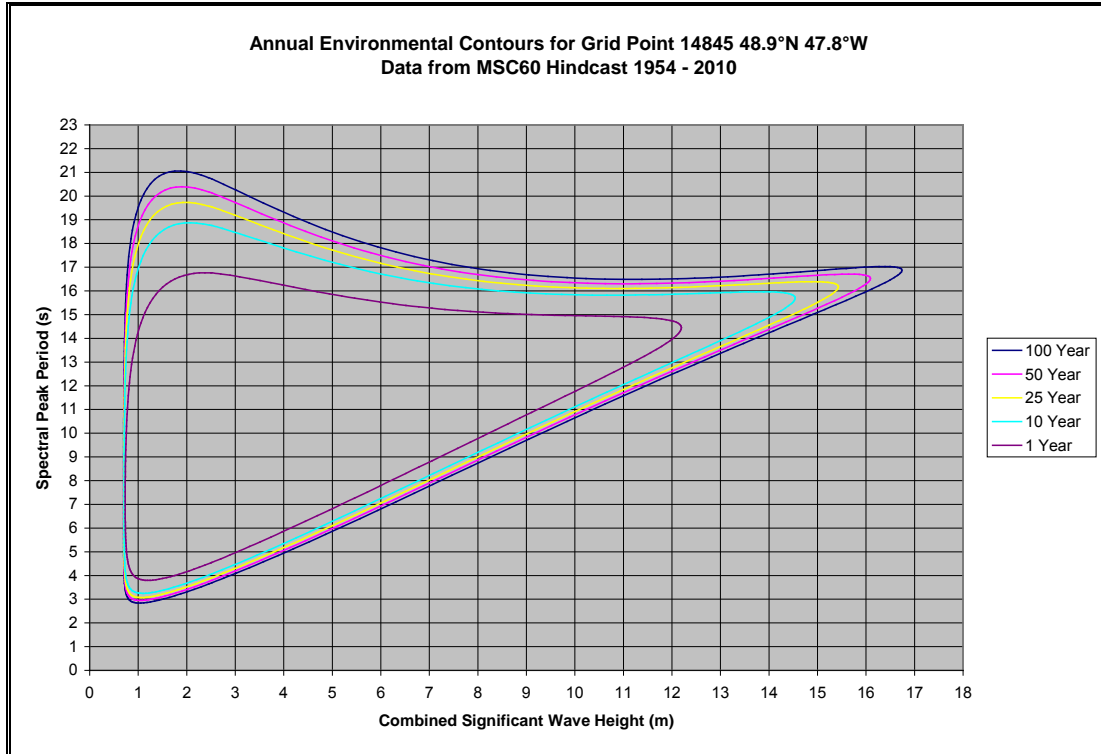


Figure 3.1 Environmental Contour Plot for Grid Point 14845 located near 48.9°N; 47.8°W. 1954 – 2010

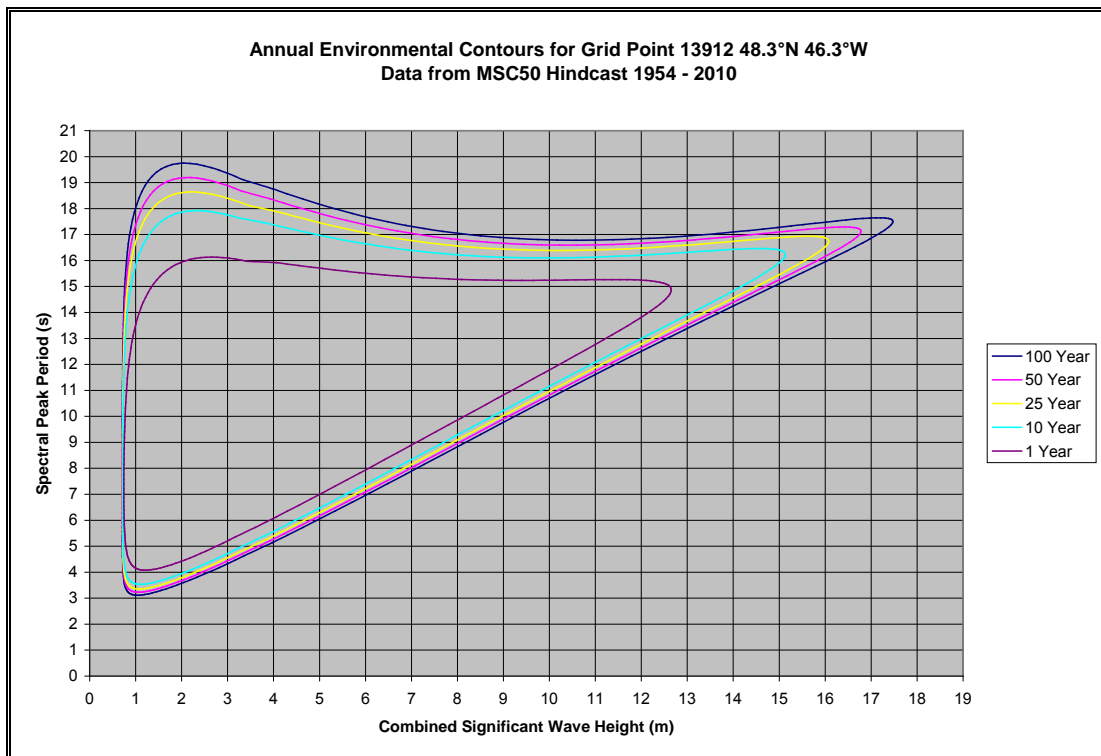


Figure 3.2 Environmental Contour Plot for Grid Point 13912 located near 48.3°N; 46.3°W. 1954 – 2010

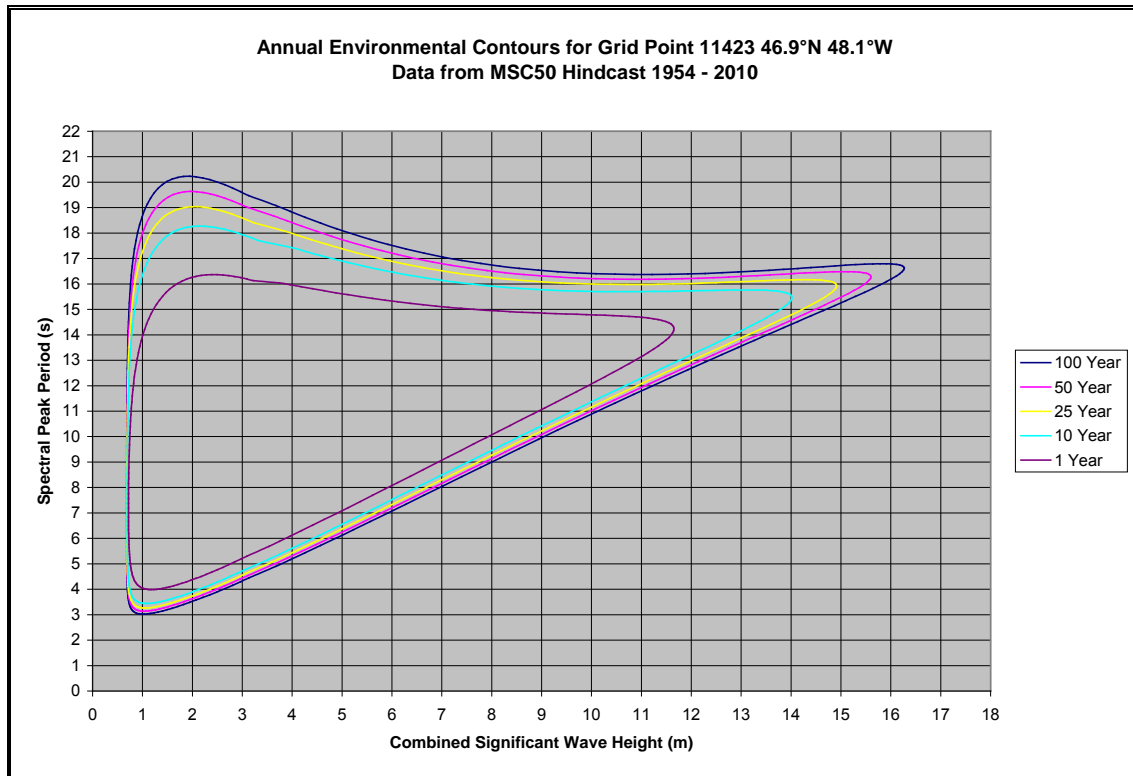


Figure 3.3 Environmental Contour Plot for Grid Point 11423 located near 46.9°N; 48.1°W. 1954 – 2010

4.0 Oceanography

4.1 Major Currents in the Study Area

The study area is the southern part of Orphan Basin, the Sackville Spur, the northeast Newfoundland Slope, northern Flemish Pass, and the Jeanne d'Arc Basin. The large scale circulation off the coast of Newfoundland and Labrador is dominated by well established currents that flow along the margins of the Continental Shelf. The two major current systems in the area are the Labrador Current and the North Atlantic Current (Colbourne & Foote, 2000). The Labrador Current is the main current in the study area and it transports sub-polar water to lower latitudes along the Continental Shelf of eastern Canada. Oceanographic studies show that this strong western boundary current follows the shelf break with relatively low variability compared to the mean flow. Over the Grand Banks a weaker current system is observed where the variability often exceeds that of the mean flow. Figure 4.1 shows the major currents off the coast of Newfoundland and Labrador.

The Labrador Current consists of two major branches. The inshore branch of the Labrador Current is approximately 100 km wide (Stein, 2007) and is steered by the local underwater topography through the Avalon Channel. The stronger offshore branch flows along the shelf break over the upper portion of the Continental Slope. The offshore branch passes between the 400 m and 1200 m isobaths (Lazier and Wright, 1993). This branch of the Labrador Current divides east of 48°W, resulting in part of the branch flowing to the east around Flemish Cap and the other flowing south around the eastern edge of the Grand Banks and through Flemish Pass. Within Flemish Pass the width of the Labrador Current is reduced to 50 km with speeds of about 30 cm/s (Stein, 2007). This flow transports cold, relatively low salinity Labrador Slope water into the region. To the southeast of the Flemish Cap the North Atlantic Current transports warmer, high salinity water to the northeast along the southeast slope of Grand Bank and the Flemish Cap (Figure 4.2).

The volume transport of the Labrador Current is variable from year to year. Han et al. (2010) found that the transport decreased by 6.3 Sv from the early to late 1990's and increased by 3.2 Sv from the late 1990's to the early 2000's. They found that the multi-year changes in the Labrador Current transport appeared to be primarily barotropic and positively correlated with the North Atlantic Oscillation at zero lag implying a fast response of the regional circulation to the atmospheric forcing variability.

The outer branch of the Labrador Current exhibits a distinct seasonal variation in flow speeds (Lazier and Wright, 1993), in which mean flows are a maximum in October and a minimum in March and April. This annual cycle is reported to be the result of the large annual variation in the steric height over the continental shelf in relation to the much less variable internal density characteristic of the adjoining deep waters. The additional freshwater in spring and summer is largely confined to the waters over the shelf. In summer, the difference in sea level between the shelf and open ocean is 0.09 m greater than in winter (Lazier and Wright, 1993). This difference produces a greater horizontal surface pressure gradient and hence, stronger mean flows.

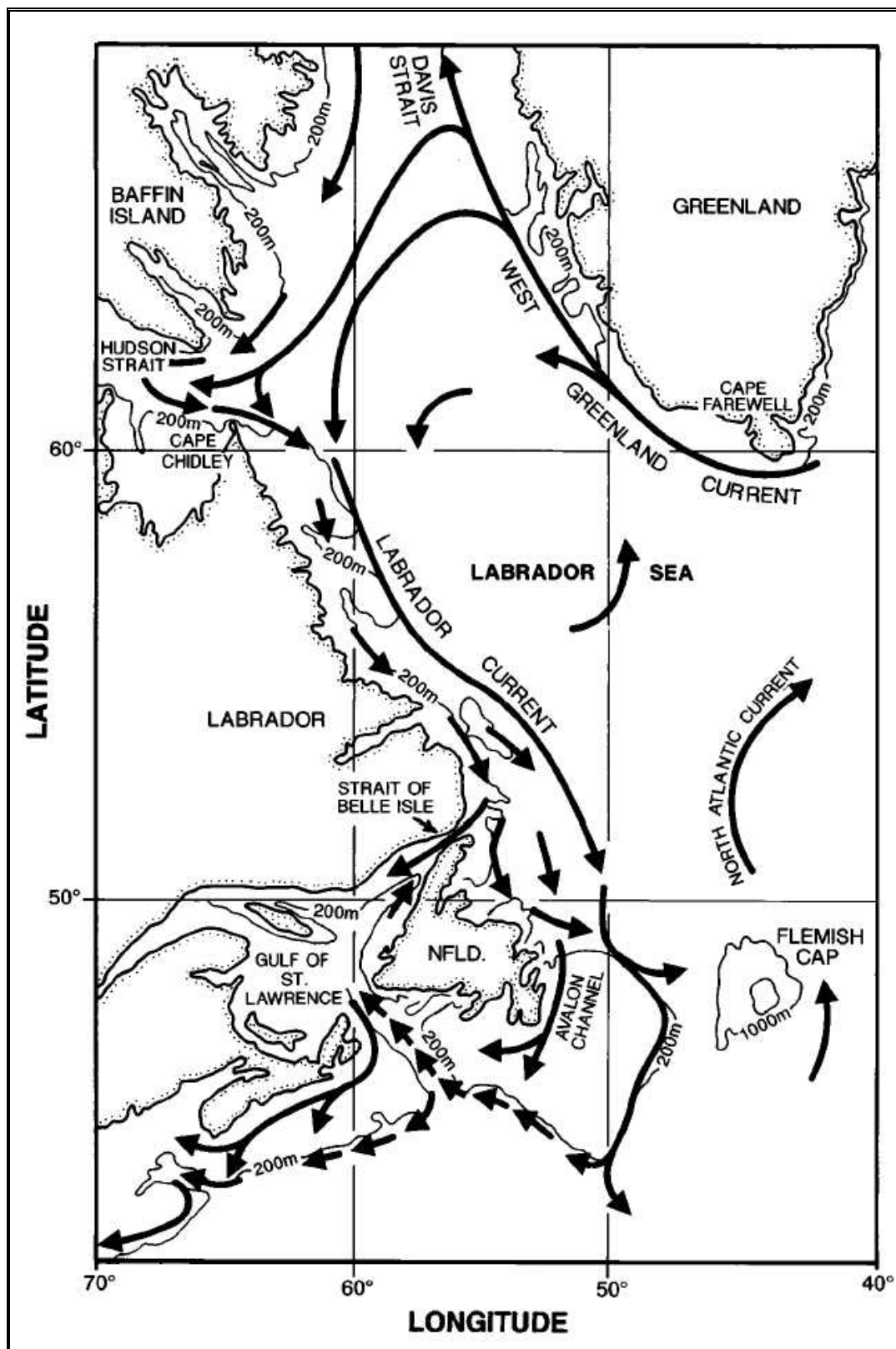


Figure 4.1 Major ocean circulation features in the Northeast Atlantic

Source: Colbourne et al., 1977

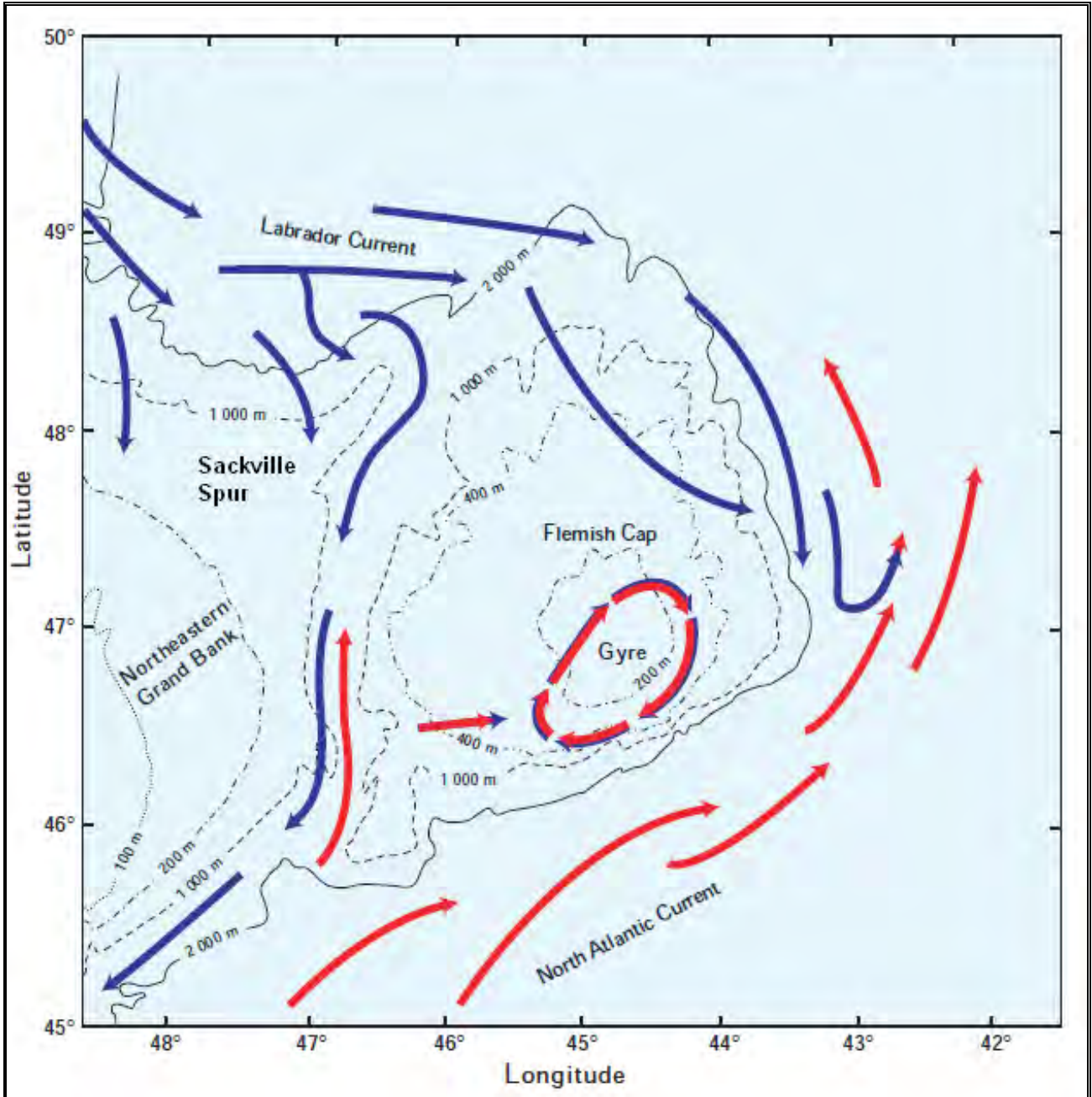


Figure 4.2 The major circulation features around the Flemish Cap and Sackville Spur

Source: (modified from Colbourne & Foote, 2000)

The International Ice Patrol has deployed satellite tracked drifter buoys in the Labrador Current to measure Lagrangian surface currents. Additional surface drifters have been deployed by the Bedford Institute of Oceanography (Petrie and Isenor, 1984; Petrie and Warnell, 1988), and by the Northwest Atlantic Research Centre in support of northern cod research (Pepin and Helbig, 1997). A composite of 144 drifter tracks was compiled by Helbig and Brett (1995). The drifter track positions and their calculated mean velocity

vectors are shown in Figure 4.3. Surface currents derived by Murphy et al. (1991) and updated by Yao et al. (1992) are presented in Figure 4.4. These surface currents were derived from the IIP's drifting buoy data between 1976 and 1989 (Murphy et al., 1991) and updated by Yao et al. (1992) using two more years of drifter data and some current meter data.

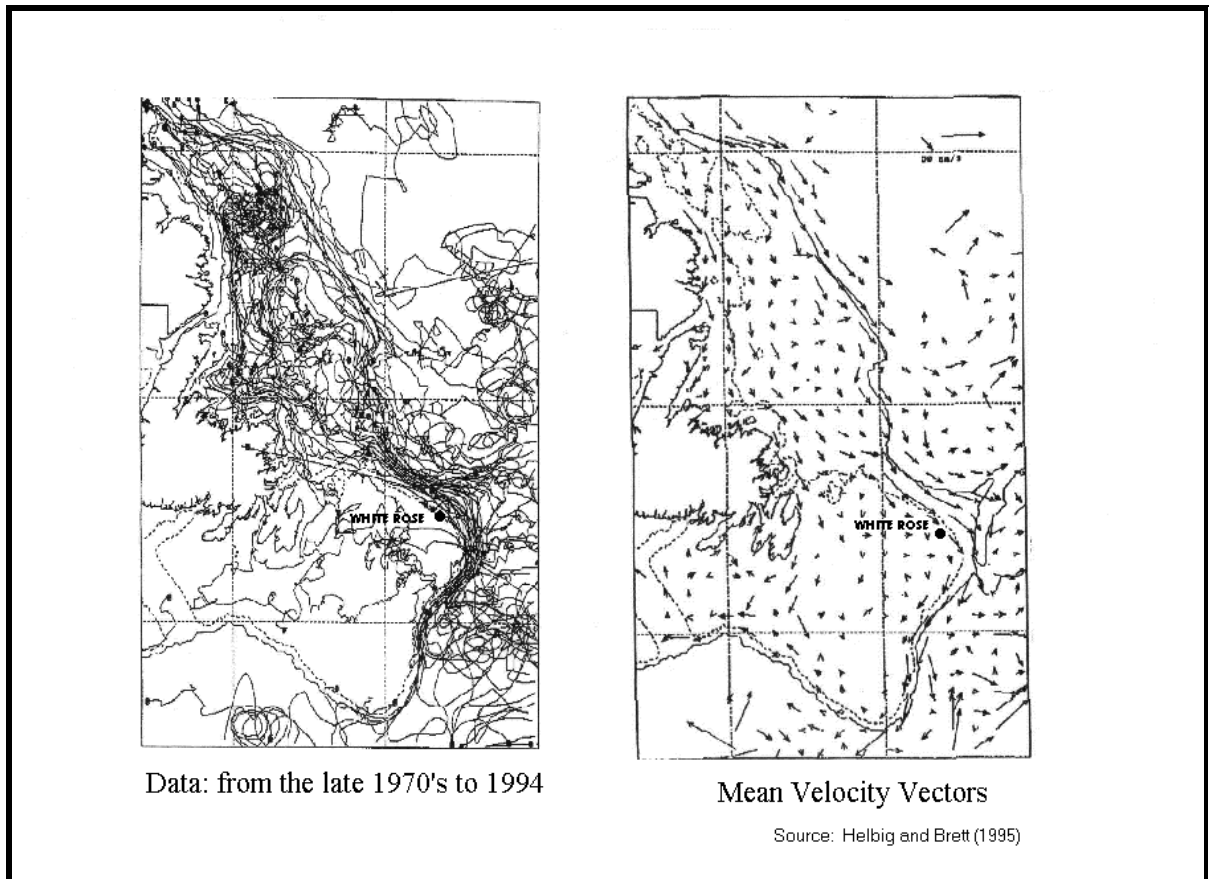


Figure 4.3 Computed Currents from Drifting Buoy Data

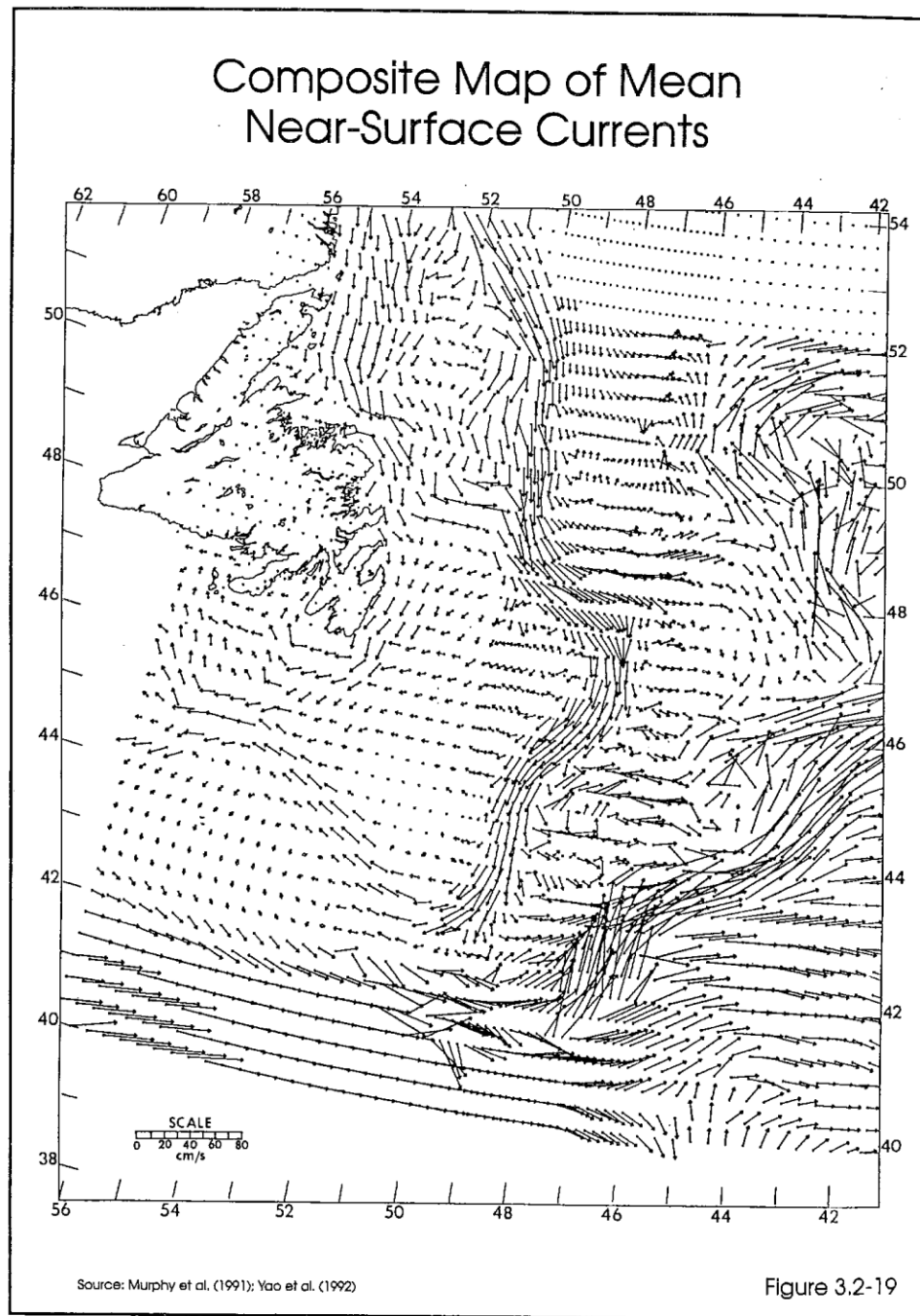


Figure 4.4 Composite Map of Mean Near-Surface Currents

The results of numerical models have also contributed to the knowledge of the circulation on the Grand Banks. The numerical model developed by Greenberg and Petrie (1988) produced a detailed, high-resolution presentation of the barotropic (vertically, uniform

currents) mean circulation on the Grand Banks and surrounding areas. The 1988 model was a first step in modeling the mean circulation in the Newfoundland Shelf region and did not take into account the effects of stratification in the water column and the effects of wind stress, both important driving forces on the Newfoundland Shelf. The barotropic model was driven by a sea surface slope at a northern boundary across Hamilton Bank and adjusted to give a specified inflow over different parts of the shelf and/or the shelf edge. A map of the currents on the Newfoundland Shelf, as calculated from the Greenberg and Petrie model is presented in Figure 4.5. The major characteristics of the circulation produced by their model were: 1) a strong topographical steering of the currents; 2) the splitting of the Labrador Current into two branches north of Flemish Pass; and 3) north-westward movement of water over the eastern part of the Grand Banks.

Narayanan et al. (1996) compared the current meter data sets obtained between 1980 and 1993 with the barotropic model results of Greenberg and Petrie (1988), and found that the model predictions were more or less in agreement with observations made at the comparison mooring sites. The model underestimated the magnitude of the offshore branch of the Labrador Current along the northeast Newfoundland Shelf. It did not duplicate the clockwise circulation on Flemish Cap as indicated by drifter data (Ross, 1980) or the eddy like features in the slope region south of Flemish Pass. The intersection between the Labrador Current and the North Atlantic Current was not taken into consideration in the model. Since the development of the 1988 barotropic model, modeling of currents on the Grand Banks has been an on-going process by Fisheries and Oceans Canada.

Hukuda et al. (1989) developed a three-dimensional model to estimate the mass exchange at different depths. Similar to the Greenberg and Petrie model (1988), their model was driven by specifying the sea level along a northern boundary. Similarly, their model reproduced the circulation pattern found by Greenberg and Petrie (1988). They examined the onshore-offshore mass exchange over the south-eastern edge of the Grand Banks and found that the southward flowing Labrador Current along the shelf break leads to an onshore flux in the upper part of the water column and an offshore flux in the bottom Ekman layer.

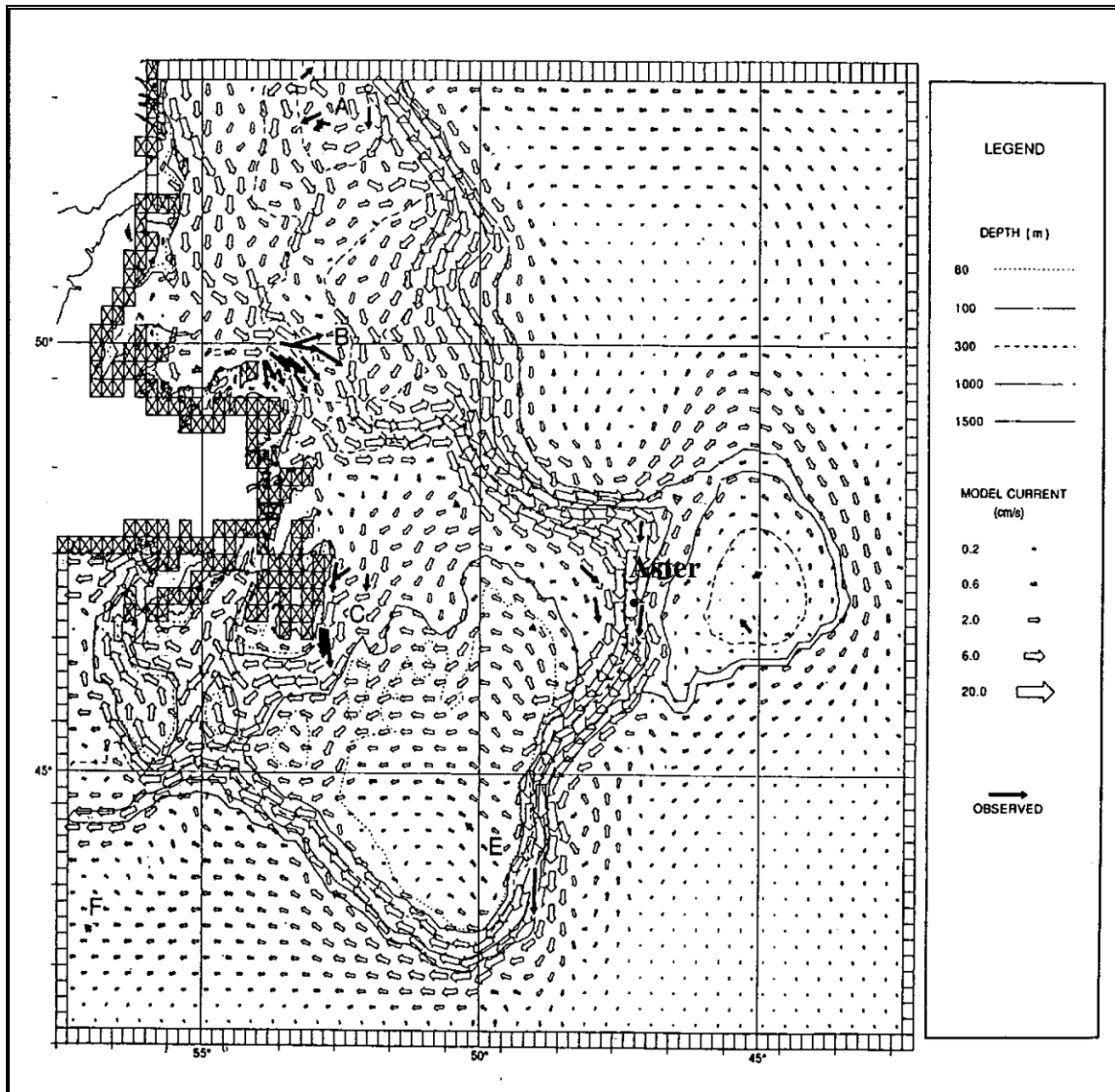


Figure 4.5 Model-Derived Depth-Averaged Currents

Source: Greenburg and Petrie (1988)

A recent modeling study by Han and Wang (2006), found that the circulation over the Newfoundland Shelf and its northeast slope is dominated by equator-ward flows associated with the inshore and offshore Labrador Current. Their model study supported a significant seasonal cycle in the current regime with strong flows during the fall/winter and weak flows in spring/summer. This is demonstrated in Figure 4.6 which shows the model currents near the surface (30 m) and near the bottom (20 m) above the ocean floor, for the months of May and November.

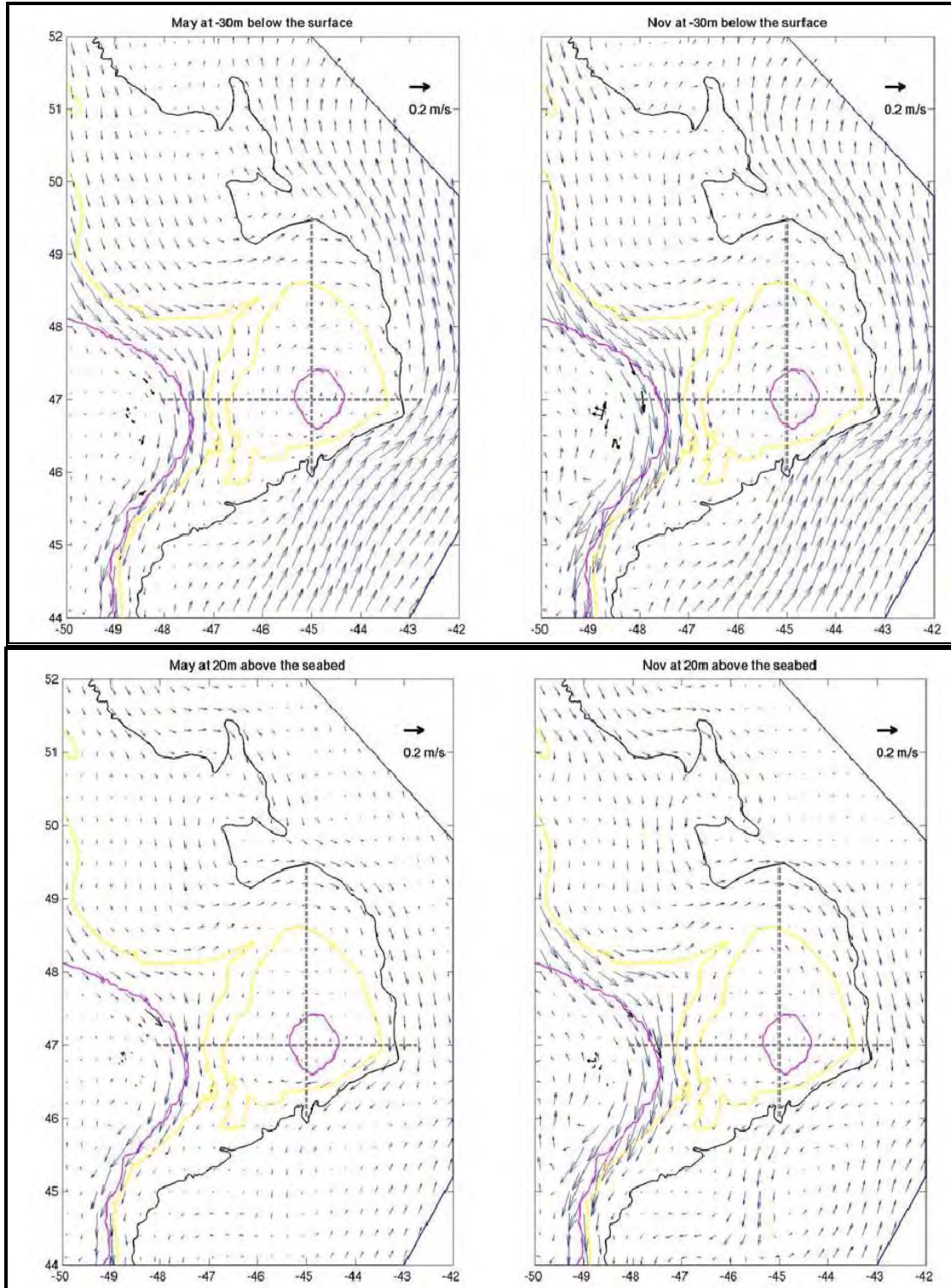


Figure 4.6 Modeled Currents at 30 m below the Surface (left) and 20 m above the Seabed (right) in May (above) and November (below)

Source: Han and Wang (2006)

4.2 Currents in the Project Area

The project study area (Figure 4.7) was divided into two sub-areas; referred to as the northern and southern sections of the study area. The northern section includes southern Orphan basin, the northeast Newfoundland Slope, Sackville Spur and northern Flemish Pass. The southern section includes western Flemish Pass and the northern Grand Banks where White Rose and Terra Nova are located.

4.2.1 Northern Section of the Study Area

Moored current meter data is available for six locations in the northern sections. The locations of the moorings are shown in Figure 4.7. The data was collected in 1976, 1979, 1992, 2003, 2007 and 2009. Information on the quantity of current meter data is presented in Table 4.1.

Table 4.1 Current meter data for the northern section of the study area

Mooring #	Location	Date	Depth (m)	Latitude	Long
1	Southern Orphan Basin	Jul 16-19, 1978	2738	49°30'N	47°05'W
2	Southern Orphan Basin	Sept 18, 2006 – Feb 10, 2007	300	49°25'N	48°11'W
2	Southern Orphan Basin	Sept 18, 2006 – Feb 10, 2007	650	49°25'N	48°11'W
2	Southern Orphan Basin	Sept 18, 2006 – Feb 10, 2007	1850	49°25'N	48°11'W
2	Southern Orphan Basin	Sept 18, 2006 – Feb 10, 2007	2328	49°25'N	48°11'W
3	NE Nfld Slope	Dec 1991- May 1992	143	47°51'N	48°01'W
3	NE Nfld Slope	Dec 1991- May 1992	293	47°51'N	48°01'W
4	Sackville Spur	Apr 11 – Jul 17, 1976	467	48°00'N	47°07'W
4	Sackville Spur	Apr 11 – Jul 17, 1976	767	48°00'N	47°07'W
5	Northern Flemish Pass	Jan 31 – Apr 13, 2003	20	48°13'N	46°15'W
5	Northern Flemish Pass	Jan 31 – Apr 13, 2003	465	48°13'N	46°15'W
5	Northern Flemish Pass	Jan 31 – Apr 13, 2003	965	48°13'N	46°15'W
6	Northern Flemish Pass	Dec 22, 2008 – Apr 4, 2009	1013	48°18'N	46°12'W

Southern Orphan Basin

Data was collected in southern Orphan Basin between September 2006 and February 2007 at depths of 300 m, 650 m, 1850 m and 2328 m at Chevron Canada's Great Barasway F-66 Well. Statistics for the mean and maximum current speeds and average velocities are presented in Table 4.2. The maximum speed varied between 36.3 cm/s at a

depth of 300 m to a speed of 23.6 cm/s at 2328 m. The mean speed varied between 11.6 cm/s and 7.1 cm/s over the same depth range. The mean velocities were only slightly lower than the mean speeds because there was little variability in the currents as shown in the progressive vector diagrams in Figure 4.8.

There was also four days of data collected in southern Orphan Basin in July 1978. For this short record, the mean speed was 6.9 cm/s and the maximum speed was 18.3 cm/s in a south southeast direction.

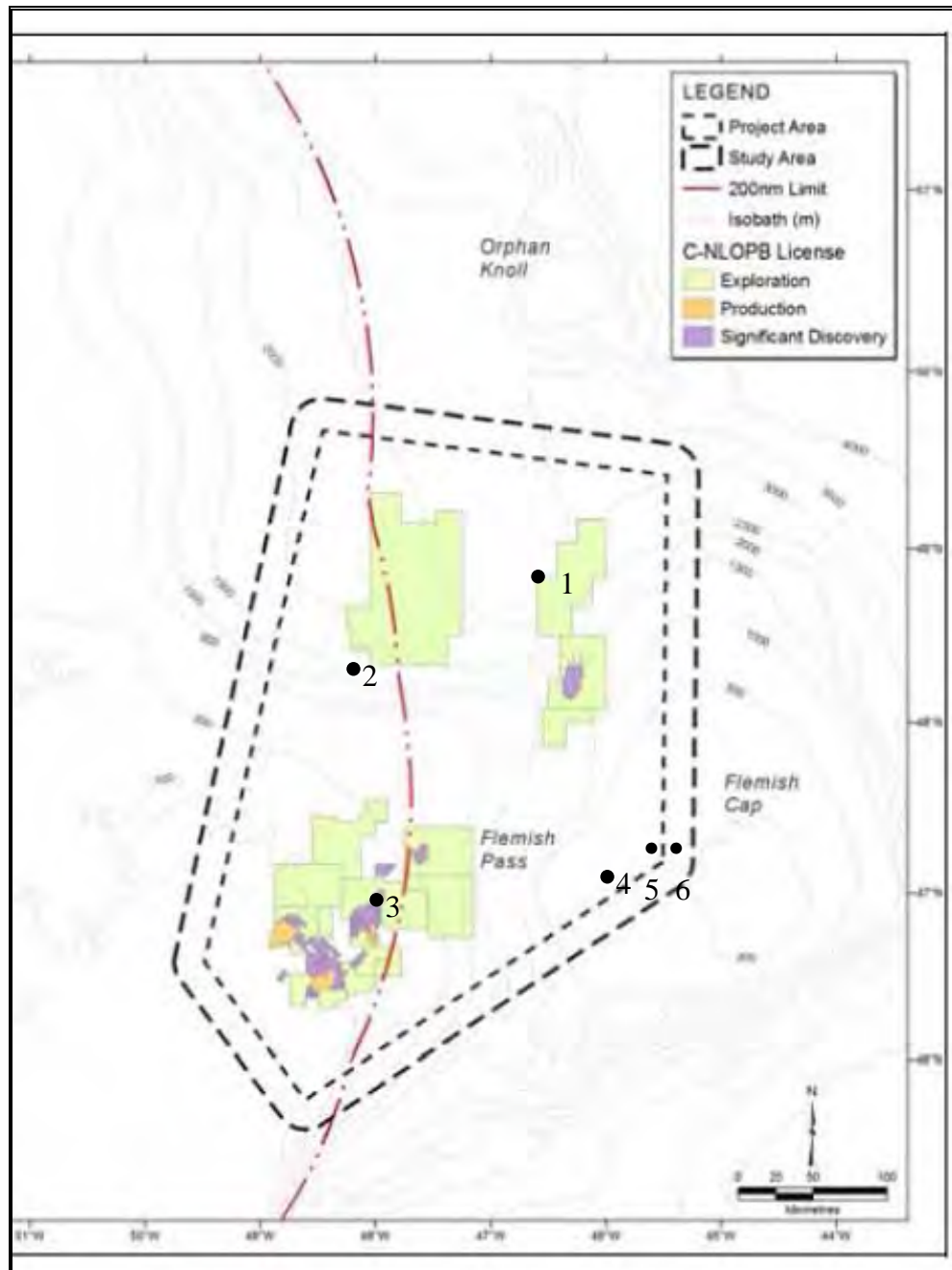


Figure 4.7 Mooring location in the northern section of the study area

Table 4.2 Current statistics for the northern section of the study area

Mooring #	Period	Depth (m)	Maximum Speed (cm/s)	Mean Speed (cm/s)	Mean Velocity (cm/s)	Direction
1	Jul, 1978	2738	18.3	6.9	6.5	south southeast
2	Sep – Feb 2007	300	36.3	11.6	8.2	south-southeast
2	Sep – Feb 2007	650	31.3	10.1	8.2	south-southeast
2	Sep – Feb 2007	1850	24.0	8.9	8.0	south
2	Sep – Feb 2007	2328	23.6	7.1	5.8	southeast
3	Dec – May, 1992	143	77.5	26.9	24.5	southeast
3	Dec – May, 1992	293	54.2	17.7	11.3	east
4	Apr – Jul, 1976	467	27.2	8.1	5.9	south
4	Apr – Jul, 1976	767	37.3	8.3	6.7	south
5	Jan – Apr, 2003	20	50.4	15.9	11.1	south
5	Jan – Apr, 2003	465	30.8	6.8	5.5	southwest
5	Jan – Apr, 2003	965	32.6	9.3	6.8	southwest
6	Dec – Apr, 2009	1013	23.3	7.1	1.9	southwest

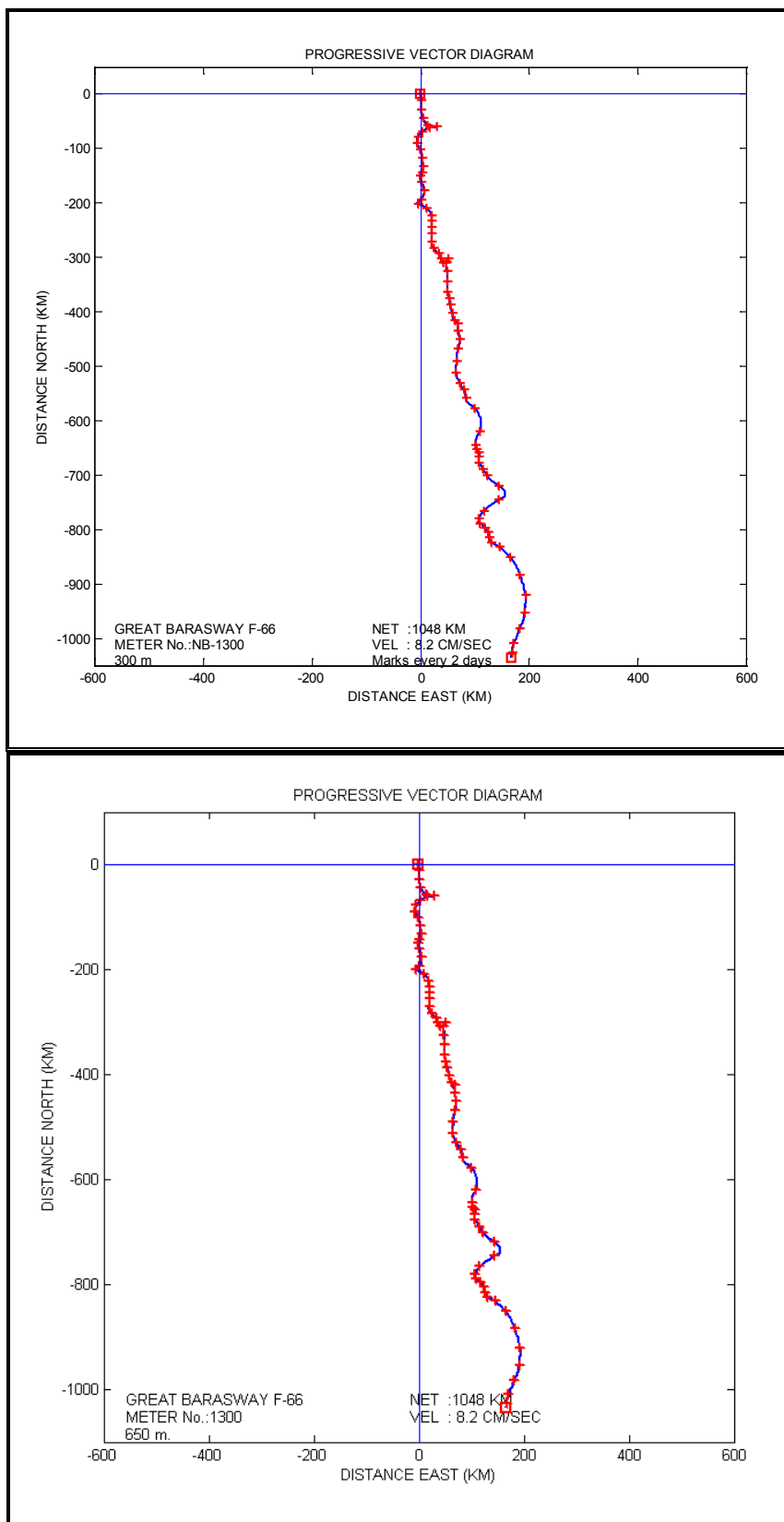


Figure 4.8 Progressive vector diagrams of currents in Orphan Basin

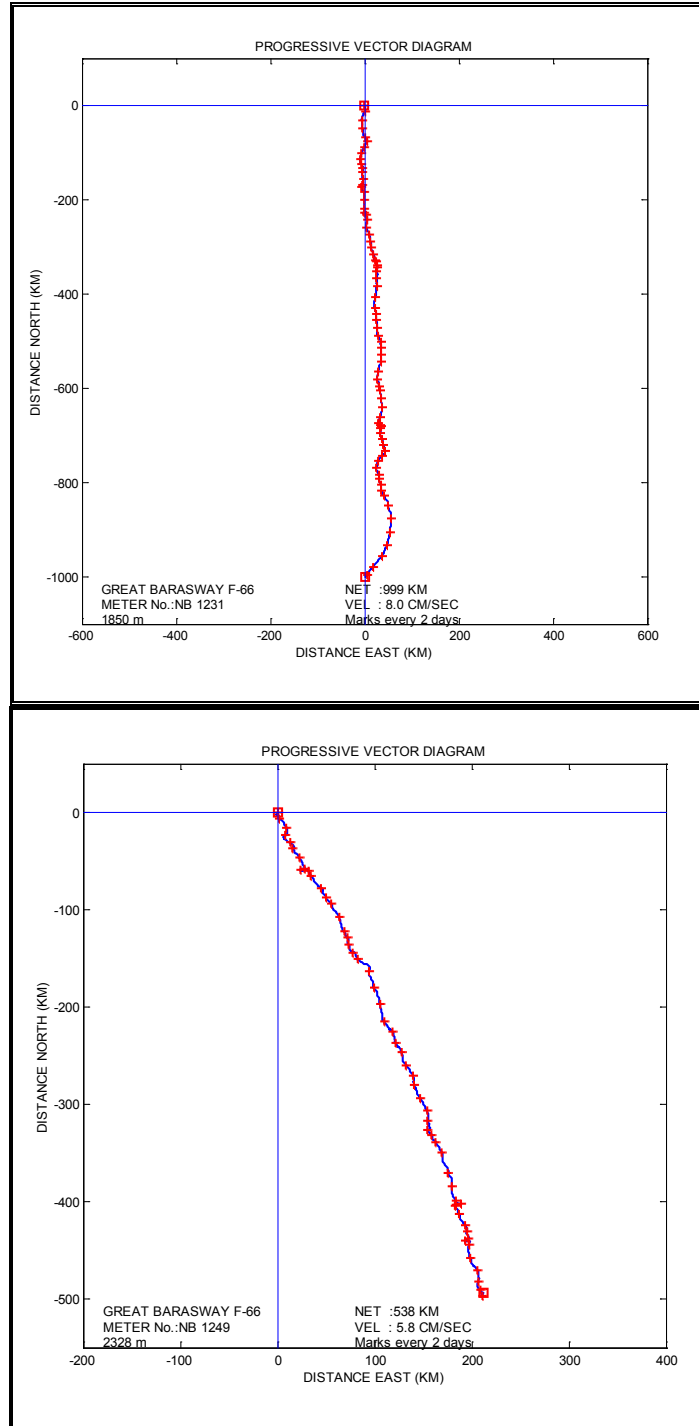


Figure 4.8 (cont.) Progressive vector diagrams of currents in Orphan Basin

Northeast Newfoundland Slope

Mooring No. 3 was on the northeast Newfoundland Slope in the area before the Labrador Current splits into two streams. At this location the current speeds were higher than on the Sackville Spur or in Flemish Pass. Statistics on the current speeds are presented in

Table 4.2 for water depths of 143 m and 293 m. At a depth of 143 m, the mean current speed was 26.9 cm/s and the maximum speed was 77.5 cm/s. At a depth of 293 m, the mean current speed was 17.7 cm/s and the maximum speed was 54.2 cm/s for depths of 143 m and 293 m, respectively. At a depth of 143 m, the mean velocity was in a southeast direction and at a depth of 293 m the current flowed in a east southeast direction (Figure 4.9).

Sackville Spur

The current meter mooring on the Sackville Spur was located in a water depth of approximately 800 m. The currents were measured at depths of 467 m and 767 m. Statistics for the mean and maximum current speeds and average velocity are presented in Table 4.2. At a depth of 467 m, the mean current speed was 8.1 cm/s and the maximum speed was 27.2 cm/s. At a depth of 767 m, the mean current speed was 8.3 cm/s and the maximum speed was 37.3 cm/s. The velocity was 5.9 cm/s in a southerly direction at a depth of 467 m and 6.7 cm/s in a south southwest direction at a depth of 767 m. During April the current flowed in a northeast direction at both depths whereas during the following months the current flowed towards the south (Figure 4.10). This is the area where the offshore branch of the Labrador splits into two streams, one stream flowing northeast around the top of Flemish Cap and the other stream flowing south through Flemish Pass.

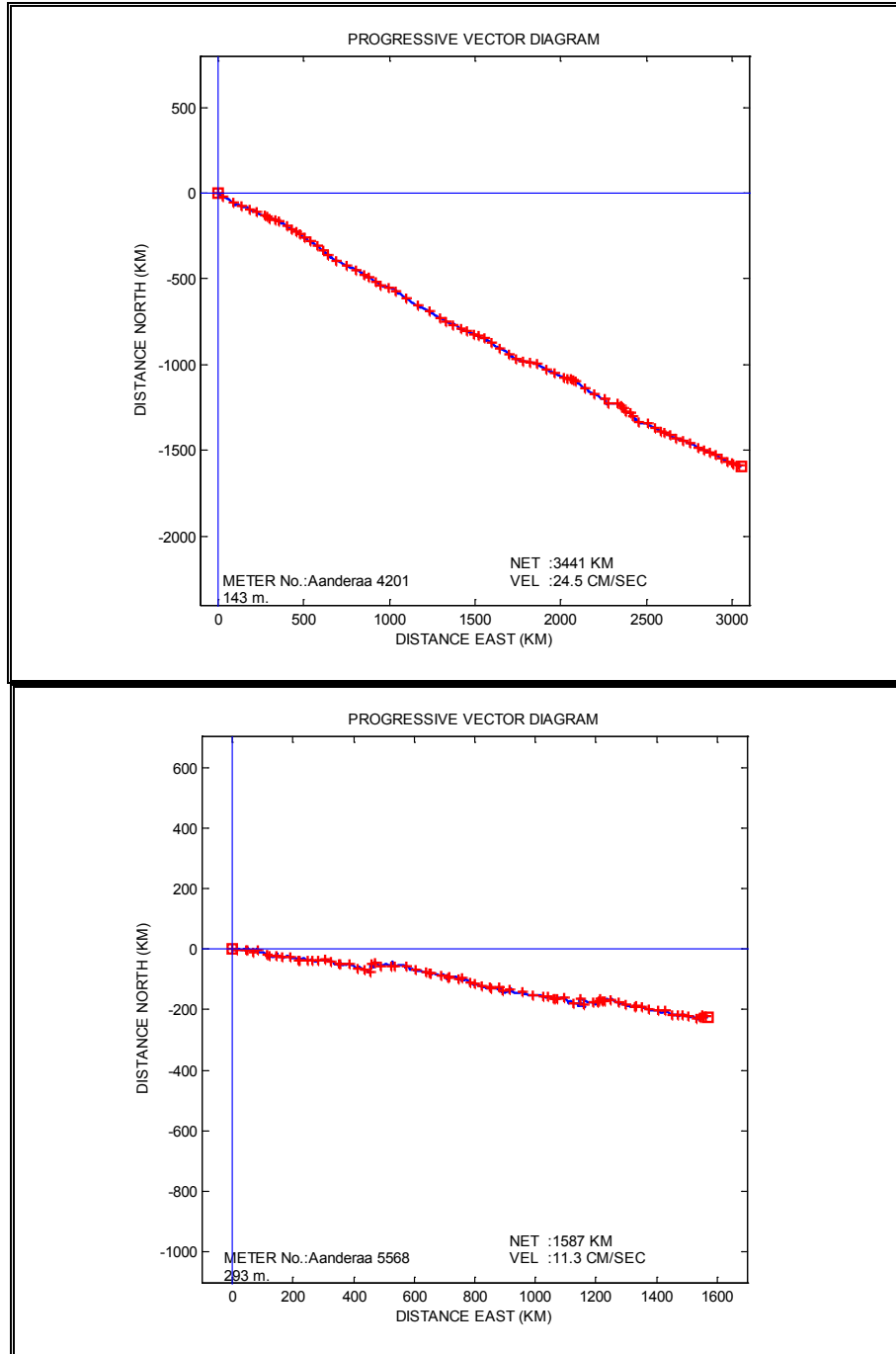


Figure 4.9 Progressive vector diagrams for the currents on the northeast Newfoundland Shelf at 143 m and 293 m

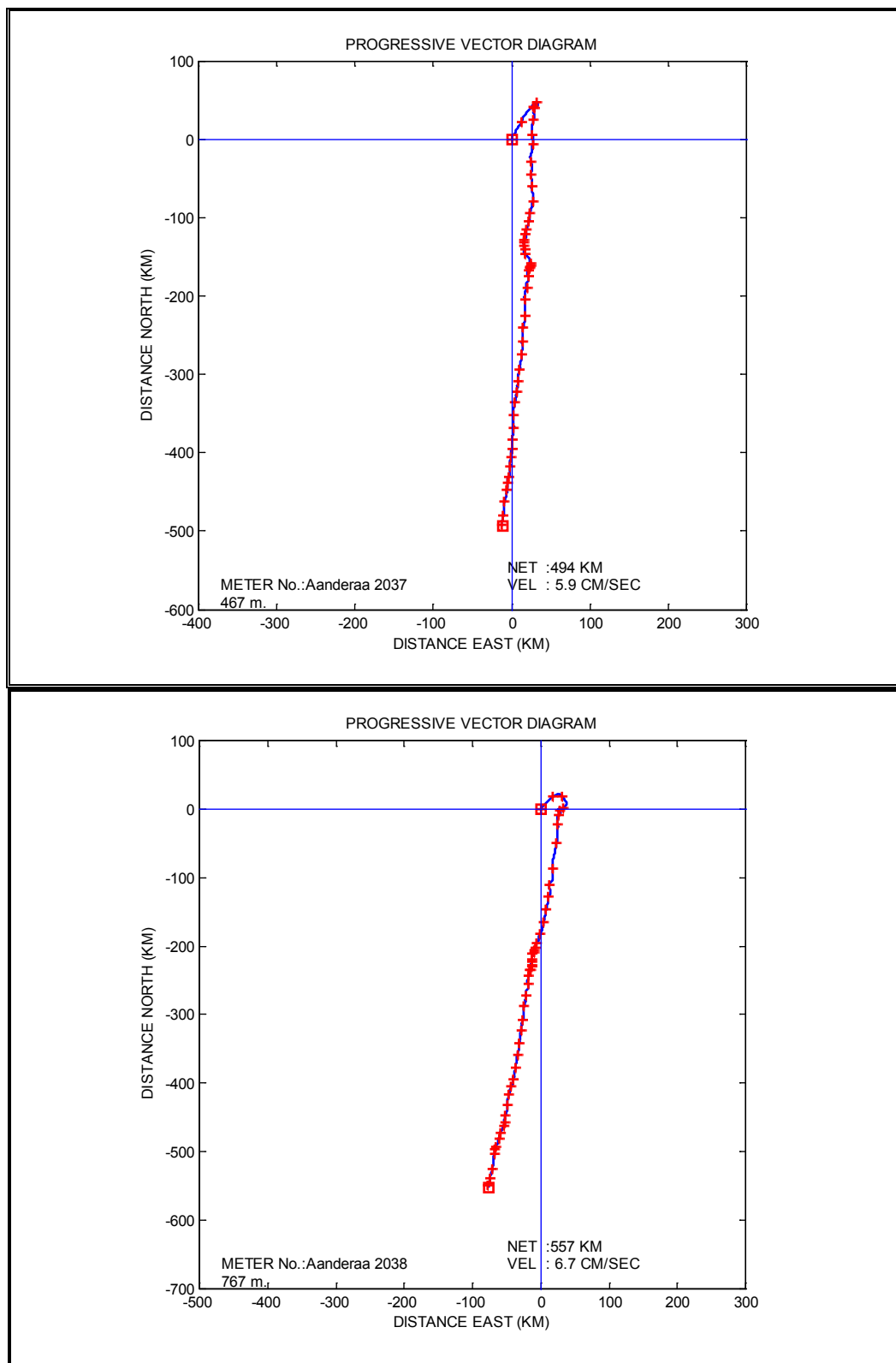


Figure 4.10 Progressive vector diagrams for the currents on the Sackville Spur at 467 m and 767 m

Northern Flemish Pass

Current data was collected at the Mizzen site in northern Flemish Pass between February and April, 2003 at depths of 20 m, 465 m and 965 m. Statistics for the mean and maximum current speeds and average velocity are presented in Table 4.2. The maximum speeds were 50.4 cm/s, 30.8 cm/s, 32.6 cm/s and the mean speeds were 15.9 cm/s, 6.8 cm/s, and 9.3 cm/s at depths of 20 m, 465 m and 965 m, respectively. The current flowed in a southerly direction near the surface and in a southwest direction in the deeper water as shown in Figure 4.11.

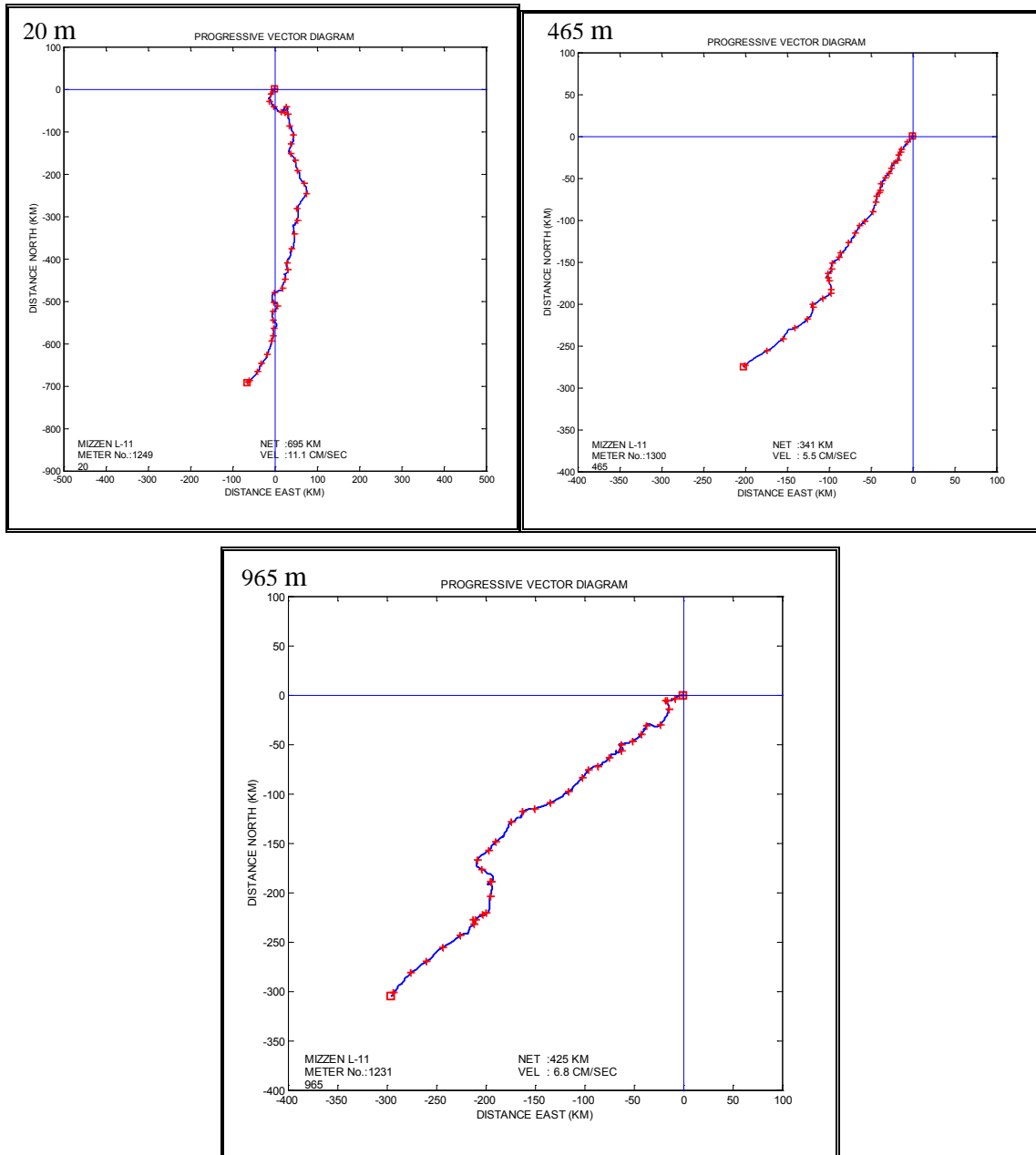


Figure 4.11 Progressive vector diagram of currents in northern Flemish Pass

4.2.2 Southern Section of the Study Area

The southern section of the study area includes the northeast Grand Banks and Flemish Pass. There are current data available from the eight moorings on the western side of Flemish Pass. These data sets are from well sites Lancaster F-70 and Tuckamore B-27 and data from the Bedford Institute of Oceanography. The locations of the moorings in Flemish Pass are shown in Figure 4.12. On the northeast Grand Banks more data is available, mainly from the Terra Nova and White Rose development sites.

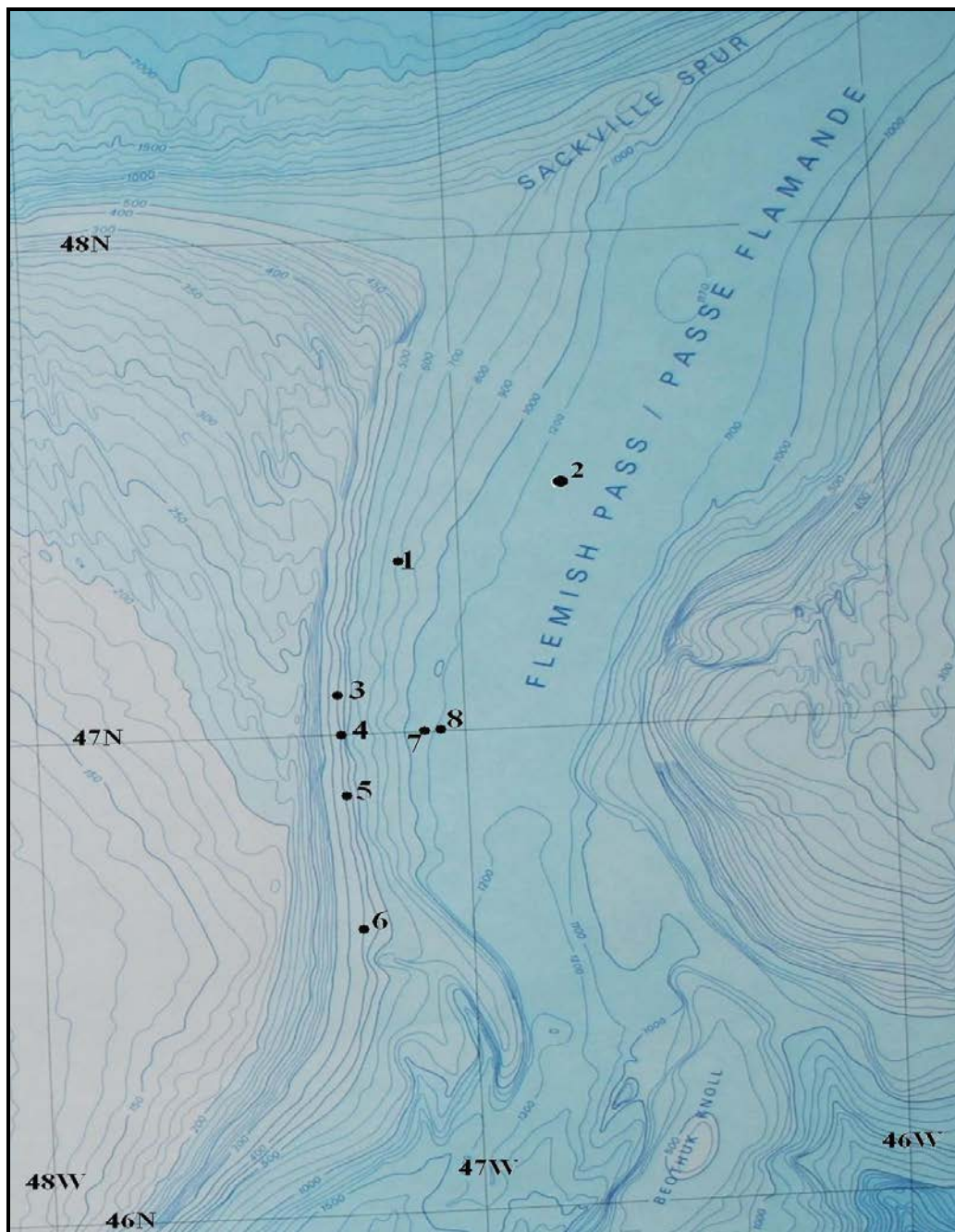


Figure 4.12 Location of current moorings in Flemish Pass

Western Flemish Pass

There is current data available for eight locations on the western side of Flemish Pass. These locations are shown in Figure 4.12. Statistics of the maximum current speeds, mean current speeds, and mean velocities are presented in Table 4.3. The maximum current speed of 86.5 cm/s was measured at a depth of 100 m at two locations near the 500 m depth contour. The mean speeds at 100 m were also high at this location with values of approximately 45 cm/s. The current speeds are high on the western side of Flemish Pass because this is the path of the offshore stream of the Labrador Current. The currents are in a southerly direction (Figure 4.13) along the bathymetric contours.

Table 4.3 Current Statistics for the western side of Flemish Pass

Mooring #	Period	Depth (m)	Max Speed (cm/s)	Mean Speed (cm/s)	Mean Velocity (cm/s)	Direction
1	Apr– Jul 1986	346	31.9	11.4	7.0	South
1	Apr- Jul, 1986	589	34.3	10.2	7.3	South southwest
1	Jul – Oct, 1986	67	63.5	30.7	29.7	South southwest
1	Jul – Oct, 1986	334	43.1	17.8	17.5	South southwest
1	Jul – Oct, 1986	592	40.6	13.4	13.0	South southwest
2	May – Jun, 2003	55	44.4	18.8	8.2	South southwest
2	May – Jun, 2003	500	19.6	11.0	9.2	South southwest
2	May – Jun, 2003	1000	25.4	10.8	8.2	South southwest
3	May – Jun, 2003	300	45.6	13.1	12.6	South
4	Oct – Dec, 1985	50	44.6	15.7	15.6	South southwest
4	Oct – Dec, 1985	100	86.5	39.4	38.5	South southwest
5	Oct – Jan, 1986	100	85.9	46.4	45.5	south
6	Oct – Jan, 1986	112	86.5	44.6	43.8	South southwest
6	Oct – Jan, 1986	260	69.7	33.3	33.3	South southwest
6	Oct – Jan, 1986	343	52.5	18.7	16.3	South southwest
6	Jul – Sep, 1983	20	67.5	23.7	5.2	Southeast
6	Jul – Dec, 1983	110	59.8	21.2	18.8	South southeast
6	Jul – Dec, 1983	214	57.9	16.4	14.7	South east
7	Jul – Oct, 1976	168	46.1	20.3	19.5	South
7	Jul – Oct, 1976	481	24.4	11.4	11.1	South southwest
7	Jul – Oct, 1976	7981	21.8	9.9	9.7	South southwest
7	Jul – Oct, 1976	961	25.9	10.3	9.9	South southwest
8	Apr – Aug, 1986	300	26.3	8.5	7.2	South southwest
8	Apr – Aug, 1986	611	17.8	6.6	5.1	South southwest
8	Apr – Aug, 1986	950	42.2	11.9	11.3	South southwest

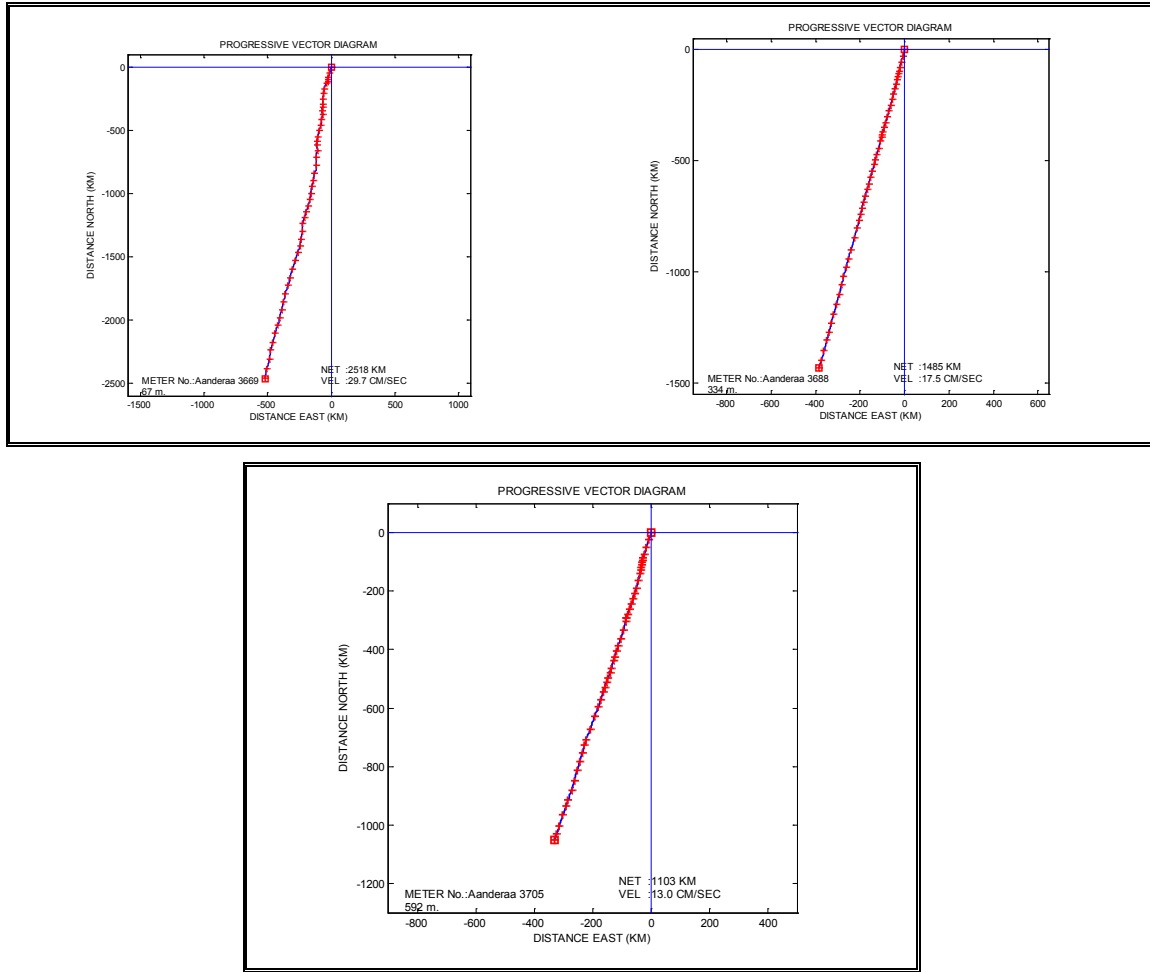


Figure 4.13 Current at the western side of Flemish Pass

Northeast Grand Banks

Tables 4.4 to 4.6 present current values at Terra Nova measured near the surface in a water depth of 20 m, mid-depth in 45 m to 50 m, and at 10 m above the seabed. Tables 4.4 to 4.6 show typical maximum speeds and directions, mean velocities, and mean speeds for each month. The identifier in the table is to identify the data set from which the values for the maximum speeds and directions were extracted. The mean speeds and velocities have been averaged from different data sets covering a few years for each month and depth. It is important to note that because the degree of variability at Terra Nova is high, different data sets will have the maximum currents in different directions and the mean velocities may also be different in both magnitude and direction. The variability and current direction is shown in a sample progressive vector diagram in Figure 4.14.

The current at Terra Nova can be divided into its main components consisting of a residual or mean velocity, tidal currents, and low frequency components. The residual flow or mean velocity tends to be small as seen from the values in Tables 4.4 to 4.7 and

range between 0.2 cm/sec to 5.6 cm/sec. The maximum speeds were 77 cm/s, 42 cm/s and 42 cm/s for near surface, mid-depth, and near bottom, respectively.

The tidal currents are a significant portion of the flow on the Grand Banks. In the near surface waters, M_2 , S_2 , O_1 , and K_1 can have values which range from 6 to 9 cm/sec, 2 to 4 cm/sec, 2 to 6 cm/sec and 2 to 6 cm/sec, respectively. At mid-depth, the tidal constituents of M_2 , S_2 , O_1 , and K_1 , have values of 6 to 7 cm/sec, 1 to 3 cm/sec, 2 to 3 cm/sec, 2 to 4 cm/sec. At 10 m above bottom the constituents of M_2 , S_2 , O_1 , and K_1 have values of 0 to 7 cm/sec, 0 to 3 cm/sec, 0 to 4 cm/sec and 0 to 4 cm/sec. The individual constituents have low values, but the combination of all the tidal constituents contribute significantly to the overall flow.

The semi-diurnal tidal currents rotate through 360° twice per day in a clockwise direction. The diurnal tidal ellipses at Terra Nova are almost circular showing no preferred direction, and the semidiurnal tidal ellipses are slightly elongated in a northwest/southeast direction. Overall, the tidal currents at Terra Nova are responsible for about 30% of the variability near the surface and at mid-depth, and for 20% of the variability near the bottom.

The low frequency components are the most important contributor to the overall flow. The strongest currents have been observed to always occur during the passage of low pressure systems. Some of the flow can be attributed to direct effects of wind stress upon the sea surface as indicated by an inertial period signal in a spectral analysis of the data. The barotropic component appears to be the largest component of the strong flows. Spectral analysis shows that the low frequency components are in the period range of 4 to 7 days.

The low frequency components are also associated with transport of warmer water onto the Grand Banks. For instance, on February 9, 2002 during the passage of a low pressure system, temperature measurements at both 1 m and 10 m above bottom showed a 0.5°C sudden increase in temperature. This event was measured at two locations at 1 m above bottom, separated by a distance of 4 nautical miles. The current flow which was in a northwest direction registered the temperature increase on the eastern side of the Terra Nova field a few hours before it was recorded on the western side. The event appears to have been an advection of warmer water onto the Banks from the southwest. This event signifies that the low frequency barotropic components are probably a major contributor to the advection and mixing of warm water from the Slope to the more shallow regions on the Grand Banks.

Wind stress is also an important driving force for the surface currents on the Continental Shelf, with a distinct annual cycle of comparatively strong winds in winter and weaker more variable winds in summer. An analysis of an array of current meter data collected from January to May 1992 by De Tracey et al. (1996) on the north-eastern section of the Grand Banks showed that the near-surface currents and local wind are highly coherent in the shallow region of the Grand Banks, suggesting that the currents on the Grand Banks have a strong wind driven component.

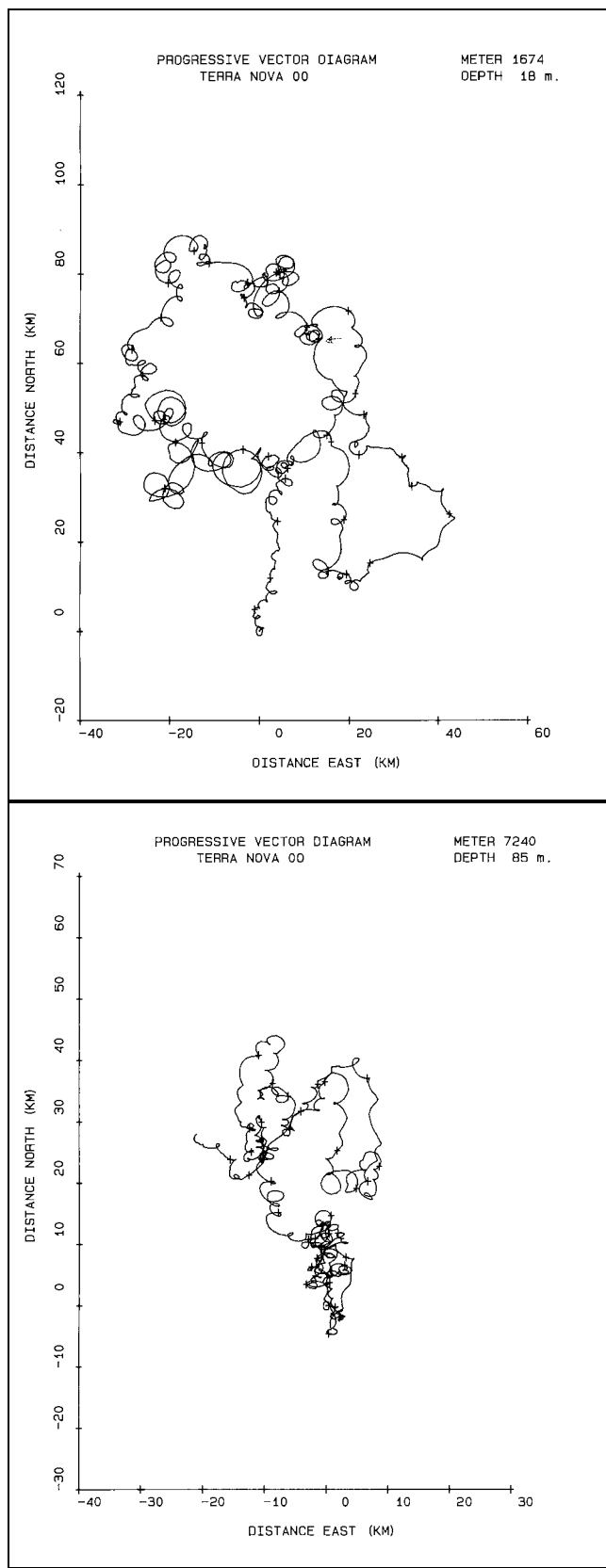


Figure 4.14 Progressive vector diagram of currents at Terra Nova

Table 4.4 Near-surface currents at Terra Nova

Month	Identifier	Max Speed (cm/sec)	Direction	Mean Speed (cm/sec)	Mean Velocity (cm/sec)	Direction (°T)
January	TN9904	48	E	13	5.6	183
February	TN0301	59	ENE	13	3.6	178
March	TH0201	45	SE,E	12	4.7	171
April	TN0101	41	N	12	1.6	170
May	TN0302	57	N	13	2.0	211
June	TN0102	52	W	12	1.7	127
July	TN0102	39	E	12	0.9	198
August	TN0003	60	NW	13	0.8	265
September	TN0003	77	SSW	18	2.0	213
October	TN0203	57	N	18	2.7	196
November	TN9904	48	E,S	14	4.3	357
December	TN9904	59	S	13	1.4	28

Table 4.5 Mid-depth currents at Terra Nova

Month	Identifier	Max Speed (cm/sec)	Direction	Mean Speed (cm/sec)	Mean Velocity (cm/sec)	Direction (°T)
January	TNC09	19	S	11	3.5	287
February	TNC09	30	W,SE,E	11	1.1	286
March	TN0201	42	SSW	10	3.0	183
April	TN0201	36	SSW	10	1.3	194
May	TN0002	31	NE	9	0.8	174
June	TN0002	34	NE,NW	10	1.7	208
July	TN0002	30	E	9	1.8	308
August	TN0102	25	E,NW	10	2.4	324
September	TN0202	25	SE,SW,W	11	1.2	177
October	TN0103	29	SW	12	1.1	305
November	TN0004	41	W	11	0.6	334
December	TN0004	37	SW	11	0.7	232

Table 4.6 Near-bottom currents at Terra Nova

Month	Identifier	Max Speed (cm/sec)	Direction	Mean Speed (cm/sec)	Mean Velocity (cm/sec)	Direction (°T)
January	TN0104	36	N	12	4.2	193
February	TN0301	42	E,SE	12	2.6	167
March	TN0201	32	SE,S,SW	11	2.5	177
April	TNC009	27	N	9	3.0	205
May	TN0002	28	E	8	1.3	159
June	TN0002	26	NE	8	0.7	169
July	TN0002	20	NE	8	0.5	296
August	TN0002	24	NW	10	2.0	310
September	TN0002	30	NE	10	0.2	135
October	TN0003	41	E	10	0.4	296
November	TN0303	29	NE,SE,SW,N	11	0.6	89
December	TN0303	32	NW,N	11	0.4	283

Table 4.7 to 4.9 show typical maximum current speeds and directions, mean velocities, and mean speeds for each month from data archived in the Bedford Institute of Oceanography for the White Rose location. The maximum current speeds have been selected from particular data sets while the mean speeds and velocities have been averaged over the available data.

There are some fundamental differences in the circulation regime at White Rose as compared with Terra Nova. At Terra Nova, the currents are characterized by a very weak residual flow because the main flow is overshadowed by the magnitude of the variabilities. At White Rose there are less variabilities overall, but the currents are more likely to be flowing in unexpected directions for a long period of time. This variability can be seen in the annual progressive vector diagrams in Figures 4.15.

The percentage of the variability of the flow attributable to the tidal currents is similar at White Rose and Terra Nova. At both locations the tidal currents are responsible for about 30% of the flow at mid-depth and for about 20% near bottom. Near the surface the tidal currents account for about 30% of the variability at Terra Nova and for 20% of the variability at White Rose.

Near surface the magnitude of the tidal constituents for M_2 , S_2 , K_1 , and O_1 vary from 0.9 to 7.0 cm/sec, 0.4 to 1.9 cm/sec, 1.5 to 5.1 cm/sec and 0.8 to 3.1 cm/sec, respectively (Oceans Ltd, 2001). At mid-depth, the values of M_2 , S_2 , K_1 , and O_1 vary from 0.2 to 5.8 cm/sec, 0.2 to 2.8 cm/sec, 1.0 to 5.3 cm/sec, and 0.4 to 3.8 cm/sec, respectively. At 10 m above the sea bed the values of M_2 , S_2 , K_1 , and O_1 vary from 0.2 to 6.1 cm/sec, 0.1 to 2.3 cm/sec, 1.0 to 5.1 cm/sec and 0.3 to 3.6 cm/sec, respectively.

The currents at White Rose will be influenced by the same driving forces as at Terra Nova. The low frequency oscillations on a synoptic scale due to the passage of low pressure systems should be as prevalent at White Rose as at Terra Nova. Since White Rose is located closer to the Continental Shelf break, there is bound to be some influence from the interactions between the Labrador Current and the branch of the North Atlantic Current which enters Flemish Pass (Figure 4.2).

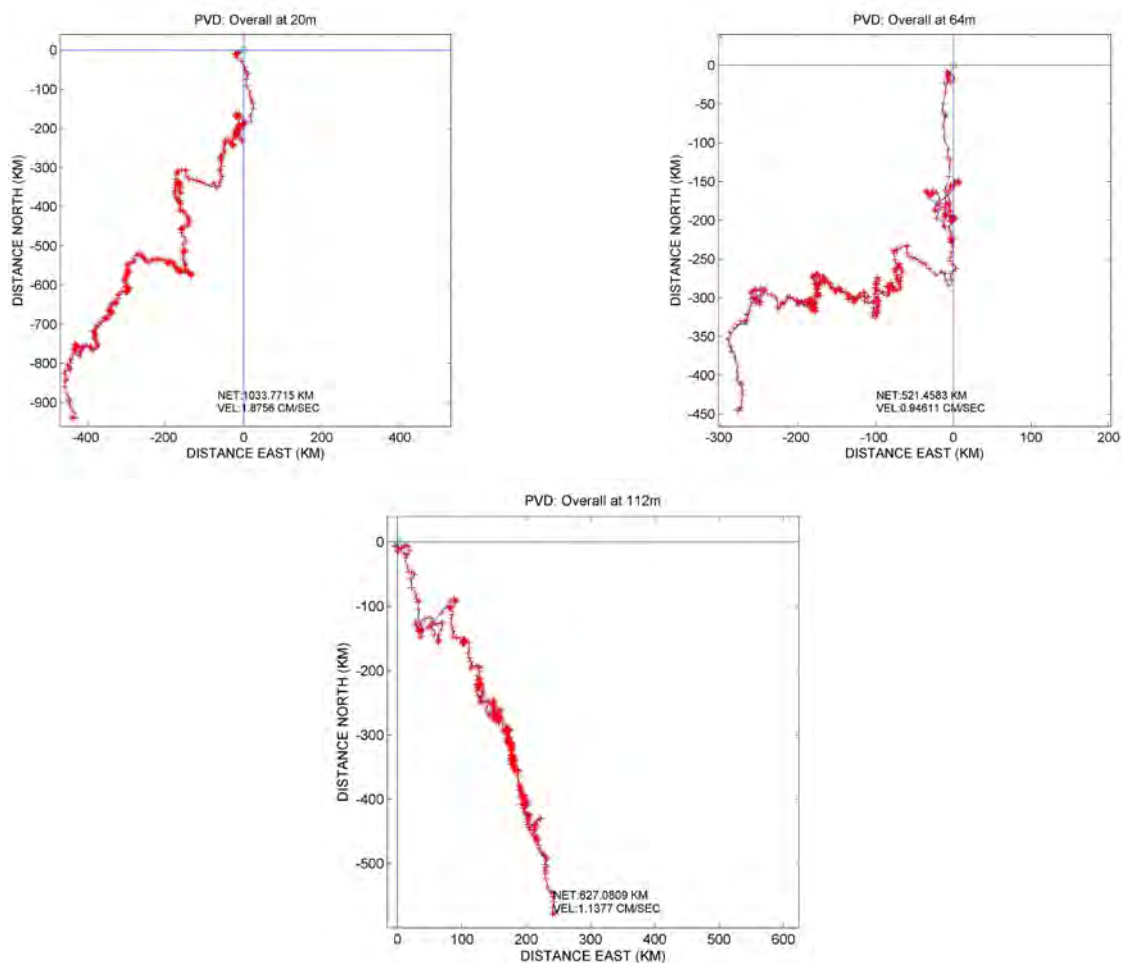


Figure 4.15 Annual progressive vector diagrams for depths of 20 m, 64 m, and 112 m at White Rose

Table 4.7 Near-surface currents at White Rose

Month	Identifier	Max Speed (cm/sec)	Direction	Mean Speed (cm/sec)	Mean Velocity (cm/sec)	Direction (°126T)
January	WRB07	51	SE	15	2.7	126
February	TRE87	38	SSE	15	9.2	127
March	TRE87	40	E	19	6.2	130
April	WRL08	40	S	11	4.0	333
May	WRH20	50	E	12	3.3	153
June	WRH20	67	SW	15	2.2	78
July	WRB07	46	WSW	13	0.8	177
August	WRB07	61	NE	16	1.6	197
September	WRN30	90	N	21	8.3	202
October	WRB07	81	SE	20	7.9	211
November	WRN02	70	S	17	3.4	172
December	TRE87	47	W,S	14	3.7	47

Table 4.8 Mid-depth currents at White Rose

Month	Identifier	Max Speed (cm/sec)	Direction	Mean Speed (cm/sec)	Mean Velocity (cm/sec)	Direction (°T)
January	WRB07	39	S,W	13	3.5	196
February	WRE09	35	ESE	12	6.4	162
March	TRE87	26	SSE	12	1.6	93
April	WRL08	29	SSE	14	6.0	180
May	WRB07	37	S,N	11	3.9	158
June	WRB07	45	S	11	1.9	151
July	WRB07	36	S	9	2.5	171
August	WRB07	62	NE	11	1.5	117
September	WRB07	57	NW	12	0.7	111
October	WRB07	75	W	13	2.1	186
November	WRB07	54	N	13	1.5	100
December	TRE87	46	S	13	1.3	48

Table 4.9 Near bottom currents at White Rose

Month	Identifier	Max Speed (cm/sec)	Direction	Mean Speed (cm/sec)	Mean Velocity (cm/sec)	Direction (°T)
January	TRE87	35	E	14	2.5	183
February	WRE09	35	SE,S,SW	12	6.0	150
March	TRE87	29	SSE,S,SSW	9	2.9	108
April	WR110	32	W	10	2.7	161
May	WRB07	41	S,N	10	2.7	162
June	WRB07	51	SW	10	1.6	142
July	WRB07	47	NE,S,W	9	1.9	196
August	WRB07	65	E	8	1.4	203
September	WRB07	72	NNW	10	1.9	221
October	WRB07	65	N	11	2.7	189
November	WRB07	58	N	12	0.9	247
December	TRE87	39	SSE	12	1.6	124

4.3 Water Mass Structure

There are three major water masses in the study area; the Labrador Current Water between the surface and approximately 400 m, the Labrador Sea Water with a depth range between 200 m and 1500 m, and the North Atlantic Deep water with a depth range between 1500 m and 4000 m. The Labrador Sea Water and the North Atlantic Deep water are nearly homogeneous with little or no seasonal variability in water properties. The Labrador Sea Water is an intermediate layer water mass with temperatures between 2°C and 4°C and salinities between 34.86‰ and 35‰. The North Atlantic Deep Water is characterized by its high salinity (34.9 to 34.97 psu) and low temperatures (2°C to 3.5°C).

In the study area, the North Atlantic Deep Water will be found only in the southern section of Orphan Basin whereas the Labrador Sea Water will be found in Flemish Pass and on the northeast Newfoundland Slope as well as in Orphan Basin.

On the north-eastern edge of the Grand Banks the water structure is characterized by three identifiable features. The first feature is the surface layer which is exposed to interaction with the atmosphere. The surface layer experiences temperature variations from sub zero values in January to above 15°C in the summer and early fall. The salinity of the surface layer is strongly affected by wave action and local precipitation. During the summer the stratified surface layer extends to a depth of 40 m or more. During the winter the surface stratification disappears and the water column becomes well mixed due to atmospheric cooling and mixing processes from wave action. The seasonal effects can be seen in the charts in Figures 4.16 to 4.17 which show the spatial distribution of temperature and salinity at 20 m and 75 m in January and July.

The second feature of the water structure is the Cold Intermediate Layer (Petrie et al., 1988). In areas where the water is deep enough, this layer of cold water is trapped during summer between the seasonally heated upper layer and warmer slope water near the seabed (Colbourne, 2002). Its temperatures range from less than -1.5°C to 0°C (Petrie et al., 1988; Colbourne et al., 1996) and salinities vary within 32 and 33 psu. It can reach a maximum vertical extent of over 200 m (Colbourne, 2004). The Cold Intermediate Layer is the residual cold layer that occurs from late spring to fall and is composed of cold waters formed during the previous winter season. It becomes isolated from the sea surface by the formation of the warm surface layer during summer, and disappears again during late fall and winter due to the intense mixing processes that take place in the surface layer from strong winds due to the intense mixing processes that take place in the surface layer from strong winds, high waves, and atmospheric cooling.

Figure 4.18 shows average bottom temperature during the decade from 1991 to 2000. The figure shows that positive bottom temperatures are found south of 46°N. The blue area to the north of 46°N in Figure 4.18 corresponds to the average spread of the Cold Intermediate Layer. The variabilities in temperature and salinity in the area have been the subject of systematic research (Colbourne, 2004; Colbourne et al., 1997; Colbourne and Foote, 2000). These studies suggest that the water properties on the Grand Banks experience notable temporal variability. Colbourne (2004) explains that bottom temperatures ranged from near record lows during 1991 to very high values in the late 90's. The areal coverage of the Cold Intermediate Layer was highest on the Newfoundland Shelf during years 1972, 1984 and 1991 (Colbourne, 2004).

Bottom temperature and salinity maps were produced by Colbourne et al. (2007) by trawl-mounted CTD data from approximately 700 fishing tows during the fall of 2005. These maps are presented in Figure 4.19. Both Figures 4.18 and 4.19 shows that the Cold Intermediate Layer is still present near the bottom over much of the Grand Banks.

During the last 50 years there have been three warming periods in the Labrador Sea; 1960 to 1971, 1977 to 1983, and 1994 to present. In 1994, the Labrador Sea water filled the entire central part of the Labrador Sea basin within the depth range of 500 to 2400 m (Yashayaev and Clarke, 2006). The warming trend since 1994 has caused the water to become warmer, saltier, and more stratified; thus making it more difficult for winter

renewal of Labrador Sea Water to take place. Unusual warming took place in 2004 believed to have originated from waters transported north and west by the North Atlantic Current and the Irminger Current (Yashayaev and Clarke, 2006).

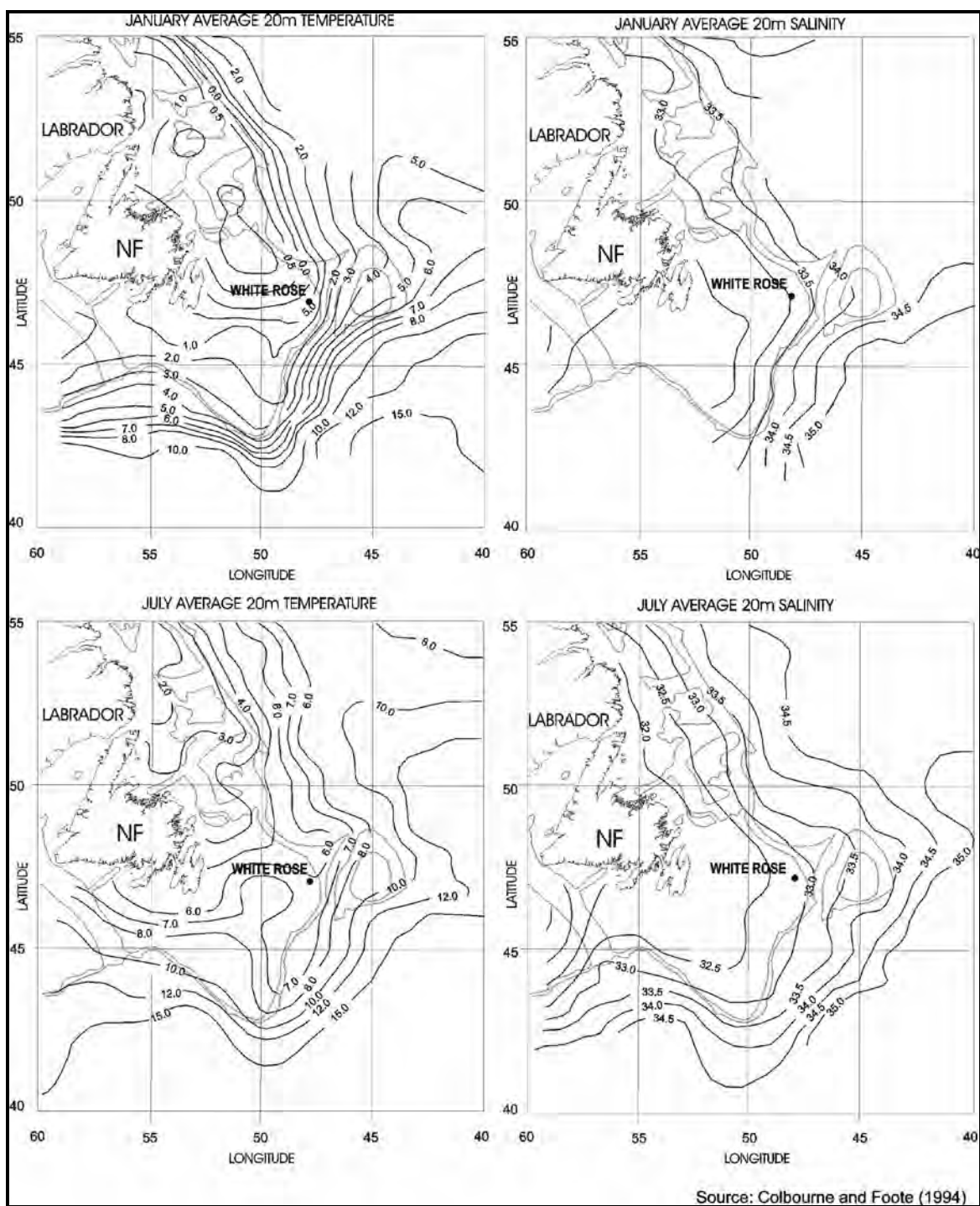


Figure 4.16 Average Spatial Distribution of Temperature and Salinity at 20 m in January and July

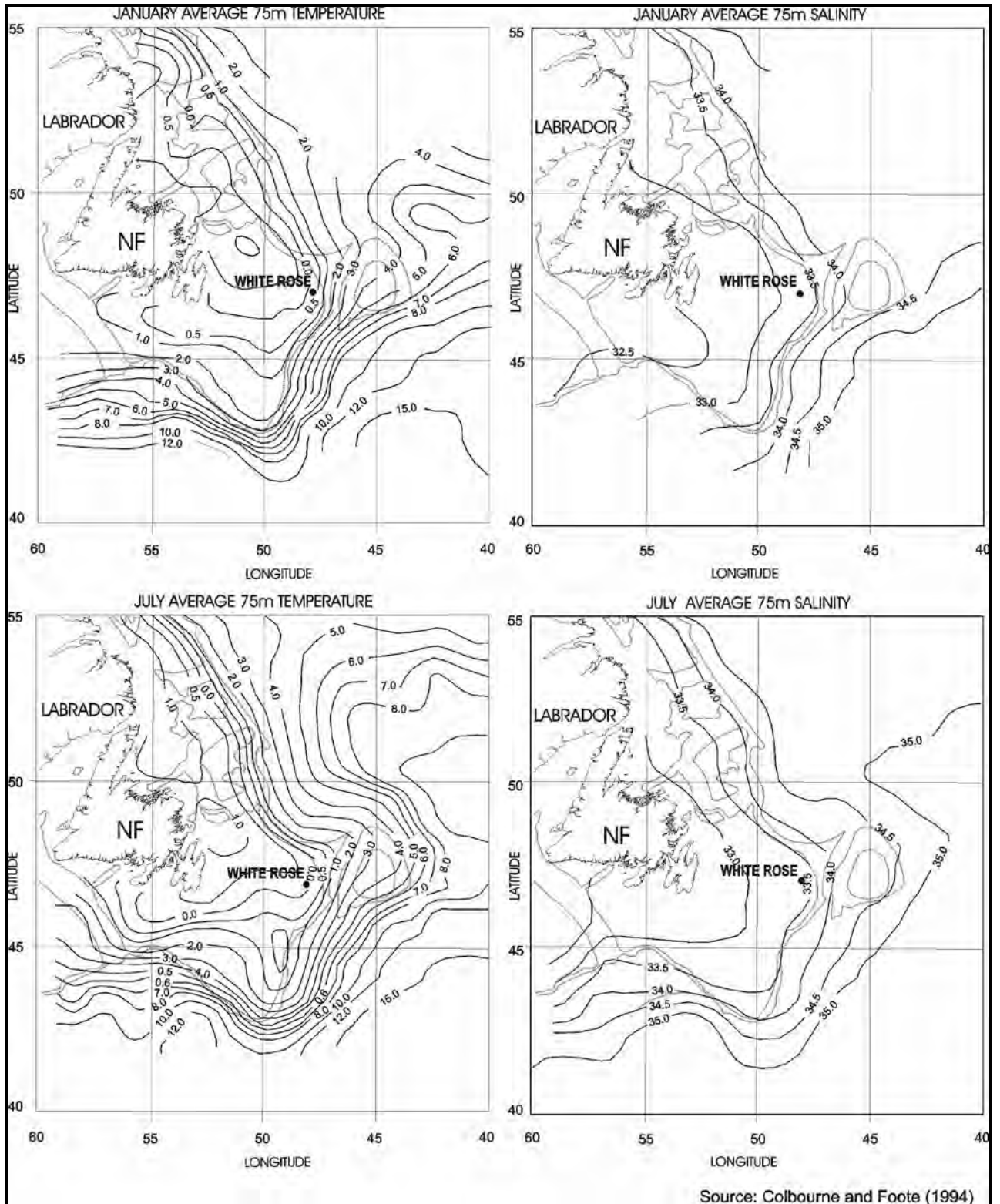


Figure 4.17 Average Spatial Distribution of Temperatures and Salinity at 75 m in January and July

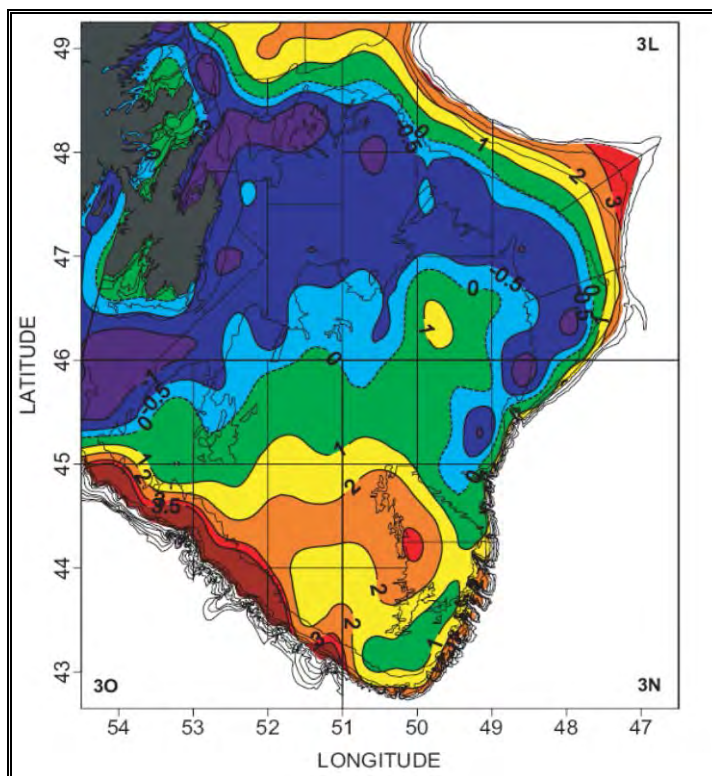


Figure 4.18 Average near bottom temperature during spring from all available data for the decade 1991-2000

Source: adapted from Colbourne, 2004

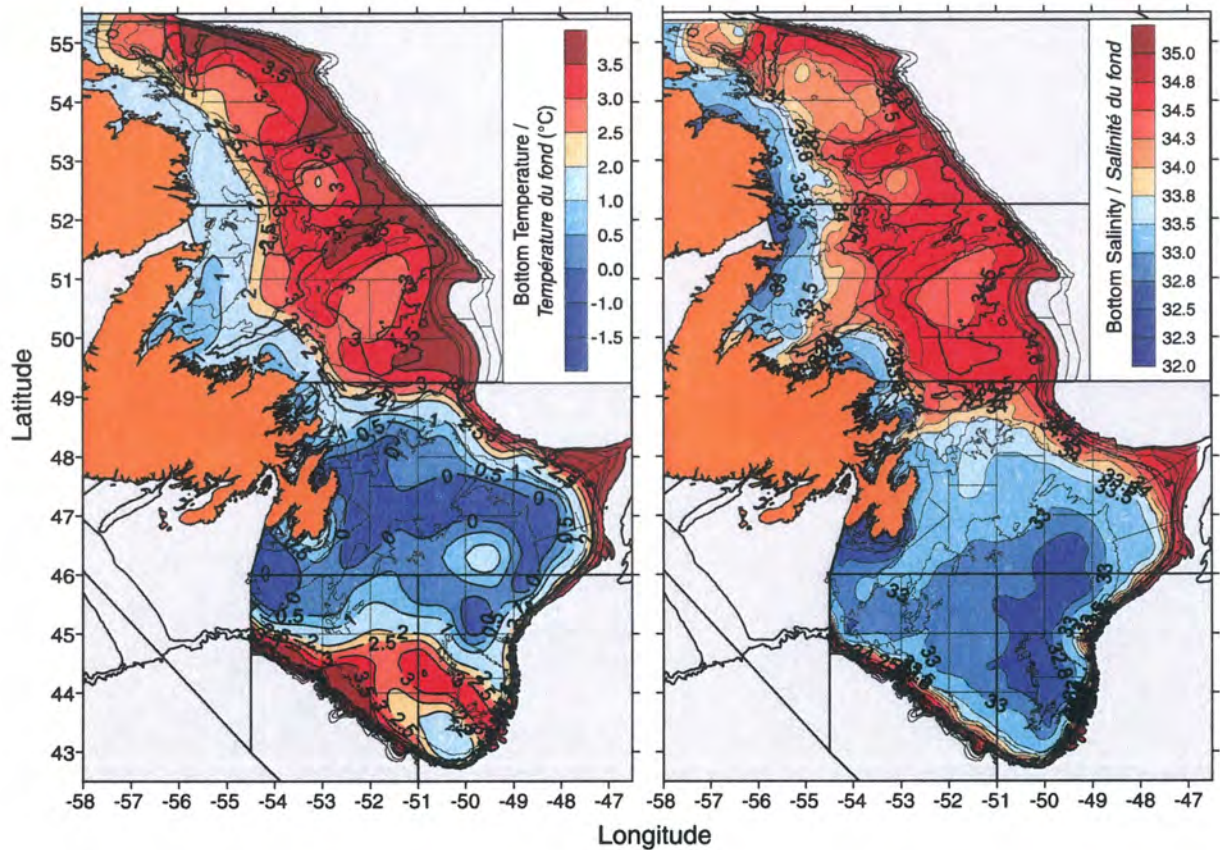


Figure 4.19 Bottom temperature and salinity maps derived for the trawl-mounted CTD data

Source: from Colbourne et al. 2007

CTD transects for the Flemish Cap and Bonavista transects are collected by Fisheries and Oceans Canada on a yearly basis. The temperature and salinity data for July and November 2011 along the Flemish Pass transect are shown in Figures 4.20 and 4.21 and those for the Bonavista transect are shown in Figures 4.22 to 4.24 for the months of May, July and November, 2011.

The temperature and salinity boundary between the water on the Shelf and the water in Flemish Pass is shown in Figures 4.20 and 4.21 from CTD data collected during 2011 along the Flemish Cap and Bonavista transects. The offshore branch of the Labrador Current flows along the Shelf break in the region of this strong density gradient. A stratified surface layer is shown in the temperature plots from July 2011, while the other monthly plot for November 2011 shows a well mixed surface layer. Figure 4.22 to 4.24 show temperature and salinity plots from the Bonavista transect. During all seasons the water is slightly colder across the Bonavista transect. In summer the salinities are similar across both transects while during the winter season the salinity is higher across the Bonavista transect.

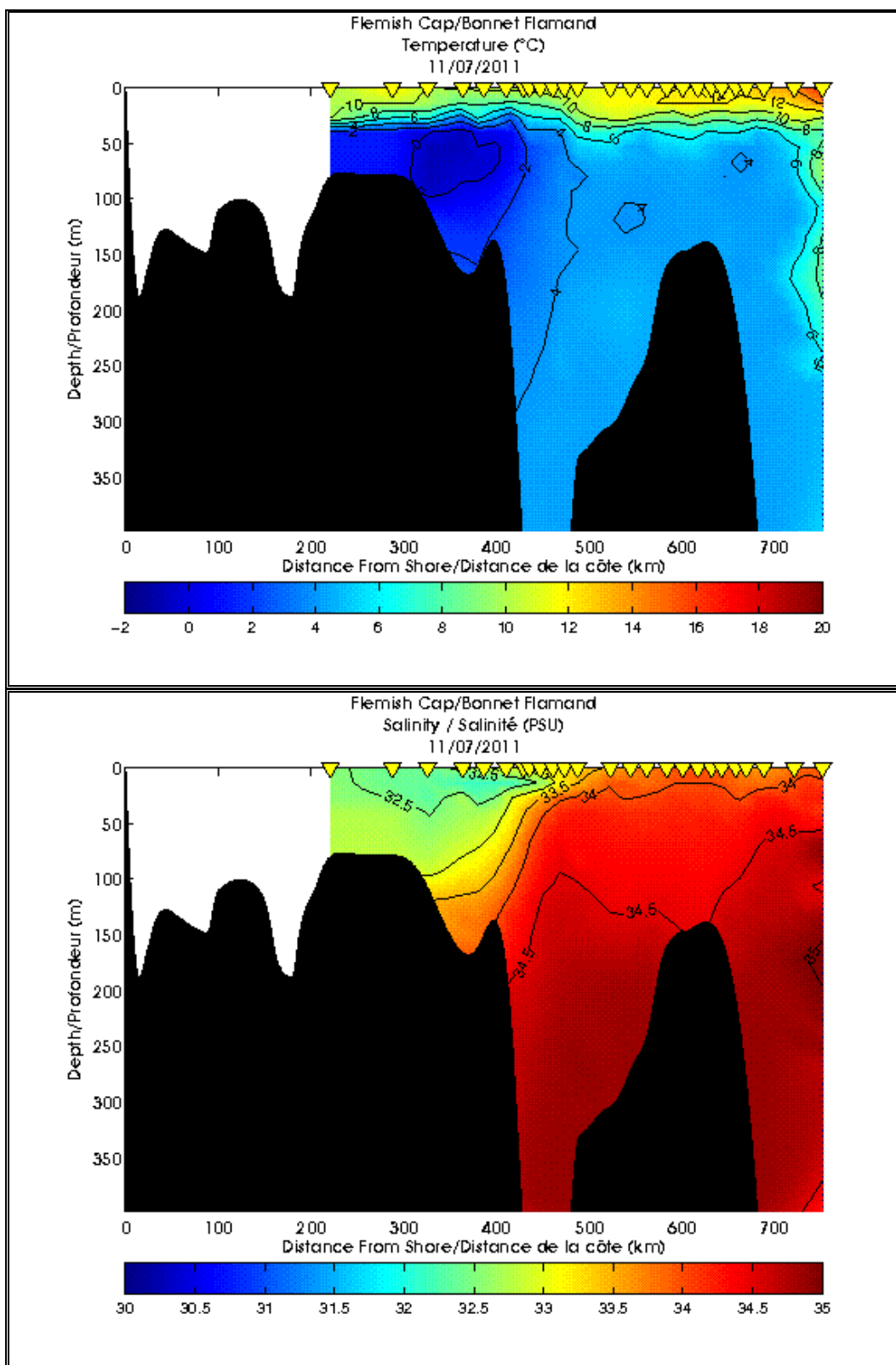


Figure 4.20 Hydrographic contours across the Flemish Cap section during July 2011

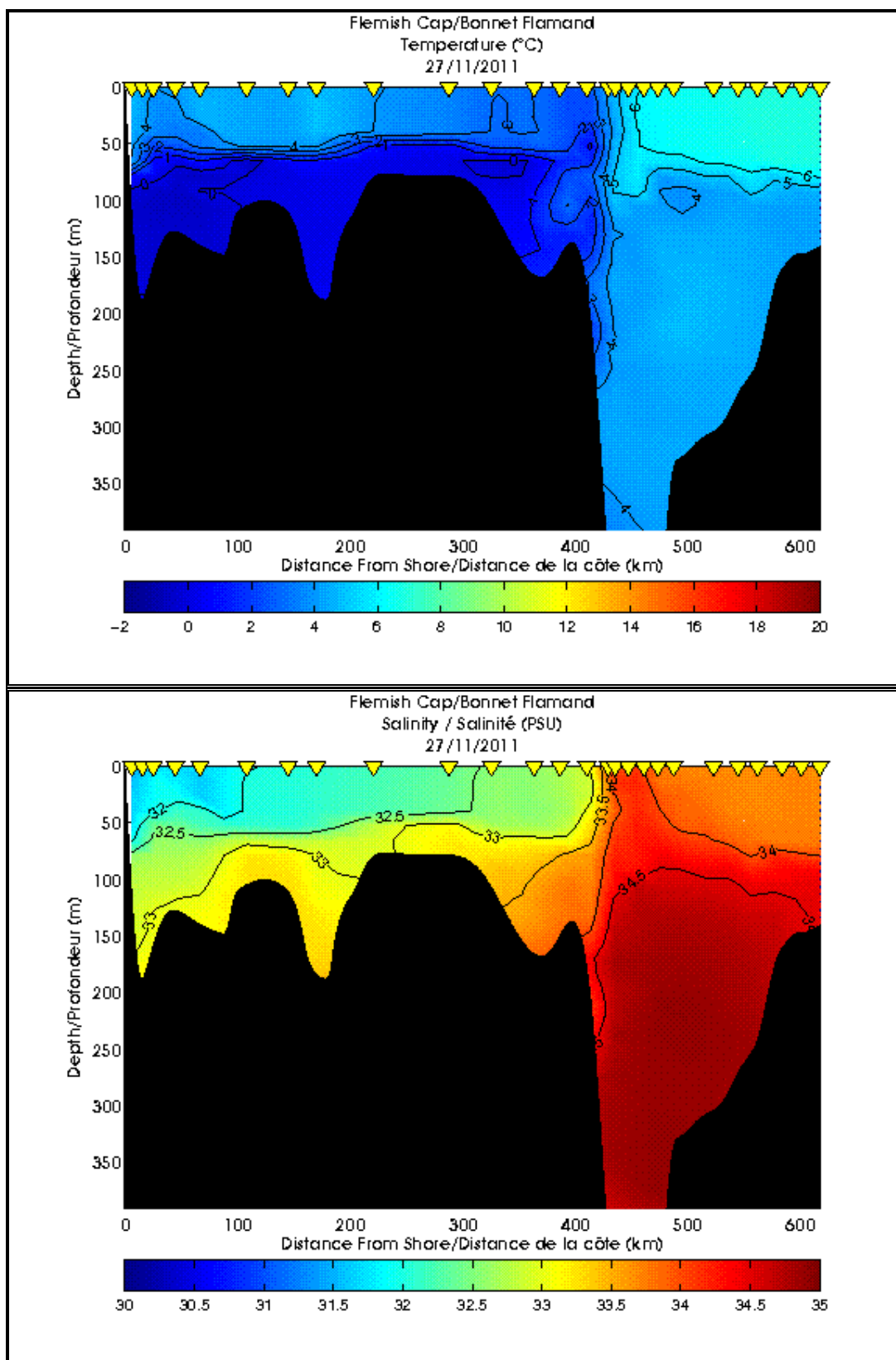


Figure 4.21 Hydrographic contours along the Flemish Cap Section during November 2011

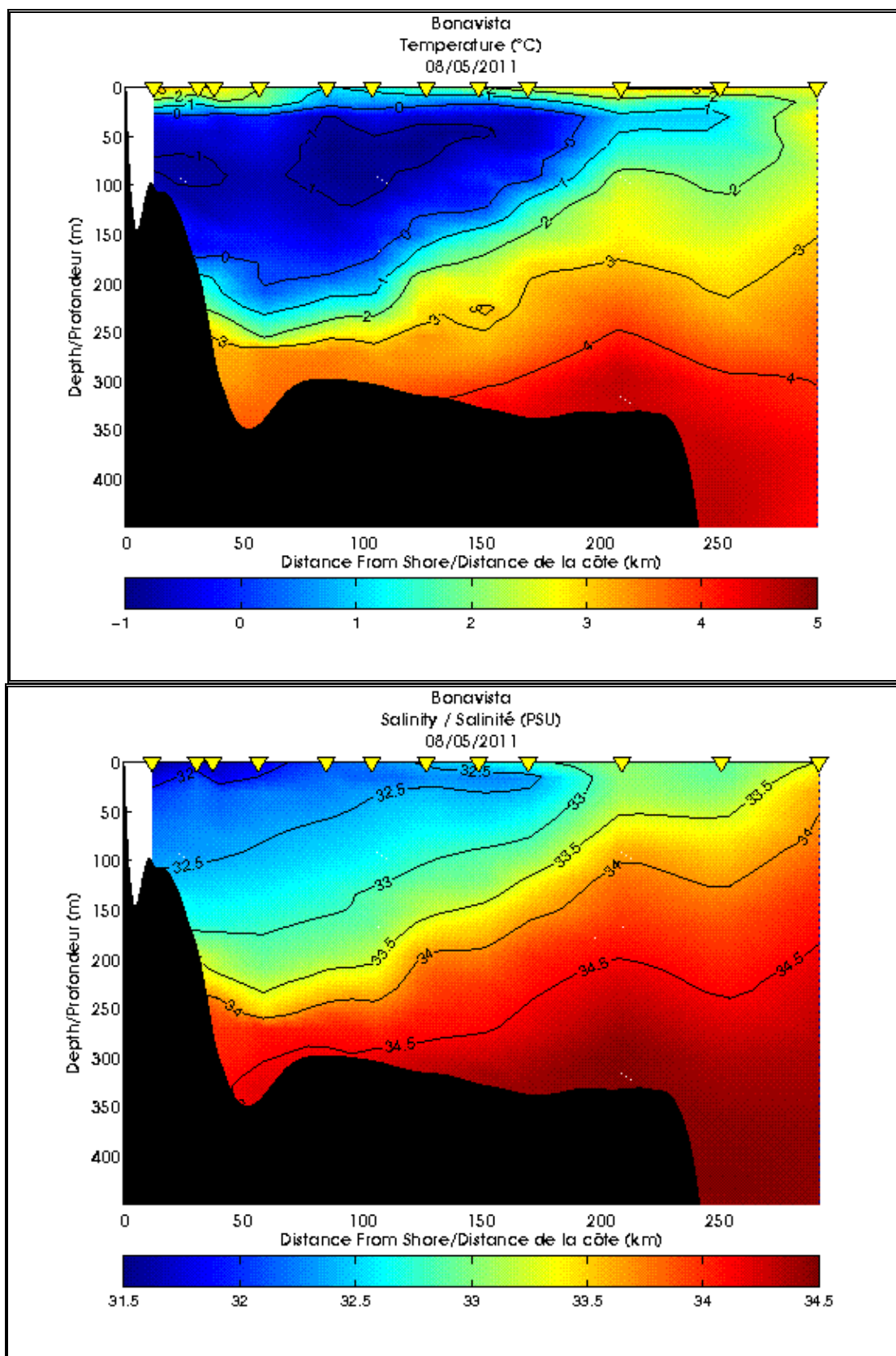


Figure 4.22 Hydrographic contours across the Bonavista section during May 2011

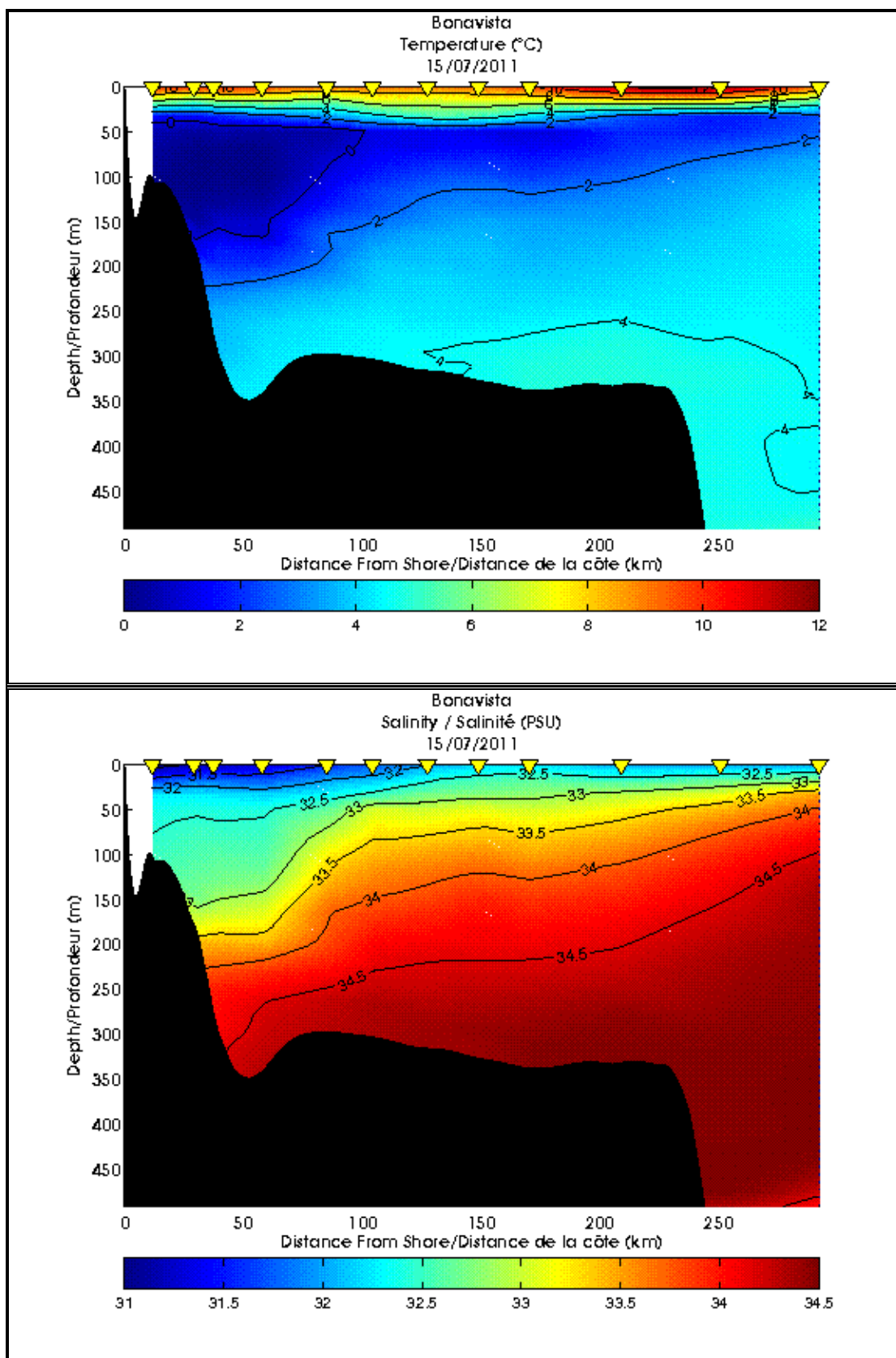


Figure 4.23 Hydrographic contours across the Bonavista section during July 2011

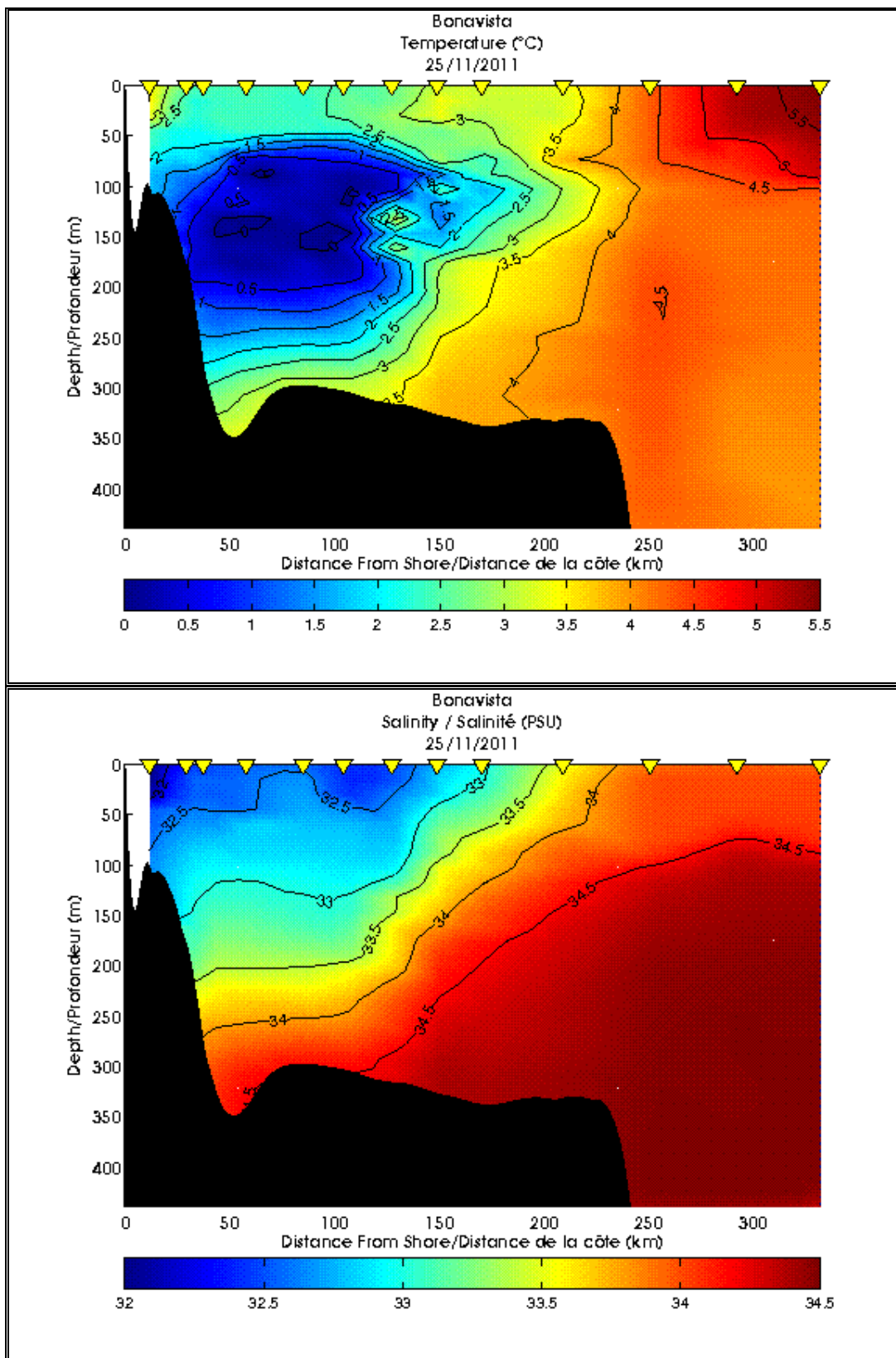


Figure 4.24 Hydrographic contours across the Bonavista section during November 2011

4.4 Water Properties in the Project Area

Temperatures and salinity data from historical measurements were extracted from the Bedford Institute of Oceanography archive. This data is presented as monthly statistics. The northern section of the study area was divided into two areas: southern Orphan Basin, and the area including Sackville Spur and northern Flemish Pass. The southern section of the study area was sub-divided according to water depth; less than 100 m, 100 to 200 m, and greater than 200 m.

Orphan Basin

In Orphan Basin, the water depth varies between 1500 m and 3000 m. Tables 4.10 to 4.15 present the temperature and salinity data by month at the surface, 50 m, 100 m, 200 m, 300 to 900 m, and 1000 to 3000 m.

The surface waters were warmest during the months of July to September with mean temperatures ranging from 9.68°C to 11.67°C. The coldest temperatures were in February and March with mean temperatures of 2.27°C and 2.26°C, respectively. The mean salinities ranged between 33.33 psu in September and 34.37 psu in January. At a depth of 50 m, the mean temperatures ranged between 2.68°C in February to 6.69°C in November. The mean salinities ranged between 33.33 psu in October and 34.47 psu in June. At a depth of 100 m, the mean temperatures ranged between 2.86°C in February and 4.74°C in December. The salinity had a standard deviation of less than 0.2 and mean salinity values that ranged from 34.51 psu in December and January to 34.70 psu in September. At a depth of 200 m, the mean temperatures ranged between 3.42°C in March to 4.04°C in December. The salinity had a standard deviation of less than 0.11 and mean salinity values that ranged from 34.73 psu in March and 34.82 psu in September. At a depth of 300 to 900 m, the mean temperatures ranged between 3.50°C in August to 3.78°C in February. The salinity had a standard deviation of less than 0.1 and mean salinity values that ranged from 34.84 psu during the summer and 34.88 psu during February. At a depth of 1000 to 3000 m, the mean temperatures ranged between 3.26°C in December to 3.42°C in February. The salinity had a standard deviation of less than 0.05 and mean salinity values that ranged between 34.88 psu and 34.90 psu.

The data is also presented in seasonal T-S plots in Figure 4.25. The seasons are spring (March-May), summer (June-August), fall/autumn (September-November), and winter (December-February). The T-S diagrams show that the water properties vary with seasons throughout the water column. In summer and fall the water is stratified to a depth between 50 m and 100 m. The T-S diagrams show that the core of the Labrador Current water is around 100 m and the core of the Labrador Sea water is around 500 m. The Atlantic Deep Water is present at 2000 m.

Table 4.10 Monthly temperature and salinity statistics for the surface water in Orphan Basin from historical CTD data

Surface Temperature (0 m)

MONTH	# Observations	Mean	Min	Max	STD
January	22	3.39	1.00	4.85	0.97
February	12	2.27	1.26	3.53	0.65
March	14	2.26	-0.48	4.96	1.58
April	84	3.23	-0.60	5.43	1.49
May	100	4.51	0.76	8.07	1.31
June	65	6.73	3.60	10.23	1.59
July	22	9.68	6.18	12.02	1.63
August	26	11.42	9.11	13.98	1.53
September	9	11.67	9.32	14.16	1.49
October	33	8.92	7.36	11.04	1.21
November	28	6.89	4.50	9.23	1.20
December	15	5.50	3.58	7.26	1.01

Surface salinity (0 m)

MONTH	# Observations	Mean	Min	Max	STD
January	22	34.37	33.64	34.58	0.23
February	12	34.23	33.76	34.40	0.18
March	14	34.24	33.42	34.74	0.43
April	84	34.29	32.85	34.76	0.39
May	100	34.22	33.13	34.91	0.39
June	65	34.26	33.58	34.81	0.31
July	22	33.69	32.70	34.50	0.65
August	26	33.68	32.89	34.45	0.44
September	9	33.67	32.61	34.20	0.55
October	33	33.90	33.32	34.31	0.24
November	28	33.96	33.03	34.26	0.33
December	15	34.21	33.85	34.37	0.15

Table 4.11 Monthly temperature and salinity data for a depth of 50 m in Orphan Basin from historical CTD data

Temperature 50 m

MONTH	# Observations	Mean	Min	Max	STD
January	25	3.76	2.26	5.50	0.78
February	12	2.68	1.41	4.15	0.82
March	18	2.77	0.80	4.94	1.25
April	75	2.95	-1.20	5.40	1.35
May	96	3.63	0.04	7.83	1.30
June	60	4.37	1.10	8.22	1.33
July	22	3.84	0.53	6.73	1.65
August	29	3.88	0.50	6.30	1.57
September	12	4.50	2.16	7.76	1.50
October	35	5.94	2.26	10.02	1.97
November	30	6.69	4.50	8.64	1.22
December	20	5.63	4.44	7.36	0.88

Salinity 50 m

MONTH	# Observations	Mean	Min	Max	STD
January	25	34.42	33.77	34.59	0.17
February	12	34.33	33.86	34.64	0.19
March	18	34.37	33.43	34.76	0.35
April	75	34.41	33.55	34.77	0.27
May	96	34.38	33.44	34.91	0.21
June	60	34.47	33.98	34.89	0.17
July	22	34.36	33.96	34.66	0.22
August	29	34.41	33.95	34.70	0.22
September	12	34.39	34.10	34.61	0.17
October	35	34.20	33.33	34.68	0.31
November	30	34.10	33.47	34.31	0.18
December	20	34.31	34.05	34.56	0.14

Table 4.12 Monthly temperature and salinity data for a depth of 100 m in Orphan Basin from historical CTD data

Temperature 100 m

MONTH	# Observations	Mean	Min	Max	STD
January	24	3.65	2.65	5.31	0.72
February	10	2.86	1.48	4.17	0.79
March	14	3.08	1.84	4.86	0.93
April	73	3.01	-0.41	5.41	0.79
May	80	3.07	0.88	7.52	0.86
June	56	3.57	2.19	8.03	1.01
July	21	3.34	2.13	4.92	0.80
August	30	3.28	1.66	4.66	0.76
September	11	3.91	3.17	4.73	0.58
October	35	3.57	2.10	4.59	0.58
November	32	4.22	2.41	7.20	0.78
December	20	4.74	3.96	6.61	0.58

Salinity 100 m

MONTH	# Observations	Mean	Min	Max	STD
January	24	34.51	34.27	34.73	0.11
February	10	34.45	34.25	34.65	0.15
March	14	34.54	34.15	34.75	0.16
April	73	34.57	33.99	34.85	0.15
May	80	34.57	34.15	34.94	0.13
June	56	34.62	34.37	34.97	0.11
July	21	34.60	34.32	34.79	0.13
August	30	34.62	34.30	34.77	0.13
September	11	34.70	34.60	34.82	0.07
October	35	34.64	34.01	34.81	0.16
November	32	34.63	34.12	34.80	0.15
December	20	34.51	34.25	34.75	0.17

Table 4.13 Monthly temperature and salinity data for a depth of 200 m in Orphan Basin from historical data

Temperature 200 m

MONTH	# Observations	Mean	Min	Max	STD
January	23	4.01	3.48	4.57	0.28
February	10	3.88	3.33	4.39	0.32
March	16	3.42	2.23	4.42	0.65
April	73	3.47	2.46	5.11	0.49
May	81	3.45	1.40	4.84	0.51
June	60	3.56	2.77	6.02	0.61
July	20	3.54	2.97	4.06	0.36
August	29	3.49	3.04	4.28	0.32
September	10	3.79	3.22	4.14	0.26
October	33	3.64	3.25	4.13	0.25
November	31	3.92	3.30	4.56	0.34
December	19	4.04	3.60	4.60	0.30

Salinity 200 m

MONTH	# Observations	Mean	Min	Max	STD
January	23	34.79	34.66	34.85	0.06
February	10	34.80	34.67	34.88	0.08
March	16	34.73	34.58	34.85	0.08
April	73	34.77	34.48	34.93	0.08
May	81	34.76	34.40	34.90	0.08
June	60	34.77	34.66	34.95	0.05
July	20	34.77	34.63	34.87	0.06
August	29	34.78	34.62	34.83	0.04
September	10	34.82	34.76	34.87	0.04
October	33	34.79	34.33	34.88	0.11
November	31	34.79	34.47	34.90	0.09
December	19	34.81	34.76	34.90	0.04

Table 4.14 Monthly temperature and salinity data for a depth of 300 to 900 m in Orphan Basin from historical CTD data

Temperature 300 to 900 m

MONTH	# Observations	Mean	Min	Max	STD
January	115	3.68	3.36	4.34	0.22
February	68	3.78	3.30	4.39	0.29
March	76	3.75	2.79	4.40	0.32
April	307	3.66	2.47	4.50	0.29
May	352	3.62	3.02	4.38	0.26
June	194	3.58	3.09	4.48	0.26
July	114	3.57	3.13	4.11	0.22
August	144	3.50	3.12	4.01	0.22
September	50	3.60	3.18	4.16	0.25
October	186	3.54	3.20	4.07	0.19
November	159	3.71	3.10	4.39	0.24
December	117	3.55	3.13	4.29	0.22

Salinity 300 to 900 m

MONTH	# Observations	Mean	Min	Max	STD
January	115	34.85	34.73	34.92	0.03
February	68	34.88	34.80	34.95	0.03
March	76	34.87	34.80	34.94	0.03
April	307	34.87	34.66	35.02	0.05
May	352	34.86	34.67	34.94	0.04
June	194	34.84	34.74	34.96	0.04
July	114	34.84	34.73	34.92	0.04
August	144	34.84	34.74	34.90	0.03
September	50	34.86	34.81	34.92	0.03
October	186	34.84	34.39	35.01	0.09
November	159	34.85	34.63	34.93	0.06
December	117	34.85	34.77	34.90	0.02

Table 4.15 Monthly temperature and salinity data for a depth of 1000 to 3000 m in Orphan Basin from historical CTD data

Temperature 1000 to 3000 m

MONTH	# Observations	Mean	Min	Max	STD
January	38	3.31	2.91	3.54	0.15
February	17	3.42	2.90	3.80	0.26
March	22	3.35	2.97	3.70	0.23
April	100	3.35	2.00	3.90	0.29
May	126	3.38	2.27	3.74	0.22
June	97	3.35	2.70	3.72	0.17
July	36	3.35	2.89	3.65	0.21
August	43	3.31	2.83	3.64	0.22
September	18	3.30	2.85	3.67	0.22
October	48	3.33	2.84	3.61	0.19
November	39	3.36	2.90	3.66	0.24
December	25	3.26	3.00	3.64	0.14

Salinity 1000 to 3000 m

MONTH	# Observations	Mean	Min	Max	STD
January	38	34.90	34.82	34.99	0.04
February	17	34.89	34.84	34.94	0.02
March	22	34.89	34.84	34.95	0.03
April	100	34.90	34.82	35.01	0.03
May	126	34.90	34.81	34.96	0.03
June	97	34.89	34.77	34.96	0.03
July	36	34.89	34.84	34.93	0.02
August	43	34.90	34.86	34.96	0.03
September	18	34.88	34.84	34.91	0.02
October	48	34.89	34.84	35.01	0.03
November	39	34.89	34.74	34.95	0.04
December	25	34.88	34.84	34.92	0.02

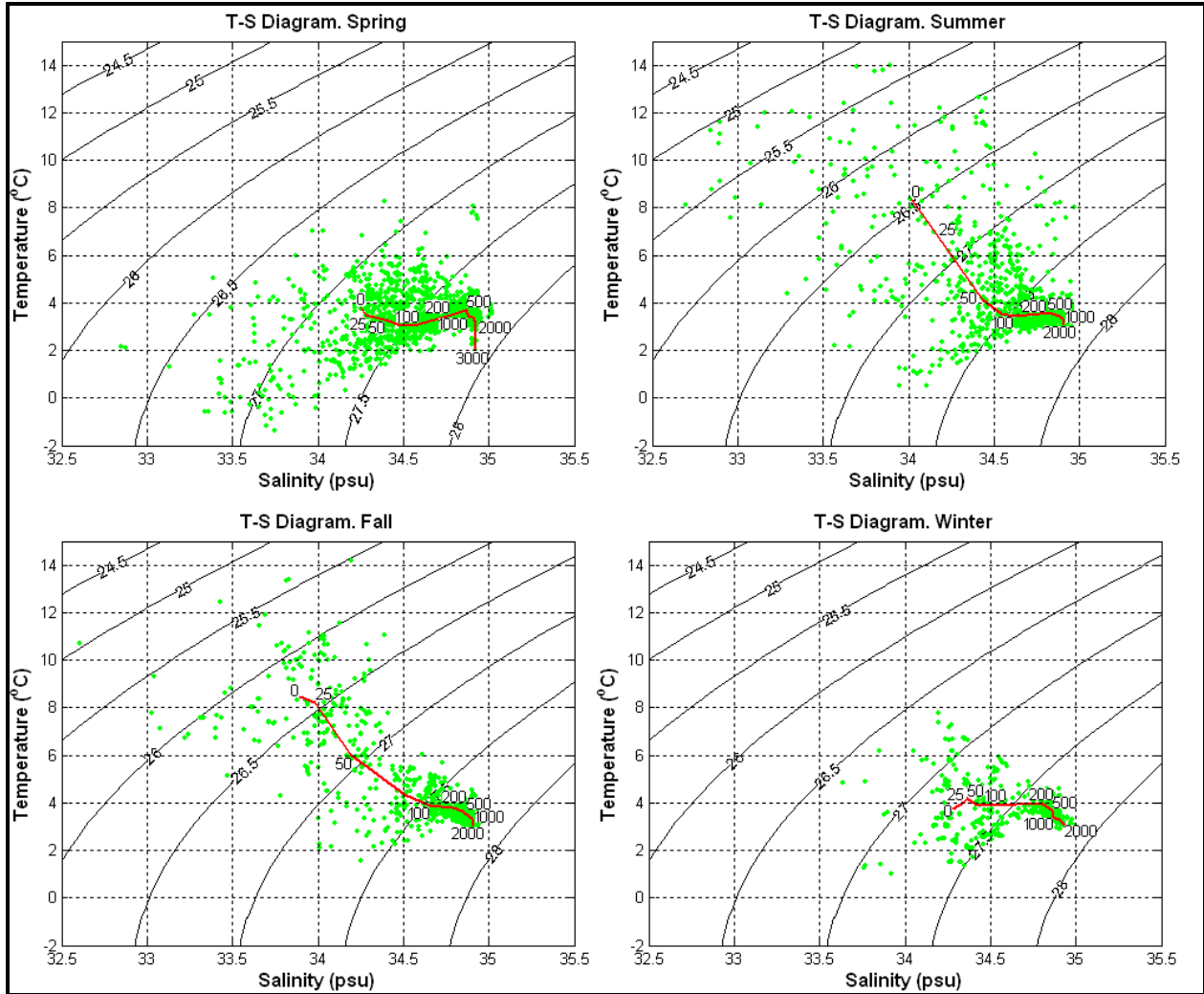


Figure 4.25 Seasonal T-S plots for Orphan Basin

Note: The red lines correspond to the average TS curve for each area. The numbers on the curves represent the water depth in metres.

Sackville Spur and Flemish Pass

Sub-area 2 contains Sackville Spur and Flemish Pass. The water depth in this area varies between the 500 m and 3000 m. Tables 4.16 to 4.21 present the temperature and salinity data by month, at the surface, 50 m, 100 m, 200 m, 300 to 900 m, and 1000 to 3000 m.

The surface waters were warmest during the months July to September with mean temperatures ranging from 10.70°C to 12.05°C. The coldest temperatures were in March and April with mean temperatures of 2.72°C and 2.88°C, respectively. The mean salinities ranged between 32.71 psu in September and 33.98 psu in February. At a depth of 50 m, the mean temperatures ranged between 2.46°C in April to 5.92°C in November. The mean salinities ranged between 33.85 psu in December and 34.10 psu in January. At a depth of 100 m, the mean temperatures ranged between 2.54°C in April to 3.94°C in December. The mean salinities ranged between 34.24 psu in April and 34.49 psu in

October and November. At a depth of 200 m, the mean temperatures ranged between 3.36°C in June to 4.04°C in December. The salinity had a standard deviation of less than 0.15 and mean salinity values ranged between 34.65 psu in April and 34.76 psu in October to December. At a depth of 300 to 900 m, the mean temperatures ranged between 3.54°C in September to 3.77°C in March. The salinity had a standard deviation of less than 0.1 and mean salinity values ranged between 34.82 psu in June and September and 34.85 psu in October, November, February and March. At a depth of 1000 to 3000 m, the mean temperatures ranged between 3.34°C in December to 3.48°C in May. The salinity had a standard deviation of less than 0.06 and mean salinity values ranged between 34.84 psu and 34.89 psu.

The data is also presented in seasonal T-S plots in Figure 4.26. The seasons are spring (March-May), summer (June-August), fall/autumn (September-November), and winter (December-February). The T-S diagrams show that the water properties vary with season throughout the water column. In summer and fall the water is stratified between 50 m and 100 m. The T-S diagrams show that the core of the Labrador Current water is around 100 m and the core of the Labrador Sea Water is around 500 m.

Table 4.16 Monthly temperature and salinity statistics for the surface water in northern Flemish Pass and the Sackville Spur

Surface temperature (0 m)

MONTH	# Observations	Mean	Min	Max	STD
January	156	3.86	-1.00	6.45	1.33
February	106	3.14	-0.44	5.80	1.16
March	162	2.72	-1.30	5.07	1.48
April	614	2.88	-1.31	8.99	1.88
May	421	4.59	-1.00	8.40	1.77
June	356	6.61	1.10	12.25	2.13
July	596	10.70	4.65	15.90	1.92
August	171	12.05	7.20	16.25	1.67
September	70	12.04	8.26	14.66	1.67
October	119	8.82	5.39	12.02	1.40
November	144	7.04	2.37	11.58	1.75
December	86	5.93	3.08	11.00	1.95

Surface salinity (0 m)

MONTH	# Observations	Mean	Min	Max	STD
January	156	33.95	32.36	34.59	0.35
February	106	33.98	33.15	34.48	0.25
March	162	33.93	33.08	34.71	0.31
April	614	33.79	32.03	34.93	0.41
May	421	33.76	32.70	34.65	0.40
June	356	33.57	31.93	34.39	0.39
July	596	33.29	31.36	34.37	0.45
August	171	32.80	31.31	34.06	0.48
September	70	32.71	31.46	34.02	0.49
October	119	33.52	32.38	34.35	0.48
November	144	33.58	32.68	34.49	0.47
December	86	33.70	32.84	34.36	0.42

Table 4.17 Monthly temperature and salinity data for a depth of 50 m in northern Flemish Pass and Sackville Spur

Temperature 50 m

MONTH	# Observations	Mean	Min	Max	STD
January	115	3.42	-0.60	6.39	1.25
February	96	3.02	-0.11	5.12	1.05
March	153	2.64	-1.56	5.40	1.30
April	588	2.46	-1.62	7.80	1.65
May	403	3.00	-1.44	8.60	1.62
June	370	3.25	-1.30	7.54	1.78
July	628	3.95	-1.20	9.81	1.68
August	159	3.28	-1.60	8.30	2.21
September	68	3.52	-0.81	10.76	2.34
October	119	5.21	0.09	10.89	2.42
November	146	5.92	0.90	9.92	1.74
December	87	5.28	1.96	9.30	1.32

Salinity 50 m

MONTH	# Observations	Mean	Min	Max	STD
January	115	34.10	33.22	34.60	0.31
February	96	34.06	33.46	34.75	0.24
March	153	34.01	33.28	34.70	0.26
April	588	33.96	32.97	34.70	0.32
May	403	33.98	32.82	34.65	0.32
June	370	34.00	33.10	34.58	0.28
July	628	34.02	33.11	34.68	0.28
August	159	33.93	32.54	34.65	0.33
September	68	34.00	33.06	34.54	0.27
October	119	33.97	32.95	34.86	0.34
November	146	33.87	32.94	34.56	0.35
December	87	33.85	33.01	34.36	0.34

Table 4.18 Monthly temperature and salinity data for a depth of 100 m in northern Flemish Pass and Sackville Spur

Temperature 100 m

MONTH	# Observations	Mean	Min	Max	STD
January	116	3.36	-0.20	4.79	0.90
February	86	3.22	0.41	5.68	0.93
March	139	2.85	-0.16	4.56	0.94
April	608	2.54	-1.40	8.10	1.08
May	356	2.82	-0.18	8.50	1.15
June	353	2.84	-0.80	7.40	1.08
July	606	3.32	-0.70	6.84	1.00
August	151	3.17	-0.79	6.37	1.52
September	66	3.13	1.18	5.47	0.90
October	110	3.25	1.12	6.26	0.87
November	146	3.88	0.98	7.31	1.10
December	90	3.94	1.35	6.28	1.06

Salinity 100 m

MONTH	# Observations	Mean	Min	Max	STD
January	116	34.33	33.23	34.66	0.20
February	86	34.27	33.63	34.84	0.24
March	139	34.30	33.75	34.79	0.21
April	608	34.24	33.42	34.89	0.24
May	356	34.31	33.45	34.81	0.22
June	353	34.33	33.47	34.72	0.20
July	606	34.36	33.66	34.82	0.19
August	151	34.35	33.65	34.79	0.25
September	66	34.40	33.69	34.75	0.18
October	110	34.49	34.08	34.77	0.20
November	146	34.49	33.93	34.93	0.20
December	90	34.39	33.84	34.82	0.23

Table 4.19 Monthly temperature and salinity data for a depth of 200 m in northern Flemish Pass and Sackville Spur

Temperature 200 m

MONTH	# Observations	Mean	Min	Max	STD
January	119	3.88	1.20	5.09	0.55
February	94	3.92	1.92	5.60	0.46
March	121	3.58	0.69	5.17	0.78
April	562	3.43	0.94	5.70	0.78
May	376	3.49	0.70	6.90	0.78
June	401	3.36	0.39	5.48	0.74
July	522	3.80	1.22	5.68	0.54
August	141	3.73	1.41	5.60	0.74
September	67	3.66	2.80	4.86	0.49
October	129	3.61	1.56	5.62	0.53
November	169	3.93	2.04	5.28	0.52
December	93	4.04	2.16	5.85	0.48

Salinity 200 m

MONTH	# Observations	Mean	Min	Max	STD
January	119	34.72	34.05	34.97	0.12
February	94	34.73	34.21	34.93	0.12
March	121	34.67	34.12	34.88	0.13
April	562	34.65	33.53	34.94	0.14
May	376	34.68	34.07	34.92	0.13
June	401	34.66	33.91	34.91	0.14
July	522	34.72	34.11	35.08	0.10
August	141	34.69	34.25	35.05	0.12
September	67	34.71	34.22	34.89	0.11
October	129	34.76	34.27	34.90	0.10
November	169	34.76	34.41	34.97	0.09
December	93	34.76	34.28	34.93	0.09

Table 4.20 Monthly temperature and salinity data for a depth of 300 to 900 m in northern Flemish Pass and Sackville Spur

Temperature 300 to 900 m

MONTH	# Observations	Mean	Min	Max	STD
January	360	3.75	2.20	4.35	0.27
February	170	3.76	3.01	4.87	0.28
March	305	3.77	1.92	4.73	0.39
April	1122	3.61	2.24	4.80	0.38
May	932	3.70	2.09	5.70	0.38
June	911	3.58	1.72	4.90	0.35
July	776	3.74	2.53	4.93	0.31
August	364	3.67	2.88	4.90	0.35
September	179	3.54	3.02	4.49	0.33
October	521	3.61	2.25	4.98	0.26
November	540	3.76	3.06	4.80	0.33
December	369	3.67	3.14	4.90	0.30

Salinity 300 to 900 m

MONTH	# Observations	Mean	Min	Max	STD
January	360	34.83	34.49	35.01	0.05
February	170	34.85	34.59	34.97	0.06
March	305	34.85	34.41	34.98	0.08
April	1122	34.83	34.44	34.98	0.07
May	932	34.84	34.45	34.99	0.07
June	911	34.82	34.12	34.99	0.08
July	776	34.84	34.60	35.14	0.06
August	364	34.84	34.61	34.97	0.05
September	179	34.82	34.36	34.94	0.06
October	521	34.85	34.49	34.94	0.05
November	540	34.85	34.63	34.99	0.05
December	369	34.83	34.74	34.98	0.03

Table 4.21 Monthly temperature and salinity data for a depth of 1000 to 3000 m in northern Flemish Pass and Sackville Spur

Temperature 1000 to 3000 m

MONTH	# Observations	Mean	Min	Max	STD
January	53	3.41	3.05	3.71	0.12
February	11	3.44	3.28	3.64	0.12
March	42	3.42	2.97	4.20	0.27
April	130	3.44	3.10	3.90	0.14
May	153	3.48	2.89	3.95	0.19
June	119	3.44	3.00	3.90	0.16
July	57	3.39	1.67	3.91	0.39
August	56	3.42	2.98	3.87	0.23
September	27	3.38	3.04	3.94	0.20
October	66	3.44	2.98	3.85	0.19
November	54	3.41	3.05	3.85	0.19
December	48	3.34	3.09	3.81	0.18

Salinity 1000 to 3000 m

MONTH	# Observations	Mean	Min	Max	STD
January	53	34.87	34.84	34.95	0.03
February	11	34.86	34.80	34.90	0.03
March	42	34.87	34.53	34.92	0.06
April	130	34.88	34.80	34.97	0.03
May	153	34.89	34.79	35.00	0.03
June	119	34.88	34.79	35.00	0.03
July	57	34.88	34.84	34.94	0.02
August	56	34.87	34.82	34.94	0.03
September	27	34.87	34.84	34.96	0.03
October	66	34.87	34.74	34.94	0.03
November	54	34.87	34.78	34.94	0.04
December	48	34.84	34.78	34.91	0.02

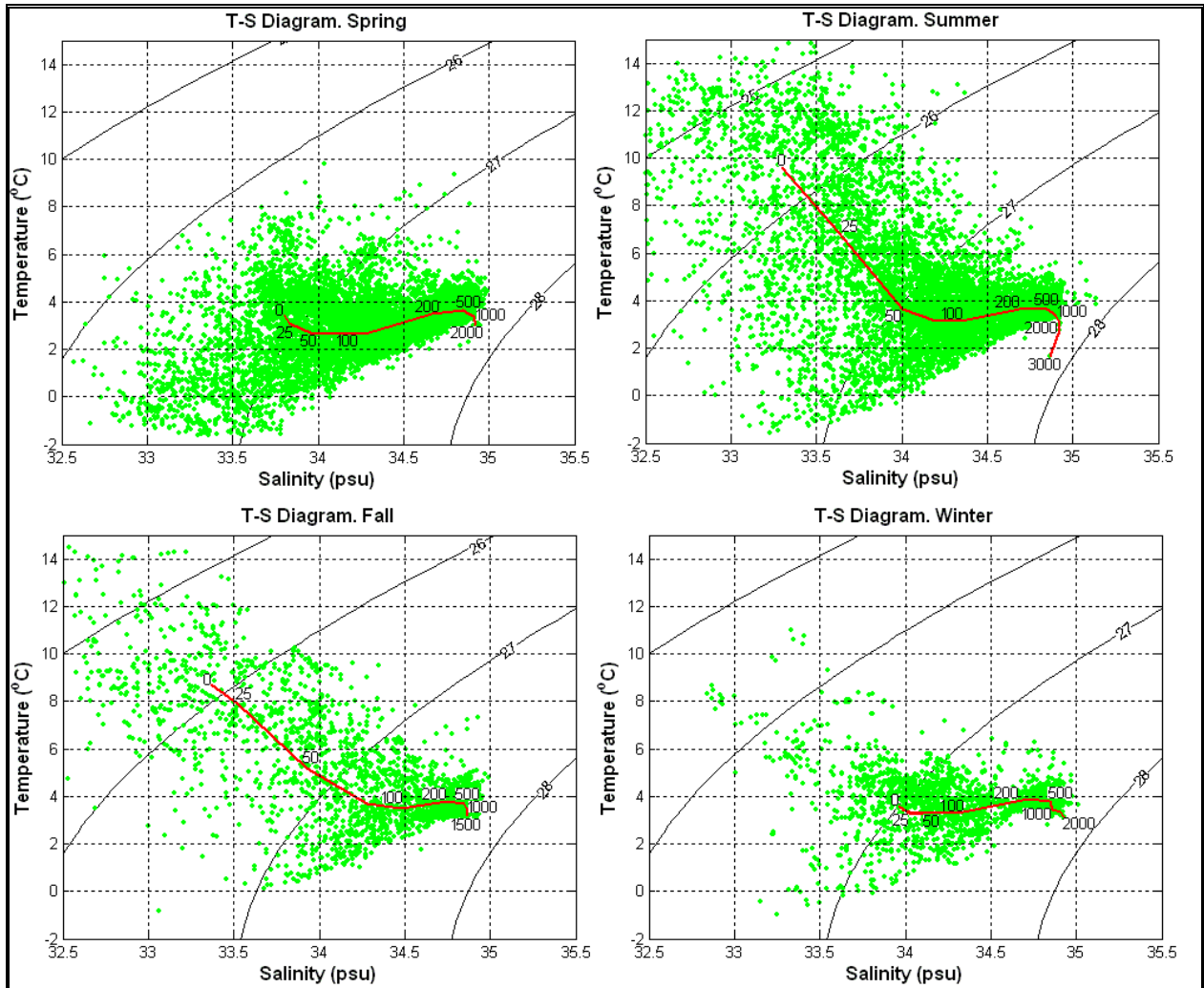


Figure 4.26 Seasonal T-S plots for northern Flemish Pass and Sackville Spur

Note: The red lines correspond to the average TS curve for each area. The numbers on the curves represent the water depth in metres.

Water Depth less than 100 m on the Northeast Grand Banks

Hibernia and Terra Nova are located on the northeast Grand Banks in less than 100 m of water. Tables 4.22 and 4.23 present CTD temperature and salinity data from the BIO database, collected at the surface and at a depth of 75 m. Table 4.22 shows that the surface water is warmest between July and September with mean temperatures ranging between 10.12°C and 12.81°C. The coldest temperatures are in February and March with a mean temperature of 0.01°C and -0.53°C, respectively. The mean salinities ranged between 32.04 psu in October to 32.97 psu in March.

At a depth of 75 m, the mean temperatures were always negative, ranging between -0.01 in January to -1.04 in March, consistent with temperatures in the Cold Intermediate Layer. The mean salinities ranged between 32.77 psu in February to 33.16 psu in December.

T-S diagrams in Figure 4.27 show how the water properties vary with season throughout the water column. In summer and fall the water is stratified to a depth of 50 m. Below 50 m the water is less stratified and shows negative temperature at 75 m and 100 m, within the core of the Cold Intermediate Layer.

In Winter and Spring, there is little to no distinction between the water properties at the surface and at 25 m because the surface layer is well mixed. However, below 75 m the water is more stratified than during summer, indicating an intrusion and mixing by the Labrador Slope water.

Table 4.22. Monthly temperature and salinity statistics for the surface water from historical CTD data for a water depth < 100 m on the Grand Banks

Surface temperature (0 m) on the Grand Banks

MONTH	# Observations	Mean	Min	Max	STD
January	14	0.90	-0.69	1.90	0.70
February	7	0.01	-1.69	0.64	0.83
March	17	-0.53	-1.75	0.96	1.05
April	177	0.48	-1.30	2.55	0.85
May	219	2.76	-0.39	6.52	1.66
June	489	5.32	1.61	14.36	1.40
July	140	10.12	5.30	13.50	1.79
August	19	12.81	10.30	16.45	1.56
September	38	11.97	6.12	18.20	2.67
October	114	9.33	5.20	12.96	2.34
November	122	6.33	2.53	10.69	1.78
December	59	2.93	0.66	6.94	1.82

Surface salinity (0 m) on the Grand Banks

MONTH	# Observations	Mean	Min	Max	STD
January	14	32.67	32.23	33.09	0.22
February	7	32.86	32.36	33.16	0.25
March	17	32.97	32.70	33.24	0.16

April	177	32.87	32.18	33.38	0.20
May	219	32.71	31.84	33.46	0.29
June	489	32.61	31.87	33.30	0.21
July	140	32.39	31.29	33.10	0.27
August	19	32.25	31.55	32.74	0.31
September	38	32.07	31.41	32.56	0.23
October	114	32.04	31.42	32.50	0.21
November	122	32.09	31.01	32.94	0.25
December	59	32.41	31.90	32.85	0.25

Table 4.23 Monthly temperatures and salinity statistics at 75 m depth from historical CTD data for a water depth of < 100 m on the Grand Banks

Temperature 75 m on the Grand Banks

MONTH	# Observations	Mean	Min	Max	STD
January	6	-0.01	-0.78	0.45	0.43
February	3	-0.83	-1.55	-0.33	0.64
March	11	-1.04	-1.73	0.09	0.83
April	130	-0.58	-1.72	2.71	0.66
May	160	-0.28	-1.57	1.26	0.75
June	284	-0.13	-1.62	1.68	0.64
July	137	-0.35	-1.54	1.05	0.55
August	20	-0.52	-1.35	0.88	0.54
September	26	-0.68	-1.47	0.72	0.53
October	111	-0.91	-1.34	1.36	0.44
November	73	-0.31	-1.35	1.82	0.74
December	51	-0.54	-1.26	1.30	0.59

Salinity 75 m on the Grand Banks

MONTH	# Observations	Mean	Min	Max	STD
January	6	32.98	32.76	33.19	0.20
February	3	32.77	32.57	32.90	0.18
March	11	33.04	32.85	33.26	0.13
April	130	33.01	32.56	34.27	0.26
May	160	33.06	32.72	33.57	0.17
June	284	33.04	32.56	34.01	0.17
July	137	33.08	32.73	33.43	0.16
August	20	33.08	32.82	33.40	0.16
September	26	33.08	32.77	33.33	0.16
October	111	33.05	32.77	33.20	0.10
November	73	33.07	32.52	33.70	0.21
December	51	33.16	32.78	33.34	0.14

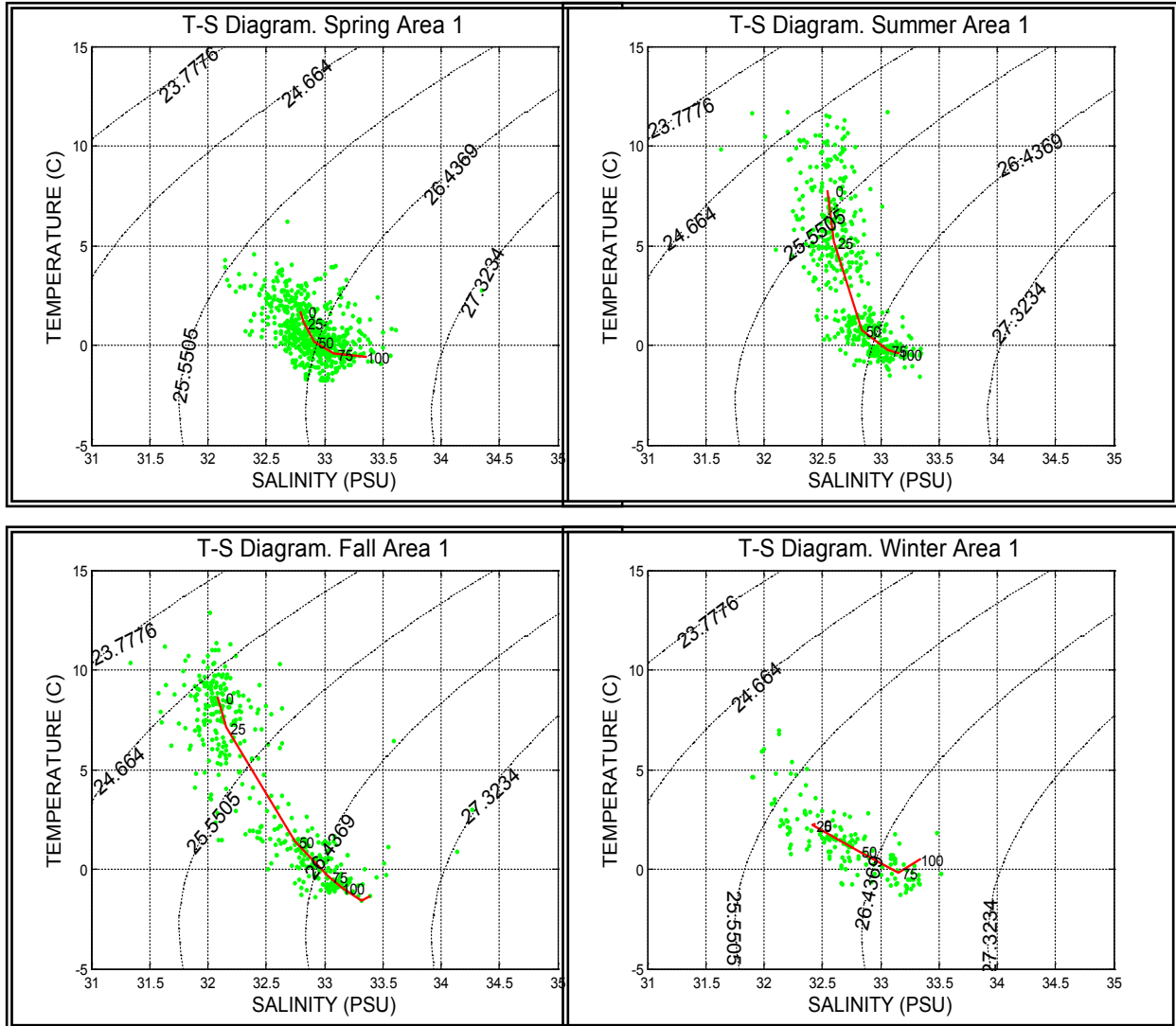


Figure 4.27 Seasonal T-S diagrams for sub-area 3 at depths less than 100 m

Note: The red lines correspond to the average T-S curve for each area. The numbers on these curves represent the depth in metres.

Water depth between 100 m and 200 m on the Northeast Grand Banks

White Rose is located within this area. Tables 4.24 and 4.25 present the temperature and salinity data by month at the surface and at 75 m. The water properties in this section of sub-area 3 are similar to those where the water depth was less than 100 m. The exception is that the waters tend to be slightly colder in between the 100 m and 200 m isobaths than where the water depth is less than 100 m. The surface waters were warmest during the months of July to September with mean temperatures ranging from 9.08°C to 11.28°C. The coldest temperatures were in February and March with mean temperatures of -0.61°C and -0.75°C, respectively. The mean salinities ranged between 31.59 psu in August and 32.94 psu in February.

At a depth of 75 m, the mean temperatures were always negative, ranging between -1.50°C in August to -0.25°C in November. The mean salinities ranged between 32.94 psu in April and 33.18 psu in February.

The colder waters in this section indicate that the water in this area is experiencing advection from the north by the Labrador Current rather than by vertical mixing through local cooling.

The T-S diagrams in Figure 4.28 show two distinct water masses and the surface seasonally mixed layer. During summer and fall strong stratification occurs in the top 50 m which disappears to being a well mixed surface layer during winter and spring. The core of the Cold Intermediate Layer occurs between the 75 m and 100 m depths. Below 100 m the water is mixed with Labrador Sea water.

Table 4.24 Monthly temperature and salinity statistics for the surface water from historical CTD data for a water depth between 100 m and 200m

Temperature surface (0 m) on the outer edge of the Grand Banks

MONTH	# Observations	Mean	Min	Max	STD
January	15	0.10	-1.40	1.40	0.90
February	23	-0.61	-1.81	0.55	0.80
March	33	-0.75	-1.77	0.50	0.78
April	235	-0.16	-1.50	2.53	0.77
May	303	1.52	-1.10	5.08	1.33
June	422	4.15	0.64	10.34	1.70
July	249	9.08	4.15	13.7	1.86
August	72	11.28	6.37	16.08	2.08
September	87	9.98	4.23	17.1	2.61
October	60	7.13	3.54	11.54	1.97
November	184	4.19	0.83	9.74	1.72
December	53	2.44	-1.00	6.06	1.37

Salinity surface (0 m) on the outer edge of the Grand Banks

MONTH	# Observations	Mean	Min	Max	STD
January	15	32.77	32.19	33.30	0.31
February	23	32.94	32.61	33.29	0.21
March	33	32.91	32.41	33.37	0.18
April	235	32.86	32.23	33.33	0.19
May	303	32.72	31.82	33.19	0.22
June	422	32.56	31.62	33.50	0.24
July	249	32.23	31.08	32.77	0.27
August	72	31.59	30.62	32.65	0.53
September	87	31.87	31.16	32.68	0.32
October	60	32.10	31.32	33.21	0.44
November	184	32.39	31.45	33.77	0.36
December	53	32.51	31.91	33.08	0.27

Table 4.25 Monthly temperature and salinity statistic for 75 m depth from historical CTD data for water depth between 100 m and 200 m

Temperature 75 m on the outer edge of the Grand Banks

MONTH	# Observations	Mean	Min	Max	STD
January	16	-0.38	-1.40	0.55	0.54
February	19	-0.71	-1.73	0.96	0.79
March	29	-0.88	-1.76	0.57	0.76
April	384	-1.11	-1.78	1.62	0.55
May	285	-0.88	-1.76	1.48	0.71
June	391	-0.99	-1.80	1.49	0.55
July	244	-0.84	-1.81	5.90	0.79
August	130	-1.50	-1.70	-0.21	0.31
September	71	-1.25	-1.68	-0.05	0.37
October	133	-1.01	-1.65	0.05	0.33
November	178	-0.25	-1.50	3.30	1.10
December	55	-0.27	-1.44	2.13	0.98

Salinity 75 m on the outer edge of the Grand Banks

MONTH	# Observations	Mean	Min	Max	STD
January	16	33.03	32.69	33.33	0.20
February	19	33.18	32.66	33.55	0.22
March	29	33.11	32.77	33.68	0.23
April	384	32.94	32.53	33.8	0.29
May	285	33.09	32.65	34.11	0.19
June	391	33.06	32.53	33.66	0.18
July	244	33.05	32.56	34.00	0.15
August	130	33.08	32.75	33.52	0.11
September	71	33.16	32.79	33.79	0.25
October	133	33.16	32.81	33.69	0.19
November	178	33.17	32.48	33.98	0.24
December	55	33.14	32.75	33.69	0.20

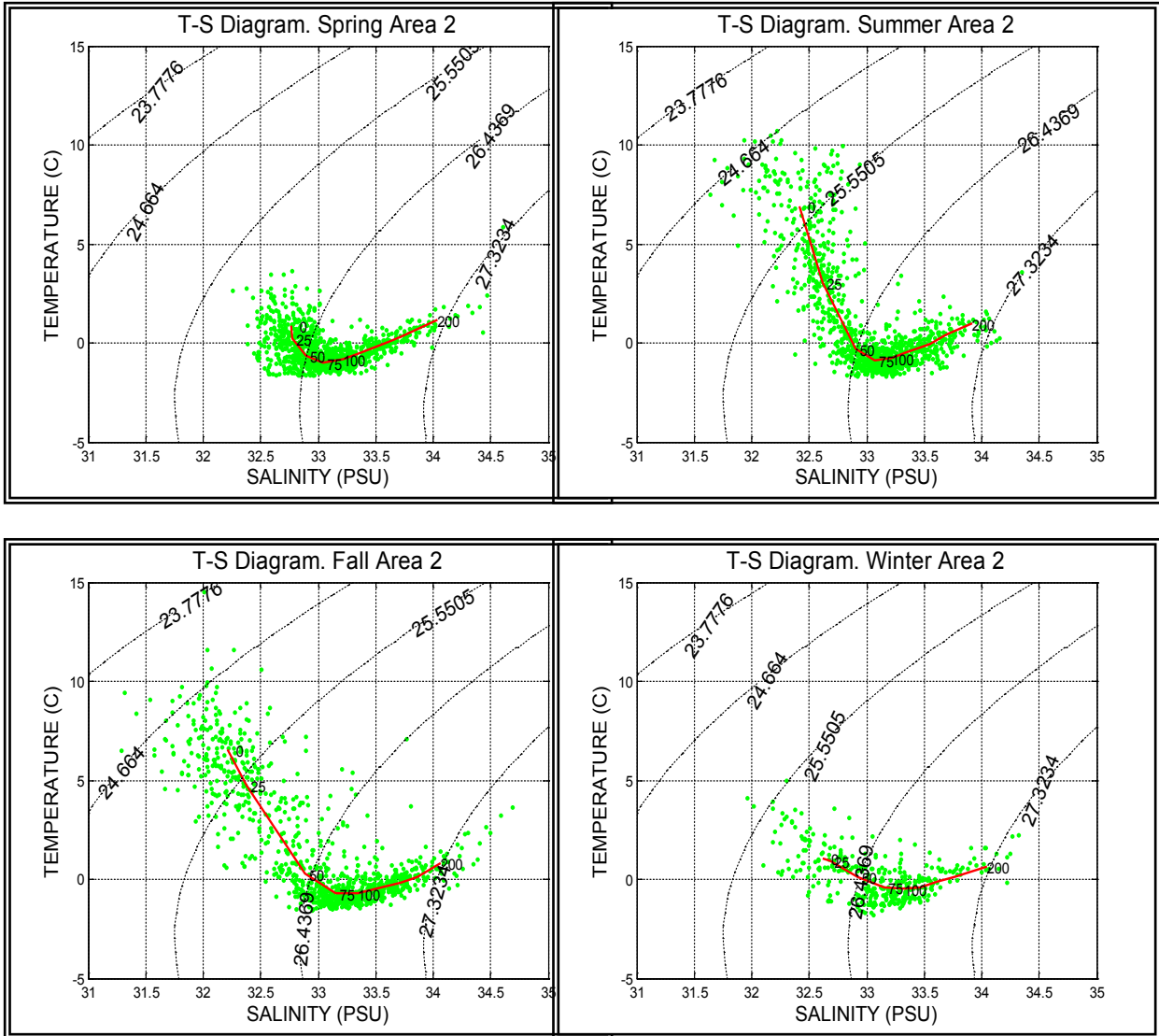


Figure 4.28 Seasonal T-S diagrams for sub-area 3 at depths from 100 m – 200 m

Note: The red lines correspond to the average T-S curve for each area. The numbers on these curves represent the depth in metres.

Water depth between 200 m and 500 m on the Northeast Grand Banks

This area is situated east of the White Rose field where the water depth is between 200 m and 500 m. Tables 4.26 and 4.27 present the temperature and salinity data by month. Similar to the two previous sections of sub-area 3, the warmest months are July to September and the coldest are February and March. The mean surface temperatures during the months of July to September ranged between 9.19°C and 10.24°C. During February and March the mean surface temperatures were -0.37°C and -0.57°C, respectively. The mean salinities ranged between 31.81 psu in August and 33.27 psu in December. Salinities above 33 psu occurred in the months of November to February. In both sub-areas 2 and 3, the lowest surface salinities are in August and the highest occur during the winter.

At a depth of 75 m, the mean temperatures are negative for most of the year, but positive during the months of November, December, and January. The temperatures range between -1.28°C in August to 2.02°C in December. The mean salinity ranges between 33.25 psu in July to 33.87 psu in December. In this area the Cold Intermediate Layer disappears in winter and is replaced by warmer, higher salinity Labrador Sea water.

The T-S diagrams in Figure 4.29 show two distinct water masses and the surface seasonally mixed layer in spring, summer and fall. The upper 50 m shows strong stratification in summer and fall and a weak stratification in spring and winter. The Cold Intermediate Layer is more pronounced in spring and summer than during the fall, and disappears in winter as mixing with the warmer and higher salinity water on the Slope intensifies.

Table 4.26. Monthly temperature and salinity statistics for the surface water from historical CTD data for water depth between 200 m and 500 m

Temperature surface (0 m) on the Continental Slope

MONTH	# Observations	Mean	Min	Max	STD
January	26	-0.14	-1.80	1.06	0.81
February	30	-0.37	-1.78	0.68	0.66
March	14	-0.57	-1.63	0.77	0.83
April	115	-0.25	-1.61	2.44	0.80
May	201	1.31	-0.99	5.52	1.41
June	308	4.03	0.57	9.55	1.66
July	82	9.22	3.42	13.7	2.14
August	56	10.24	5.55	13.8	1.92
September	22	9.19	6.63	14.13	1.75
October	41	5.84	2.32	8.24	1.61
November	141	3.47	-0.19	7.23	1.48
December	38	1.93	0.78	4.52	0.94

Salinity surface (0 m) on the Continental Slope

MONTH	# Observations	Mean	Min	Max	STD
January	26	33.15	32.36	34.01	0.35
February	30	33.26	32.75	34.58	0.37
March	14	32.98	32.76	33.42	0.18
April	115	32.94	32.24	33.87	0.27
May	201	32.82	31.81	33.79	0.30
June	308	32.59	31.36	33.97	0.35
July	82	32.10	30.95	33.02	0.35
August	56	31.81	30.29	33.04	0.56
September	22	32.02	30.77	33.46	0.56
October	41	32.71	31.50	33.86	0.61
November	141	33.03	31.24	34.37	0.56
December	38	33.27	32.38	34.04	0.45

Table 4.27. Monthly temperature and salinity statistics for 75 m depth from historical CTD data for water depth between 200 m and 500 m

Temperature 75 m on the Continental Slope

MONTH	# Observations	Mean	Min	Max	STD
January	34	0.01	-1.76	2.05	0.89
February	18	-0.10	-1.82	1.69	0.99
March	15	-0.40	-1.61	1.59	1.00
April	146	-0.73	-1.78	1.77	0.90
May	181	-0.53	-1.75	5.78	1.12
June	297	-0.61	-1.88	3.64	1.03
July	84	-1.13	-1.78	0.66	0.54
August	109	-1.28	-1.72	0.38	0.43
September	15	-0.69	-1.65	2.18	0.96
October	38	-0.09	-1.53	4.04	1.63
November	141	1.09	-1.38	5.90	1.73
December	32	2.02	-0.67	4.24	1.31

Salinity 75 m on the Continental Slope

MONTH	# Observations	Mean	Min	Max	STD
January	34	33.5	32.98	34.18	0.32
February	18	33.55	32.85	34.34	0.39
March	15	33.28	32.77	33.89	0.29
April	146	33.31	32.62	34.20	0.33
May	181	33.34	32.74	34.30	0.35
June	297	33.33	32.48	34.30	0.33
July	84	33.25	32.80	33.99	0.26
August	109	33.36	32.84	34.10	0.22
September	15	33.53	33.13	34.43	0.34
October	38	33.56	33.07	34.42	0.33
November	141	33.64	32.83	34.49	0.35
December	32	33.87	32.92	34.43	0.36

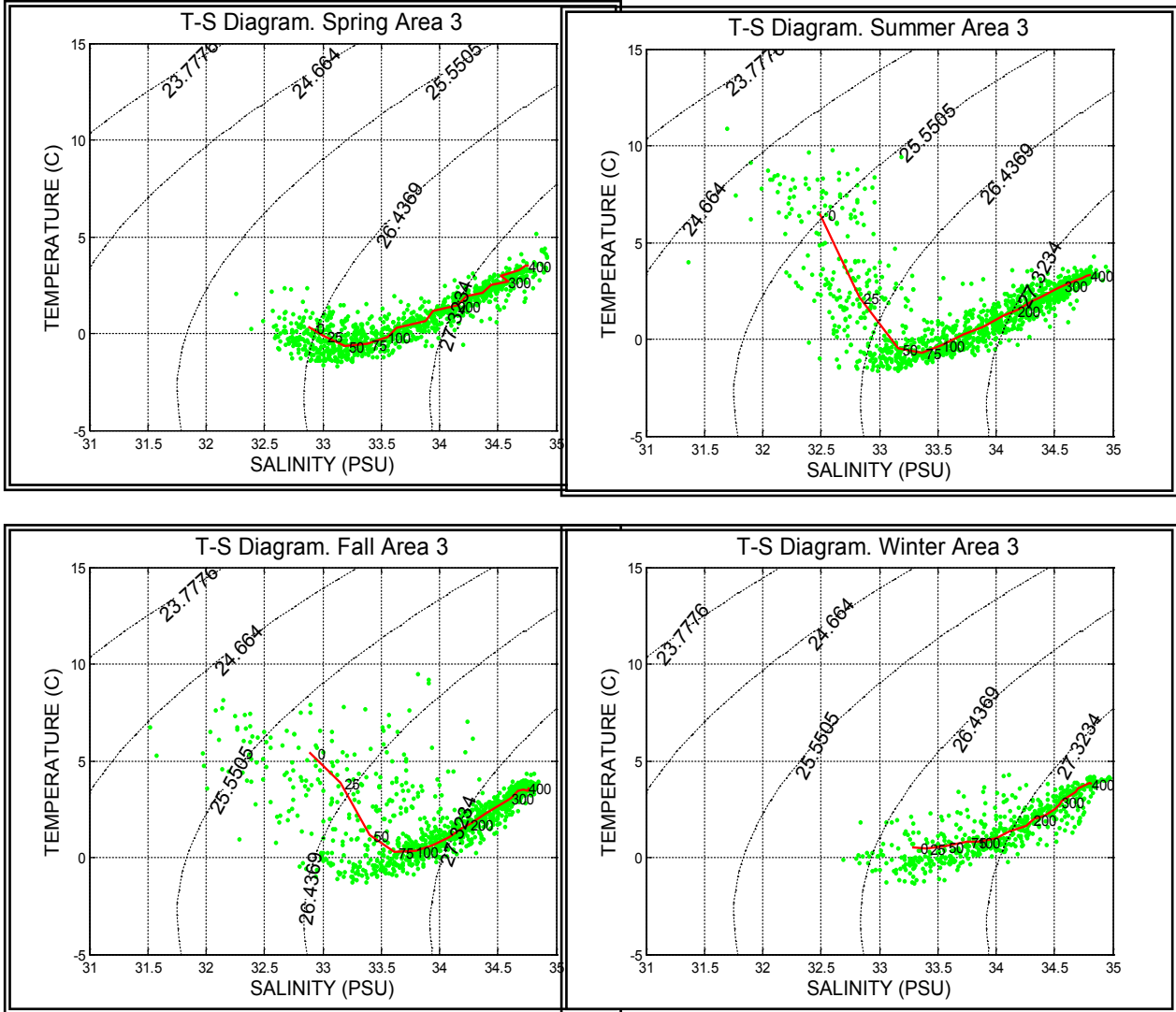


Figure 4.29. Seasonal T-S diagrams for sub-area 3 at water depths from 200 m to 500 m

Note: The red lines correspond to the average T-S curve for each area. The numbers on these curves represent the depth in metres.

5.0 Sea Ice and Icebergs

The sea ice and iceberg analysis was broken up into the same three regions as the ICOADS regions.

5.1 Sea Ice

A table defining the types of sea ice is presented below:

Table 5.1 Classifications of Sea Ice

Ice Type	Definition
New	Recently formed ice which includes frazil ice, grease ice, sluch and shuga. These types of ice are composed of ice crystals which are only weakly frozen together (if at all) and have a definite form only while they are afloat. In Canada, the term 'new ice' is applied to all recently formed sea ice having thickness up to 10cm. This includes ice rind, light nilas and dark nilas
Grey	Young ice 10 to 15 cm thick which is less elastic than nilas and breaks on swell. Usually rafts under pressure
Grey-White	Young ice 15 to 30 cm thick. Under pressure more likely to ridge than raft
First-Year	Sea ice of not more than one winter's growth, developing from young ice; thickness 30cm to 2m. May be subdivided into: Thin first year ice: 30-70 cm thick Medium first year ice: 70-120 cm thick Thick first year ice: over 120 cm thick
Old	Sea ice which has survived at least one summers melt. Most topographic features are smoother than on first year ice.
Fast	Sea ice which forms and remains fast along the coast where it is attached to the shore, to an ice wall, to an ice front, between shoals or grounded icebergs. Vertical fluctuations may be observed during changes of sea level. Fast ice may be forms in situ from sea water or by freezing of floating ice of any age to the shore and may extend a few metres or several hundred kilometres from the coast.

5.1.1 30-Year Median Ice Concentration

The 30-year median concentration of sea ice reaches its maximum during the week of March 05. Figure 5.1 the median of ice concentration does not extend into either of the three Regions covering the project area. The maximum median sea ice extent reaches to approximately 48°N; 49°W.

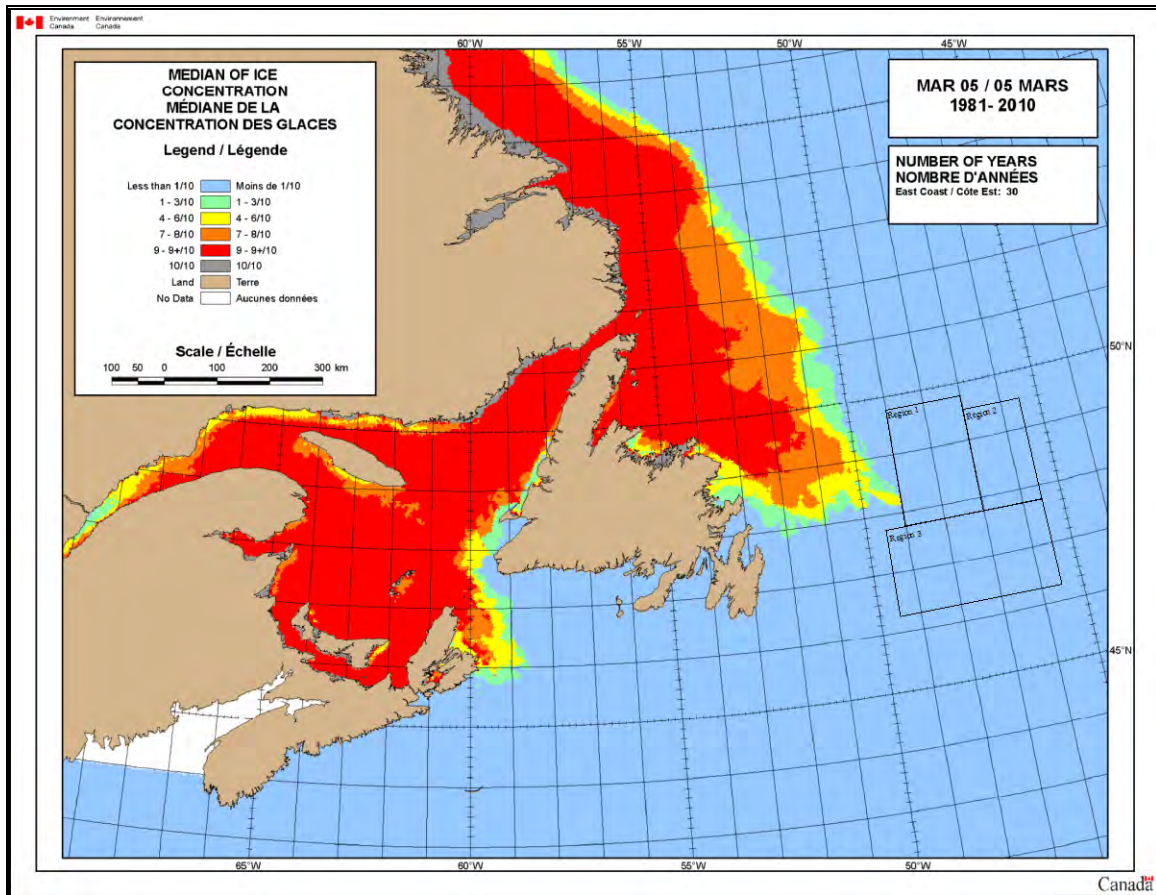


Figure 5.1 30-Year Frequency of Presence of Sea Ice within the Project Area (March 05)

(Source: Environment Canada, 2011).

5.1.2 30-Year Frequency of Presence of Sea Ice

Region 1

A weekly analysis of the Canadian Ice Service's 30-Year Frequency of Presence of Sea Ice over the area shows that the region is first affected by sea ice beginning the week of January 15 and lasting until the week beginning May 28. Figure 5.2 shows the week of March 12, the time when the frequency of presence of sea ice is the greatest over the area. The frequency of presence of sea ice over the majority of Region 1 is 1 – 15%. The

frequency of presence of sea ice is greatest in the southwest corner of Region 1 with the highest frequency between 34 – 50%.

The predominant ice type within the area from January 15th to the week of February 05th is a mixture of grey and grey-white. By February 19th, thin first-year ice begins to form in the northern part of Region 1 and new ice forms to the northwest. Thin first-year ice is the predominate ice type from February 19 until the week of April 02, with a small amount of medium and thick first-year ice also present. Thick first-year and some old ice is predominate for the remainder of the season.

Region 2

A weekly analysis of the Canadian Ice Service's 30-Year Frequency of Presence of Sea Ice over the area shows that the region is first affected by sea ice beginning the week of January 29 and lasting until the week beginning April. Figure 5.2 shows the week of March 12, the time when the frequency of presence of sea ice is the greatest over the area. The frequency of presence of sea ice over the majority of the southern half of Region 2 is 1 – 15%, while the northern half is mostly ice free.

The predominant ice type within the area from January 15th to the week of February 12th is a mixture of grey and grey-white. By February 19th, thin first-year ice begins to form in the southwest region of Region 2. Thin first-year ice is the predominate ice type from February 19 until the week of March 26, with a small amount of Grey-White, Medium first-year and thick first-year ice also present. Thick first-year and some old ice are predominate for the remainder of the season.

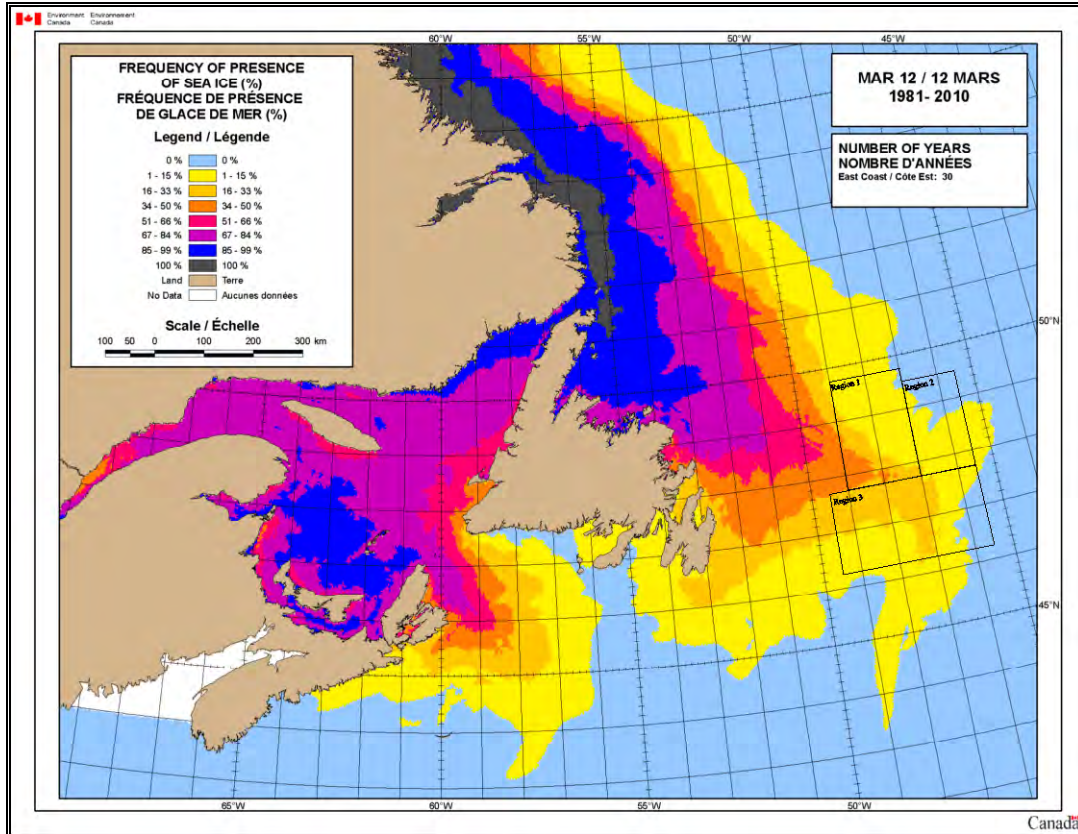


Figure 5.2 30-Year Frequency of Presence of Sea Ice within the Project Area (March 12)

(Source: Environment Canada, 2011)

Region 3

A weekly analysis of the Canadian Ice Service's 30-Year Frequency of Presence of Sea Ice over the area shows that the region is first affected by sea ice beginning the week of January 15 and lasting until the week beginning May 21. Figure 5.3 shows the week of March 19, the time when the frequency of presence of sea ice is the greatest over the area. The frequency of presence of sea ice over the majority of southern half of Region 3 is 1 – 15% while the frequency of presence of sea ice in the northern half is highest at 16 – 33%. There is a small sector in the southeast corner that is ice free.

The predominant ice type within the area from January 15th to the week of February 12th is a mixture of grey and grey-white. By February 19th, thin first-year ice begins to form in the eastern part of Region 3. Thin first-year ice is the predominate ice type from February 19 until the week of April 02, with a small amount of Grey-White, Medium first-year and thick first-year ice also present. Medium and thick first-year ice is predominate for the remainder of the season.

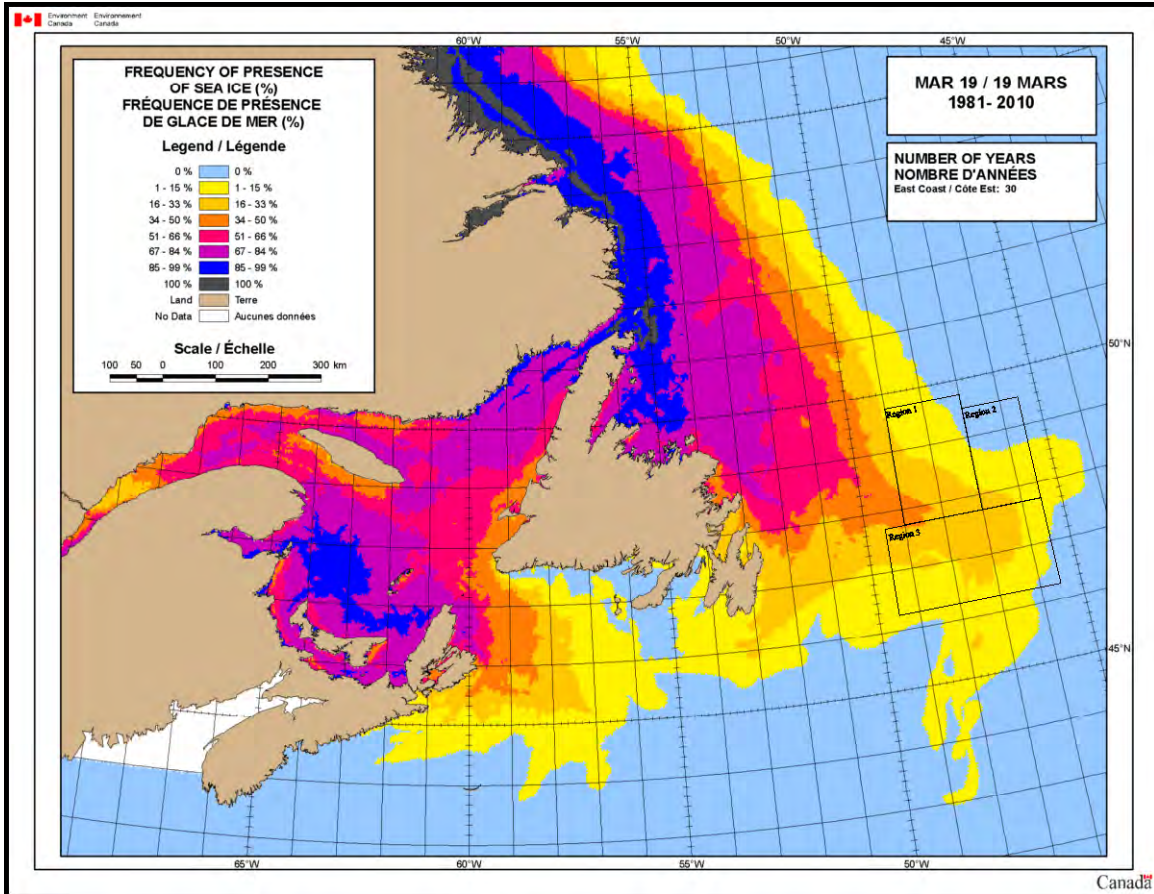


Figure 5.3 30-Year Frequency of Presence of Sea Ice within the Project Area for the week of March 19

(Source: Environment Canada, 2011)

5.2 Icebergs

An analysis was performed to determine the threat posed by icebergs in the Project area. The International Ice Patrol Iceberg Sightings Database from 1974-2009 was used as the primary data source in this analysis (NSIDC, 2009).

Overall there is a good distribution of iceberg sightings ranging from a total of 1474 in all 3 regions for 1974 to only one over all three regions in 2006 (Figure 5.4). Only iceberg sightings that occurred within the project area were considered in this analysis. Duplicate sightings of the same iceberg were also eliminated from the data set so that only the initial sighting was counted.

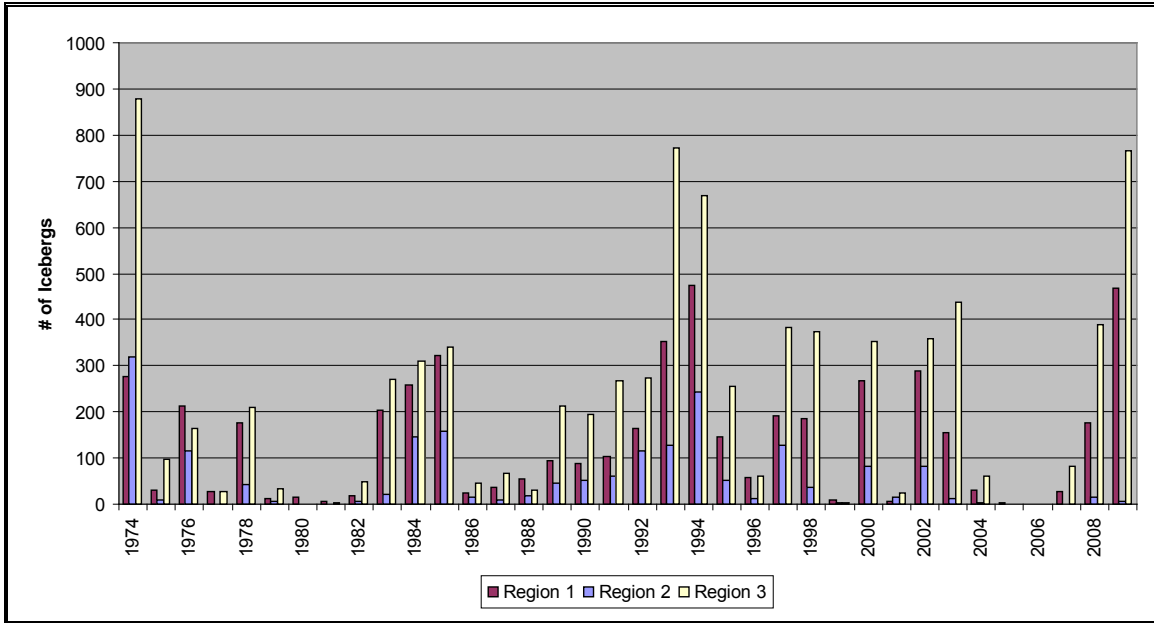


Figure 5.4 Iceberg Sightings within the Project Area

(Source: IIP)

Region 1

Figure 5.1 shows the positions of all icebergs within Region 1 from 1974-2009. Iceberg concentration is concentrated towards the southern portion of the region. Over the 35 years studied, 3546 icebergs have been sighted inside Region 1. Environmental factors such as iceberg concentration, ocean currents and wind determine how icebergs drift through the area.

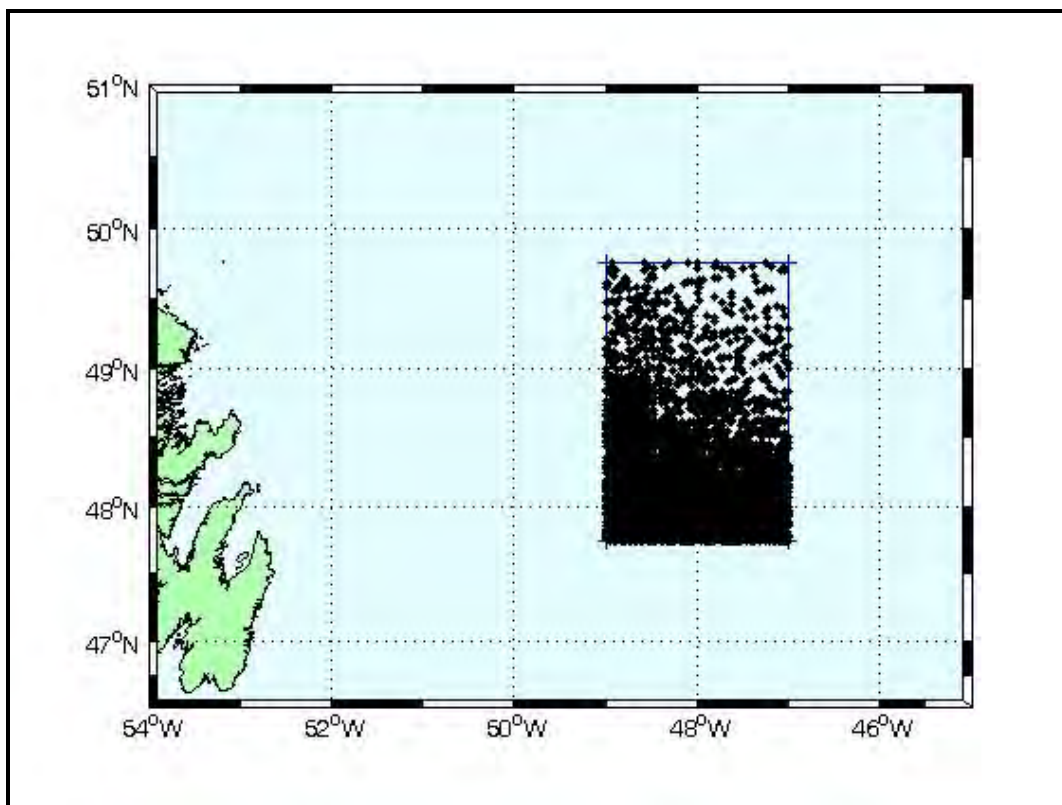


Figure 5.4 Iceberg sightings within Region 1 from 1974 - 2009

A monthly analysis shows that icebergs have been spotted within the region in all months, with the exception of September and November. They are most prominent during the month of May (Figure 5.6 and Table 5.2). With respect to size, the most prominent icebergs are small, accounting for 28.1% of observed icebergs within the region. Large icebergs occur 8.4% of the time and very large icebergs for 1.0% of the time.

Table 5.2 Iceberg Size by month within Region 1

(source:IIP)

	Jan	Feb	Mar	Apr	May	Jun	Jul	Aug	Sep	Oct	Nov	Dec	Year
General	13	21	90	316	323	115	51	1	0	0	0	0	930
Unidentified Target	26	23	43	5	18	13	7	0	0	4	0	1	140
Growler	0	4	41	31	69	8	19	0	0	0	0	0	172
Bergy Bit	8	3	20	20	29	9	1	1	0	0	0	0	91
Small	21	108	277	260	243	52	33	4	0	0	0	0	998
Medium	14	49	246	198	262	73	34	5	0	0	0	0	881
Large	1	18	60	93	70	42	13	0	0	0	0	0	297
Very Large	0	1	9	18	4	3	0	2	0	0	0	0	37
Total	83	227	786	941	1018	315	158	13	0	4	0	1	3546

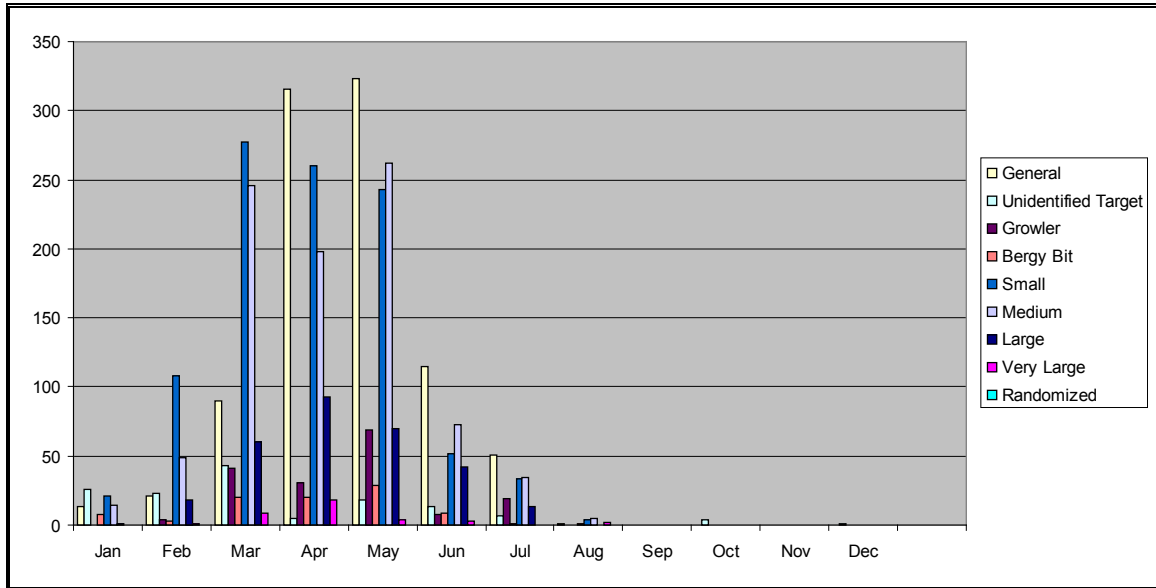


Figure 5.6 Iceberg Size by month within Region 1

Region 2

Figure 5.7 shows the positions of all icebergs within Region 2 from 1974-2009. Iceberg concentration is concentrated towards the southern portion of the region. Over the 35 years studied, 1002 icebergs have been sighted inside Region 2. Environmental factors such as iceberg concentration, ocean currents and wind determine how icebergs drift through the area.

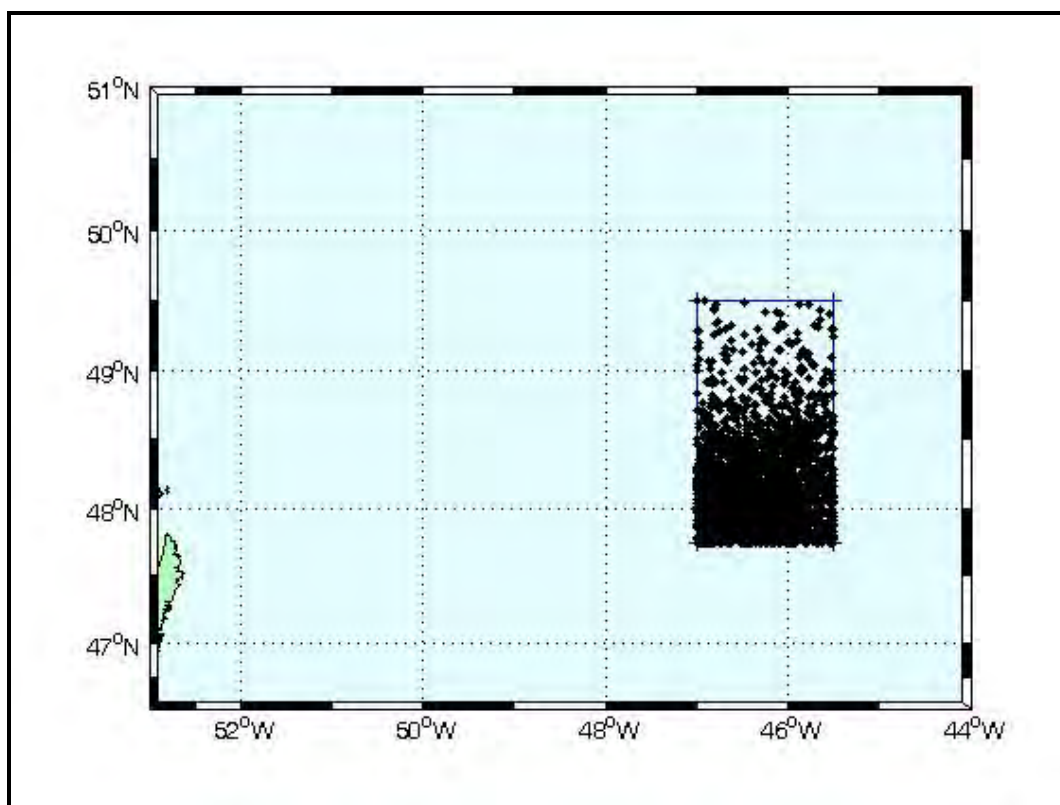


Figure 5.7 Iceberg sightings within Region 2 from 1974 – 2009

A monthly analysis shows that icebergs have been spotted within the region in all months between January and August. They are most prominent during the month of March (Figure 5.8 and Table 5.3). With respect to size, the most prominent icebergs are medium, accounting for 25.3% of observed icebergs within the region. Large icebergs occur 8.5% of the time and very large icebergs for 0.3% of the time.

Table 5.3 Iceberg Size by month within Region 2

(source:IIP)

	Jan	Feb	Mar	Apr	May	Jun	Jul	Aug	Sep	Oct	Nov	Dec	Year
General	0	3	50	69	112	37	25	1	0	0	0	0	297
Unidentified Target	11	18	8	9	23	14	3	0	0	0	0	0	86
Growler	0	4	13	3	3	0	3	0	0	0	0	0	26
Bergy Bit	0	4	11	3	3	1	0	0	0	0	0	0	22
Small	1	45	97	42	26	11	4	3	0	0	0	0	229
Medium	7	13	97	48	57	20	9	3	0	0	0	0	254
Large	0	1	27	15	27	11	2	2	0	0	0	0	85
Very Large	0	0	0	2	1	0	0	0	0	0	0	0	3
Total	19	88	303	191	252	94	46	9	0	0	0	0	1002

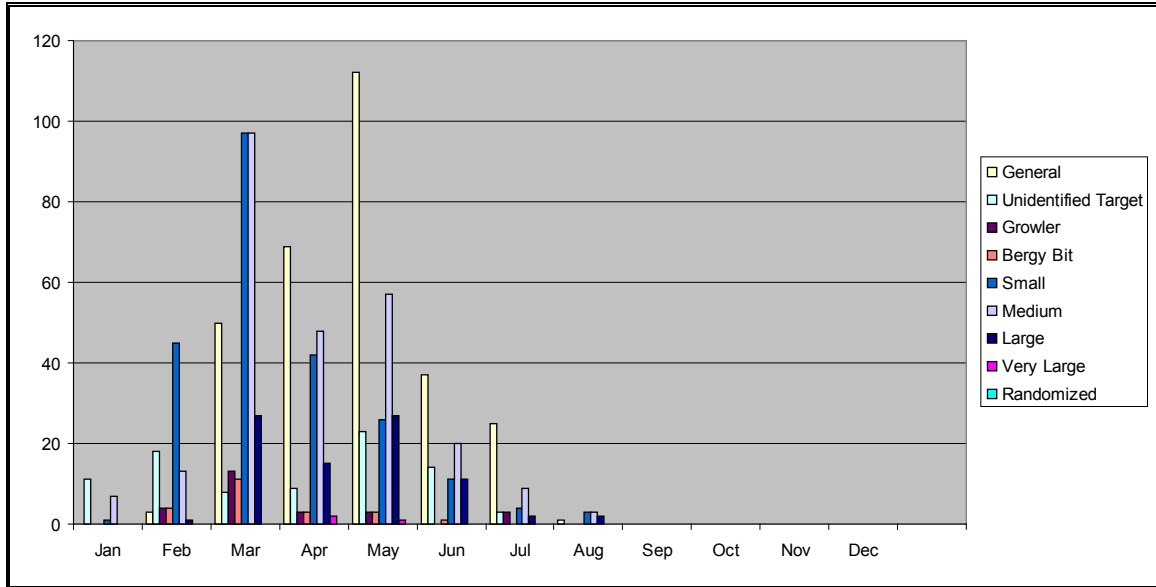


Figure 5.8 Iceberg Size by month within Region 2

Region 3

Figure 5.9 shows the positions of all icebergs within Region 3 from 1974-2009. The greatest overall distribution of all three sectors occurs within Region 3 with icebergs having been spotted over nearly the entire region. Over the 35 years studied, 9527 icebergs have been sighted inside the region. Environmental factors such as iceberg concentration, ocean currents and wind determine how icebergs drift through the area.

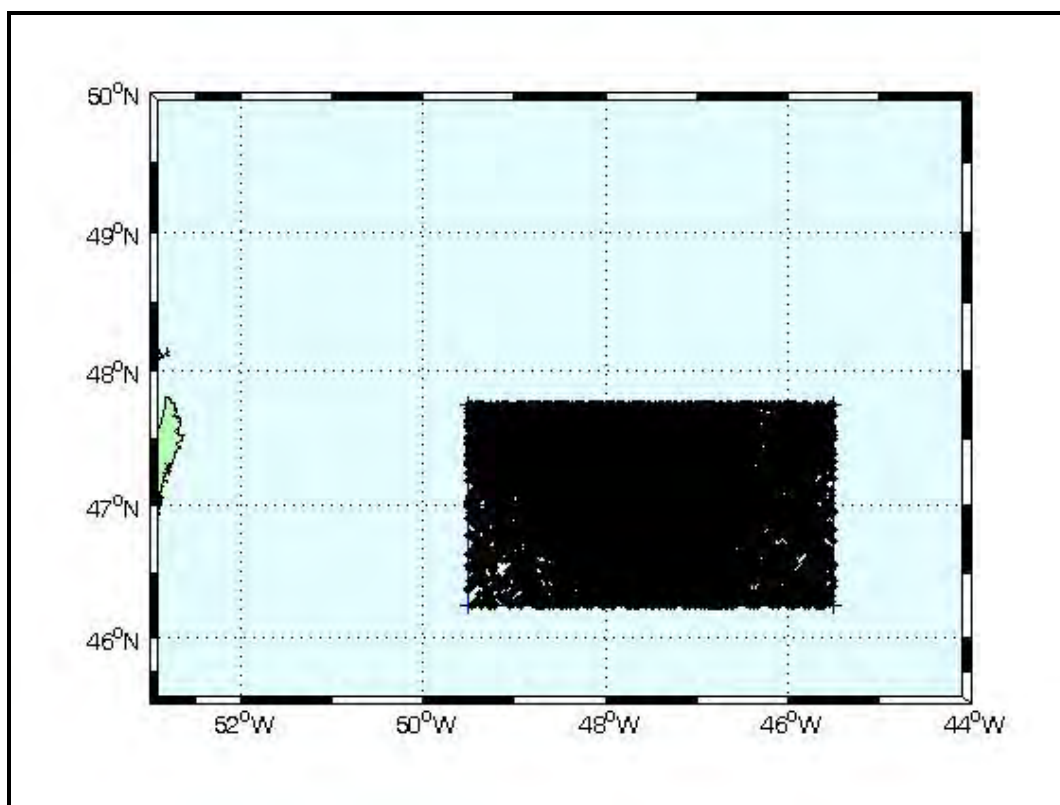


Figure 5.9 Iceberg sightings within Region 3 from 1974 - 2009

A monthly analysis shows that icebergs have been spotted within the region in all months with the exception of September and November. They are most prominent during the month of April (Figure 5.8 and Table 5.3). With respect to size, the most prominent icebergs are medium, accounting for 27.0% of observed icebergs within the region. Large icebergs occur 9.7% of the time and very large icebergs for 0.8% of the time.

Table 5.4 Iceberg Size by month within Region 3

(source:IIP)

	Jan	Feb	Mar	Apr	May	Jun	Jul	Aug	Sep	Oct	Nov	Dec	Year
General	5	30	426	540	716	300	71	0	0	0	0	0	2088
Unidentified Target	19	93	123	33	110	28	11	1	0	5	0	4	427
Growler	1	11	87	163	227	32	16	0	0	2	0	0	539
Bergy Bit	4	4	64	102	75	22	4	0	0	0	0	1	276
Small	30	231	730	844	604	140	48	0	0	0	0	1	2628
Medium	14	109	640	830	686	237	51	1	0	0	0	1	2569
Large	1	16	198	314	249	134	15	0	0	0	0	0	927
Very Large	0	0	16	27	22	5	3	0	0	0	0	0	73
Total	74	494	2284	2853	2689	898	219	2	0	7	0	7	9527

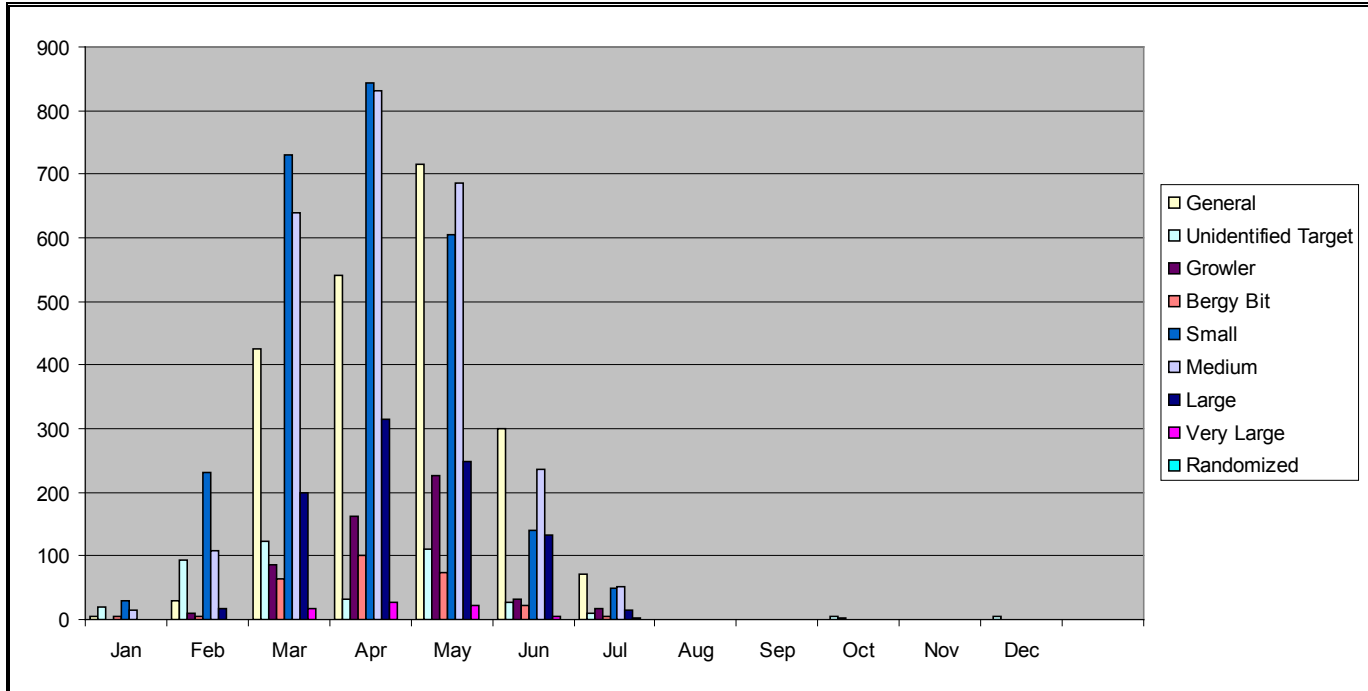


Figure 5.10 Iceberg Size by month within Region 3

References

- Archer, C.L., and K. Caldeira, 2008. Historical trends in the jet streams, *Geophys. Res. Lett.*, 35, L08803.
- Bell, G.D., and M. Chelliah, 2006. Leading Tropical Modes Associated with Interannual and Multidecadal Fluctuations in North Atlantic Hurricane Activity. *J. Climate*, V.19, 590–612.
- Borgman, L.E., 1973. Probabilities for the highest wave in a hurricane. *J. Waterways, Harbors and Coastal Engineering Div.*, ASCE, p.185-207
- Colbourne, E., 2002. Physical Oceanographic Conditions on the Newfoundland and Labrador Shelves during 2001. CSAS Res.Doc. 2002/023.
- Colbourne, E.B., 2004. Decadal Changes in the Ocean Climate in Newfoundland and Labrador Waters from the 1950s to the 1990s. *J. Northw. Atl. Fish. Sci.*, 34. 41–59.
- Colbourne, E., B. deYoung, S. Narayanan, and J. Helbig, 1997. Comparison of hydrography and circulation on the Newfoundland Shelf during 1990-1993 with the long-term mean. *Can. J. Fish. Aquat. Sci.* V.54 (Suppl. 1), 1997.
- Colbourne, E.B., C. Fitzpatrick, D. Senciall, W. Bailey, and P. Stead, 2007. Oceanographic Observations from Travel-Mounted CTDs on Multi-Species

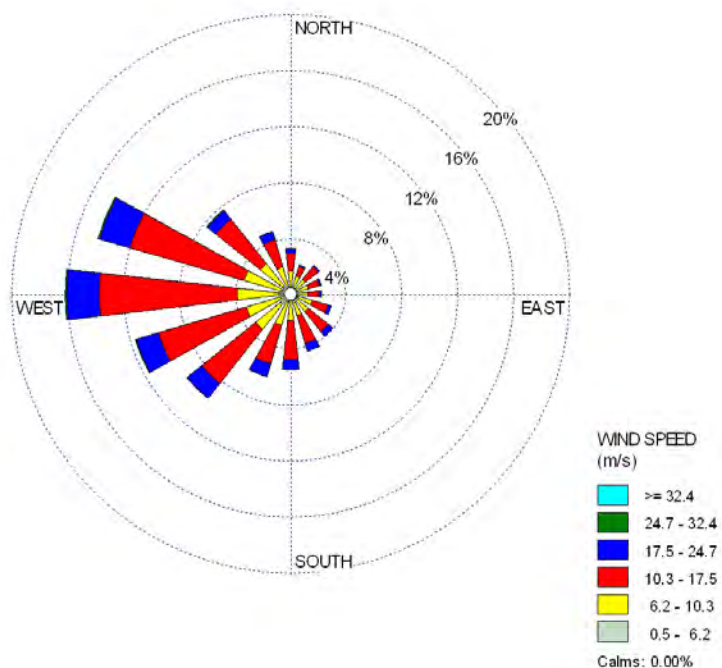
- Surveys in the Newfoundland and Labrador Region. AZMP Bulletin, No. 6, Fisheries and Oceans Canada, p. 43-47.
- Colbourne, E.B., and K.D. Foote, 2000. Variability of the Stratification and Circulation on the Flemish Cap during the Decades of the 1950's-1990's. J. Northw. Atl. Fish. Sci., V.26, p.103-122.
- Colbourne, E.B., and K.D. Foote, 1994. Spatial Temperature and Salinity Fields over the Shelves of Newfoundland and Labrador. Can. Tech. Rep. Hydrog. Ocean Sci., V.160, 128 p.
- Colbourne, E.B., and D.R. Senciall, 1996. Temperatures, Salinity and Sigma-t along the standard Flemish Cap. Transect. Can. Tech. Rep. Hydrog. Ocean Sci. 172, 222.
- DeTracey, B.M., C.L. Tanf, and P.C. Smith, 1996. Low-frequency currents at the northern edge of the Grand Banks. J. Geophys. Res., V.101, C6, P.12, 223-14,236.
- Environment Canada, 1997. The Canada Country Study: Climate Impacts and Adaptation, Atlantic Canada Summary.
- Forristall, G.Z., 1978. On the statistical distribution of wave heights in a storm. J. Geophys. Res., V.83, p.2353-2358.
- Greenberg, D.A., and B.D. Petrie, 1988. The Mean Barotropic Circulation on the Newfoundland Shelf and Slope 1951-1980. J. Geoph. Res., V.93 (C 12), PERD Project, 15541-15550.
- Han, G., K. Ohashi, N. Chen, P.G. Myers, N. Nunes, J. Fischer, 2010. Decline and partial rebound of the Labrador Current 1993-2009. Monitoring ocean currents from altimetric and CTD data. J. Geophys., Res. V.115, C12012, doi:10.1029/2009/JC006091, 2010.
- Harris, Erin. Personal Correspondence. Oceanweather, October 15, 2007
- Hart, R.E., and J.L. Evans, 2001. A Climatology of extratropical transition of Atlantic tropical cyclones. J. Climate, V.14, p.546-564
- Helbig, J.A., and P. Brett, 1995. A Compendium of Satellite Tracked Drifting Buoy Observations Collected on the Labrador Shelf, Northeast Newfoundland Shelf, and Grand Banks. Unpublished Report.
- Hukuda, H., R.J. Greatbach and A.E. Hay, 1989. A Simple Three-Dimensional Model of the Circulation off Newfoundland. J. Geoph. Res., V.94 (C9), p.12607-12618.
- Jarvinen, B.R., C.J. Neumann, and M.A.S. Davis, 1984. A tropical cyclone data tape for the North Atlantic basin, 1886-1983: Contents, limitations, and uses. NOAA Tech. Memo. NWS NHC 22, NOAA/National Hurricane Center, Miami, FL, 21 pp. [Available from NOAA/Tropical Prediction Center, 11691 SW 17th St., Miami, FL 33165-2149.]
- Kent, E.C., P.K. Taylor, B.S. Truscott and J.S. Hopkins, 1993. The Accuracy of Voluntary Observing Ships' Meteorological Observations - Results of the VSOP-NA. J. Atmosph. Oceanic Technol., V.10, p.591-608.

- Lazier, J.R.N., and D.G. Wright, 1993. Annual velocity Variations in the Labrador Current. *J. Phys. Oceanog.*, V.23, p.659-678.
- McCabe, G.J., M.P. Clark, M.C. Serreze, 2001. Trends in Northern Hemisphere Surface Cyclone Frequency and Intensity. *J. Climate*, V.14, p.2763–2768.
- Murphy, D.L., W.E. Hanson, and R.L. Tuxhorn, 1991. Modifications to Ice Patrol's Mean Current Base. Report of the International Ice Patrol in the North Atlantic. US Coast Guard Bulletin, No. 76, CGC /188 /45.
- Narayanan, S., S. Prinsenberg and P.C. Smith, 1996. Current Meter Observations from the Labrador and Newfoundland Shelves and Comparisons with Barotropic Model Predictions and IIP Surface Currents. *Atmosphere - Ocean*, V.34, No. 1, 227-255.
- NSIDC, 2009. International Ice Patrol (IIP) Iceberg Sightings Data base. Boulder, Colorado USA: National Snow and Ice Data Center/World Data Center for Glaciology. Digital media
- Neumann, C.J., B.R. Jarvinen, C.J. McAdie, and J.D. Elms, 1993. Tropical cyclones of the North Atlantic Ocean, 1871–1992. National Climatic Data Center in cooperation with the National Hurricane Center, Coral Gables, FL, 193 pp. [Most recent track information available online at <http://www.nhc.noaa.gov>.]
- Pepin, P., and J.A. Helbig, 1997. Distributions and Drift of Atlantic Cod (*Gadus morhua*) Eggs and Larval on the Northeast Newfoundland Shelf. *Can. J. Fish Aquat. Sci.*, V.4, p.670-685.
- Petrie, B., and A. Isenor, 1984. An analysis of Satellite - Tracked Drifter Observations Collected in the Grand Banks Region. *Can. Tech. Rep. Hydrog. Ocean Sci.*, V.39, 64 p.
- Petrie, B., S. Akenhead, J. Lazier, and J. Loder, 1988. The cold intermediate layer on the Labrador and Northeast Newfoundland Shelves, 1978-1986. *NAFO Sci. Council. Stud.*, 12, 57-69.
- Petrie, B., and D. Warnell, 1988. Oceanographic and Meteorological Observations from the Hibernia Region of the Newfoundland Grand Banks. *Canadian Data Report of Hydrography and Ocean Science*, No. 69, 270 p.
- Rogers, E., and L.F. Bosart, 1986. An Investigation of Explosively Deepening Oceanic Cyclones. *Monthly Weather Review*, V.114, p.702-718.
- Ross, C., 1980. The Drift of Satellite - Tracked Buoys on Flemish Cap, 1979-80. *NAFO Sci. Council. Res. Doc. 80/Ix/127*, 12 p.
- Stein, M., 2007. Oceanography of the Flemish Cap and Adjacent Waters. *J. Northw. Atl. Fish. Sci.*, V.37, p.135-146.
- Swail, V.R., V.J. Cardone, M. Ferguson, D.J. Gummer, E.L. Harris, E.A. Orelup and A.T. Cox, 2006. The MSC50 Wind and Wave Reanalysis. 9th International Wind and Wave Workshop, September 25-29, 2006, Victoria, B.C.

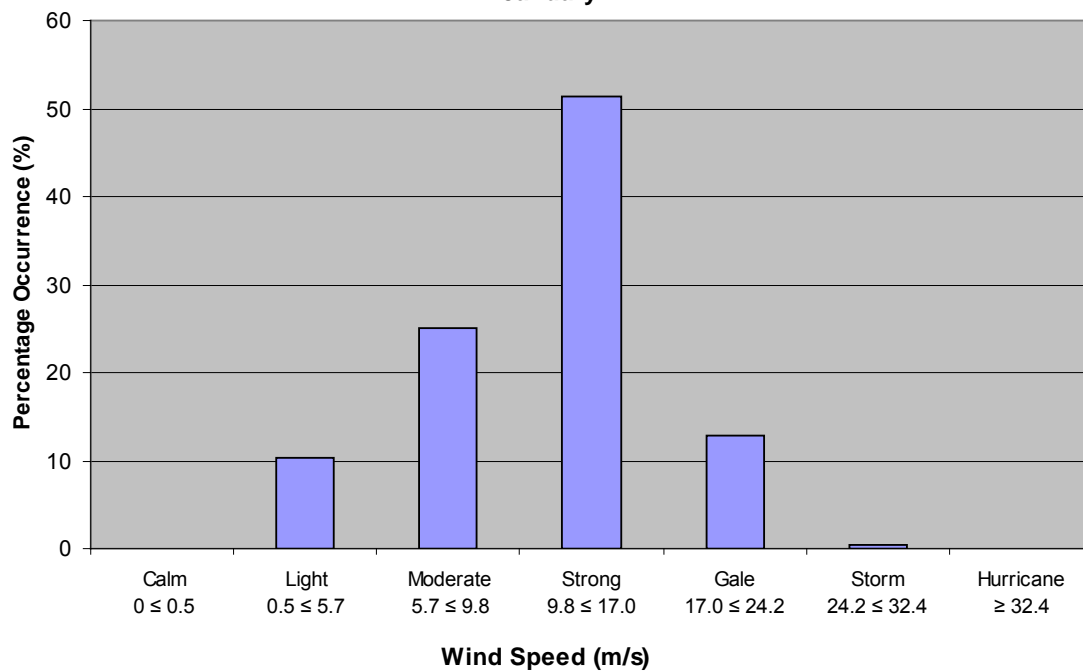
- United States Geological Survey, Conservation Division, 1979. OCS Platform Verification Program. Reston, Virginia.
- Winterstein, S.R., T. Ude, C.A. Cornell, P. Jarager, and S. Haver, 1993. Environmental Parameters for Extreme Response: Inverse FORM with Omission Factors. ICOSsar-3, Paper No 509/11/3, Innsbruck, 3-12 August 1993.
- Yao, T., T. Brown, and D. Fissel, 1992. Verification Study of Regional Sea Ice Models. Report by Active Sciences Ltd. to Ice Centre, Environment Canada, 286 p.
- Yashayaev, I, and A. Clarke, 2006. Recent warming of the Labrador Sea. DFO AZMP Bulletin, No. 5, 2006.

APPENDIX 1
Monthly Wind Roses
and
Percentage Occurrence Graphs
for MSC50 Grid point 14845

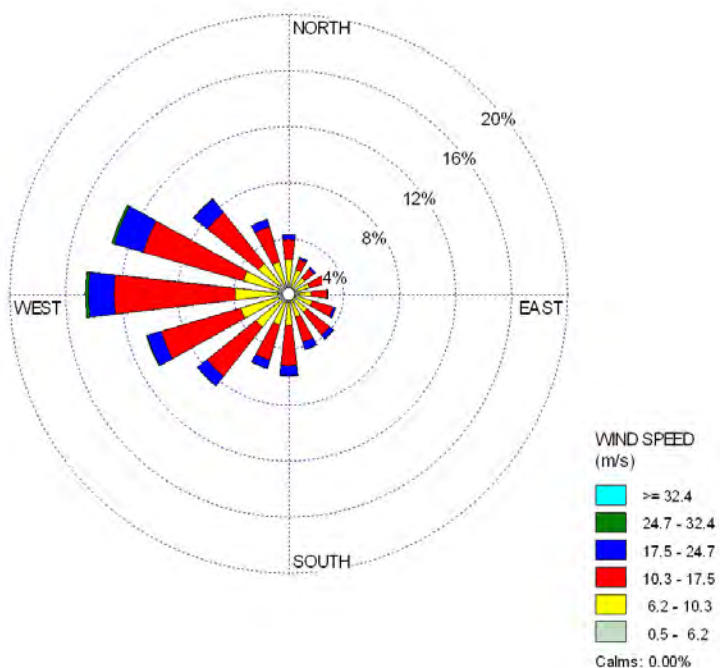
January



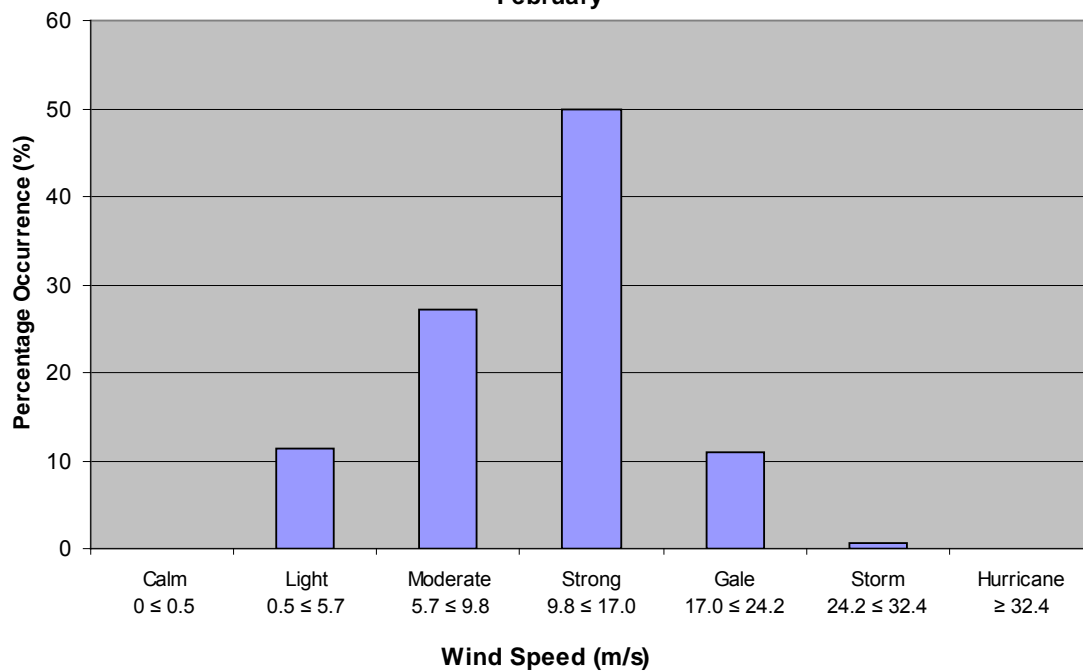
Wind Speed Percentage Occurrence Grid Point 14845 January



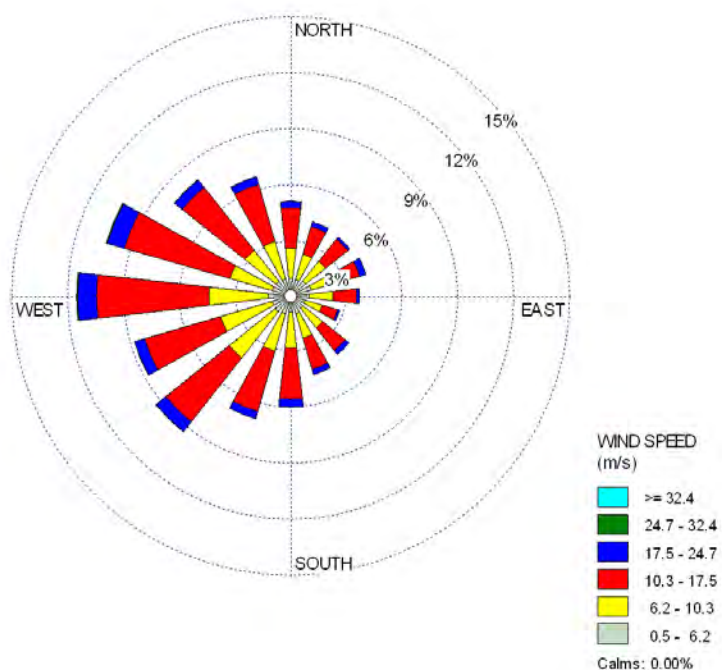
February



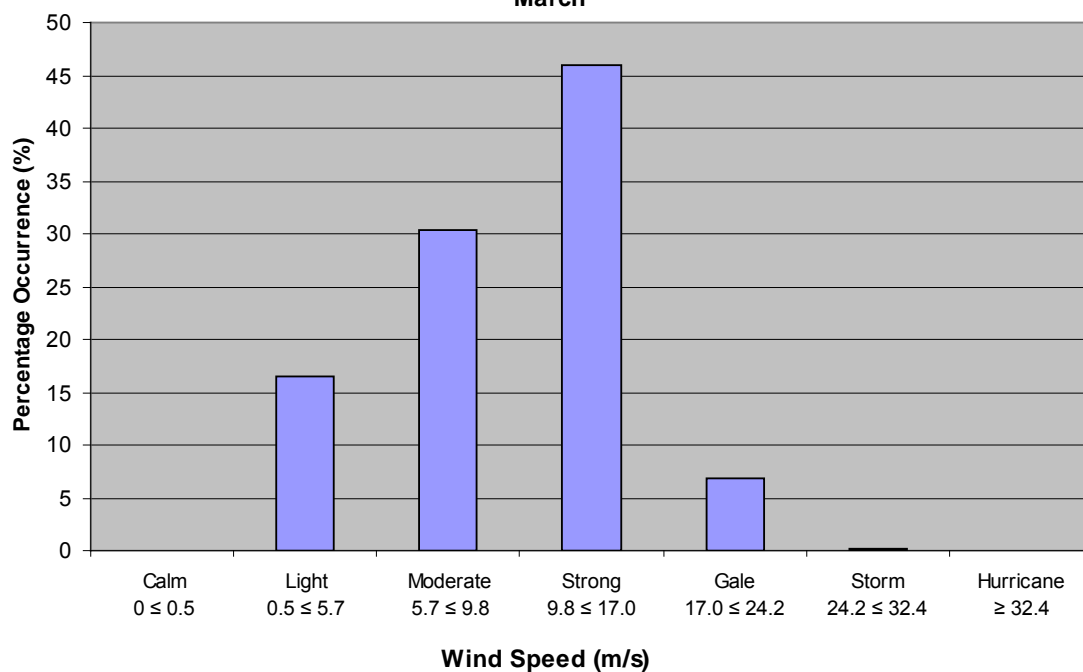
**Wind Speed Percentage Occurrence
Grid Point 14845
February**



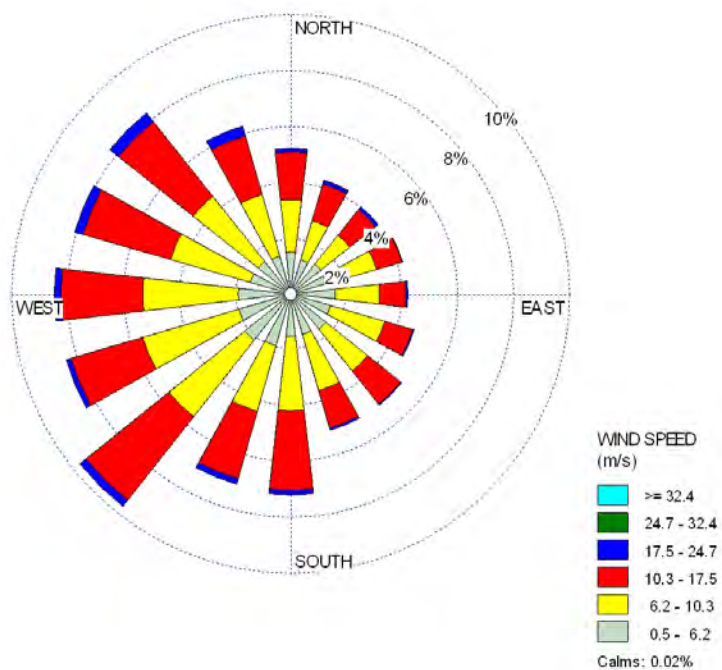
March



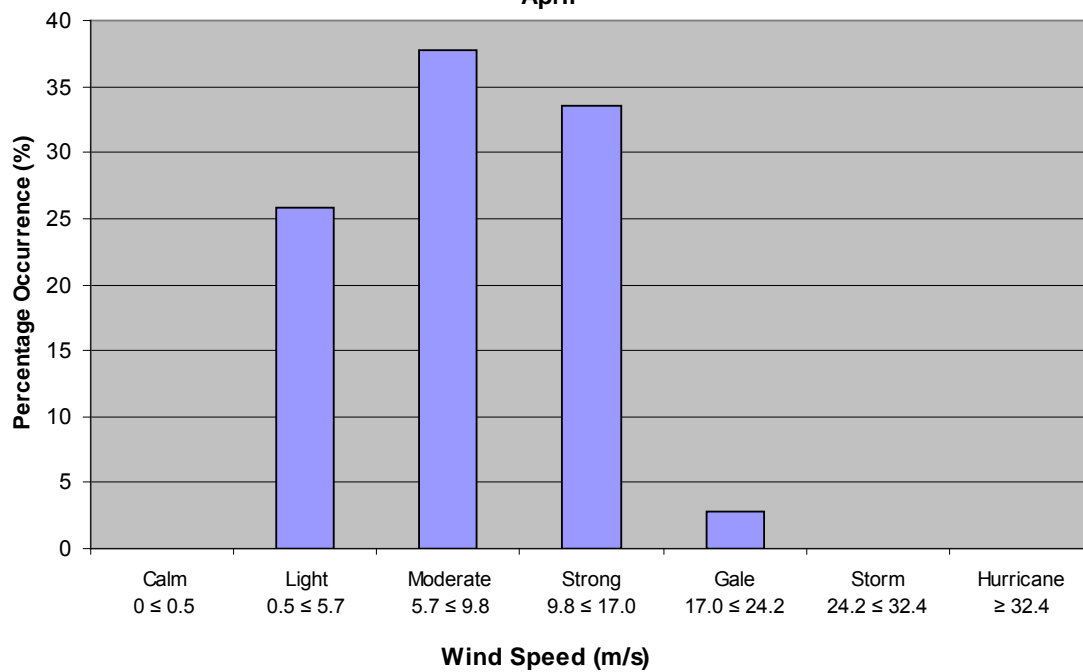
**Wind Speed Percentage Occurrence
Grid Point 14845
March**



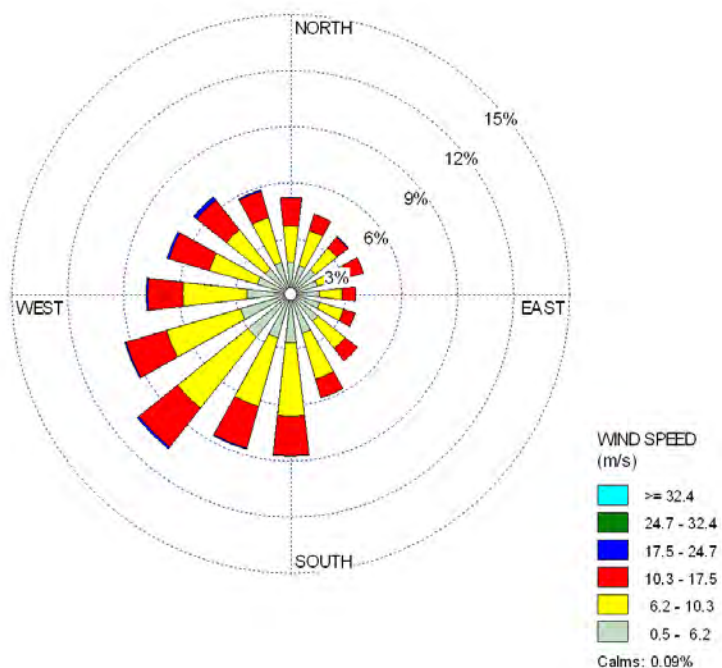
April



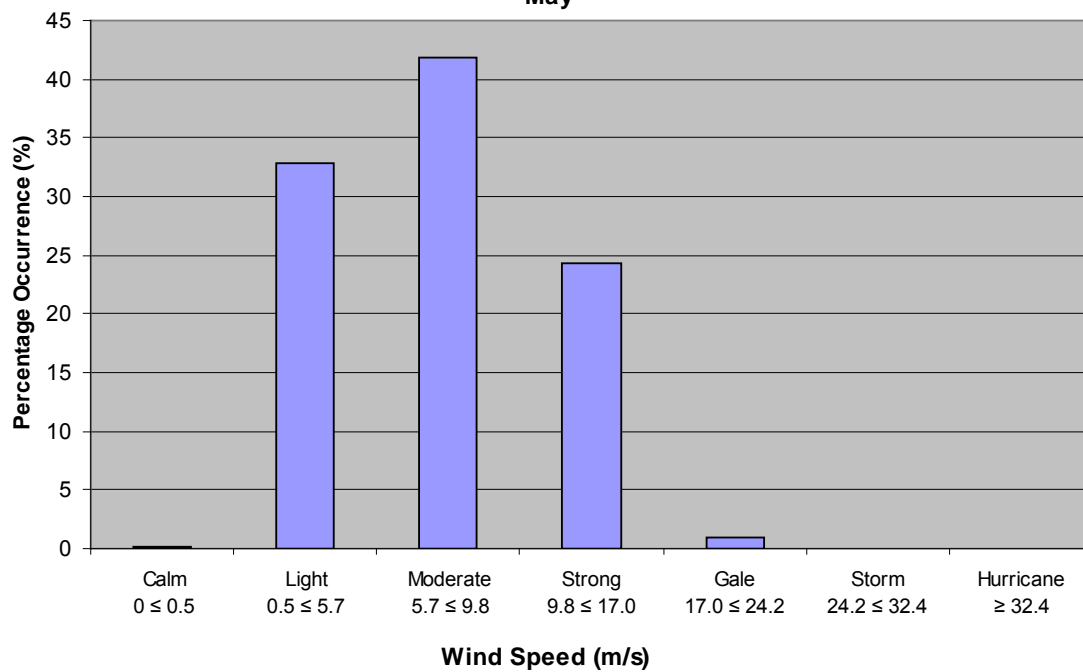
**Wind Speed Percentage Occurrence
Grid Point 14845
April**



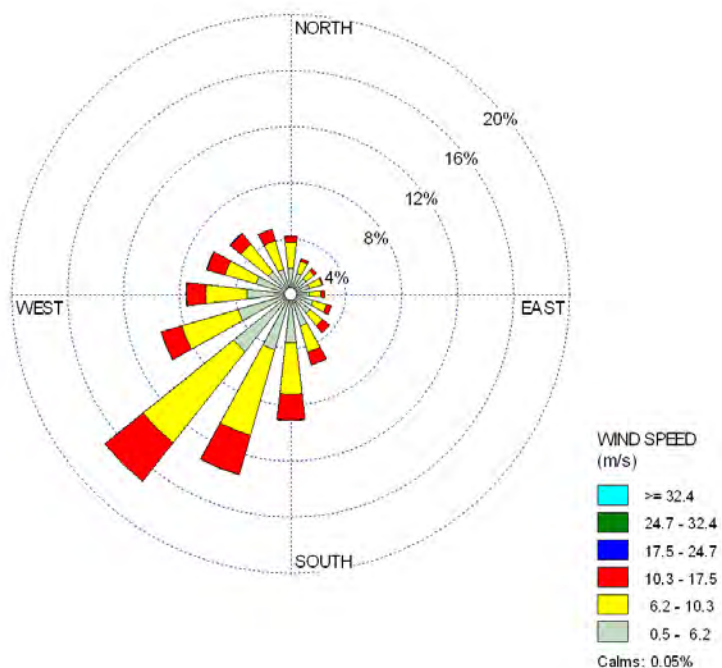
May



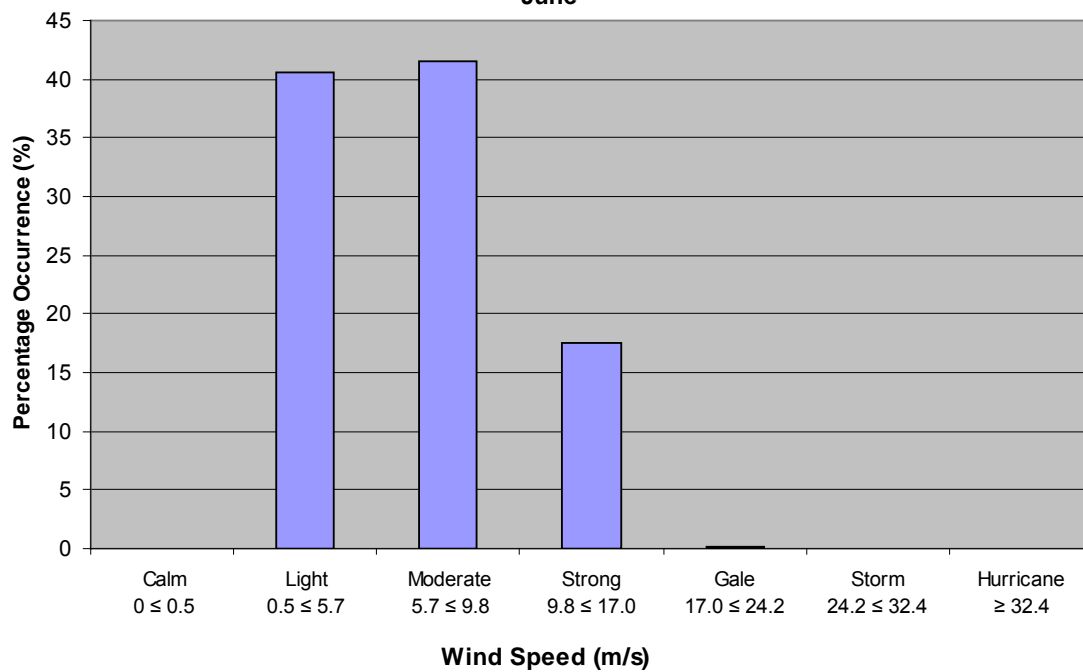
Wind Speed Percentage Occurrence
Grid Point 14845
May



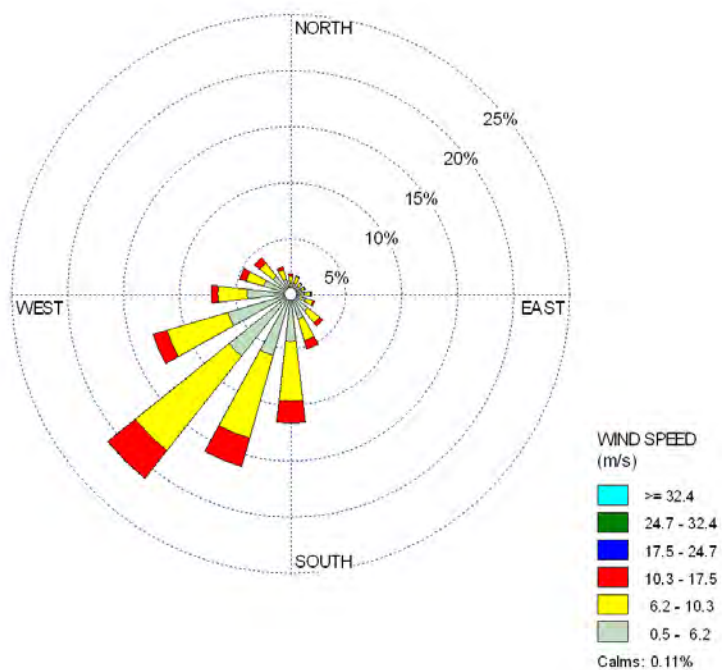
June



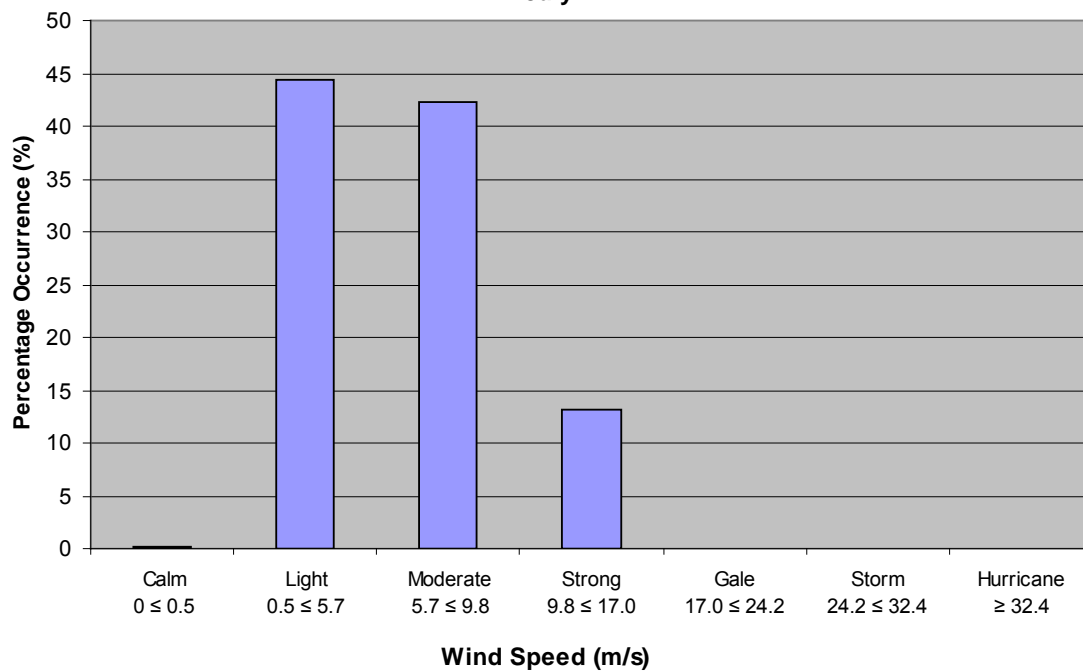
Wind Speed Percentage Occurrence
Grid Point 14845
June



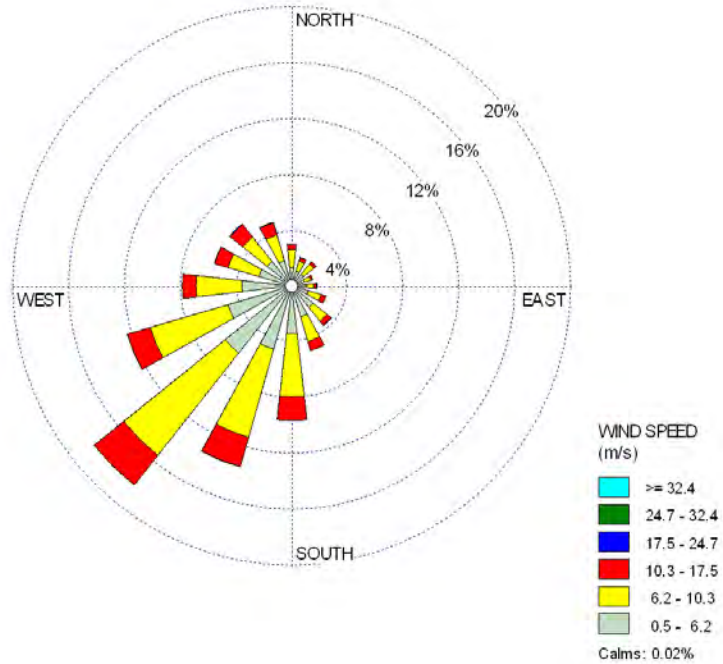
July



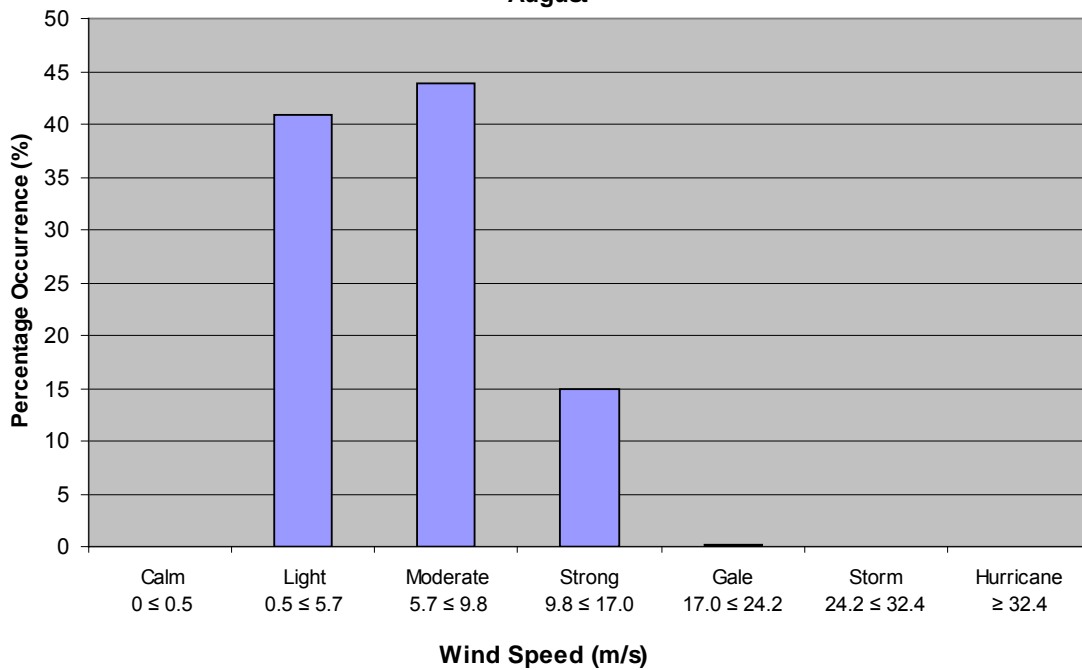
Wind Speed Percentage Occurrence
Grid Point 14845
July



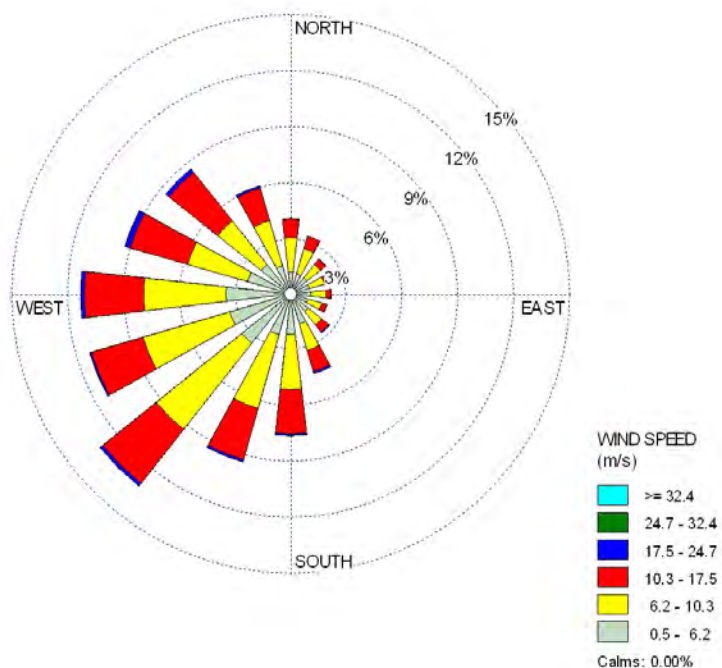
August



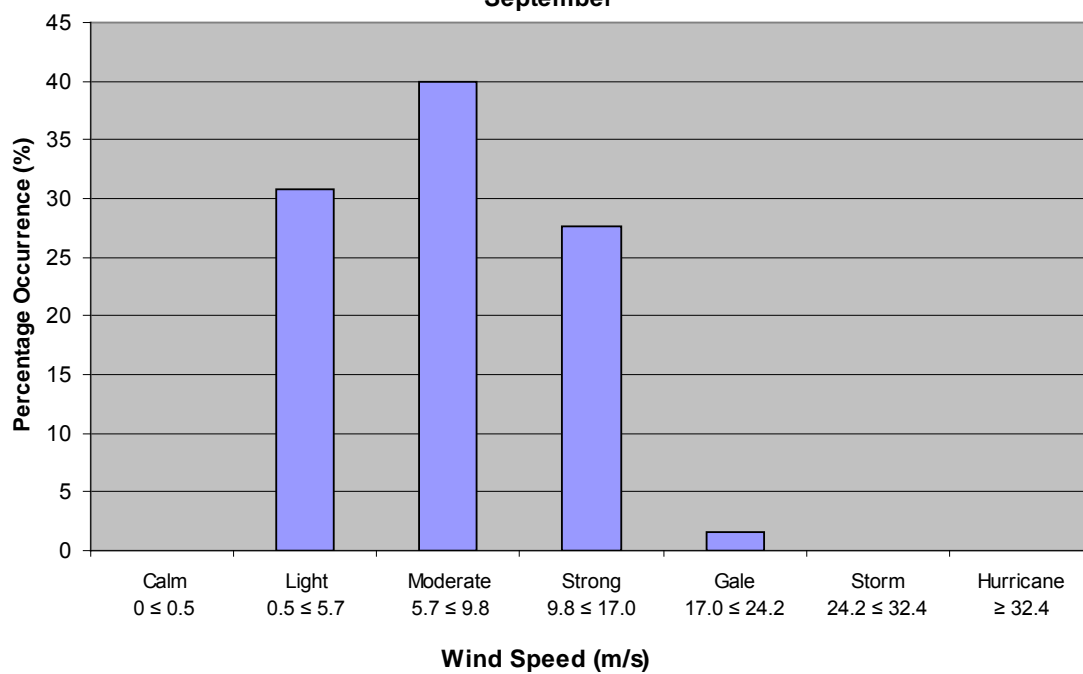
**Wind Speed Percentage Occurrence
Grid Point 14845
August**



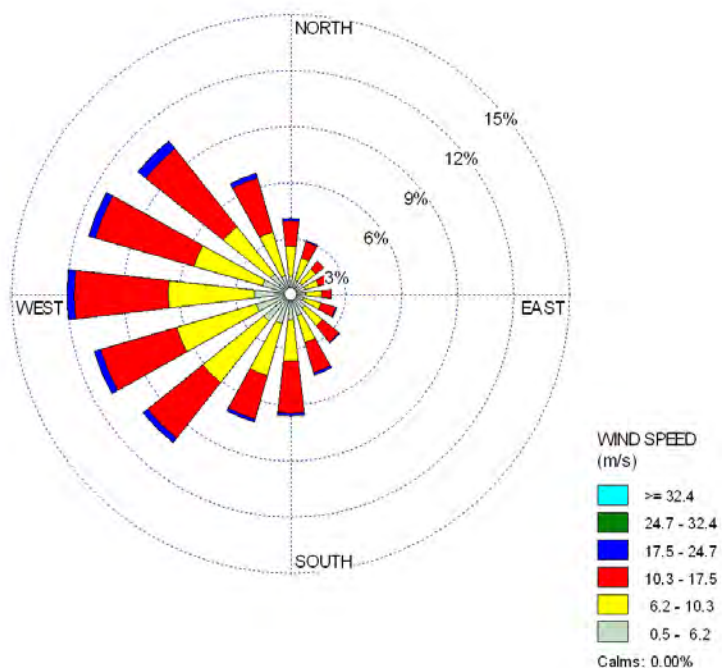
September



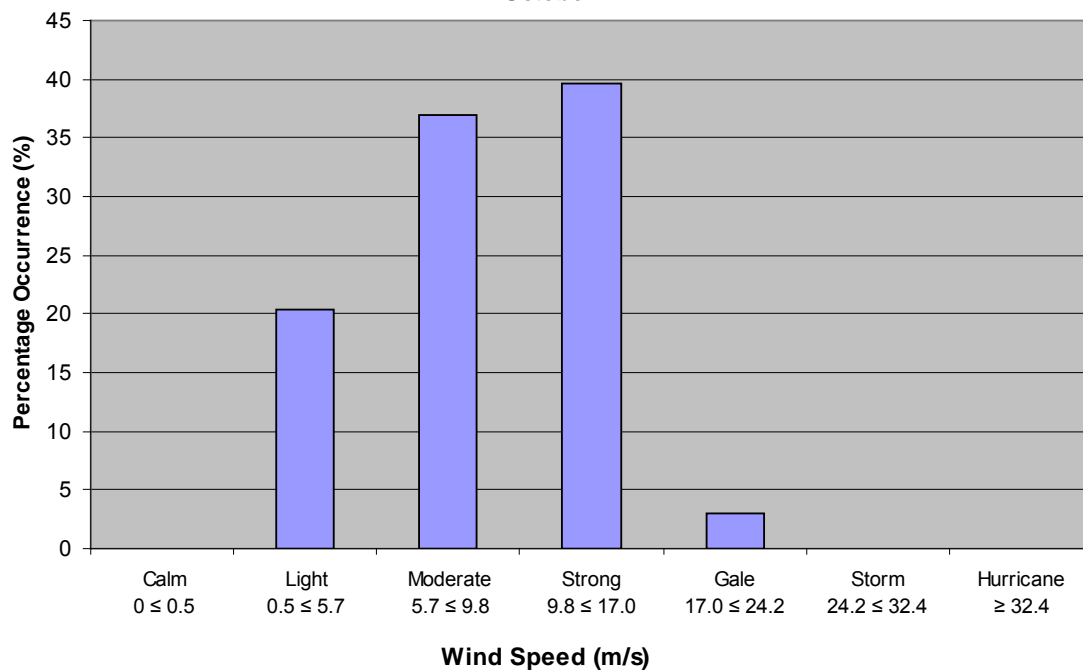
**Wind Speed Percentage Occurrence
Grid Point 14845
September**



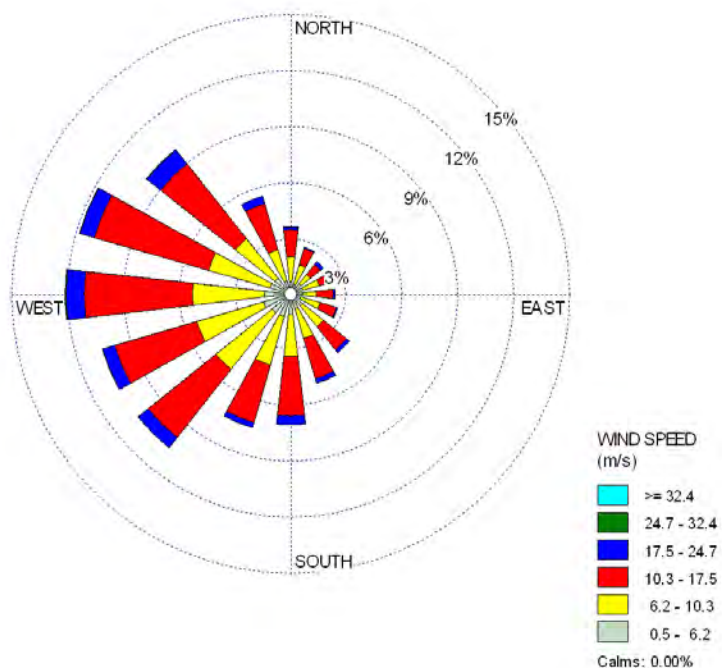
October



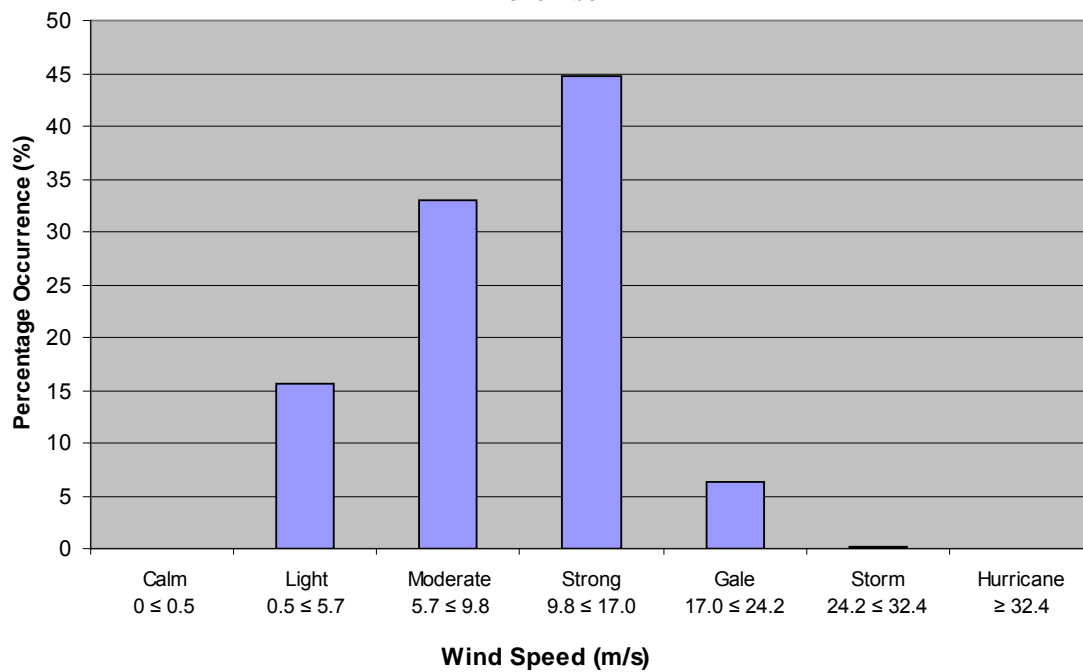
Wind Speed Percentage Occurrence
Grid Point 14845
October



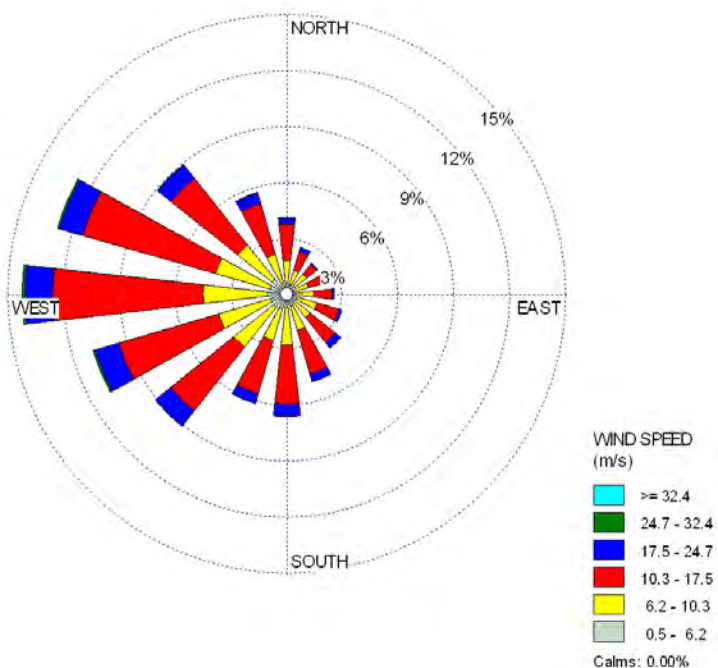
November



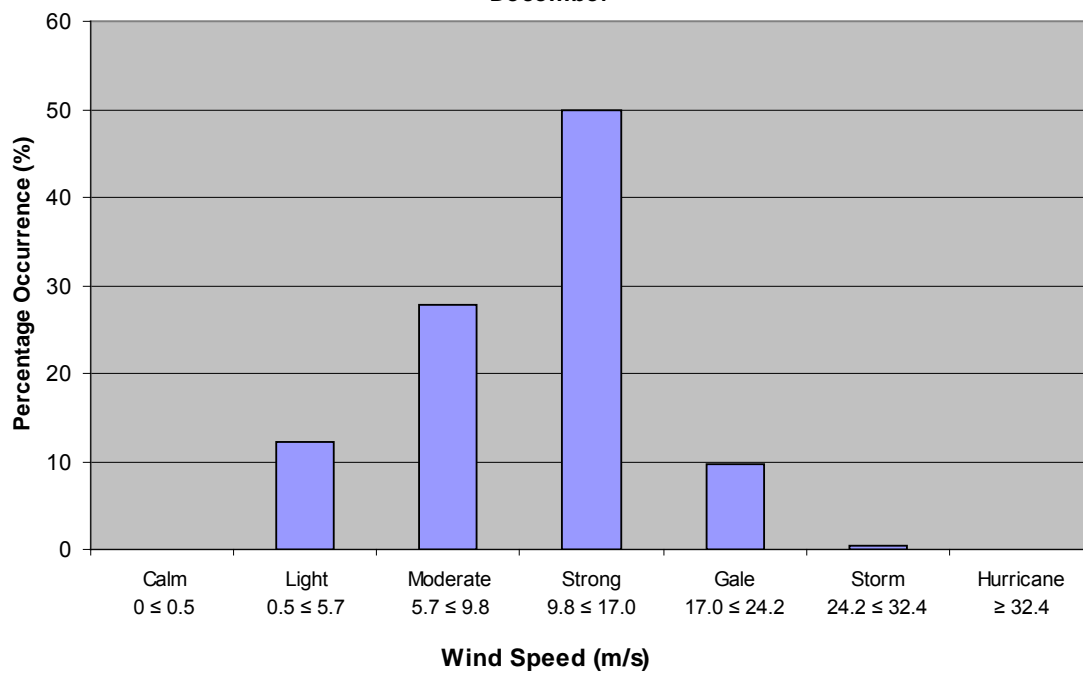
Wind Speed Percentage Occurrence
Grid Point 14845
November



December

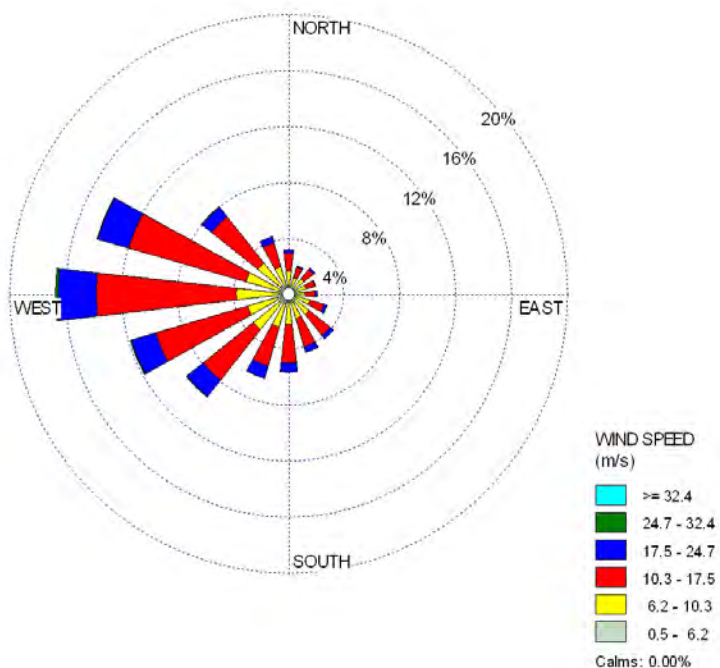


Wind Speed Percentage Occurrence
Grid Point 14845
December

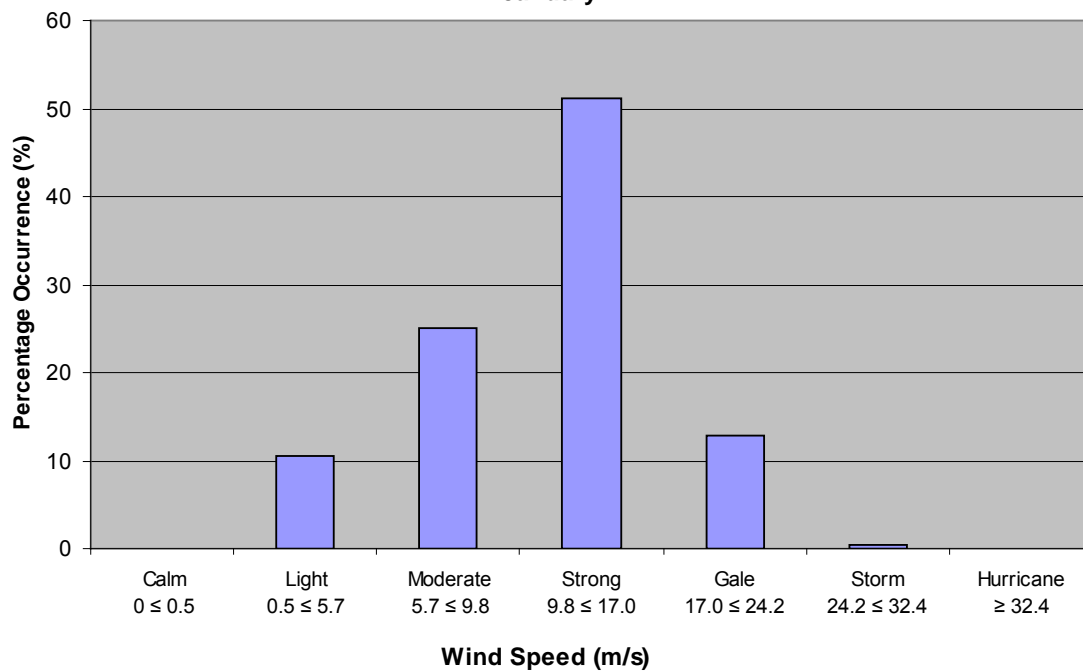


APPENDIX 2
Monthly Wind Roses
and
Percentage Occurrence Graphs
for MSC50 Grid point 13912

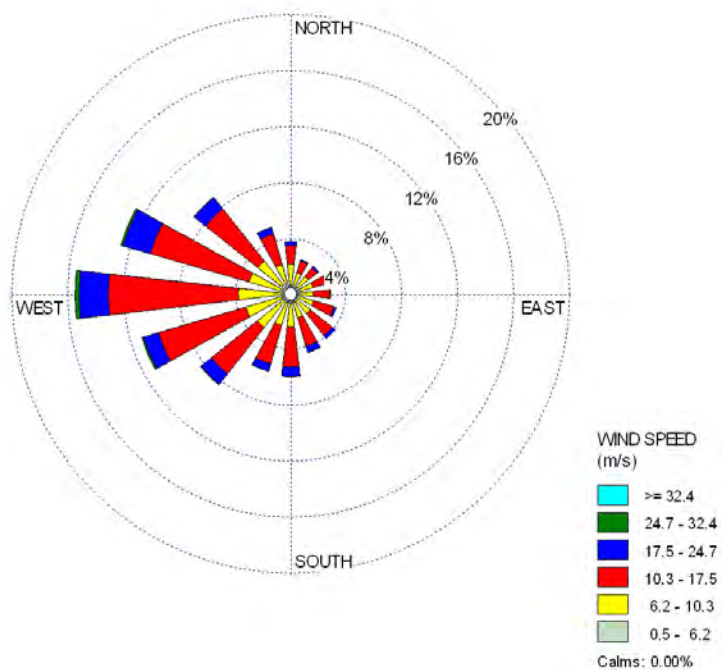
January



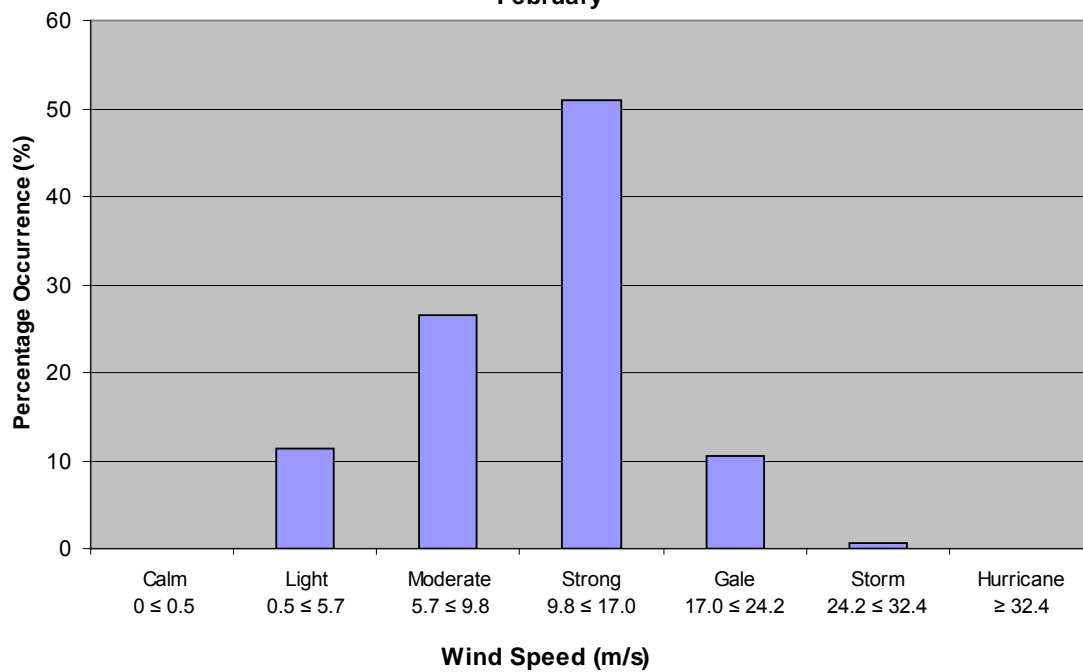
Wind Speed Percentage Occurrence Grid Point 13912 January



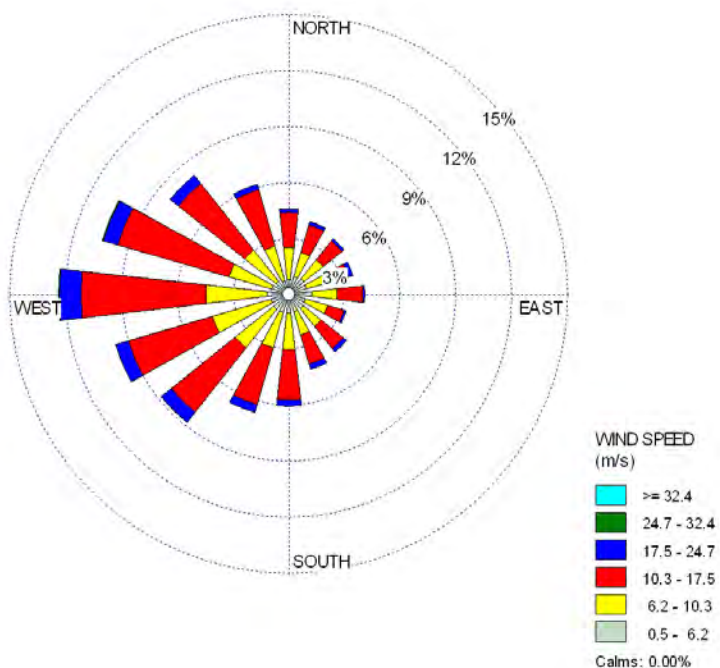
February



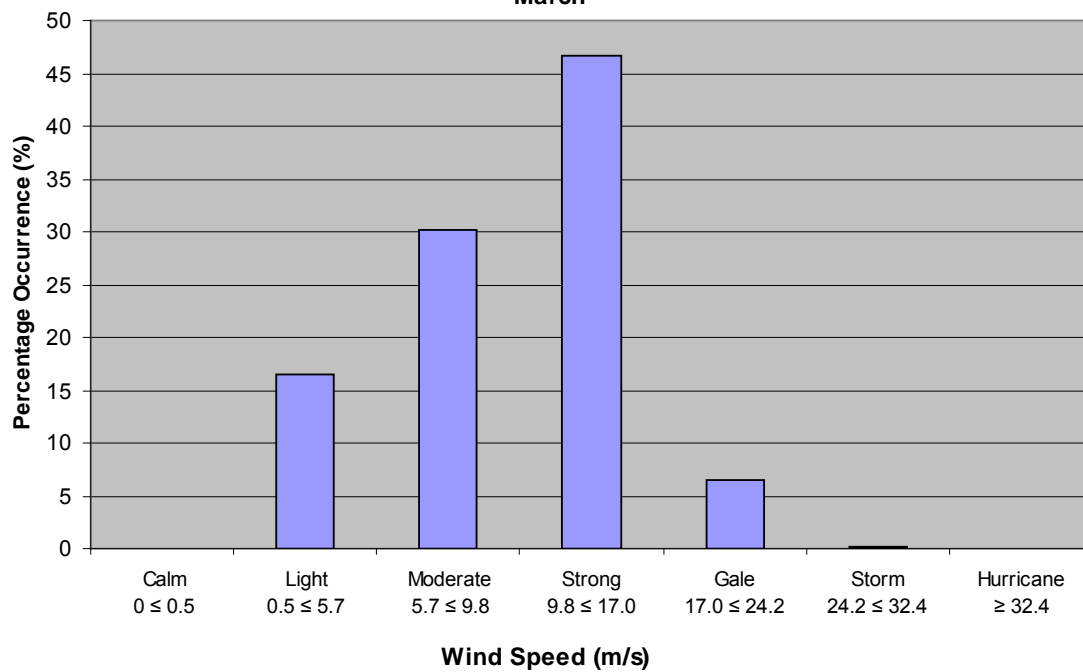
Wind Speed Percentage Occurrence Grid Point 13912 February



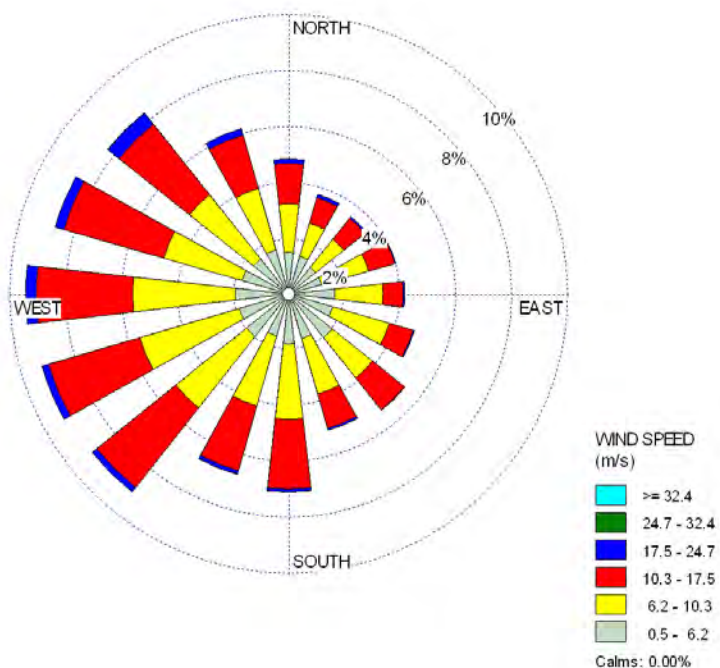
March



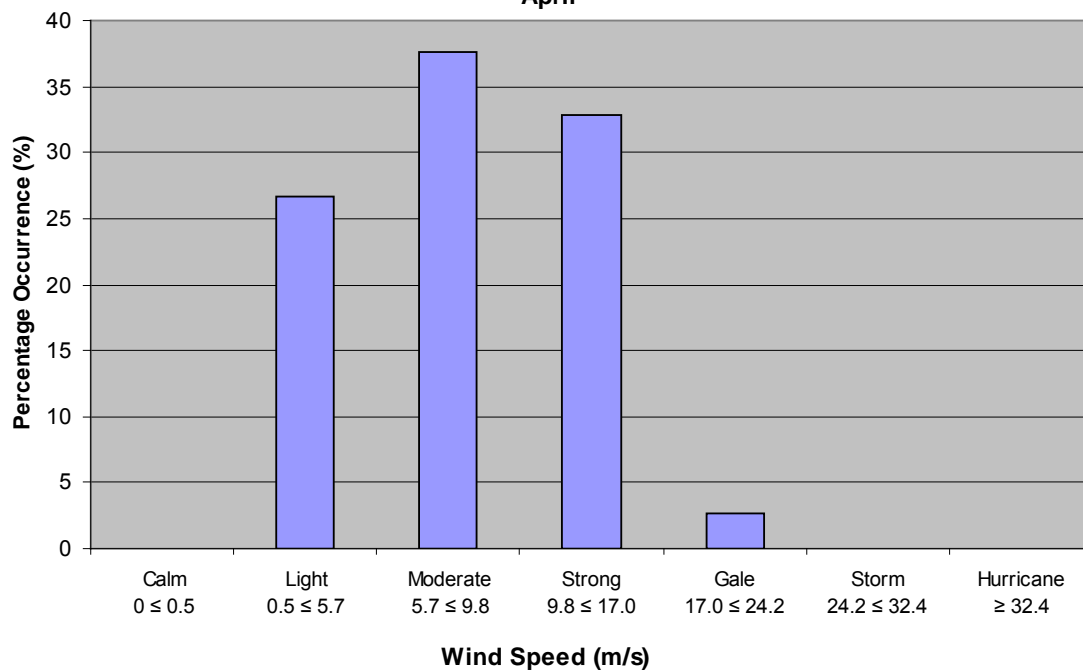
**Wind Speed Percentage Occurrence
Grid Point 13912
March**



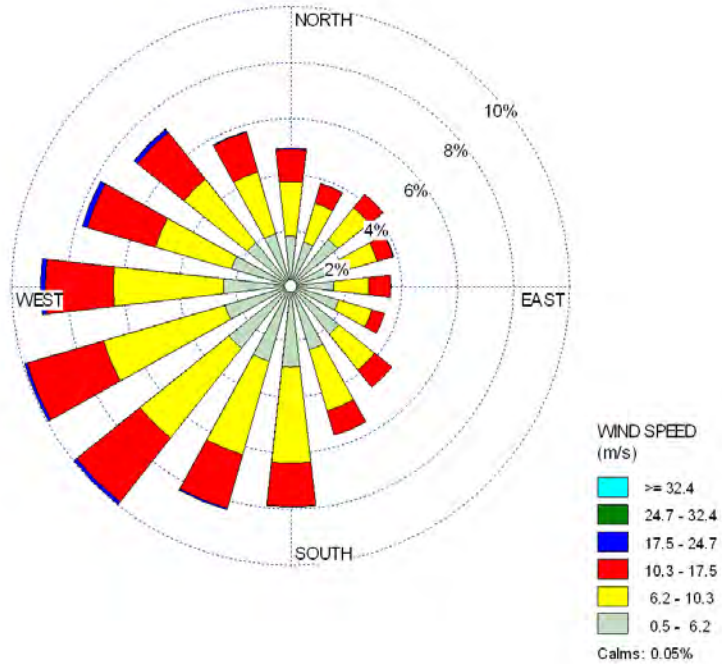
April



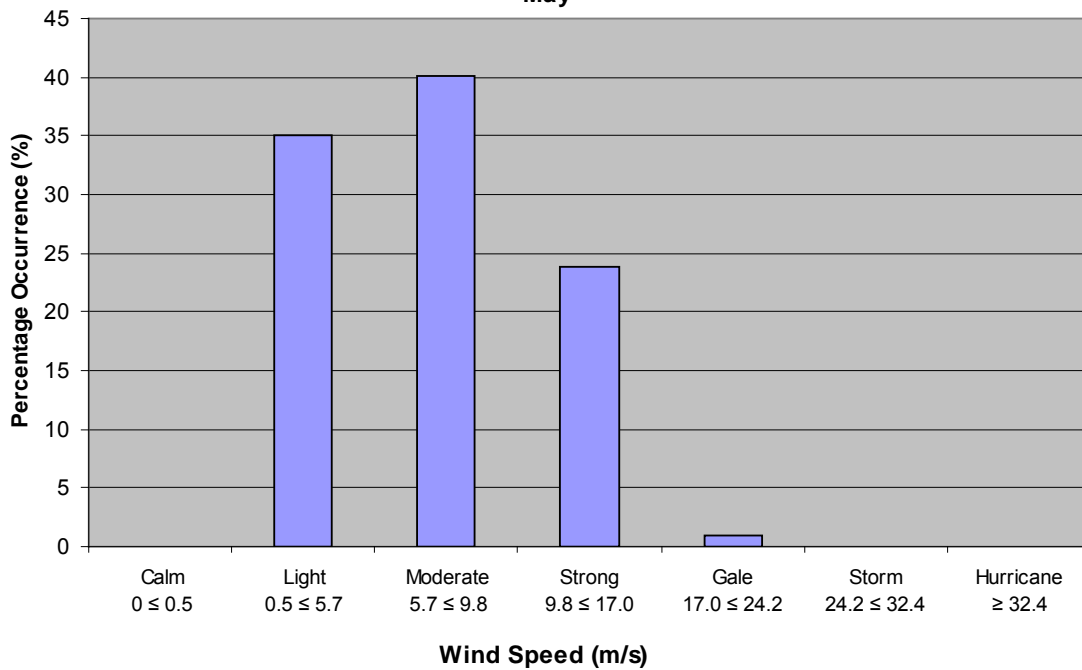
Wind Speed Percentage Occurrence
Grid Point 13912
April



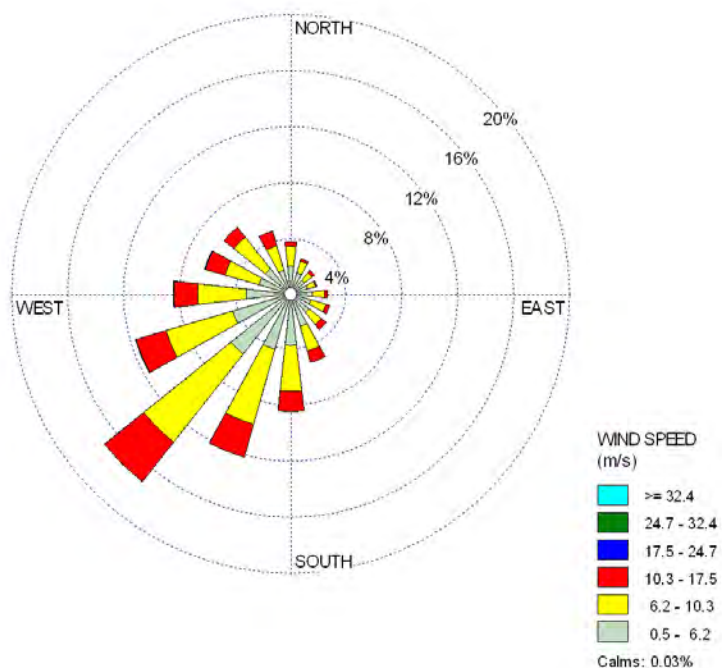
May



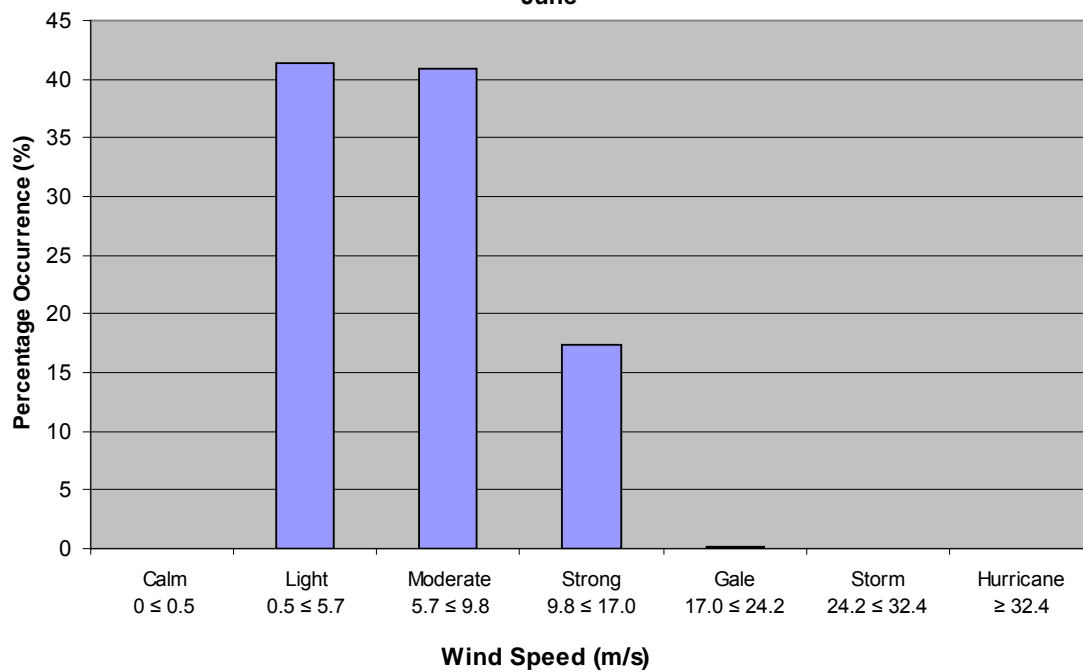
**Wind Speed Percentage Occurrence
Grid Point 13912
May**



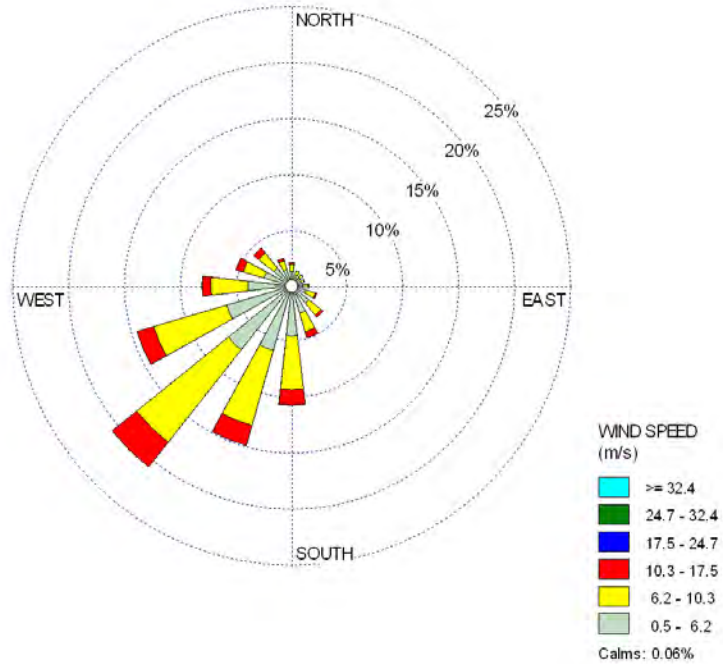
June



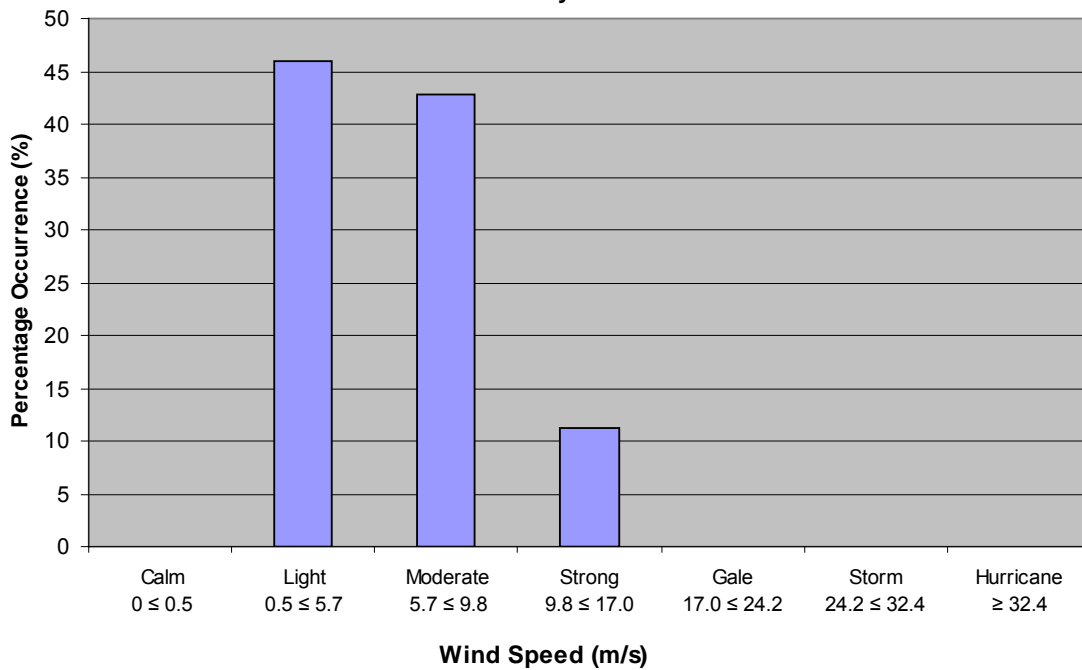
**Wind Speed Percentage Occurrence
Grid Point 13912
June**



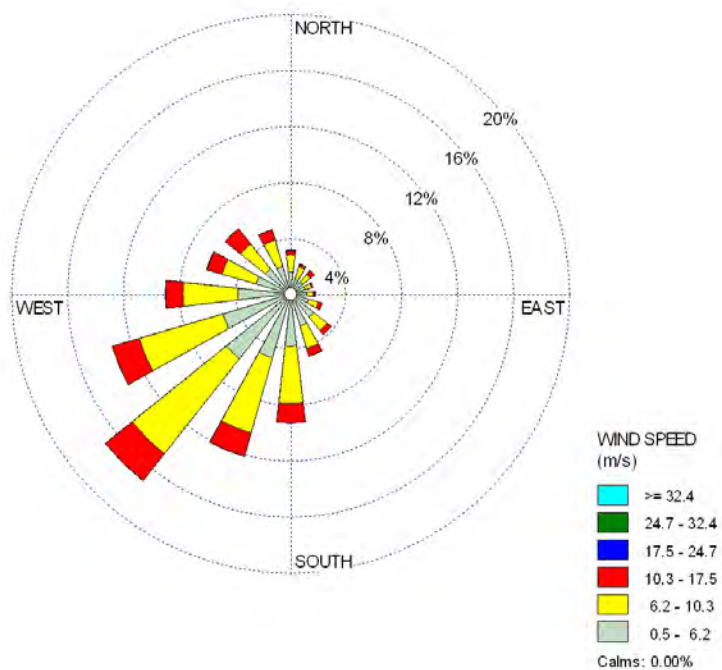
July



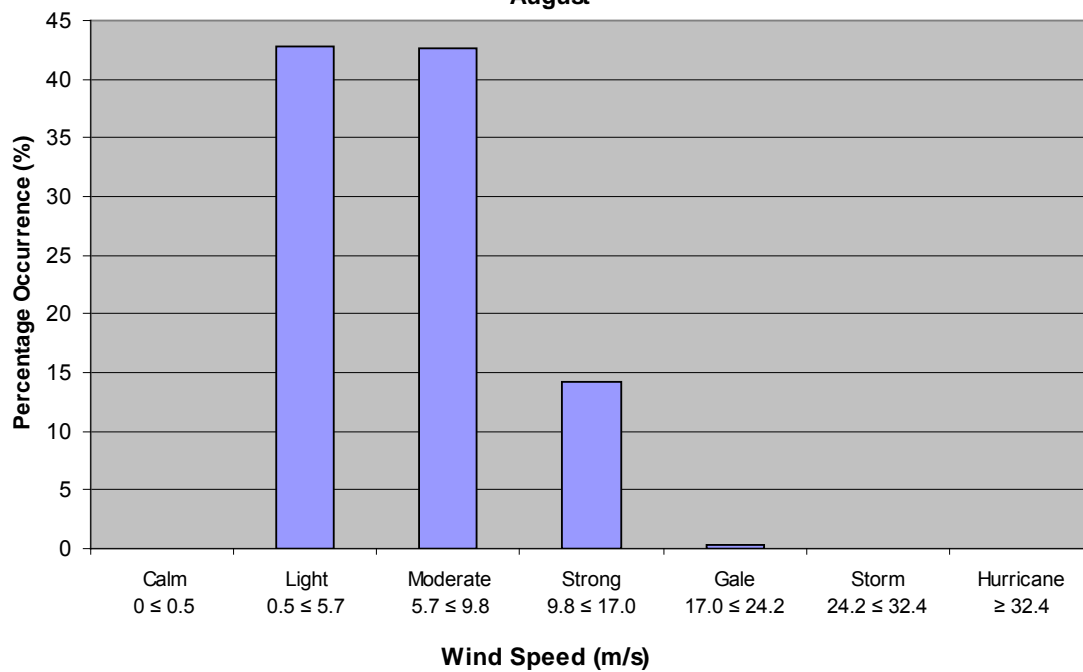
Wind Speed Percentage Occurrence
Grid Point 13912
July



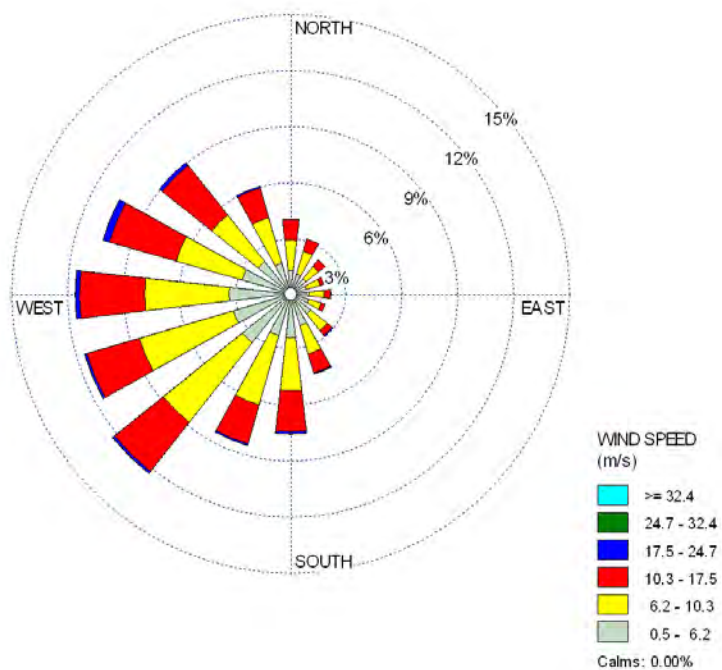
August



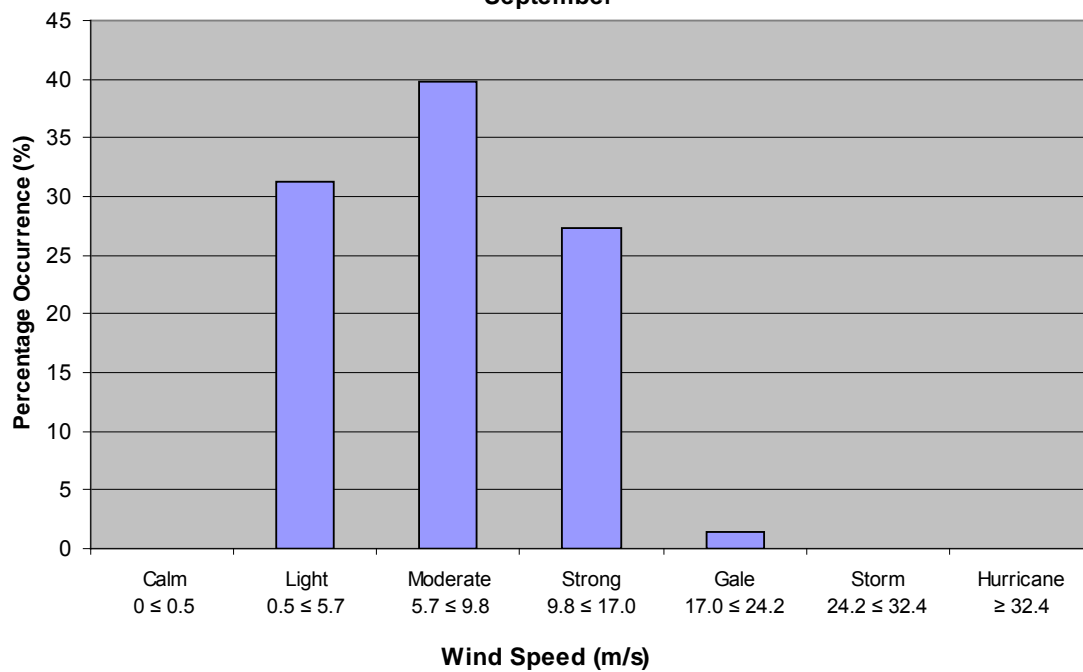
**Wind Speed Percentage Occurrence
Grid Point 13912
August**



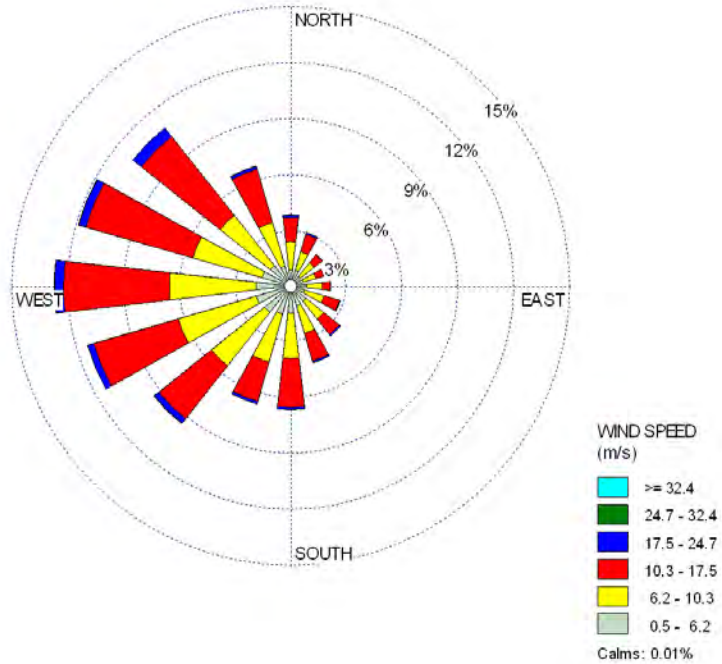
September



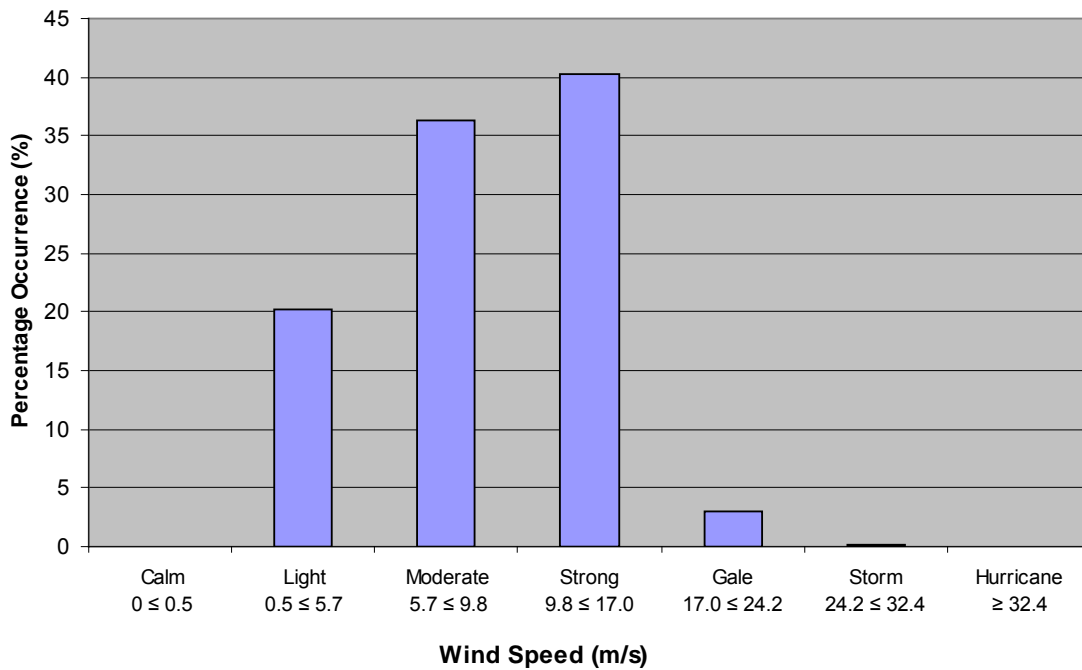
**Wind Speed Percentage Occurrence
Grid Point 13912
September**



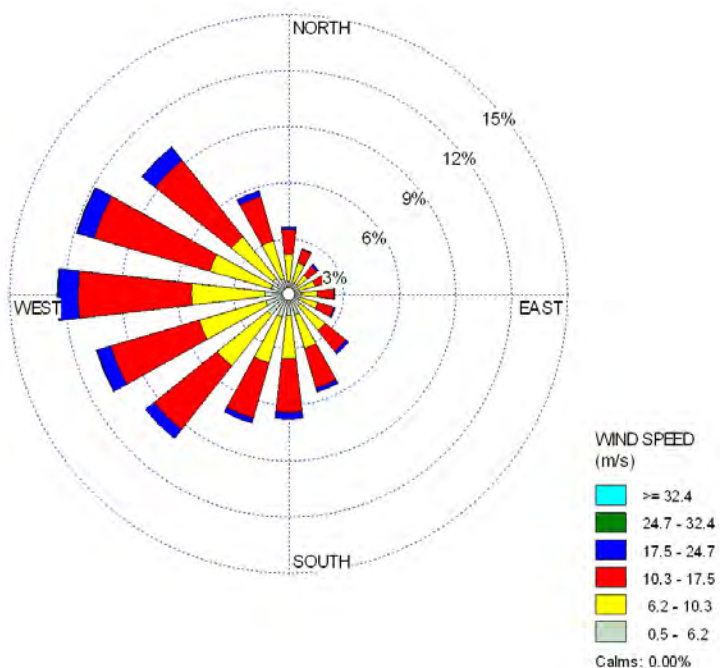
October



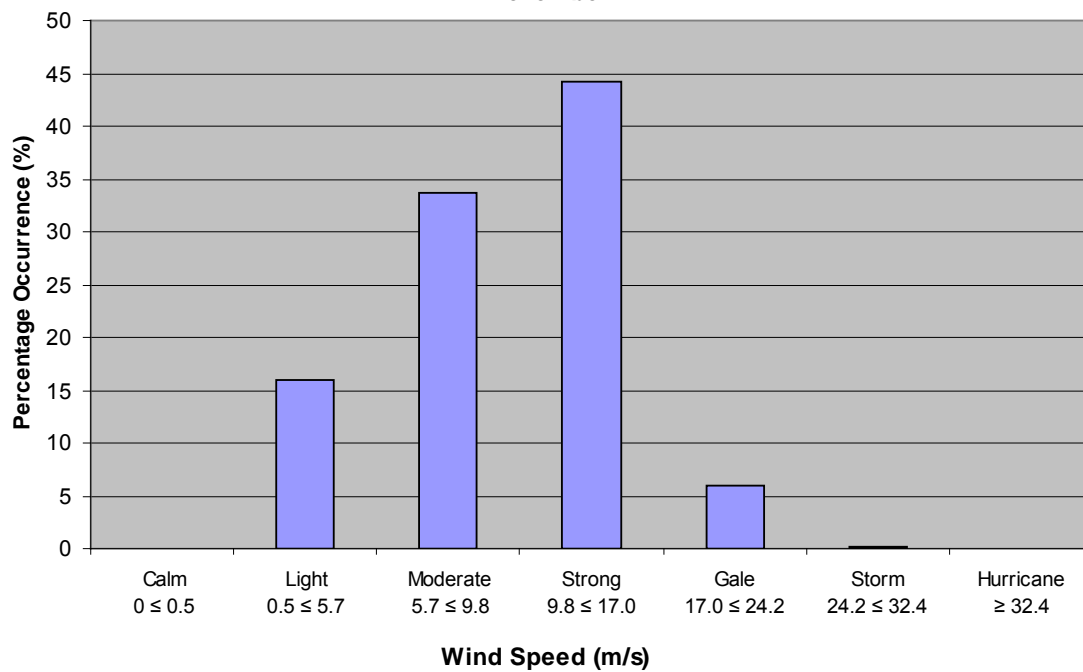
**Wind Speed Percentage Occurrence
Grid Point 13912
October**



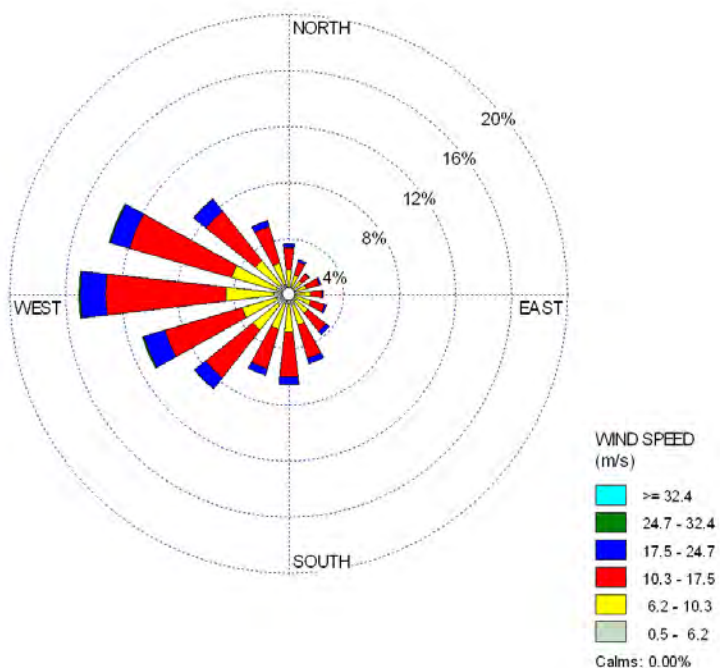
November



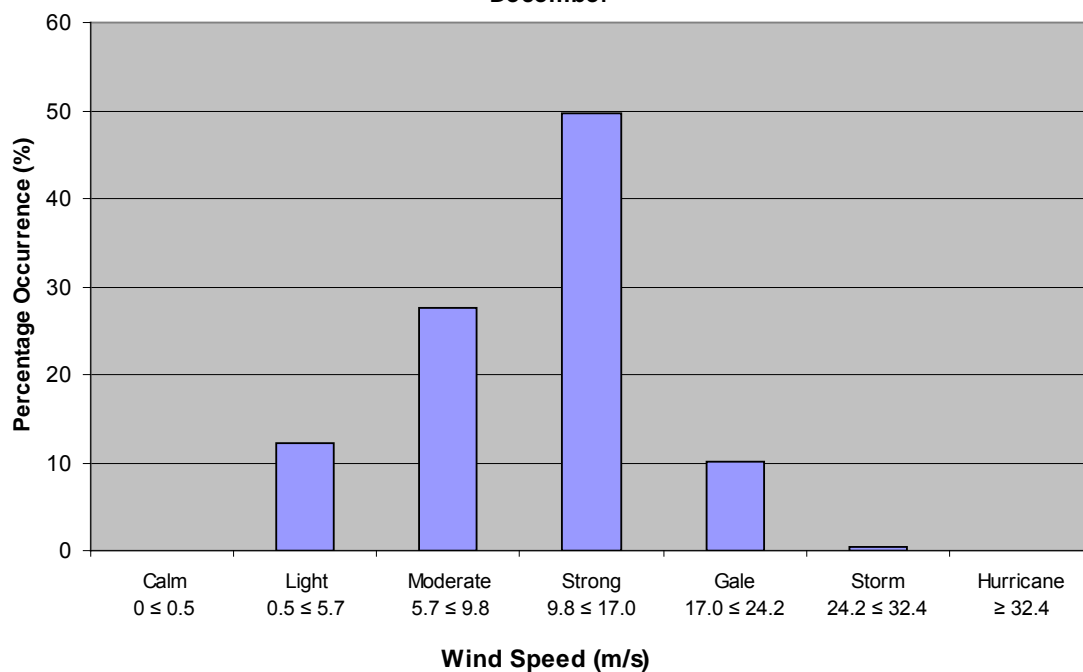
Wind Speed Percentage Occurrence
Grid Point 13912
November



December

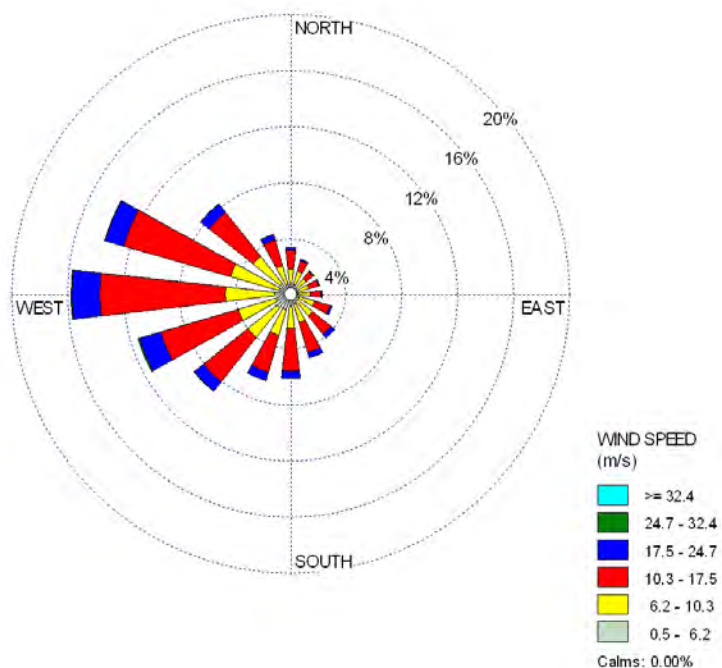


Wind Speed Percentage Occurrence Grid Point 13912 December

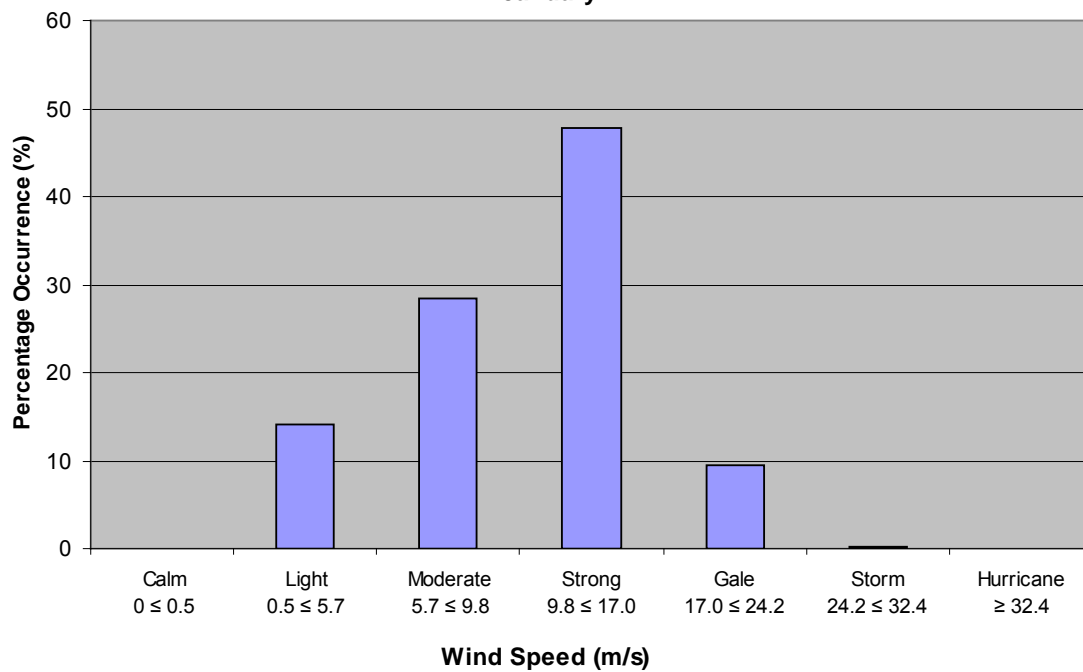


APPENDIX 3
Monthly Wind Roses
and
Percentage Occurrence Graphs
for MSC50 Grid point 11423

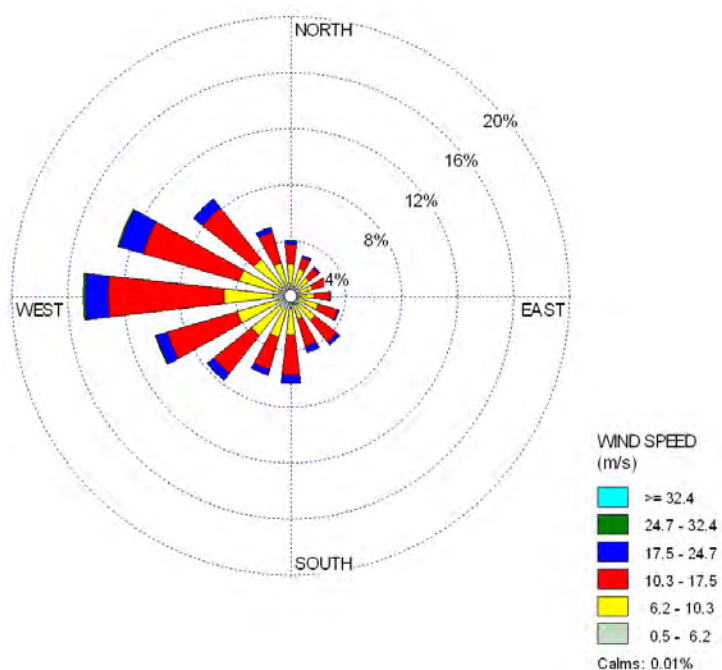
January



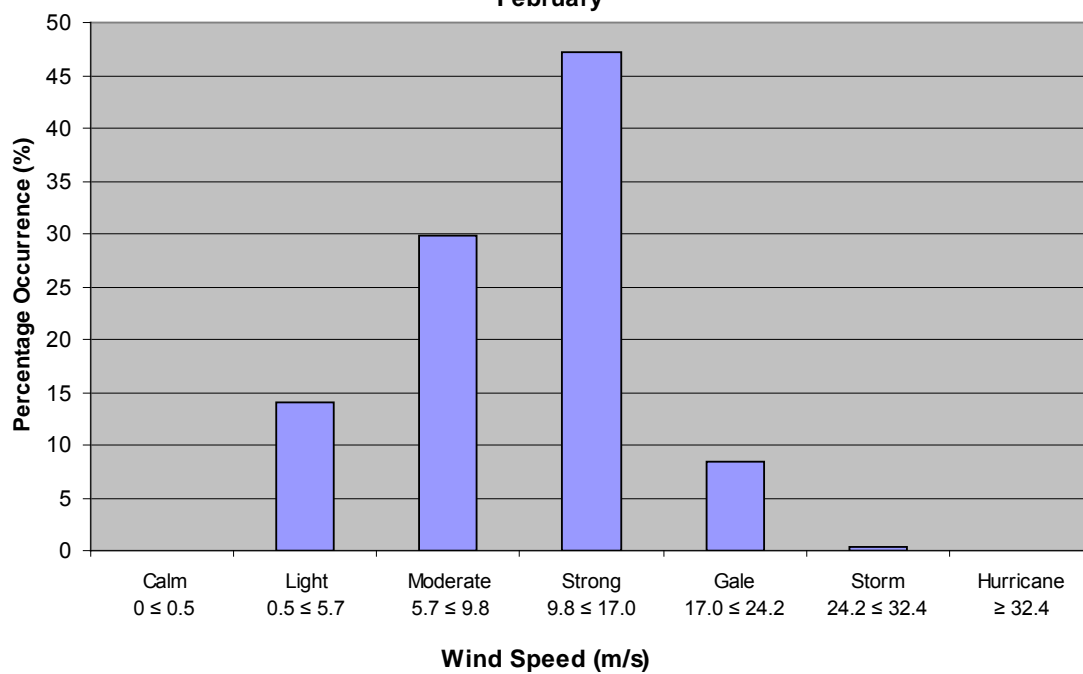
Wind Speed Percentage Occurrence Grid Point 11423 January



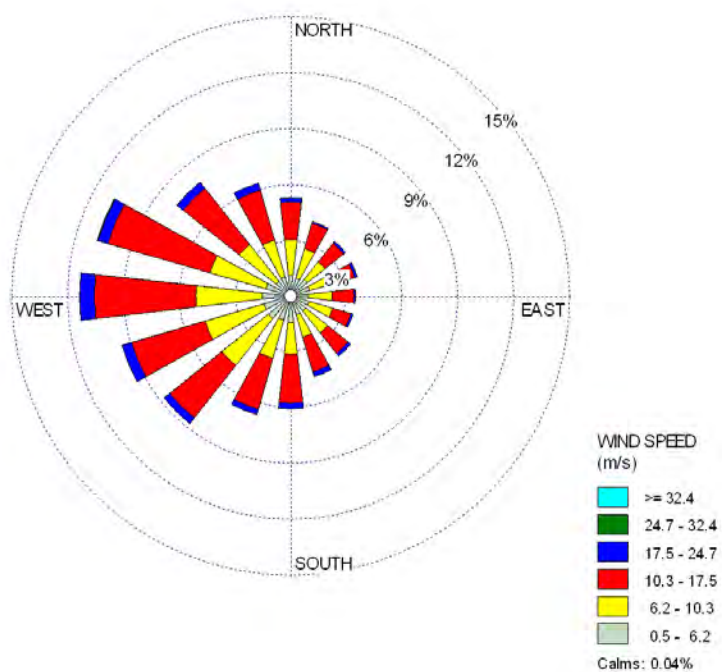
February



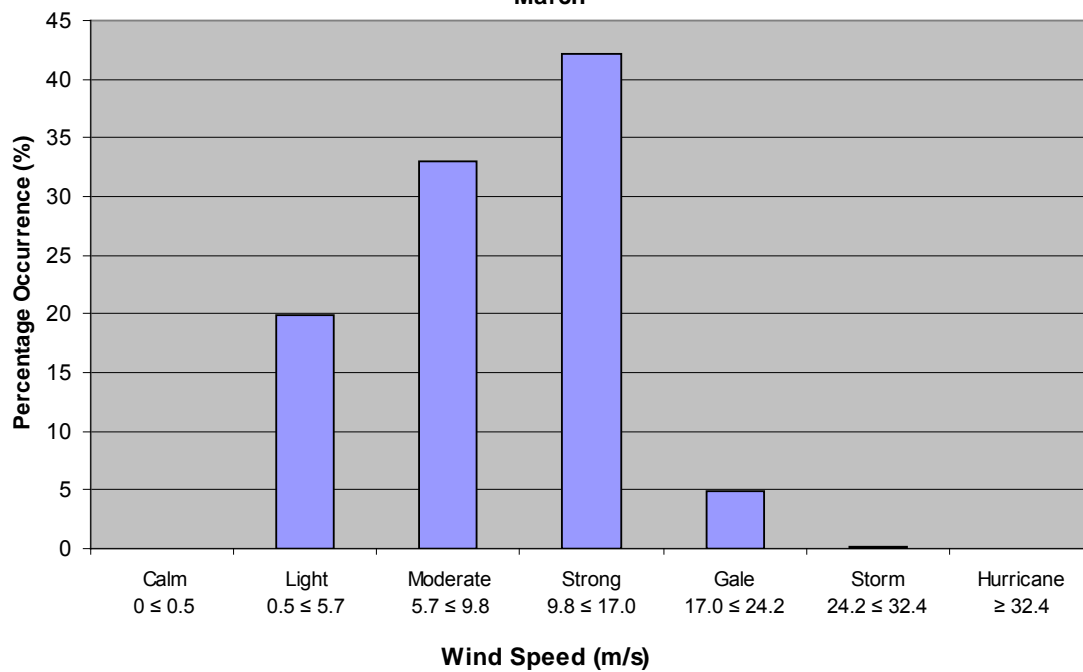
Wind Speed Percentage Occurrence Grid Point 11423 February



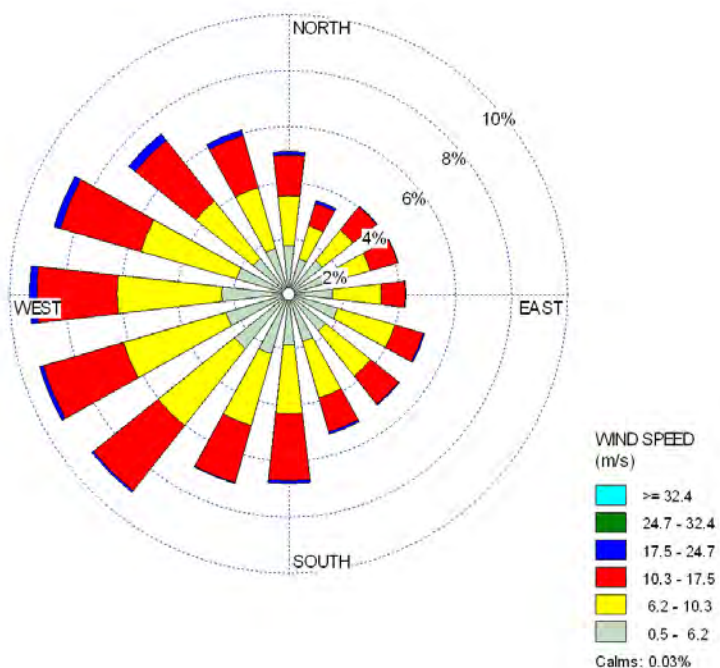
March



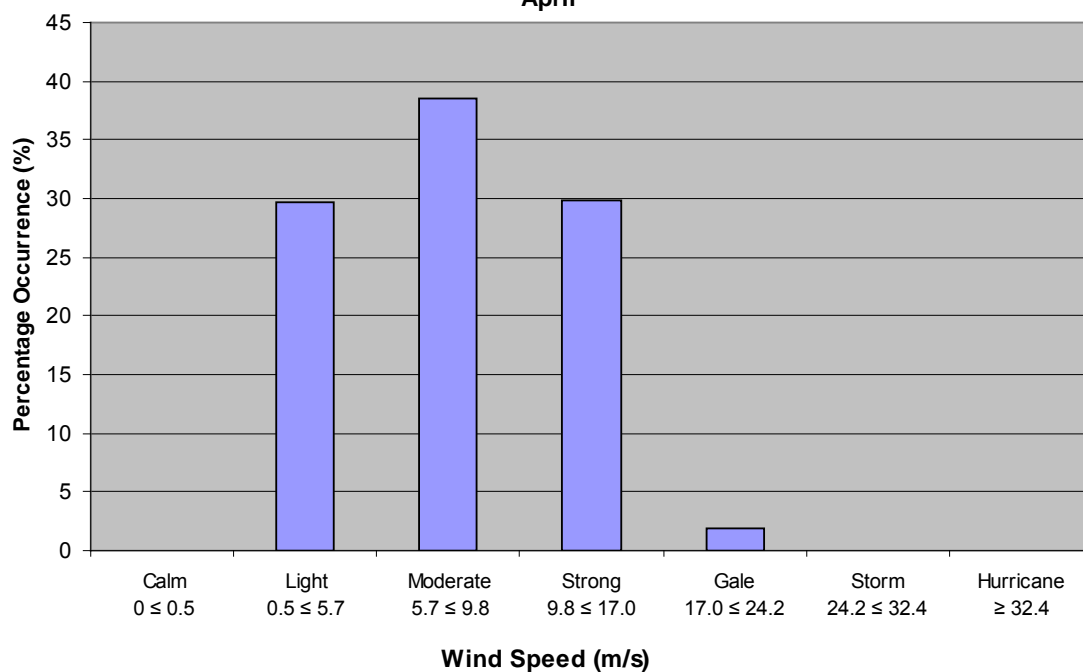
Wind Speed Percentage Occurrence
Grid Point 11423
March



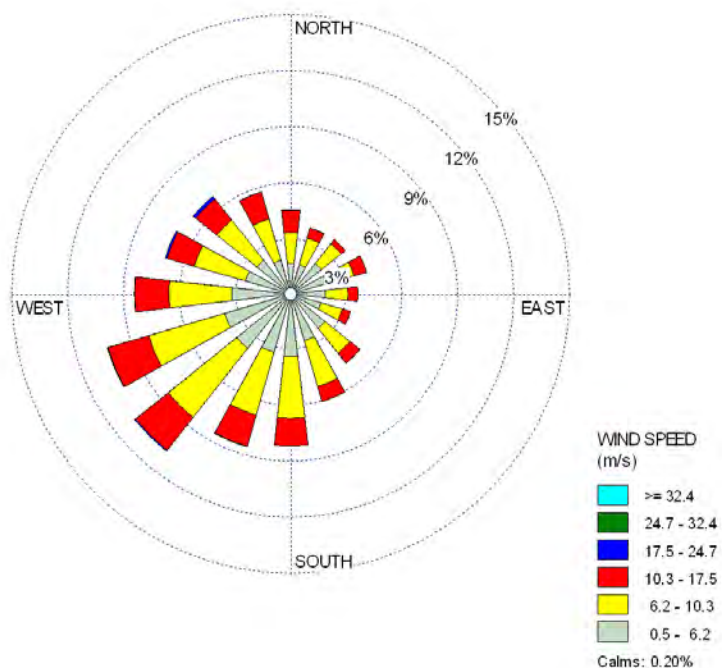
April



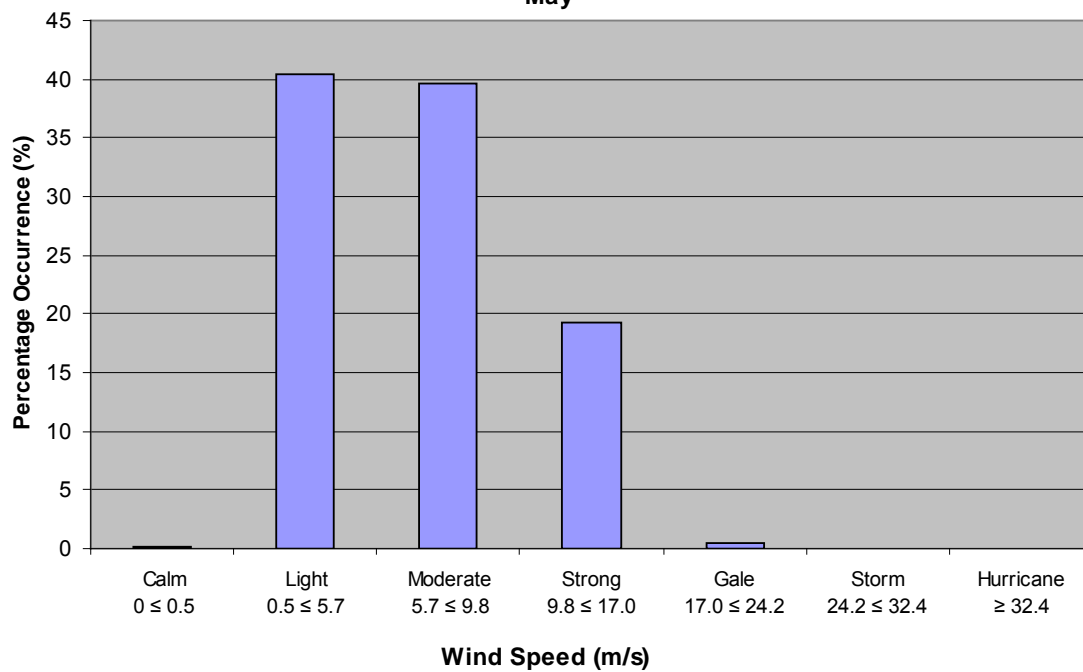
**Wind Speed Percentage Occurrence
Grid Point 11423
April**



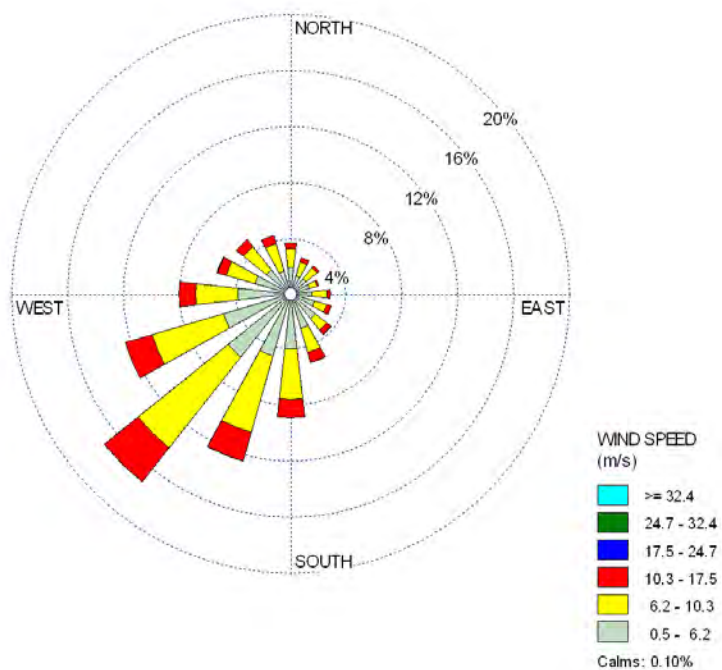
May



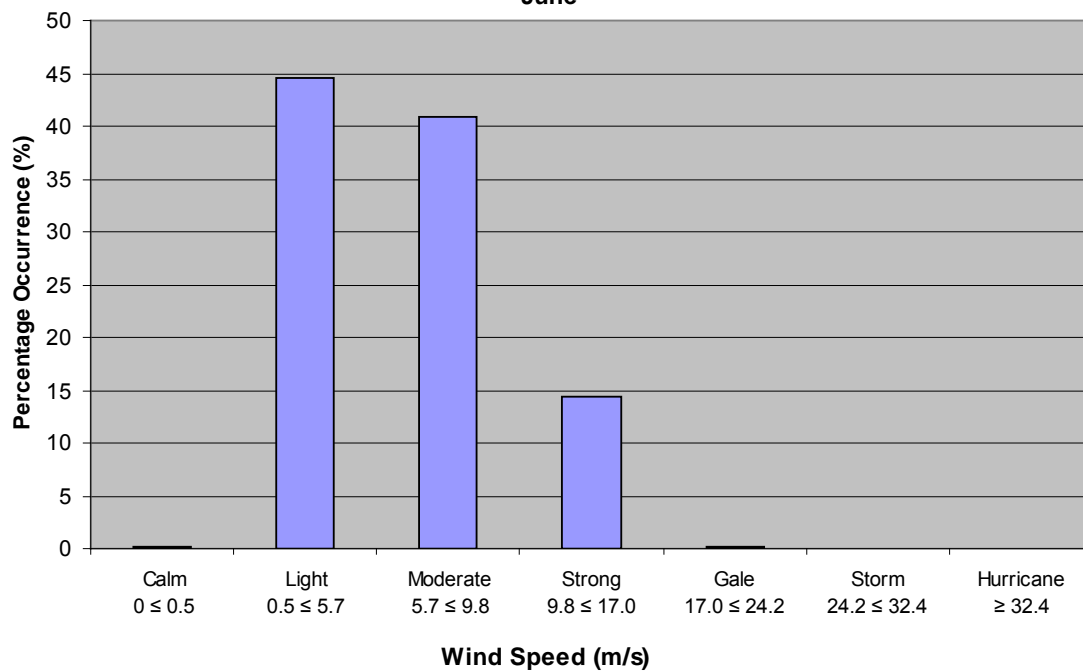
Wind Speed Percentage Occurrence
Grid Point 11423
May



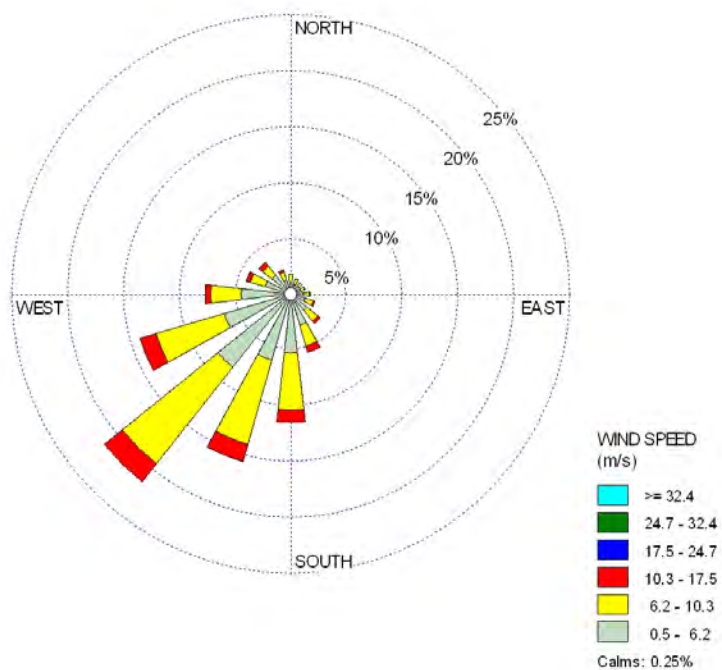
June



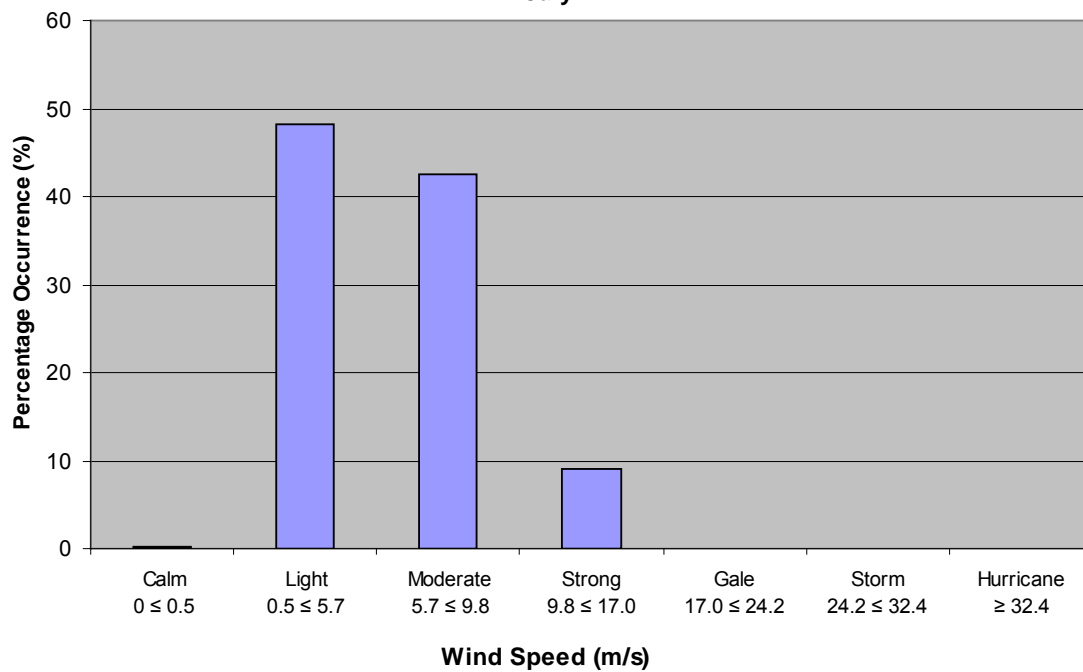
**Wind Speed Percentage Occurrence
Grid Point 11423
June**



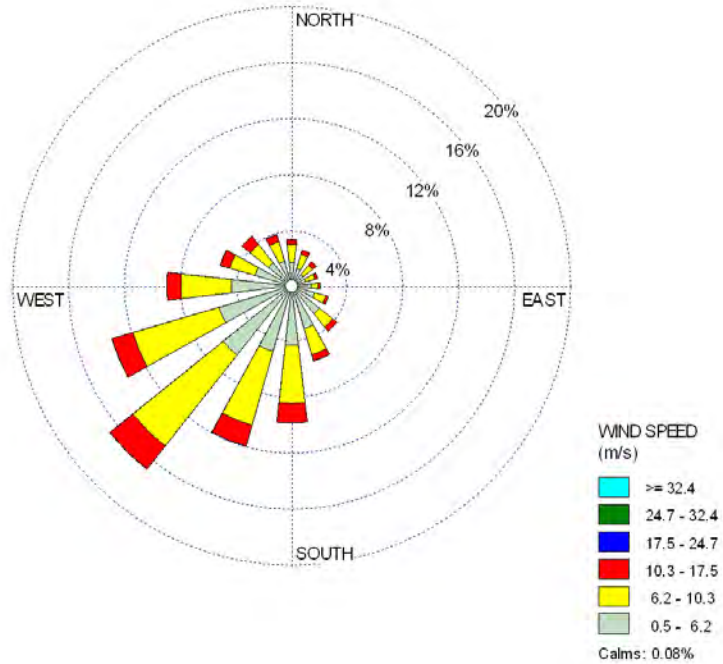
July



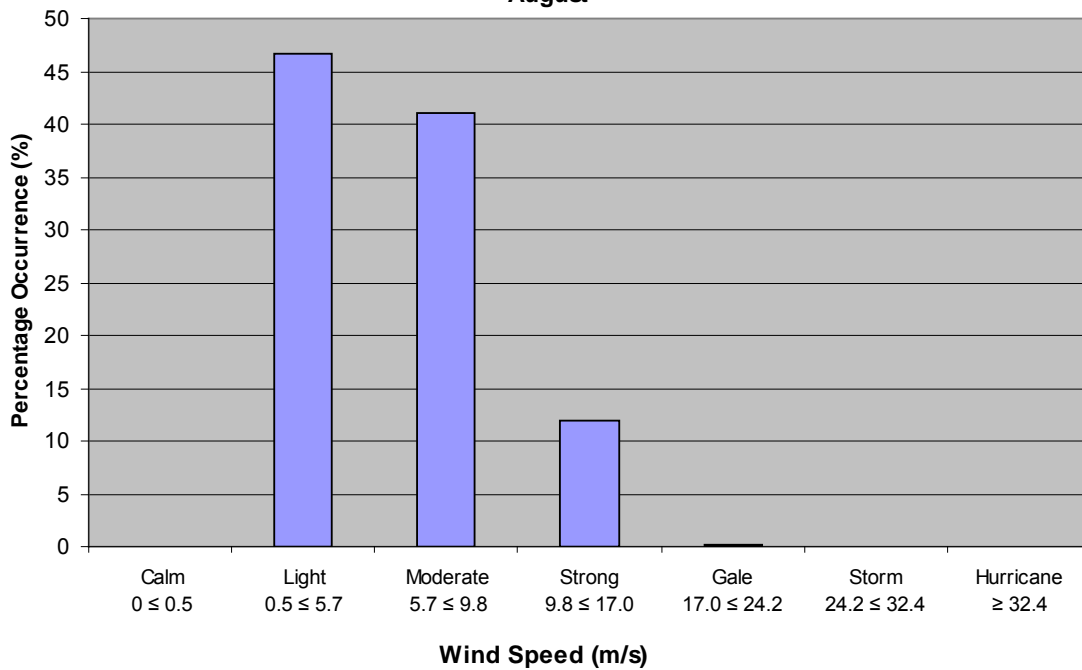
Wind Speed Percentage Occurrence
Grid Point 11423
July



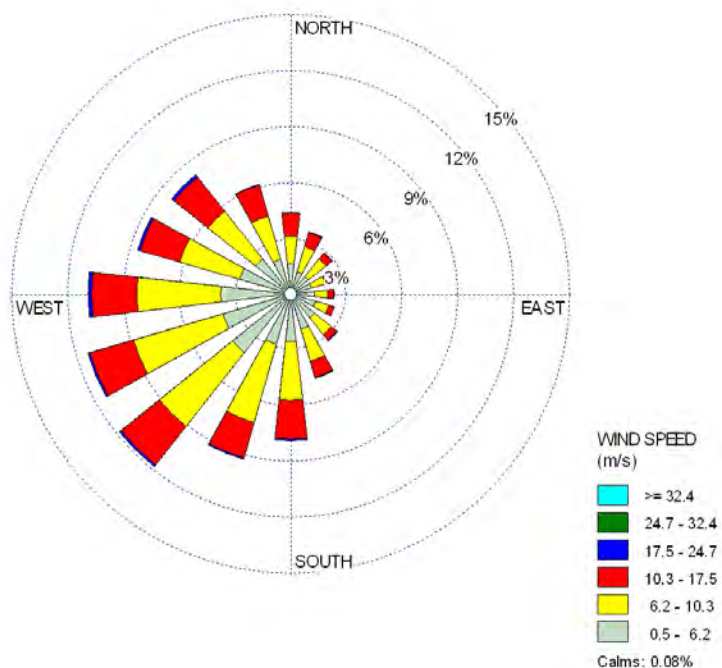
August



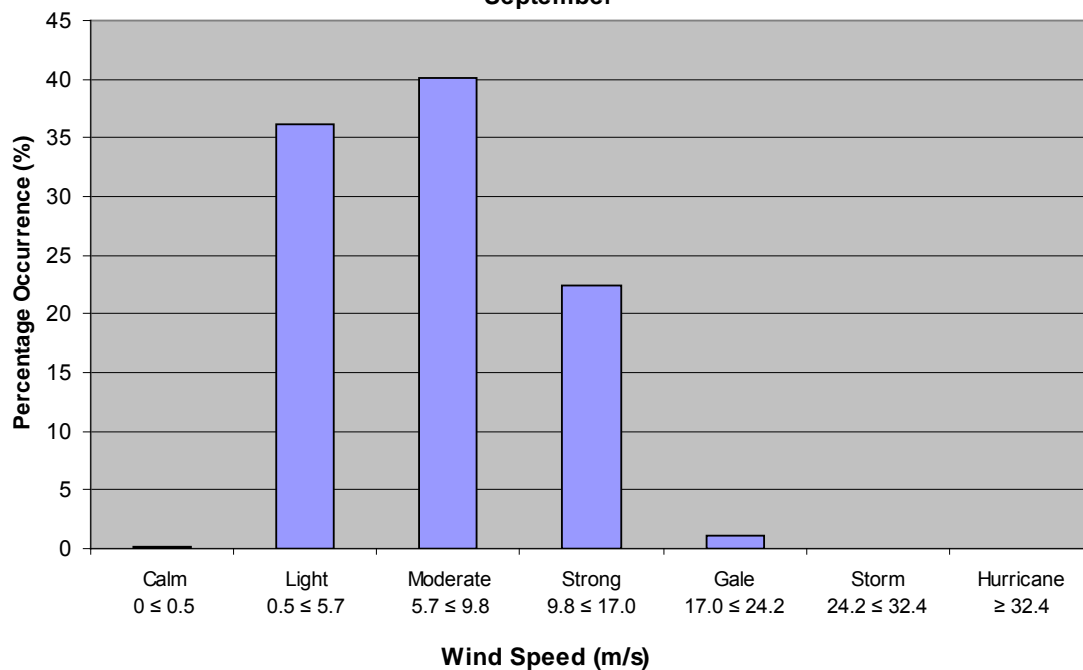
**Wind Speed Percentage Occurrence
Grid Point 11423
August**



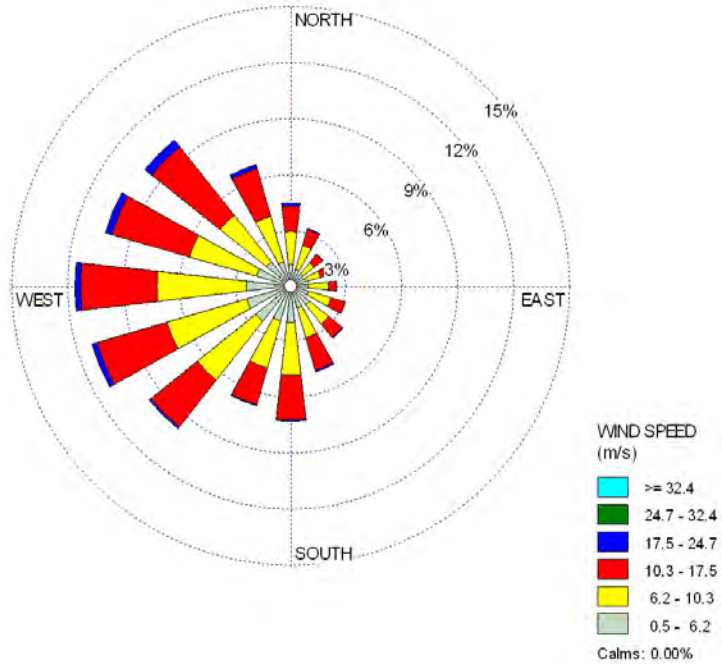
September



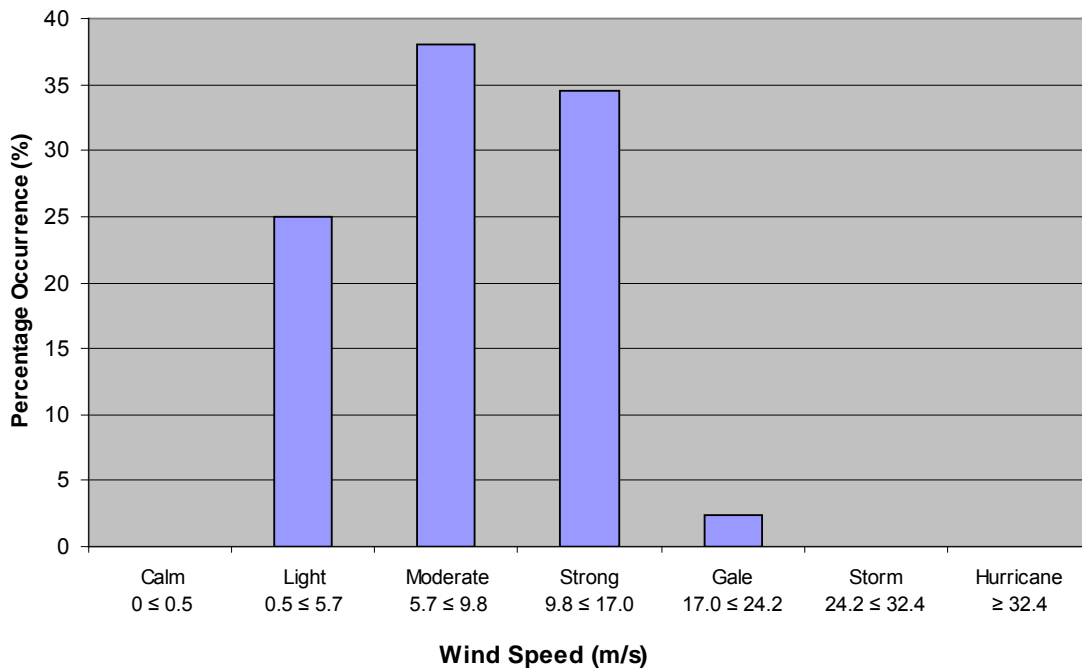
**Wind Speed Percentage Occurrence
Grid Point 11423
September**



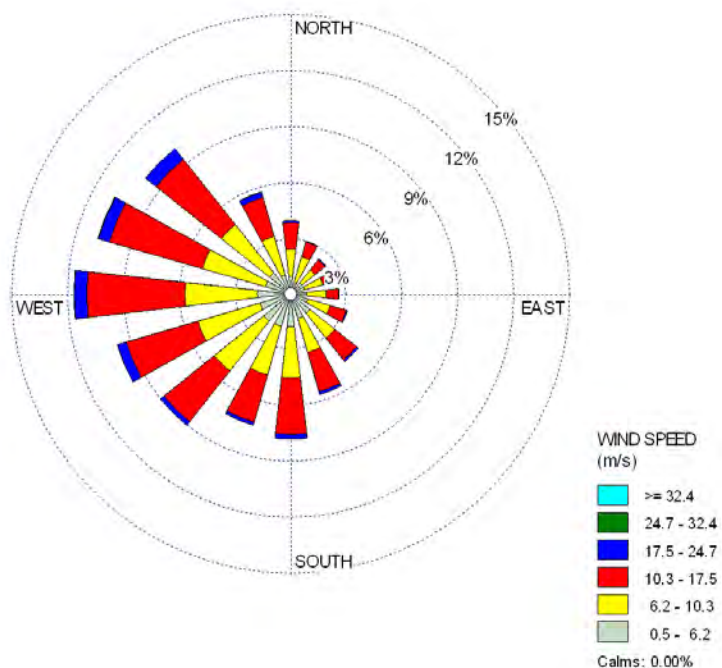
October



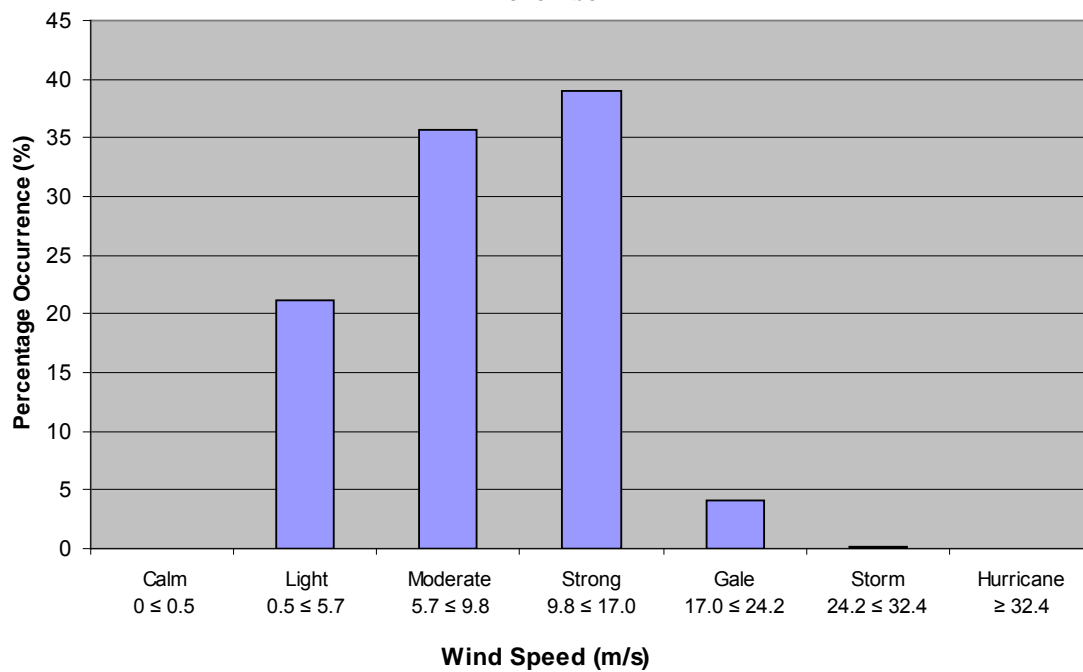
**Wind Speed Percentage Occurrence
Grid Point 11423
October**



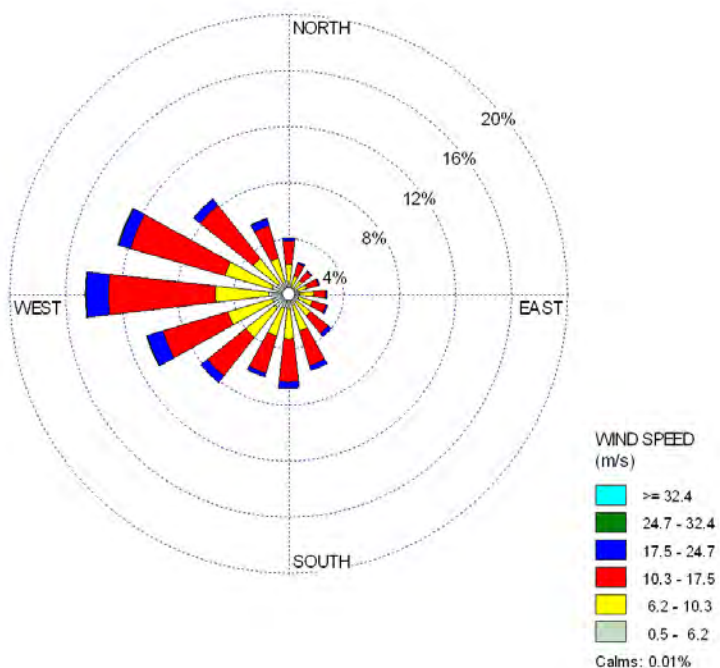
November



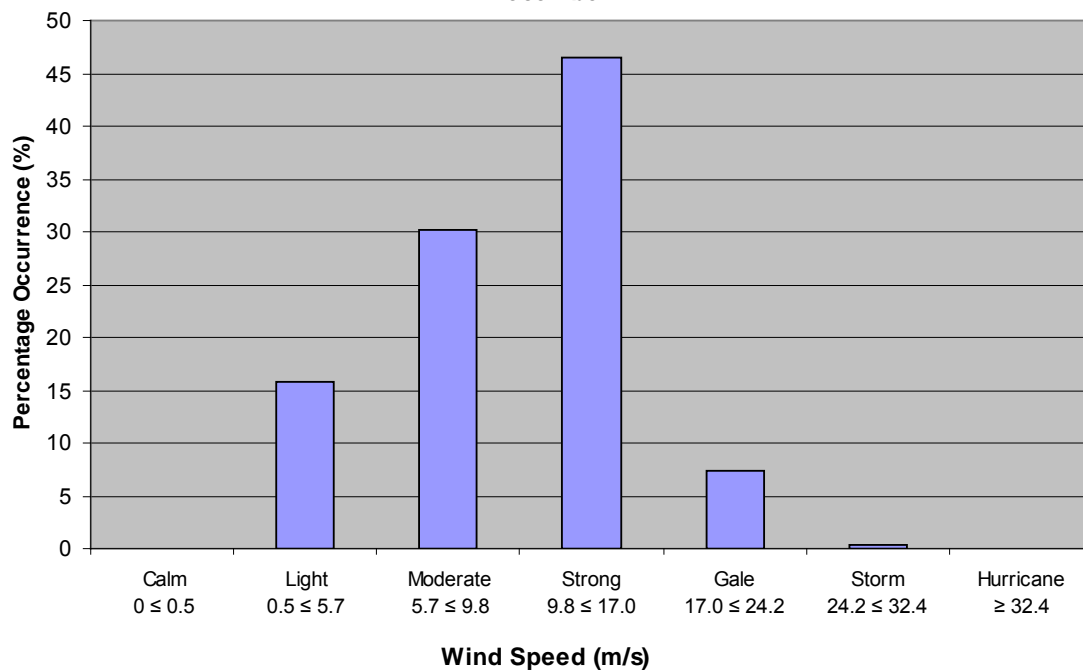
Wind Speed Percentage Occurrence Grid Point 11423 November



December

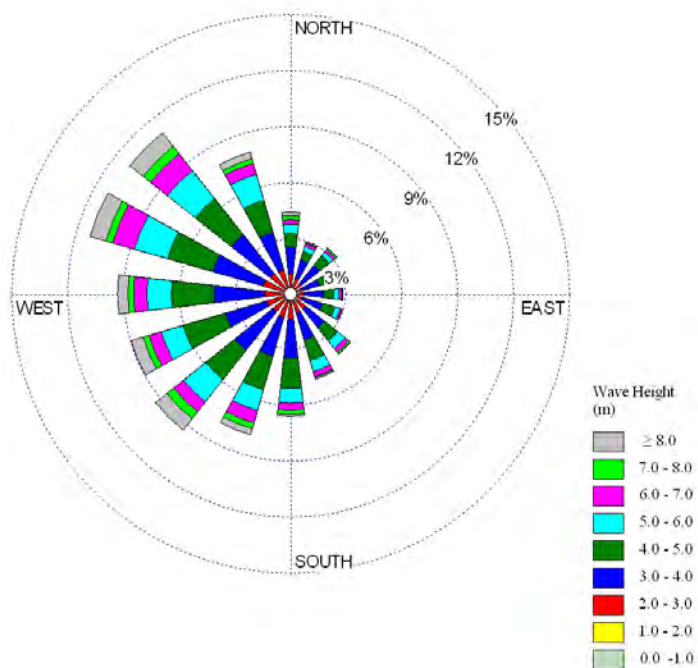


Wind Speed Percentage Occurrence Grid Point 11423 December

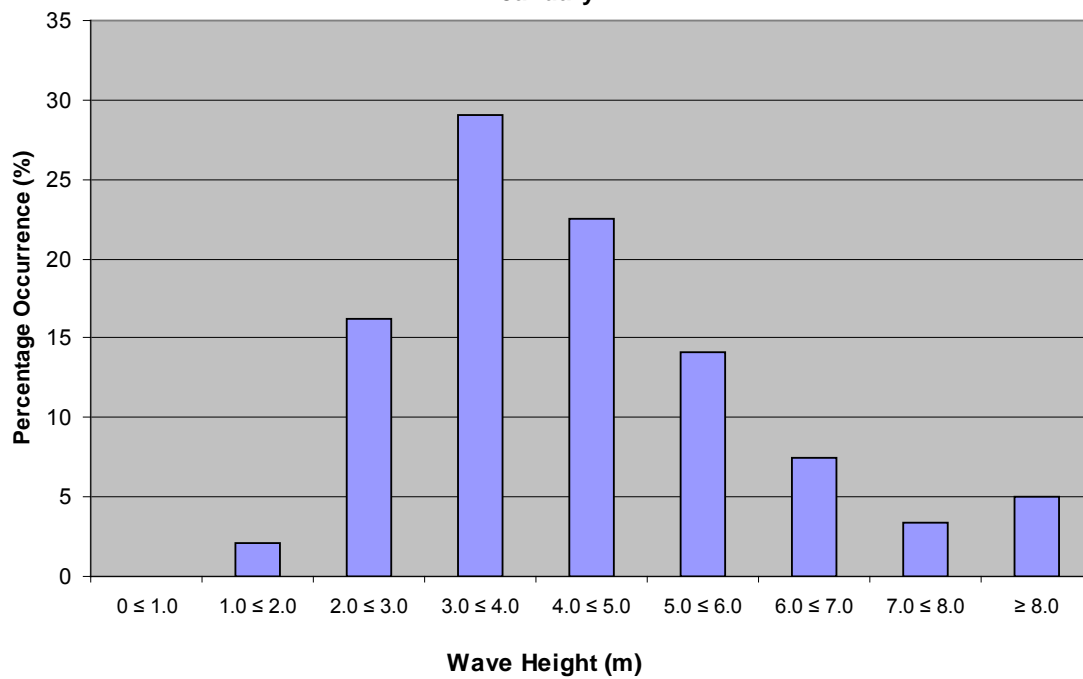


APPENDIX 4
Monthly Wave Roses
and
Percentage Occurrence Graphs
for MSC50 Grid point 14845

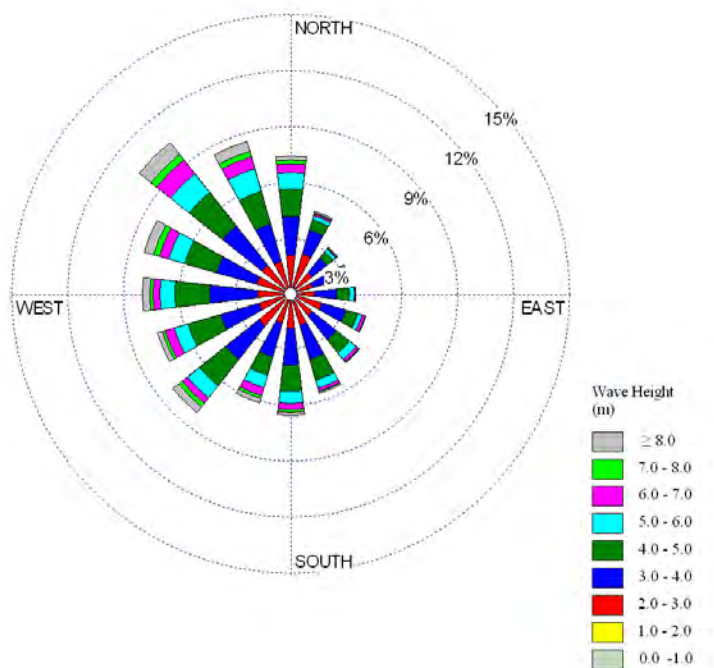
January



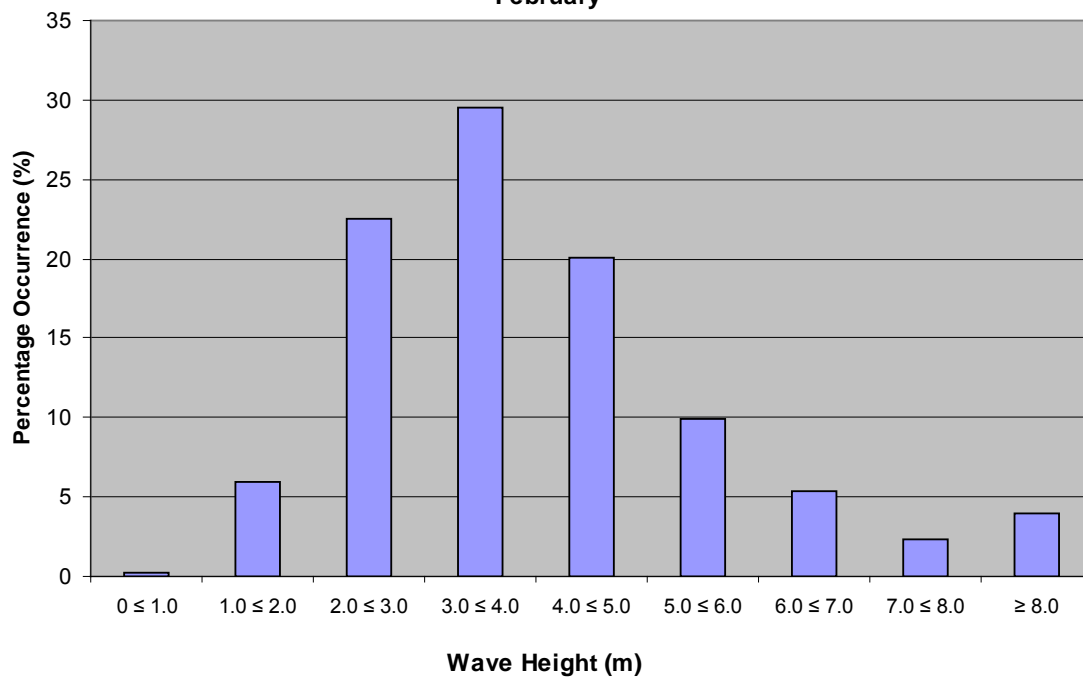
**Wave Height Percentage Occurrence
Grid Point 14845
January**



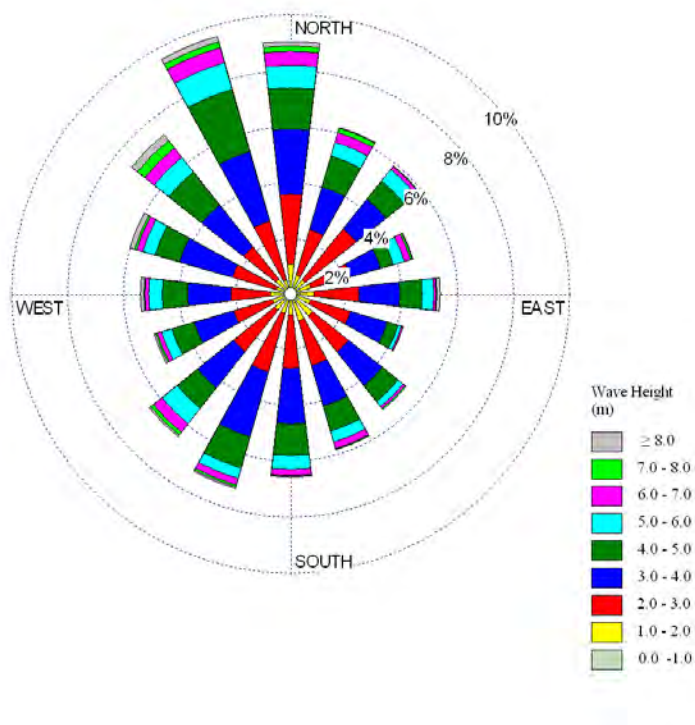
February



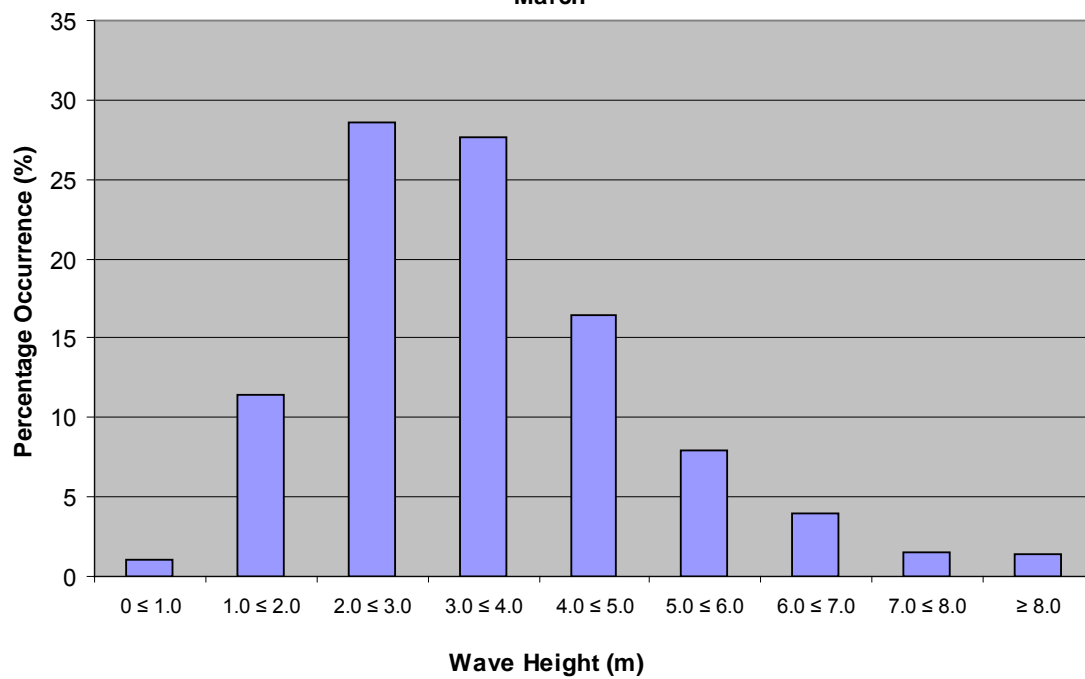
**Wave Height Percentage Occurrence
Grid Point 14845
February**



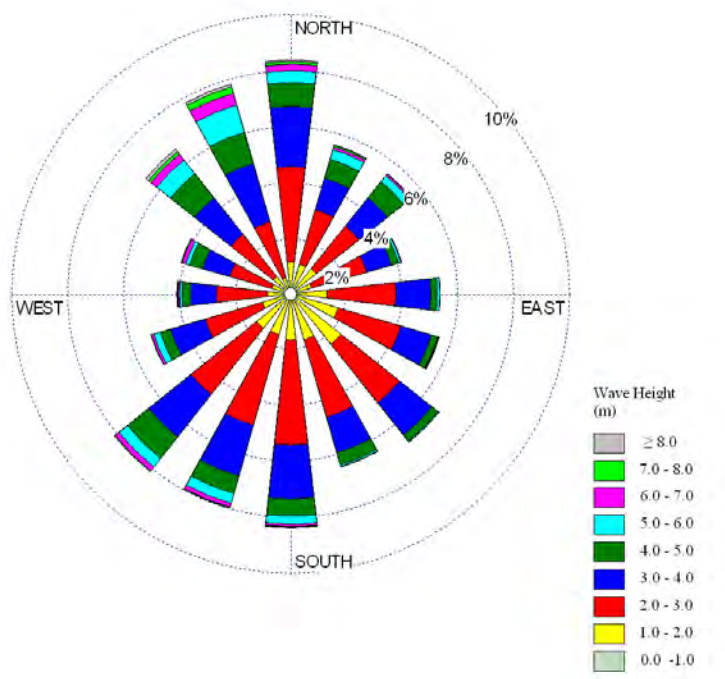
March



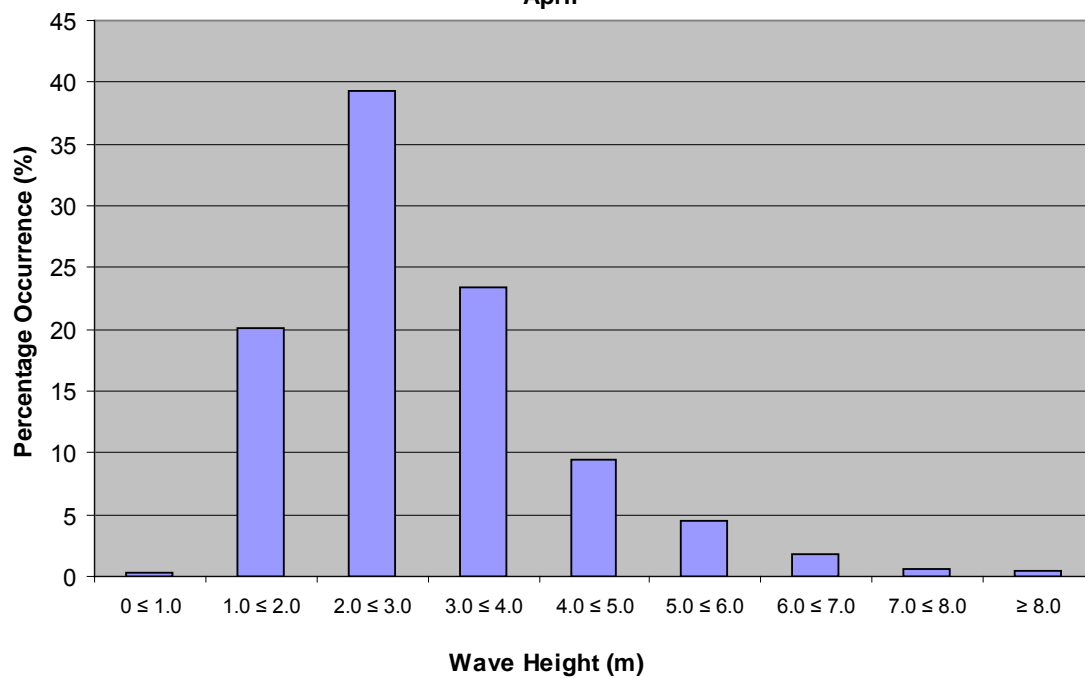
**Wave Height Percentage Occurrence
Grid Point 14845
March**



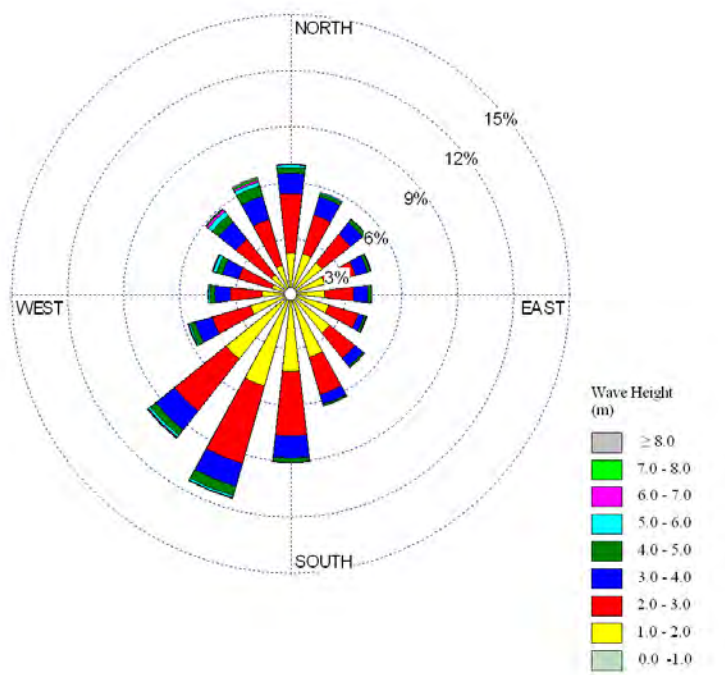
April



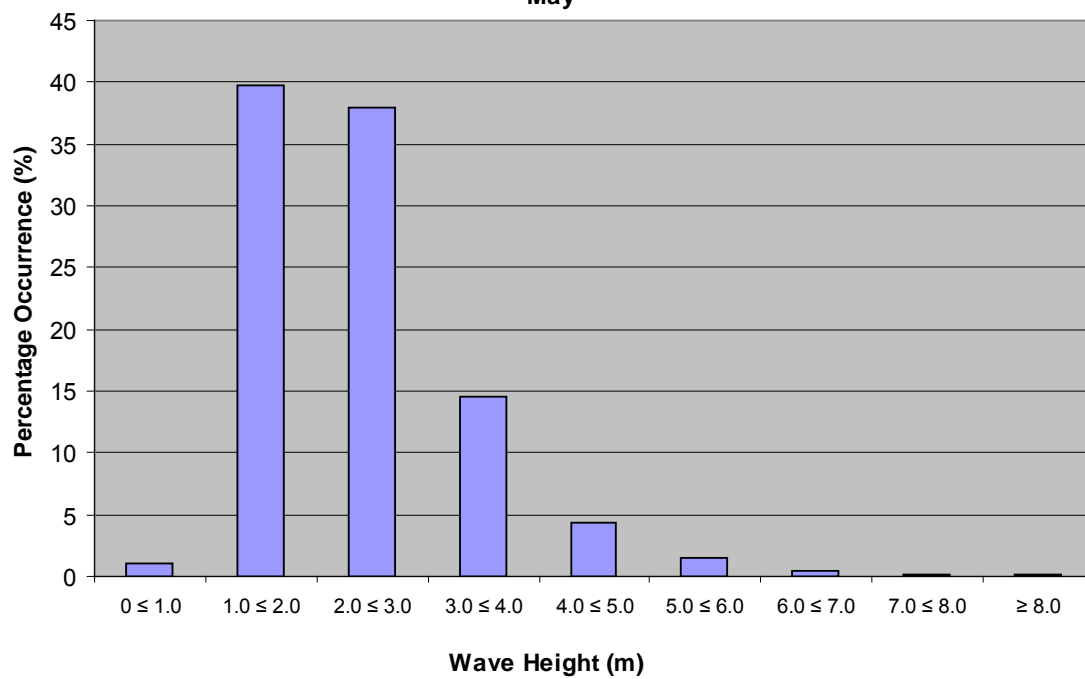
**Wave Height Percentage Occurrence
Grid Point 14845
April**



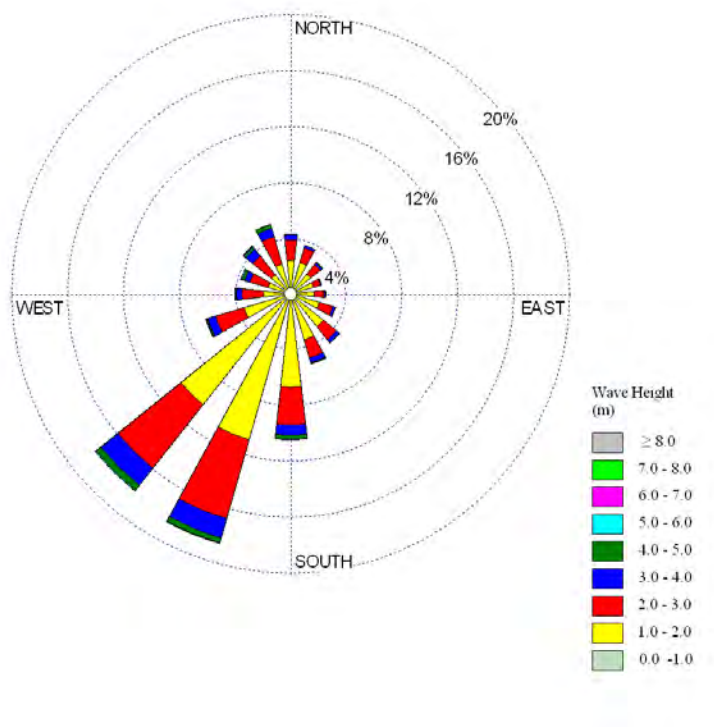
May



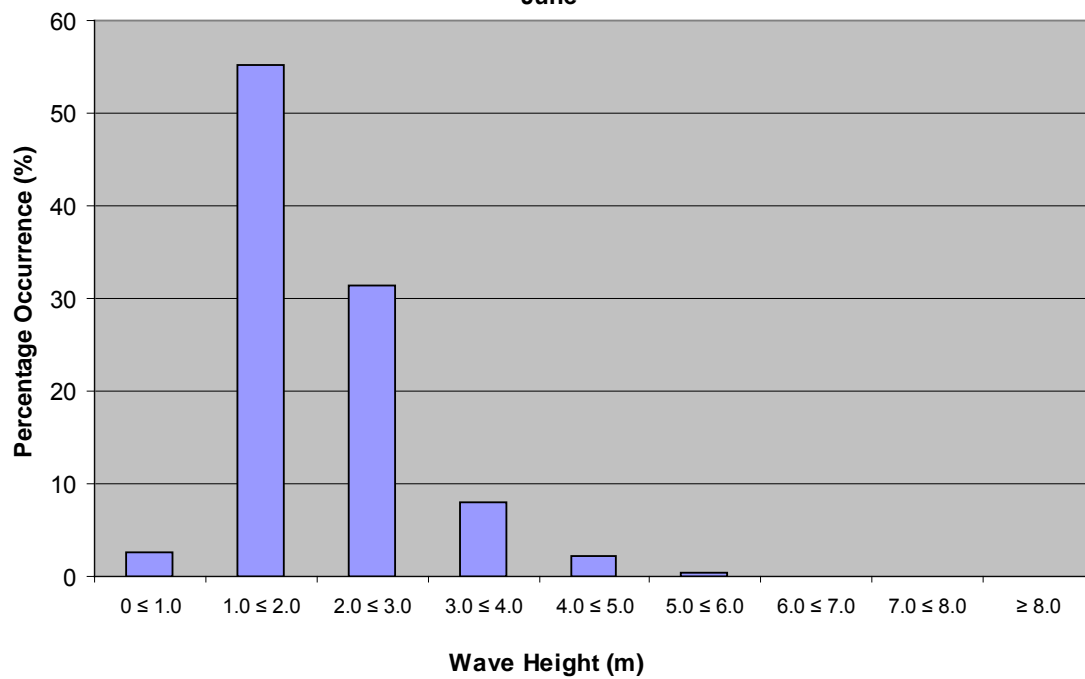
**Wave Height Percentage Occurrence
Grid Point 14845
May**



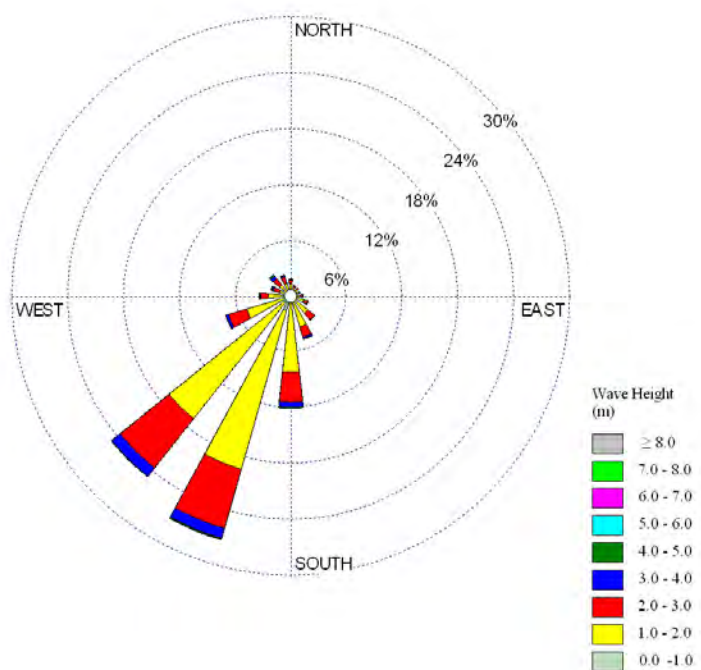
June



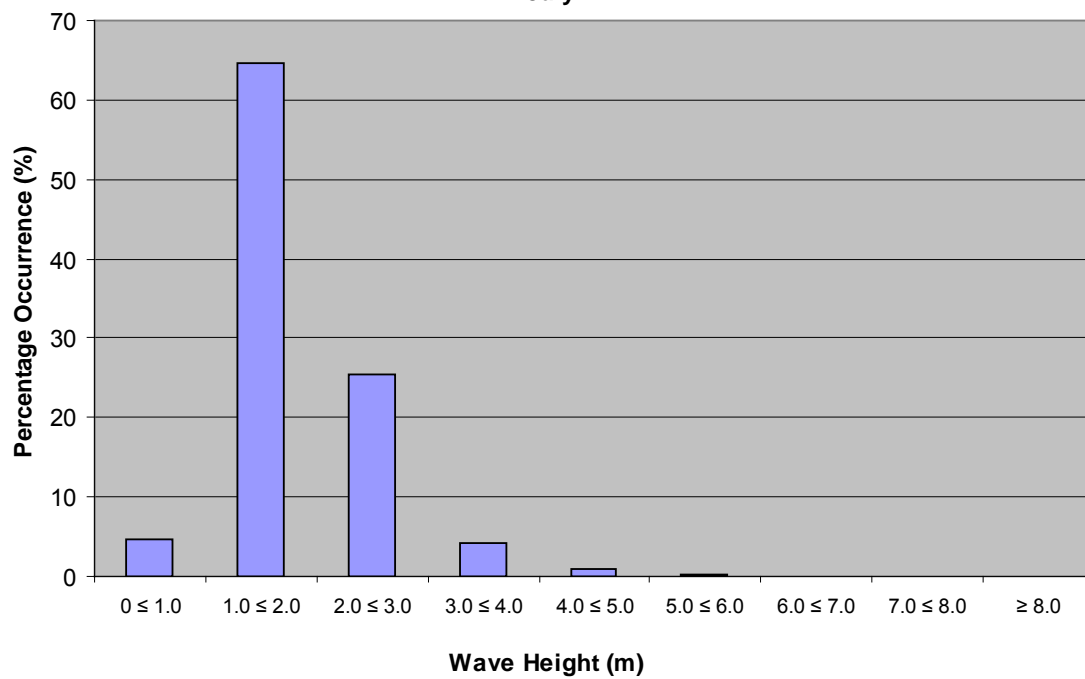
**Wave Height Percentage Occurrence
Grid Point 14845
June**



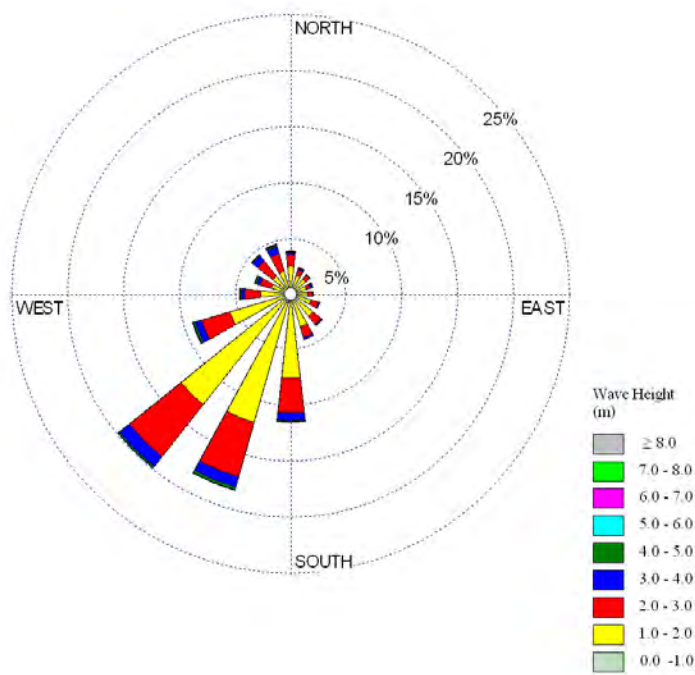
July



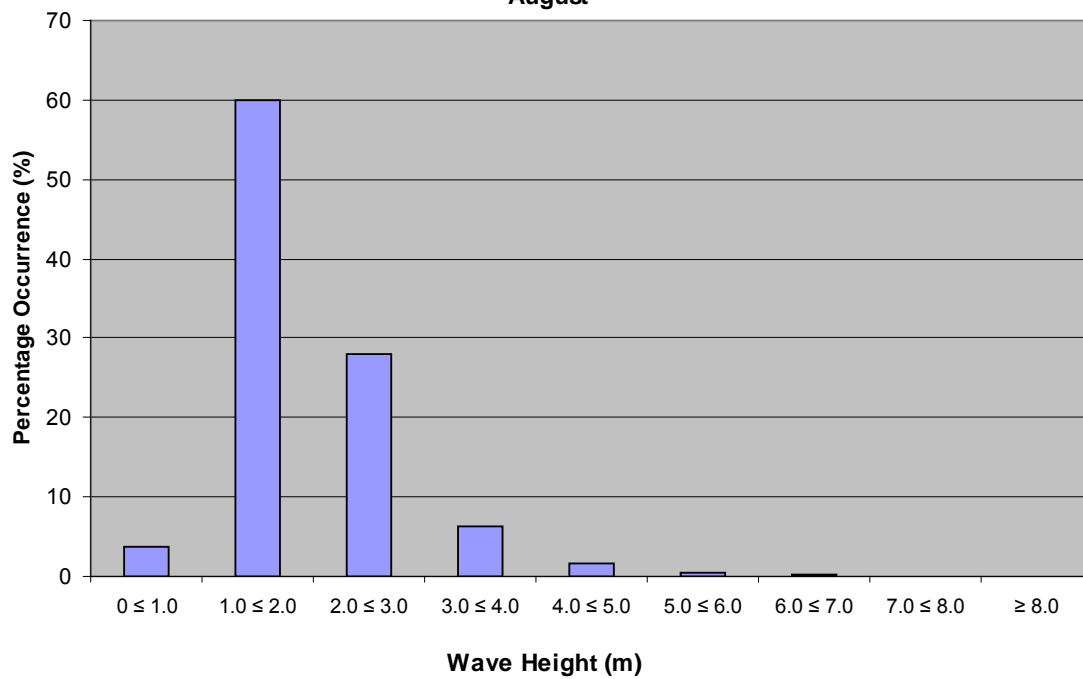
Wave Height Percentage Occurrence
Grid Point 14845
July



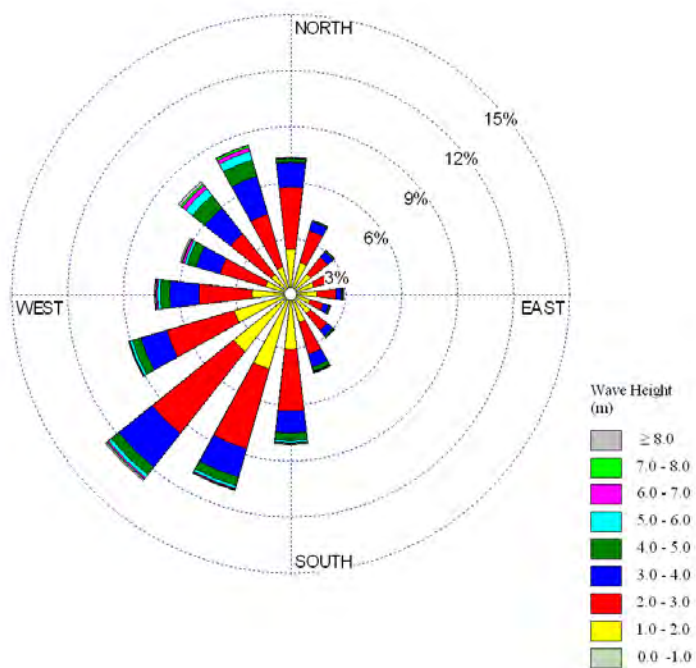
August



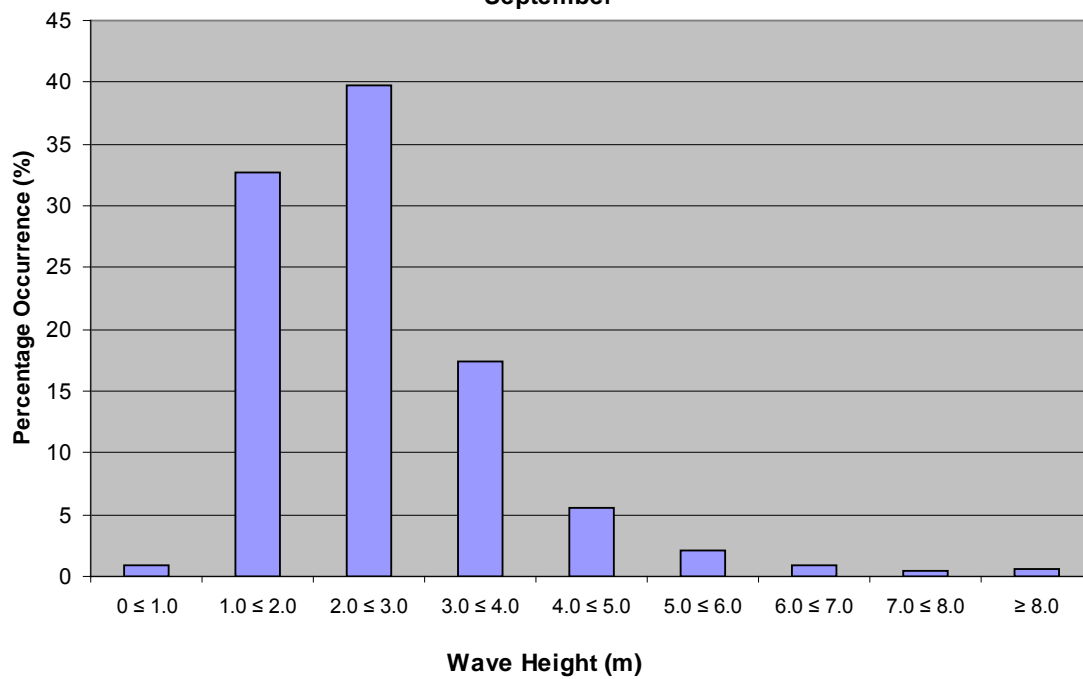
**Wave Height Percentage Occurrence
Grid Point 14845
August**



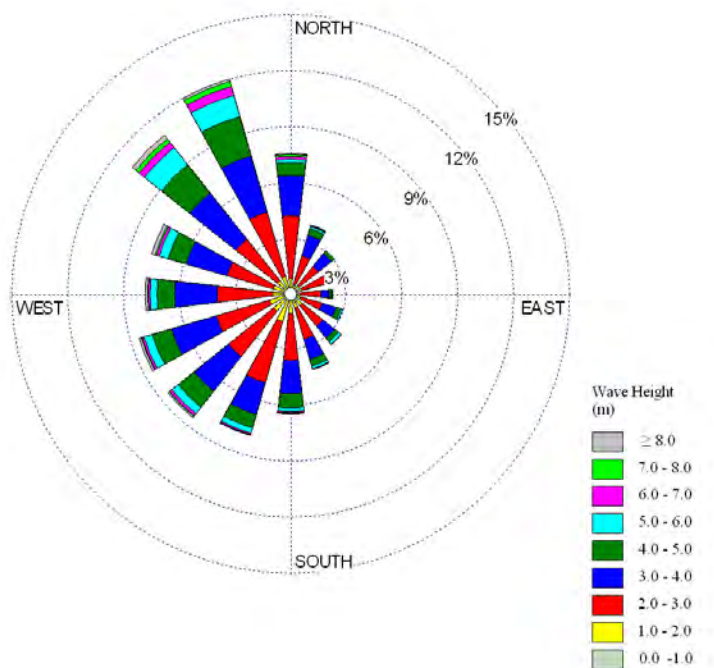
September



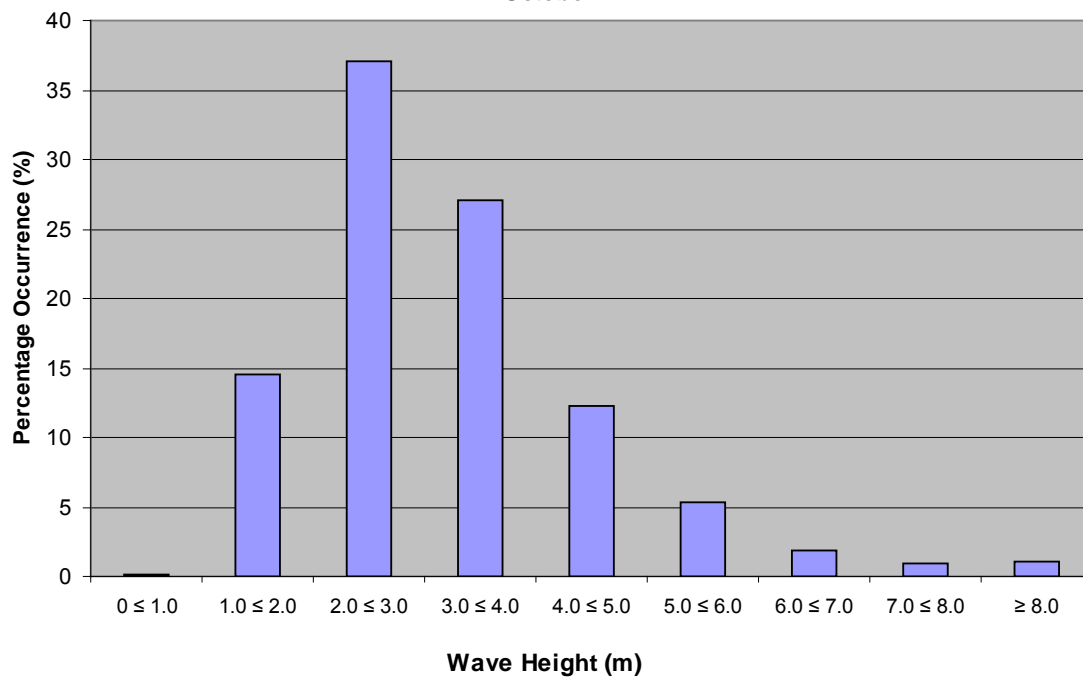
**Wave Height Percentage Occurrence
Grid Point 14845
September**



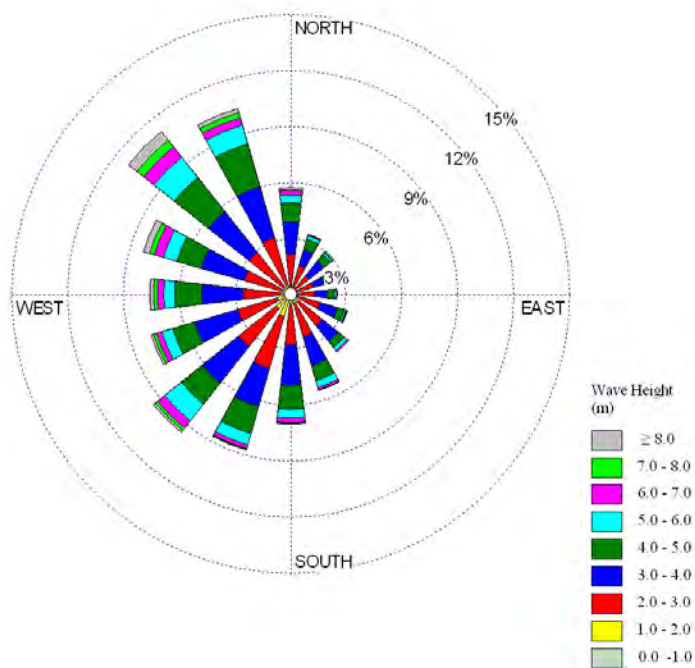
October



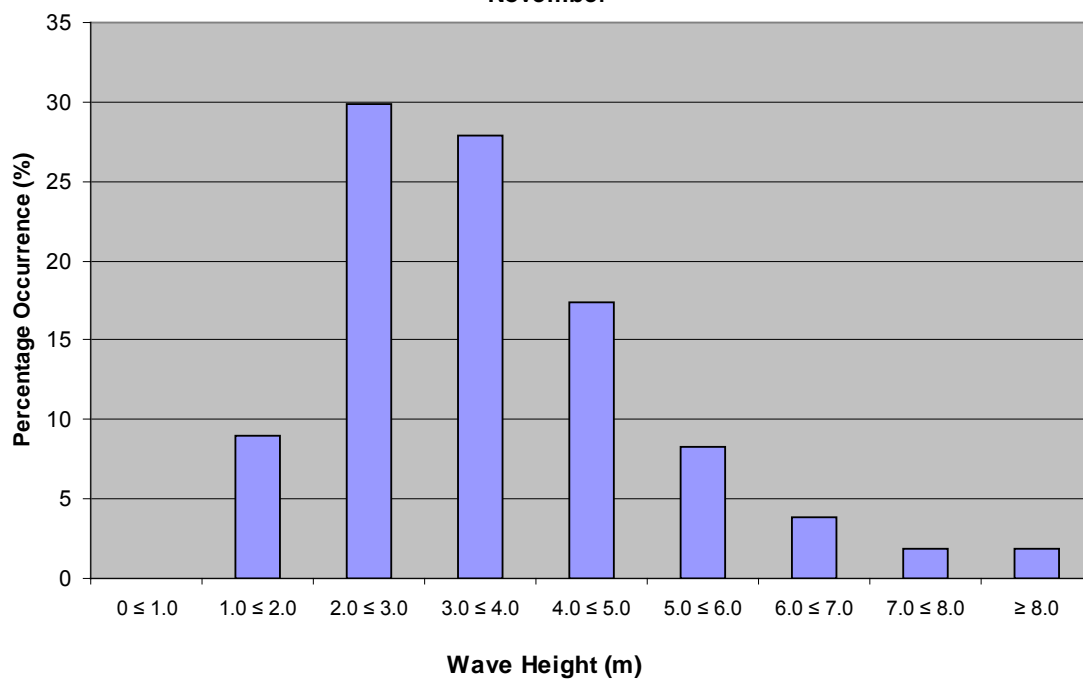
**Wave Height Percentage Occurrence
Grid Point 14845
October**



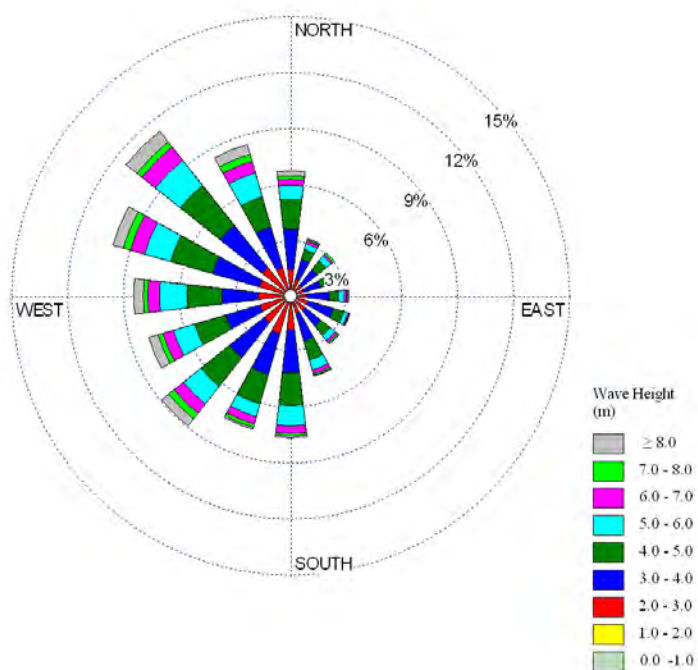
November



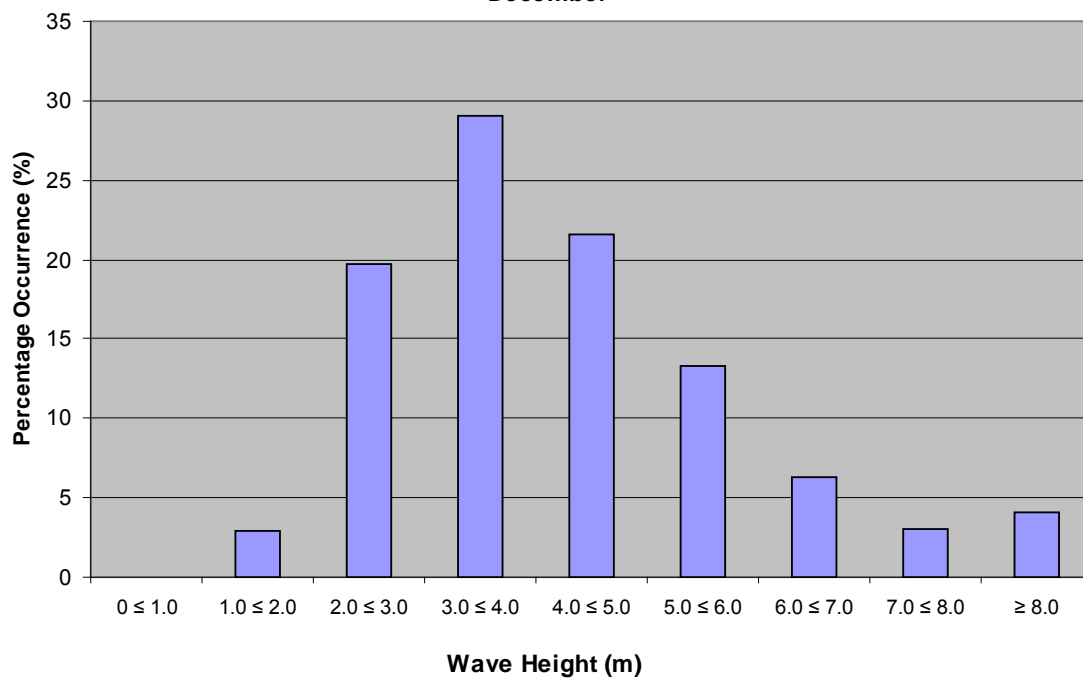
**Wave Height Percentage Occurrence
Grid Point 14845
November**



December

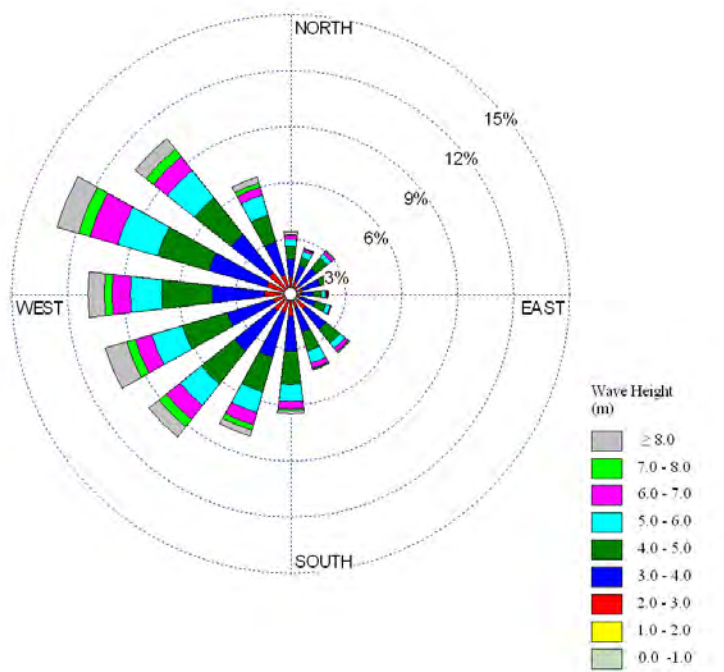


**Wave Height Percentage Occurrence
Grid Point 14845
December**

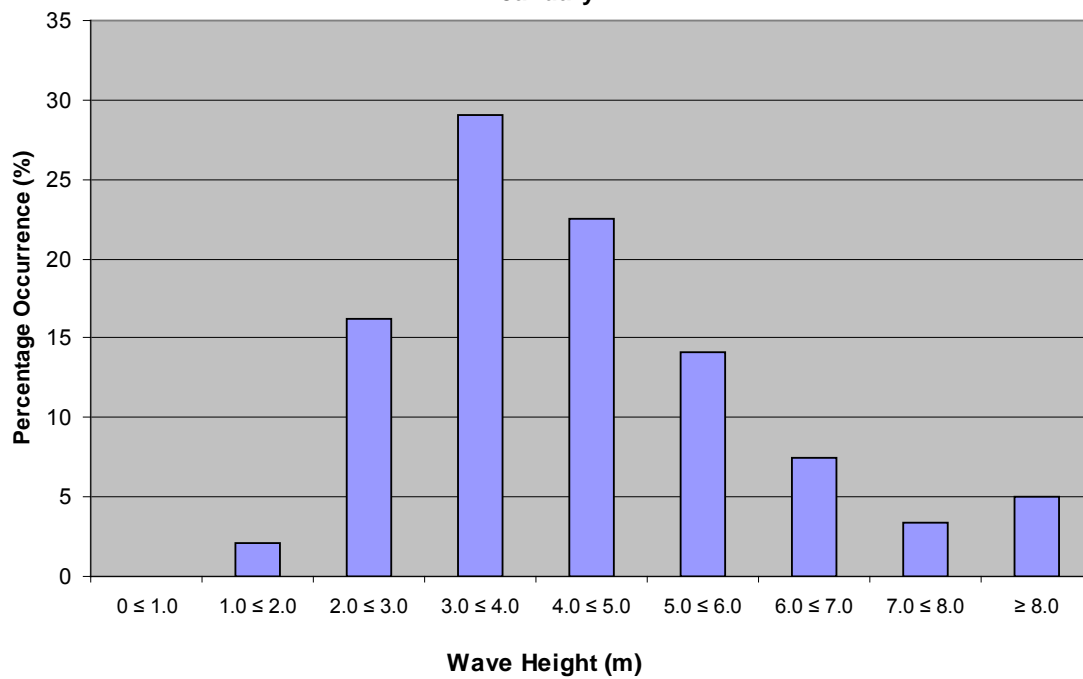


APPENDIX 5
Monthly Wave Roses
and
Percentage Occurrence Graphs
for MSC50 Grid point 13912

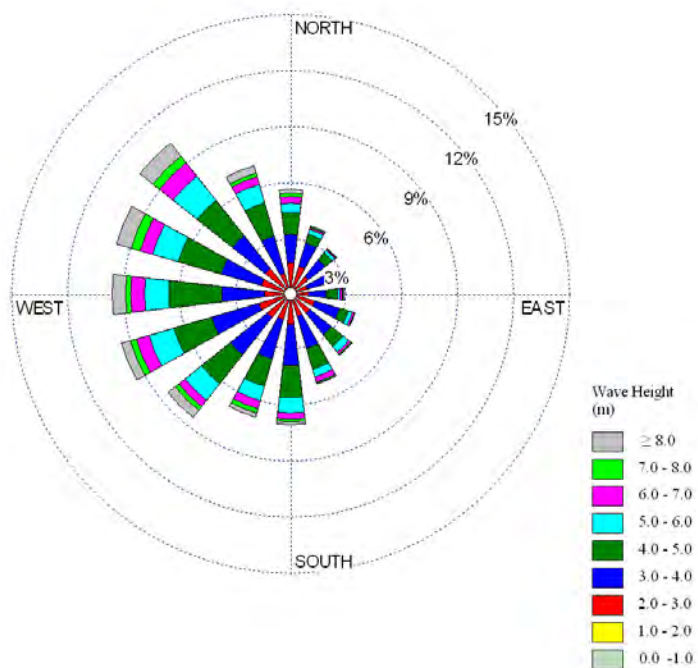
January



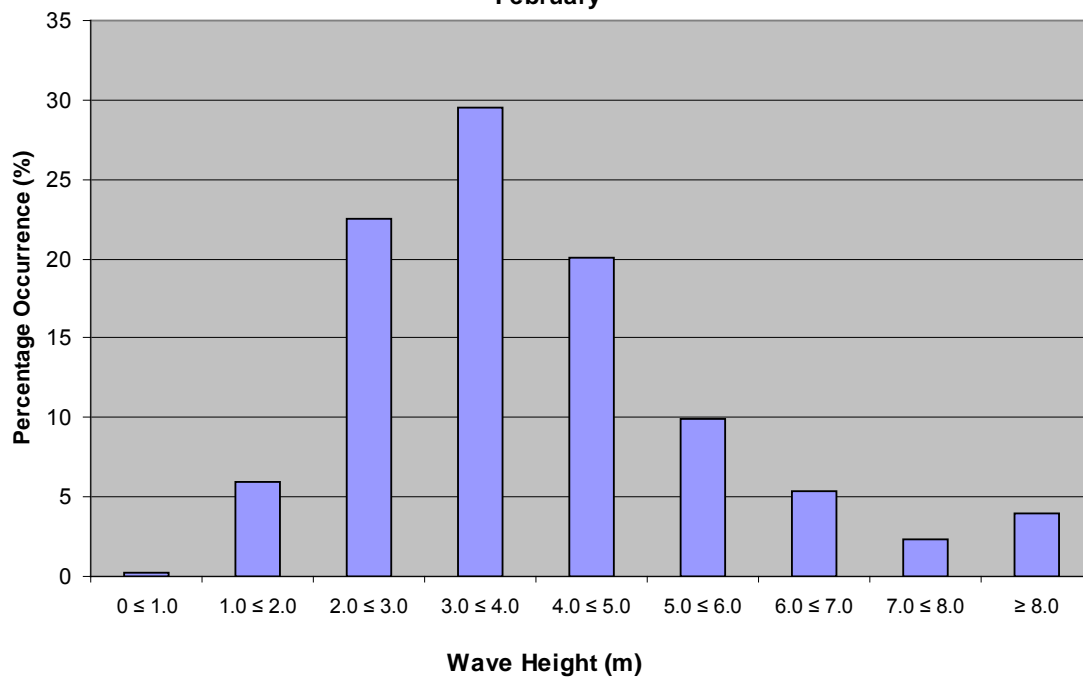
**Wave Height Percentage Occurrence
Grid Point 13912
January**



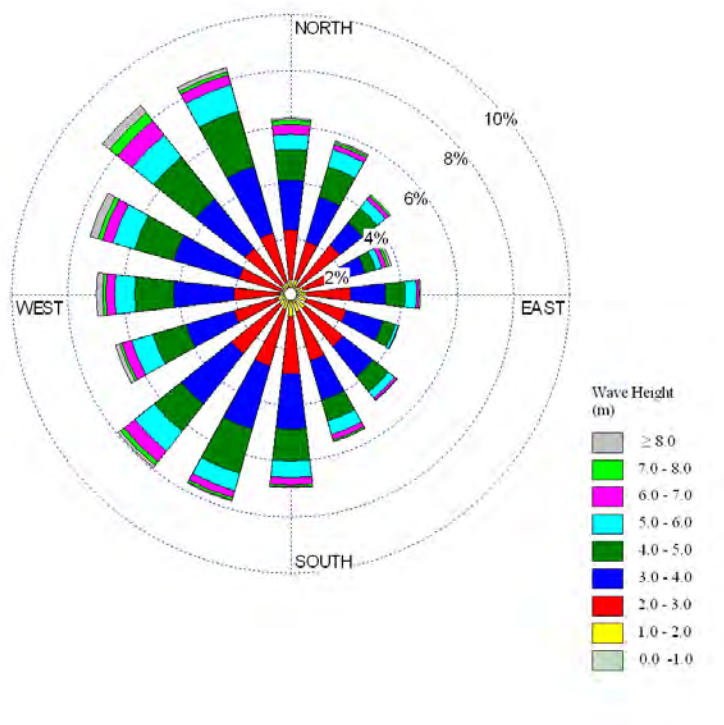
February



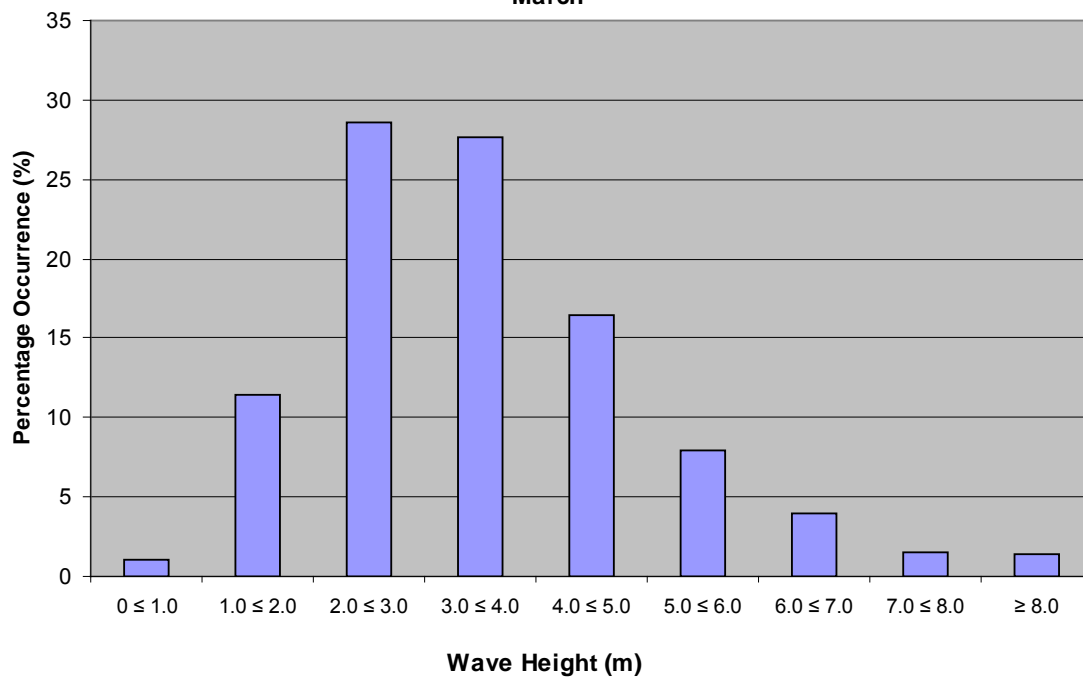
**Wave Height Percentage Occurrence
Grid Point 13912
February**



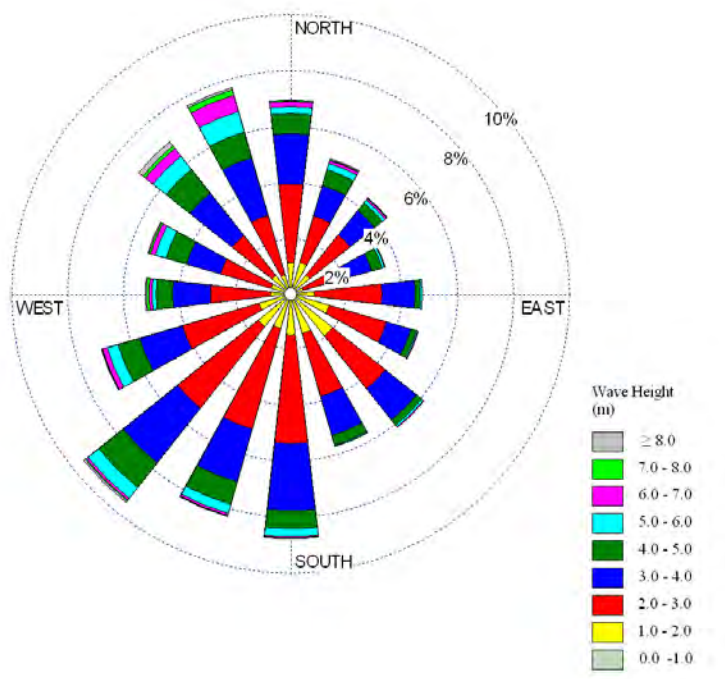
March



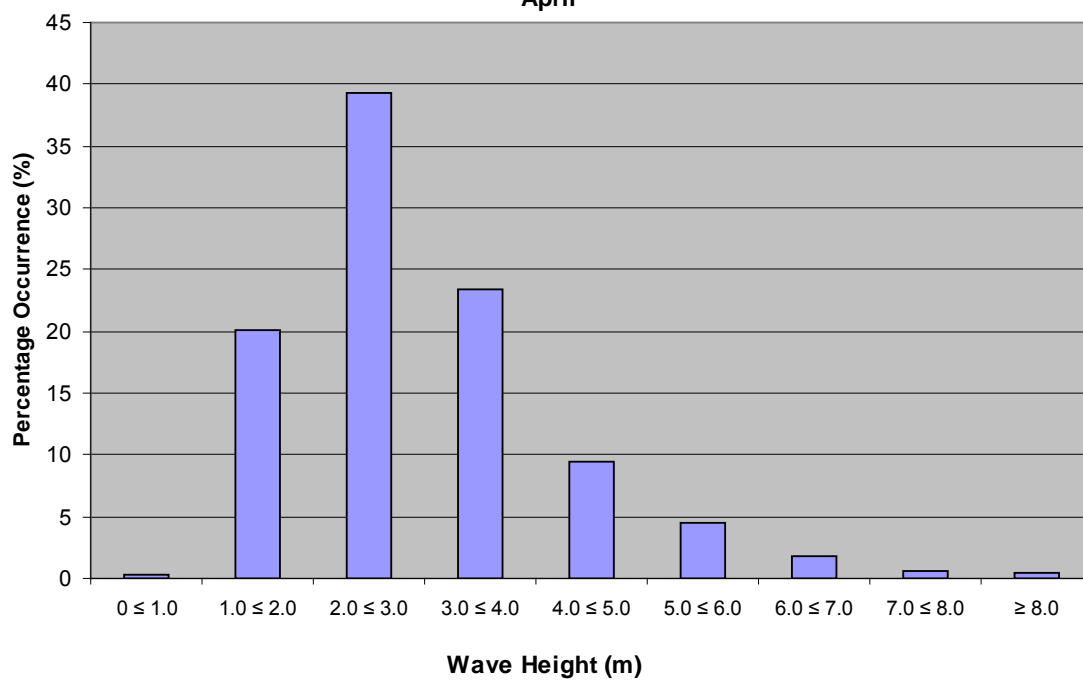
**Wave Height Percentage Occurrence
Grid Point 13912
March**



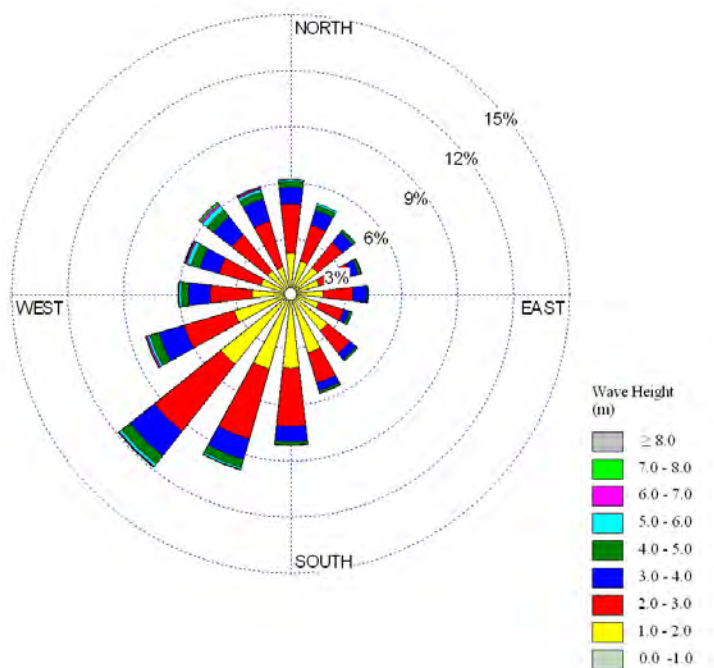
April



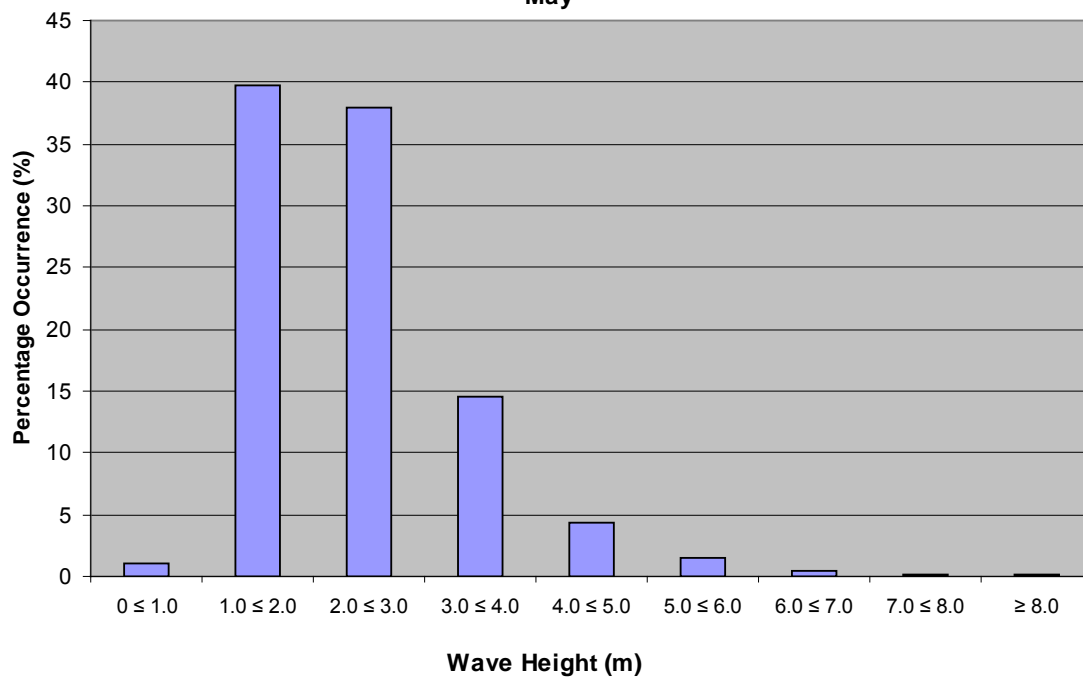
**Wave Height Percentage Occurrence
Grid Point 13912
April**



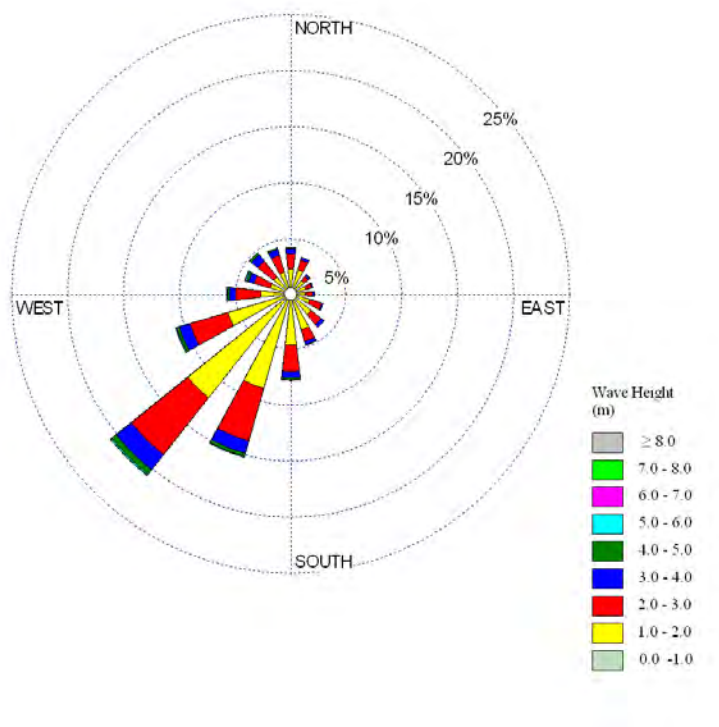
May



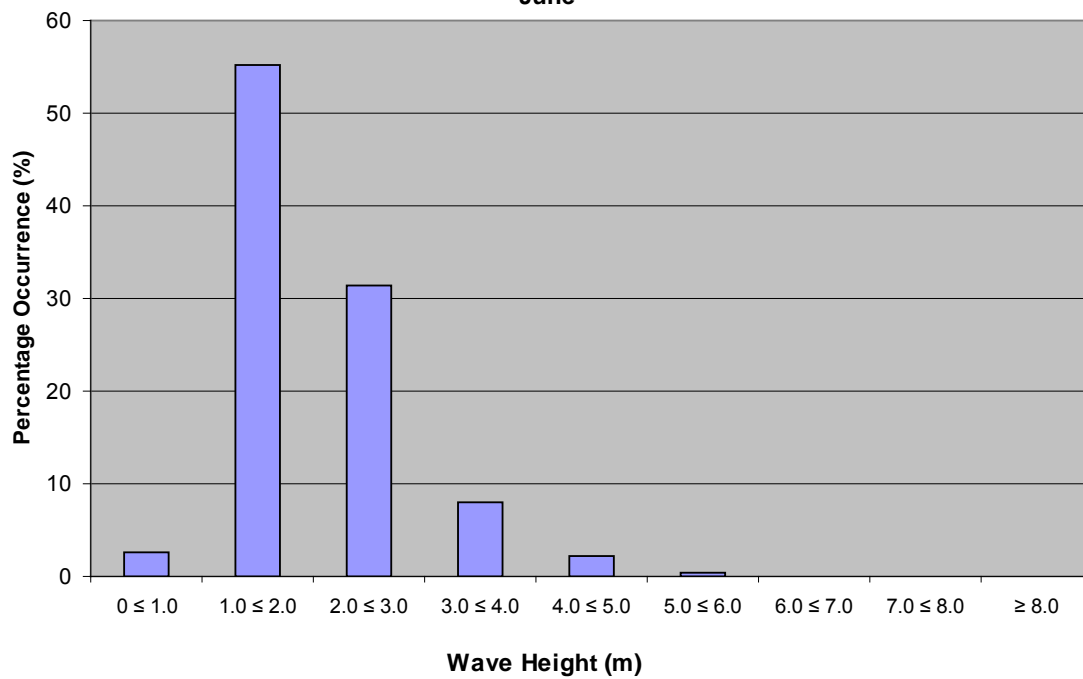
**Wave Height Percentage Occurrence
Grid Point 13912
May**



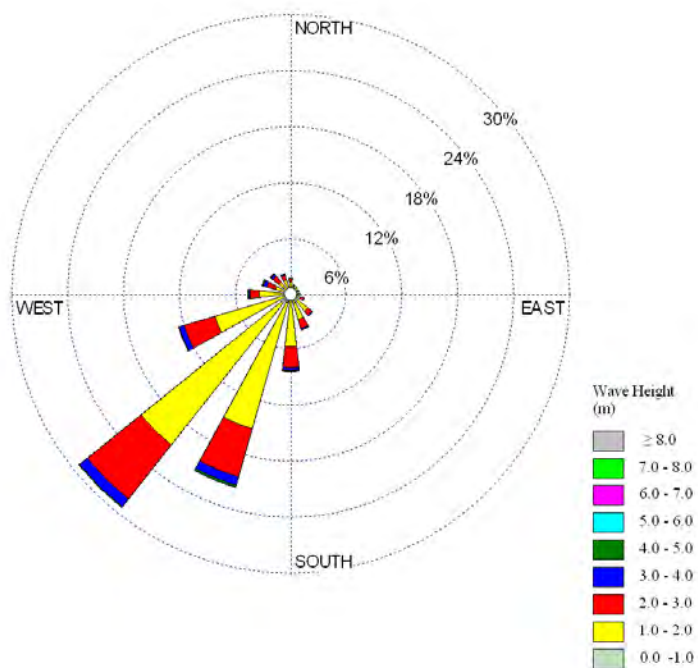
June



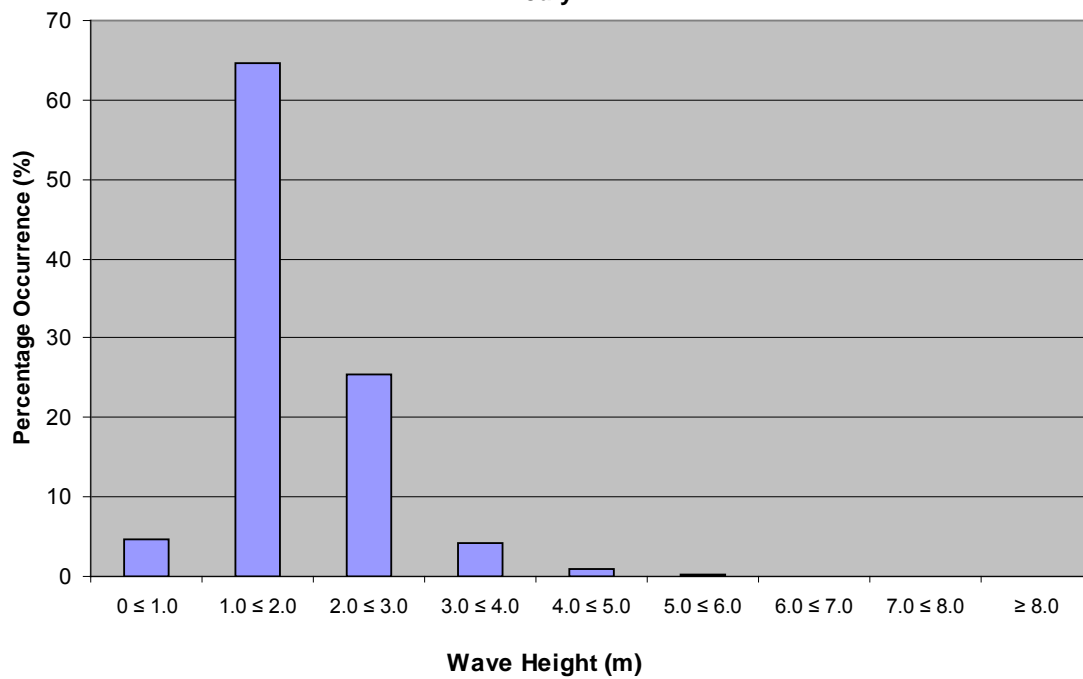
**Wave Height Percentage Occurrence
Grid Point 13912
June**



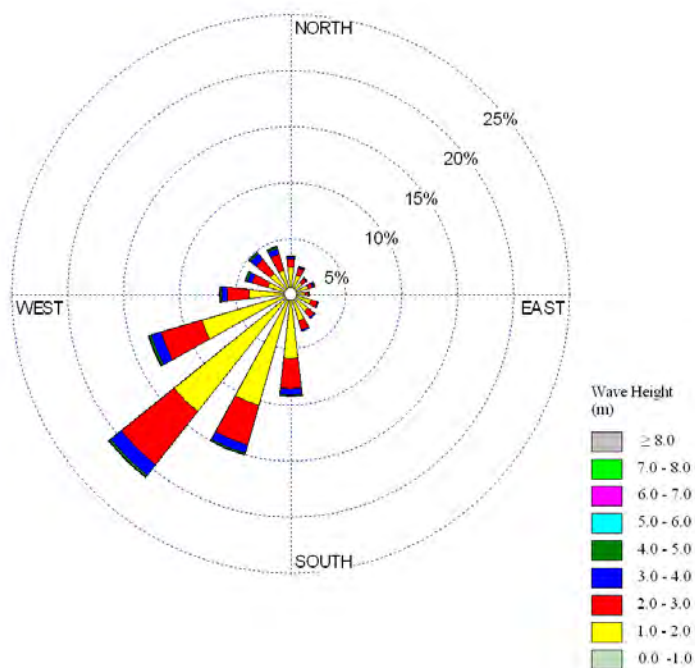
July



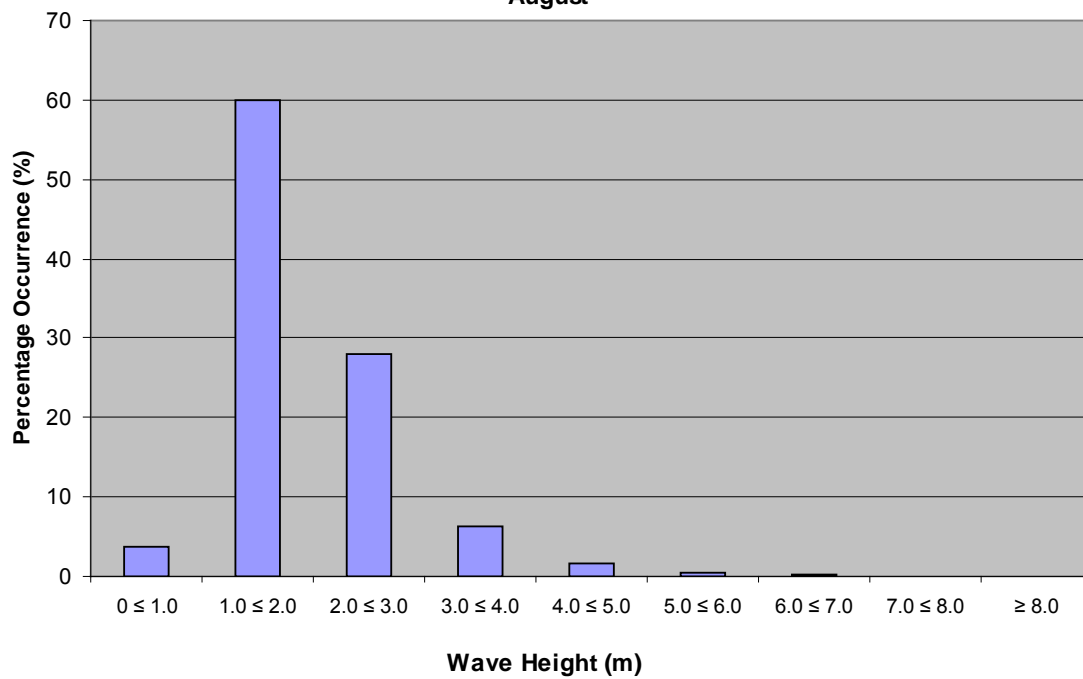
Wave Height Percentage Occurrence
Grid Point 13912
July



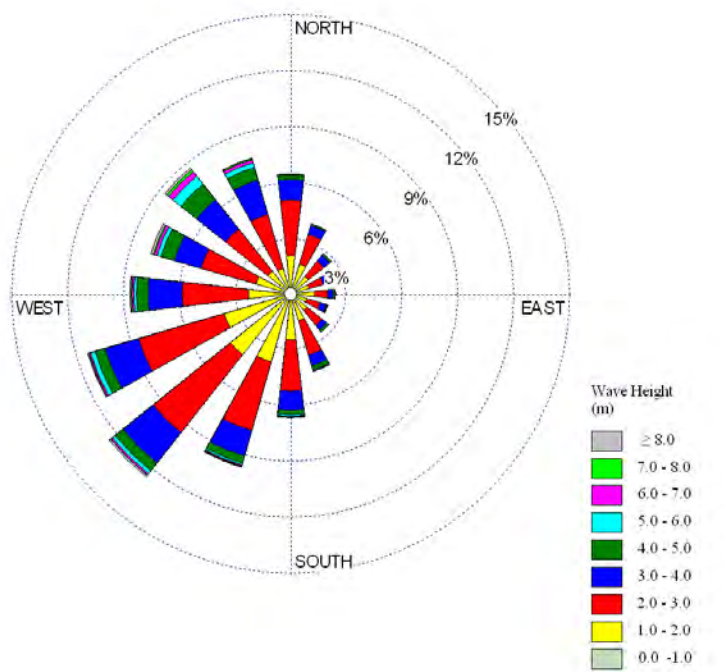
August



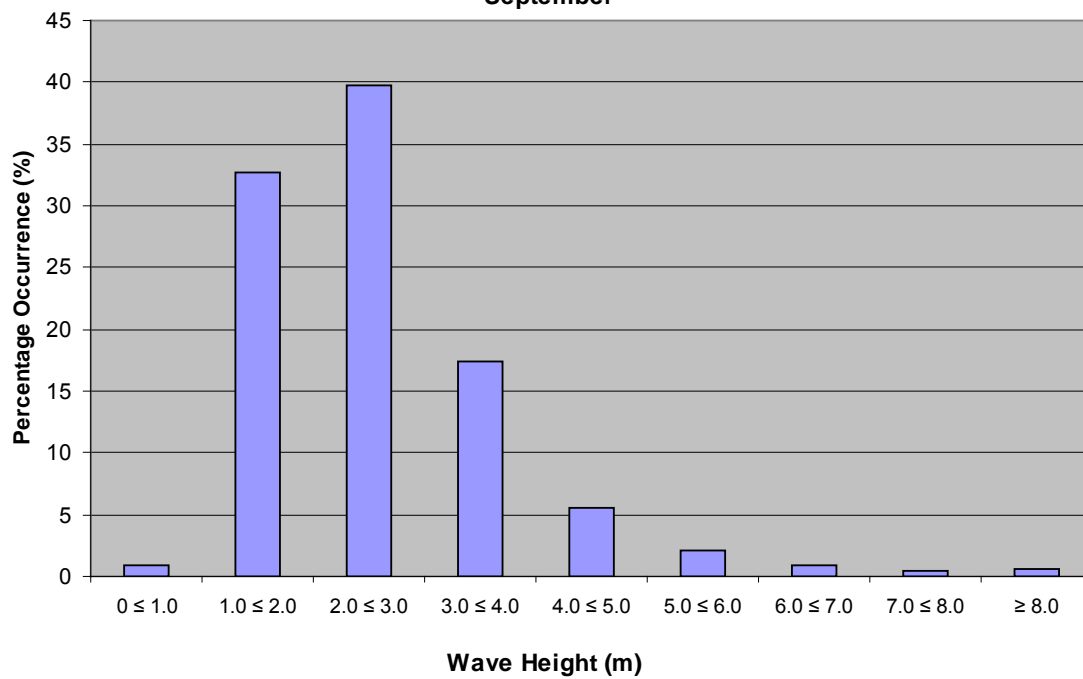
**Wave Height Percentage Occurrence
Grid Point 13912
August**



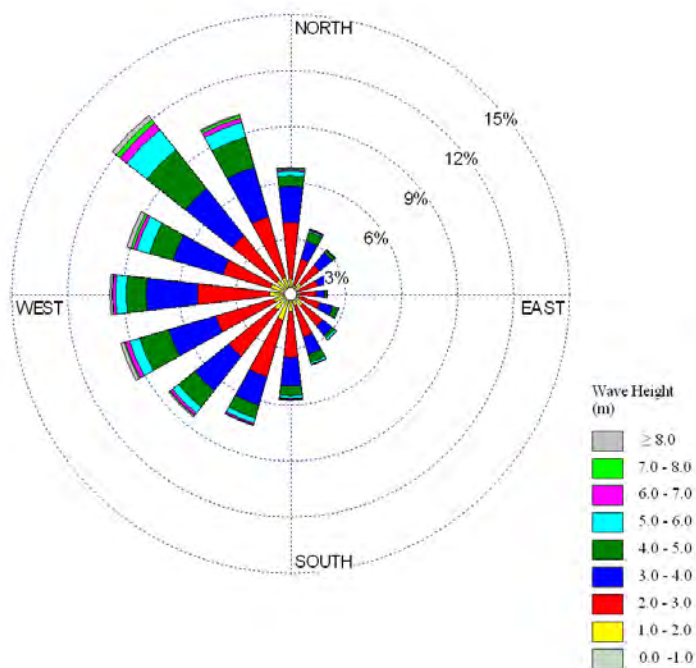
September



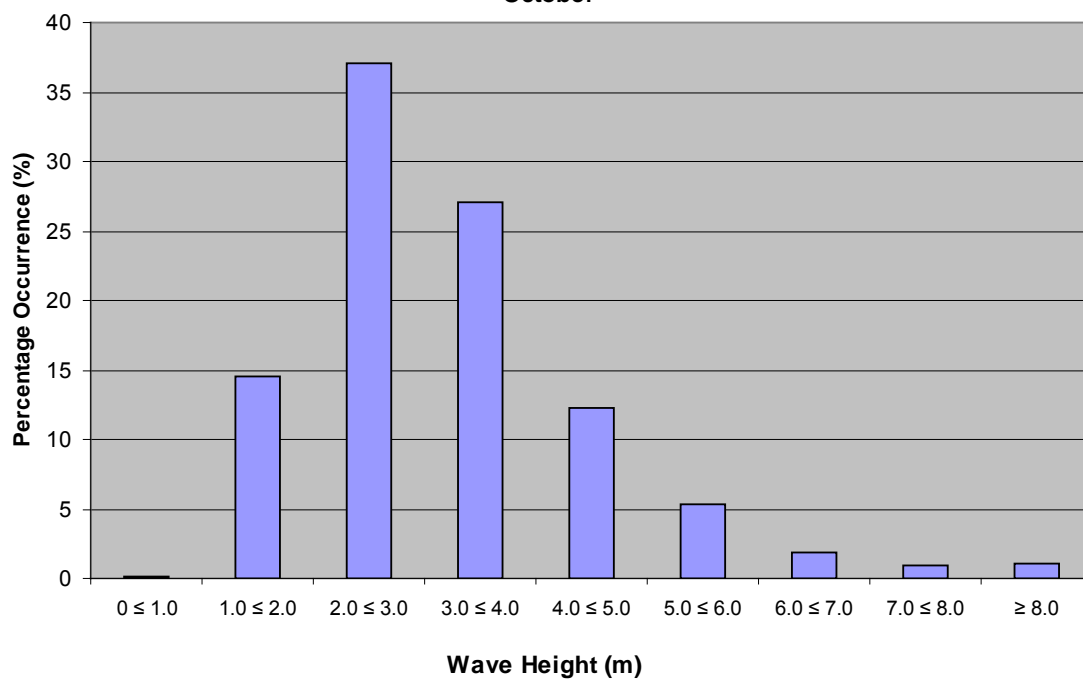
**Wave Height Percentage Occurrence
Grid Point 13912
September**



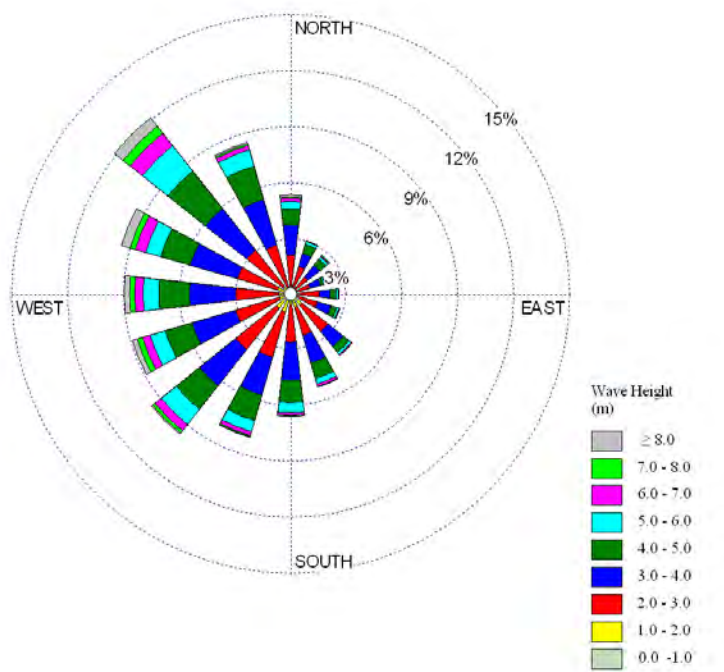
October



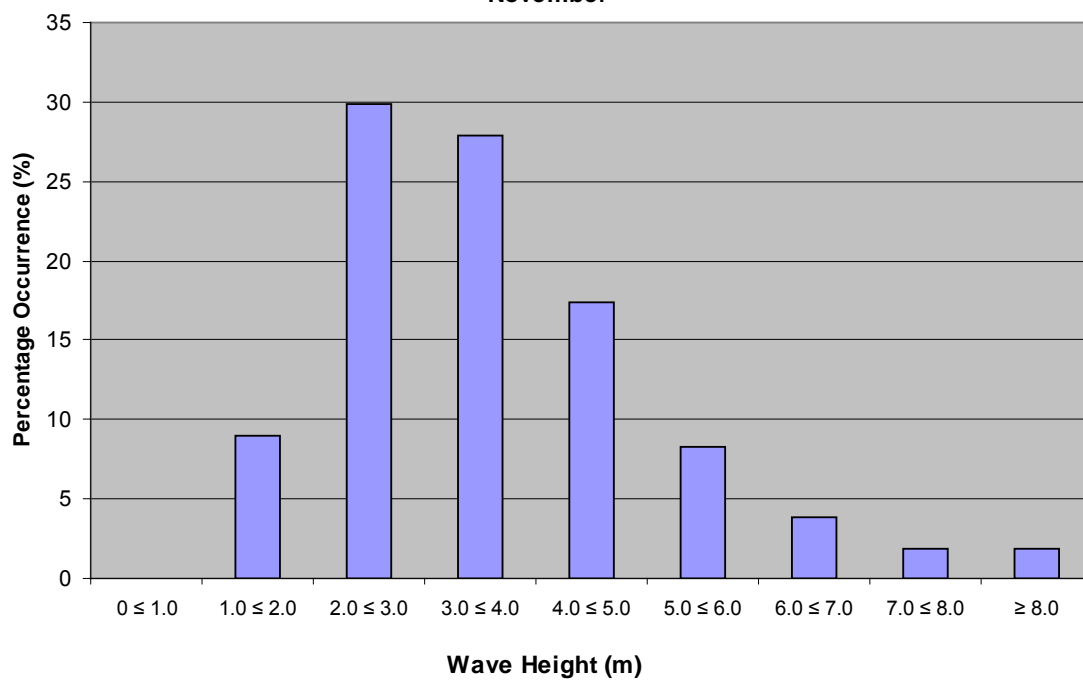
**Wave Height Percentage Occurrence
Grid Point 13912
October**



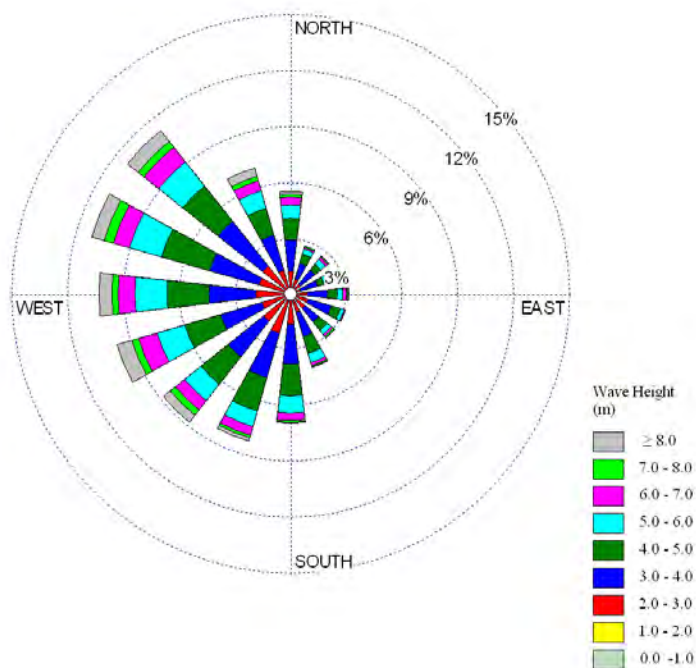
November



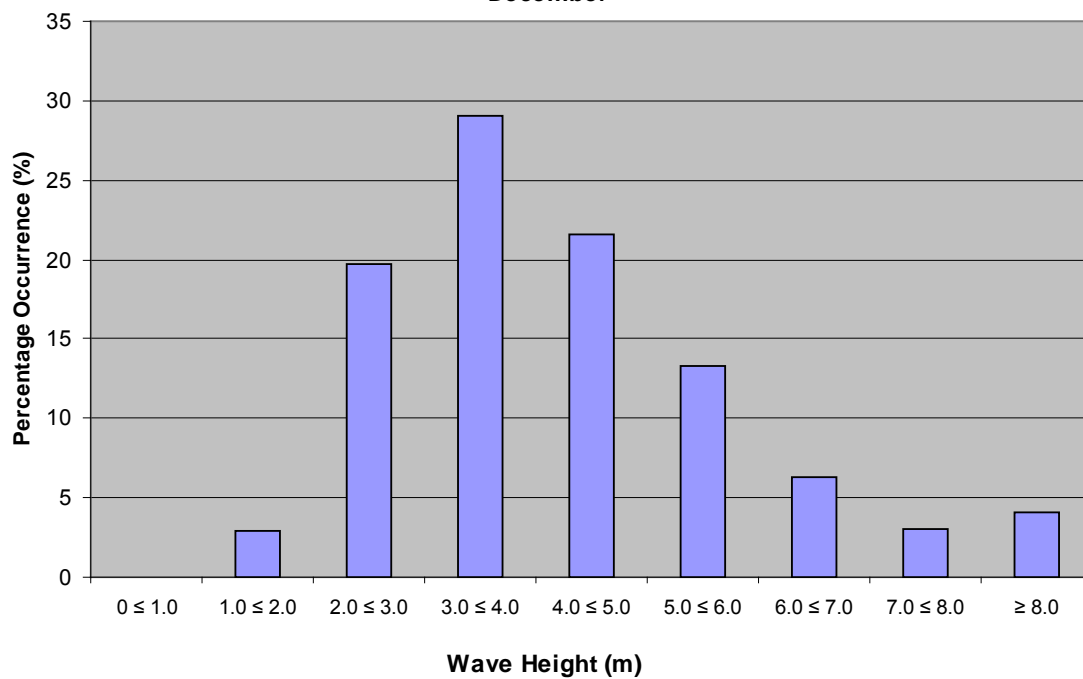
**Wave Height Percentage Occurrence
Grid Point 13912
November**



December

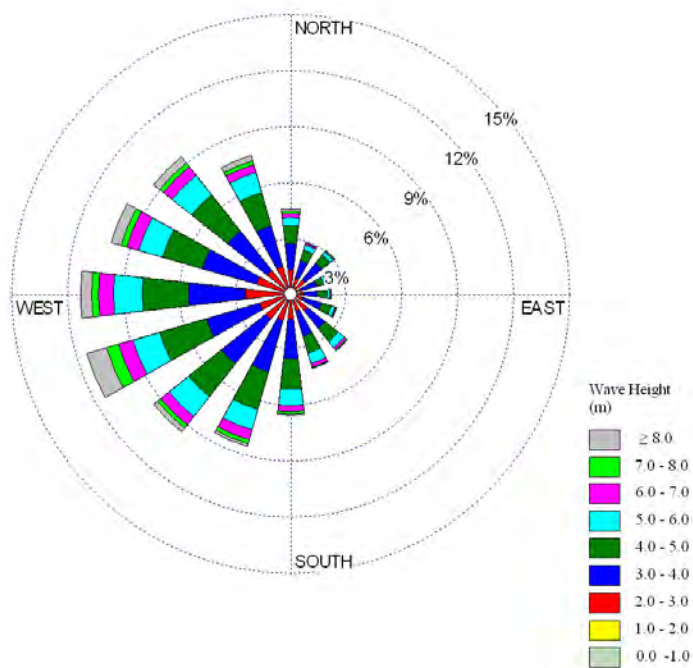


Wave Height Percentage Occurrence
Grid Point 13912
December

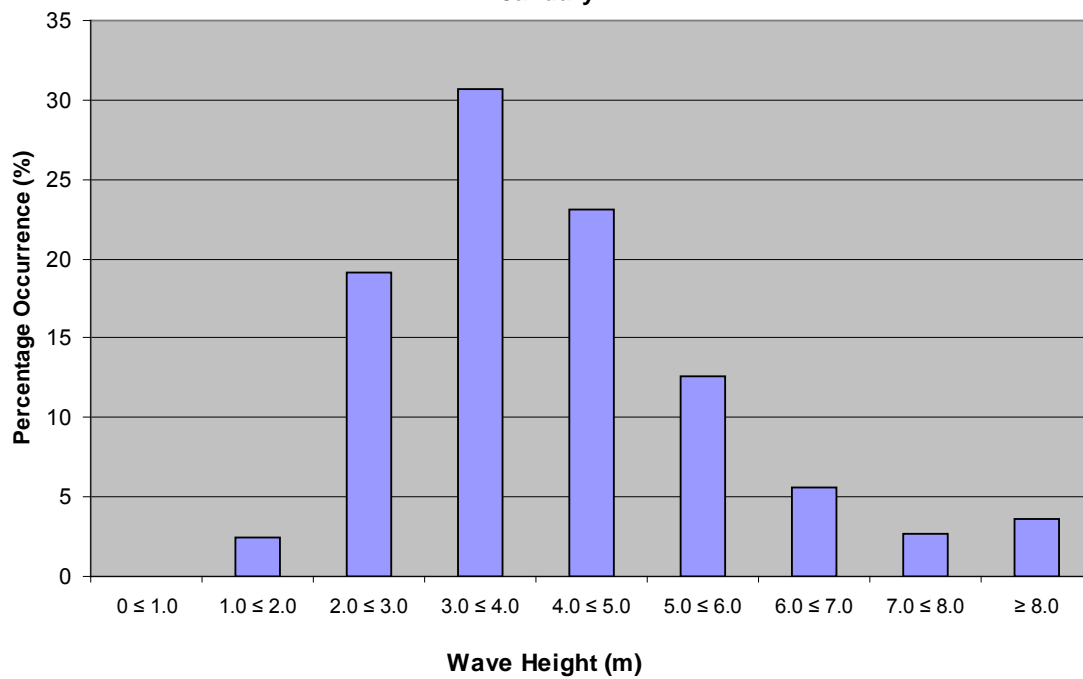


APPENDIX 6
Monthly Wave Roses
and
Percentage Occurrence Graphs
for MSC50 Grid point 11423

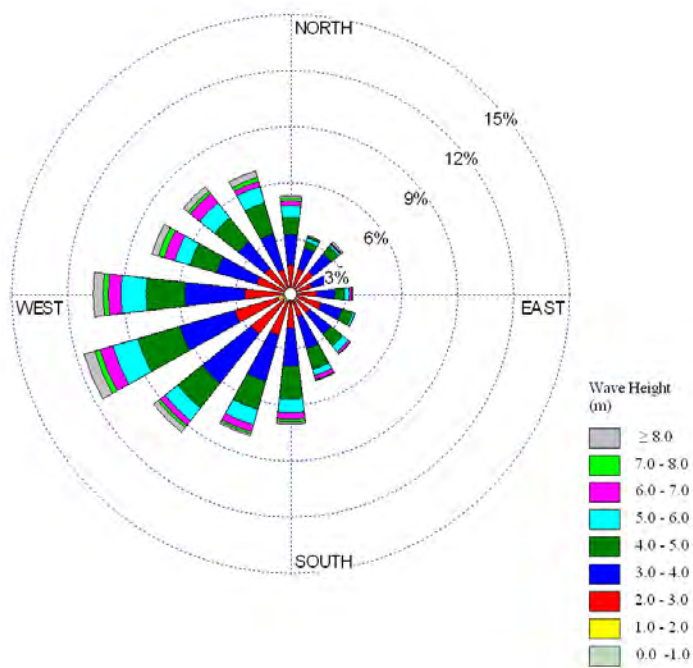
January



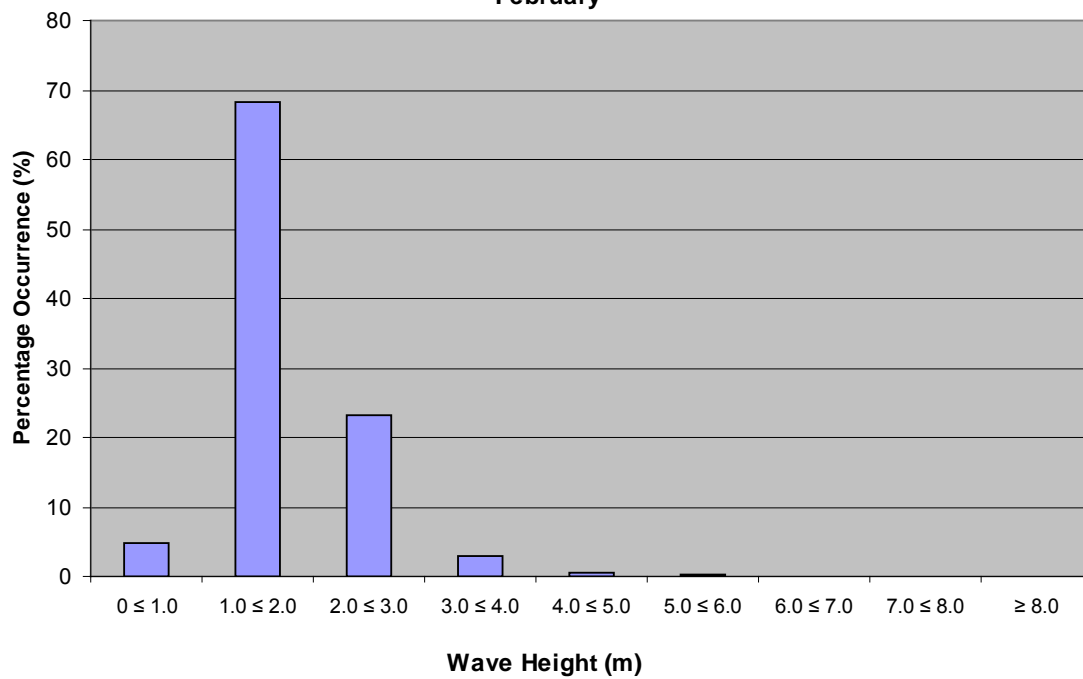
**Wave Height Percentage Occurrence
Grid Point 11423
January**



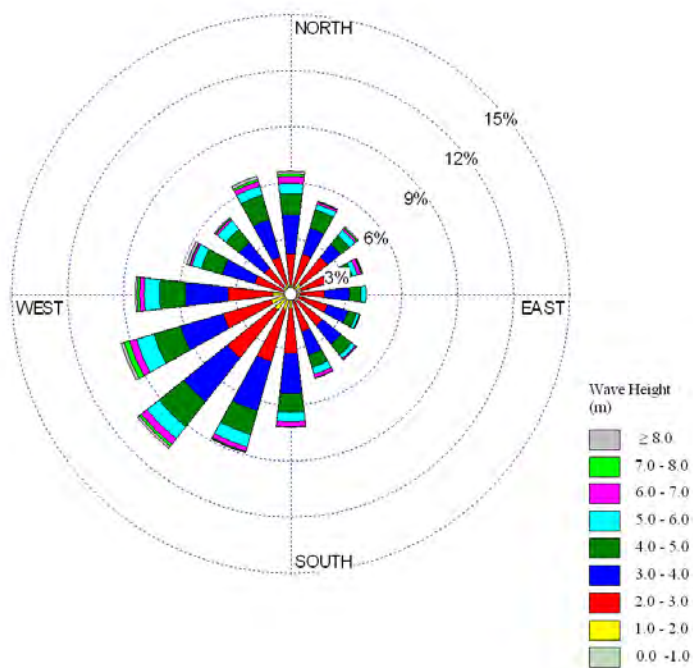
February



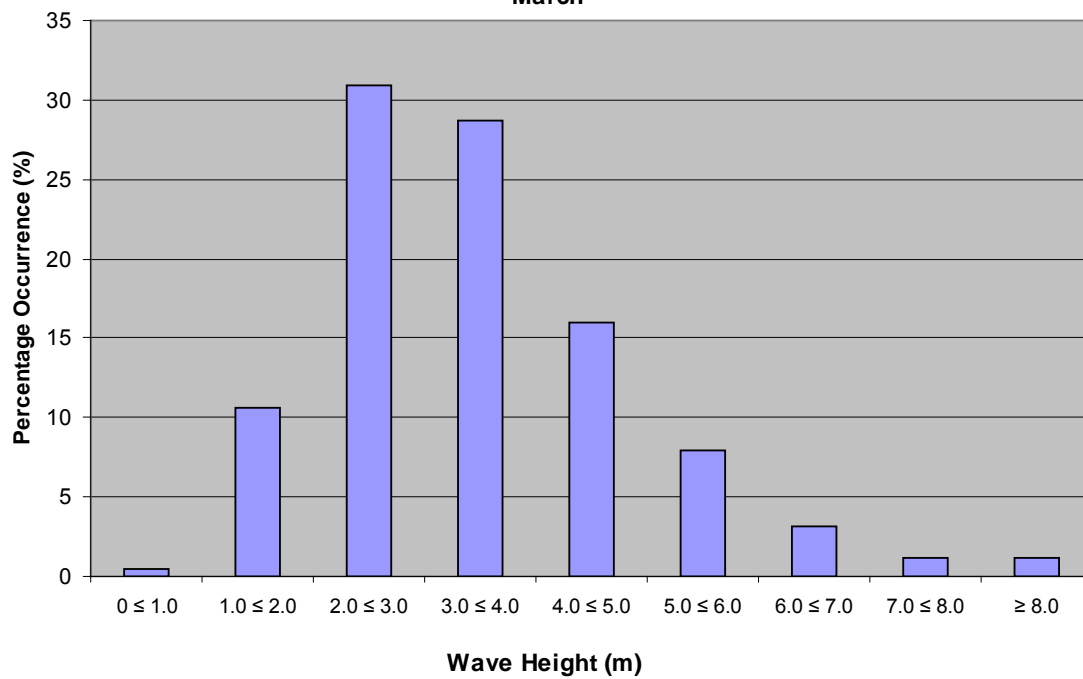
**Wave Height Percentage Occurrence
Grid Point 11423
February**



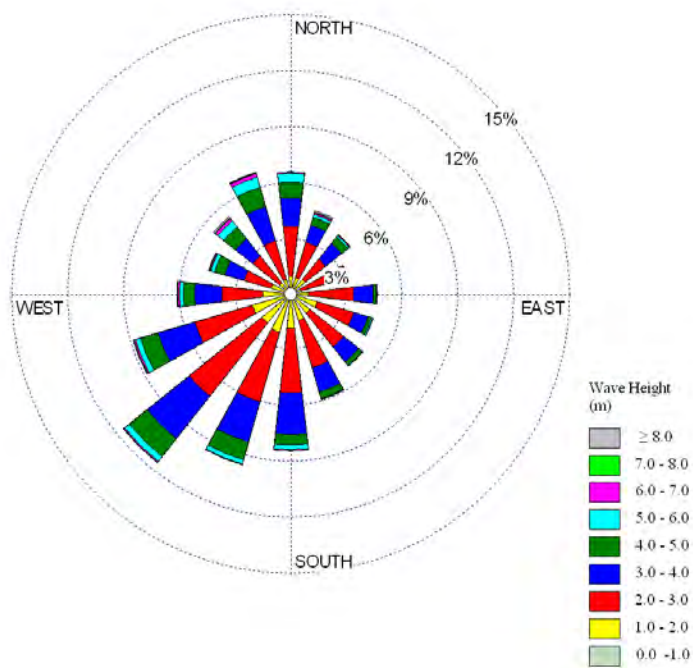
March



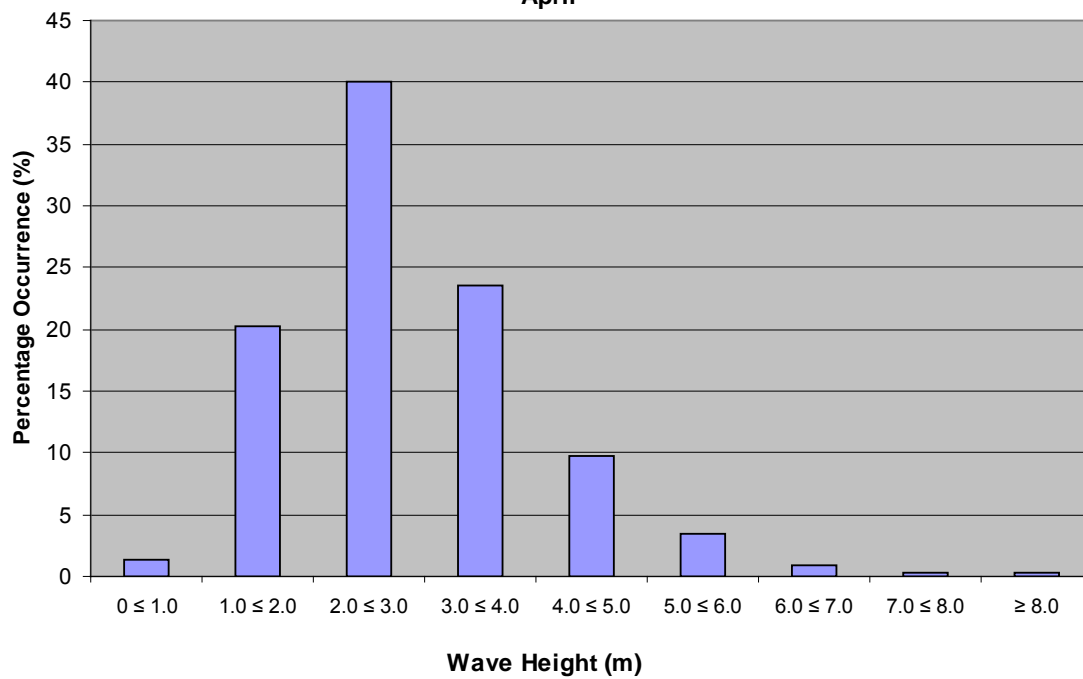
**Wave Height Percentage Occurrence
Grid Point 11423
March**



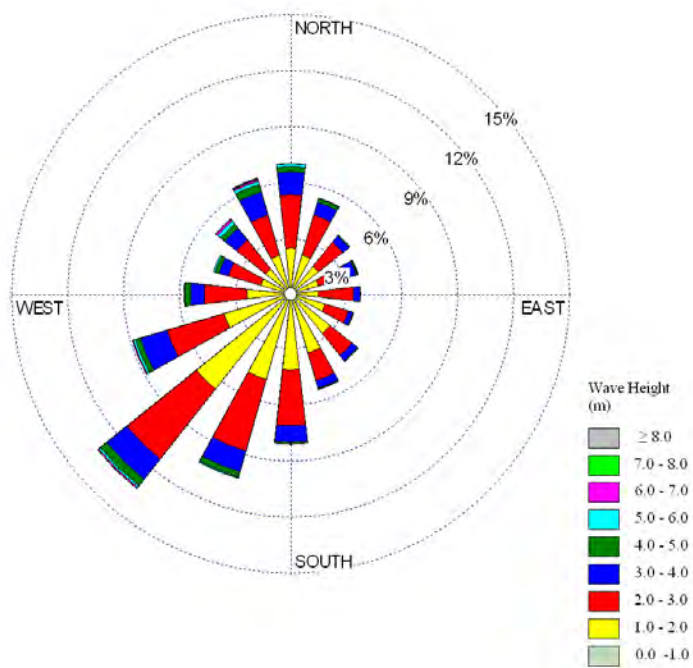
April



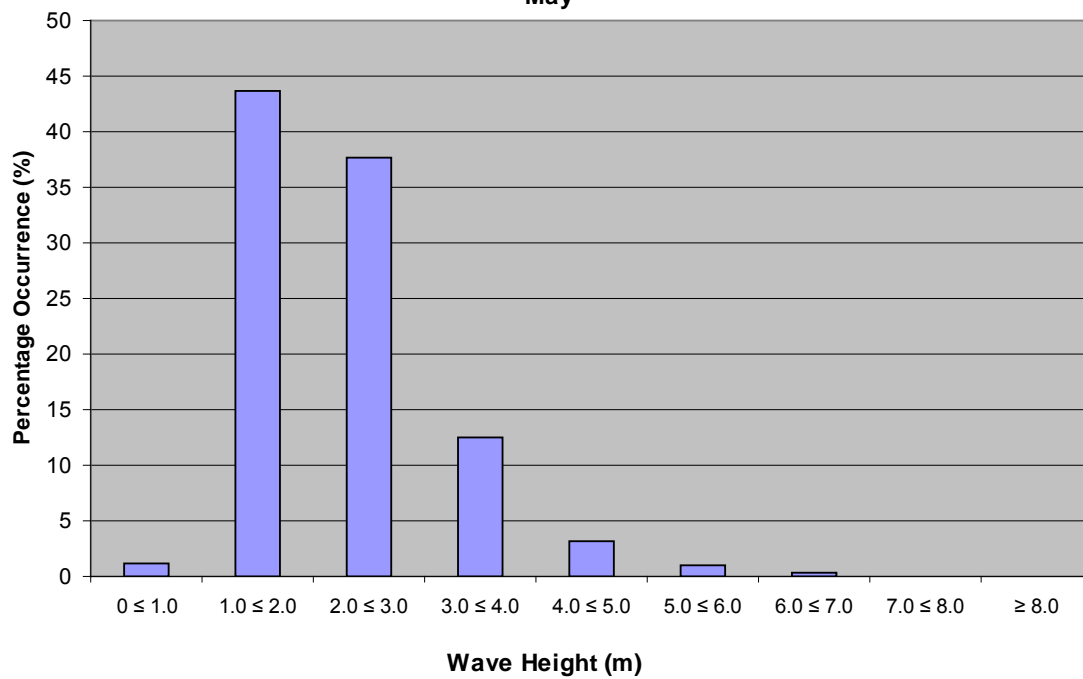
**Wave Height Percentage Occurrence
Grid Point 11423
April**



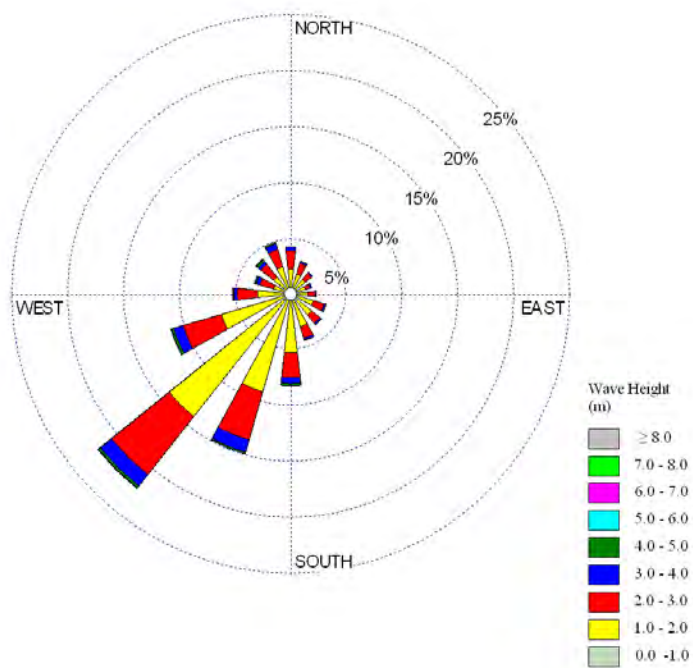
May



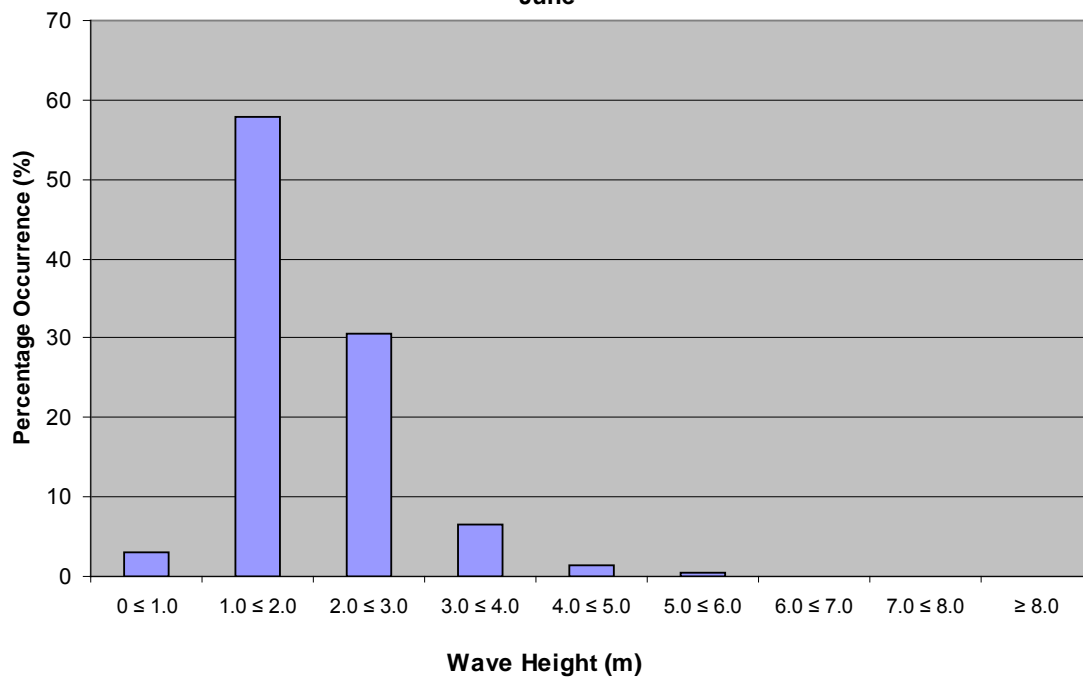
**Wave Height Percentage Occurrence
Grid Point 11423
May**



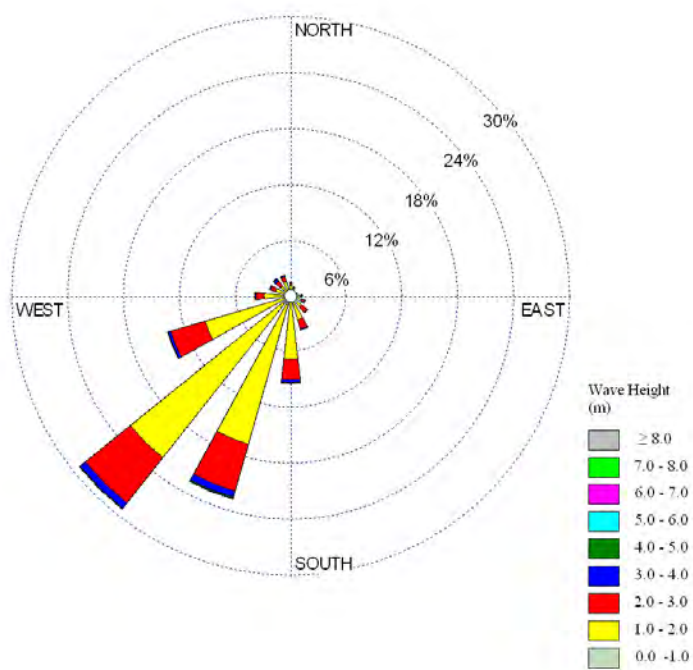
June



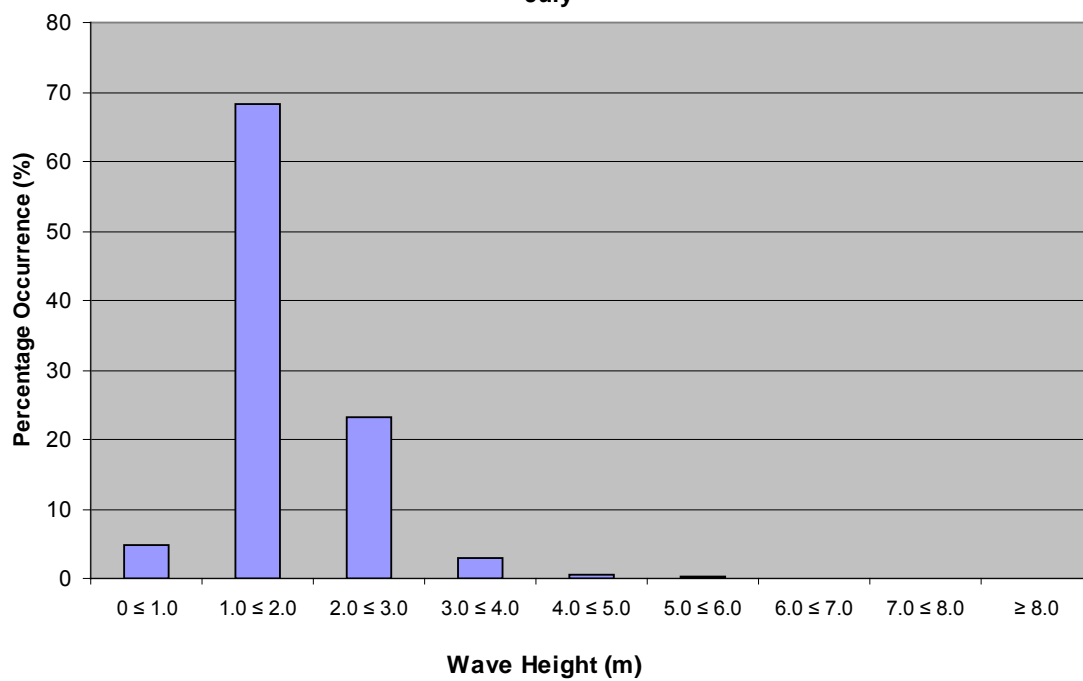
**Wave Height Percentage Occurrence
Grid Point 11423
June**



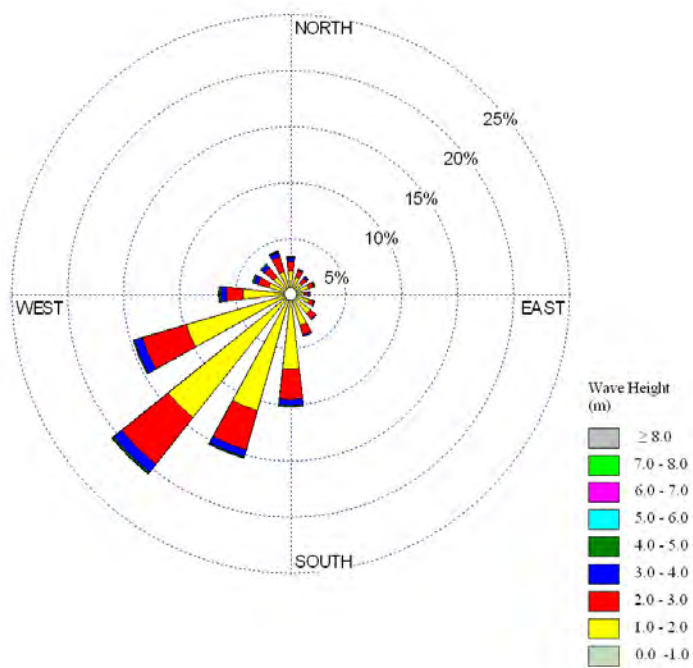
July



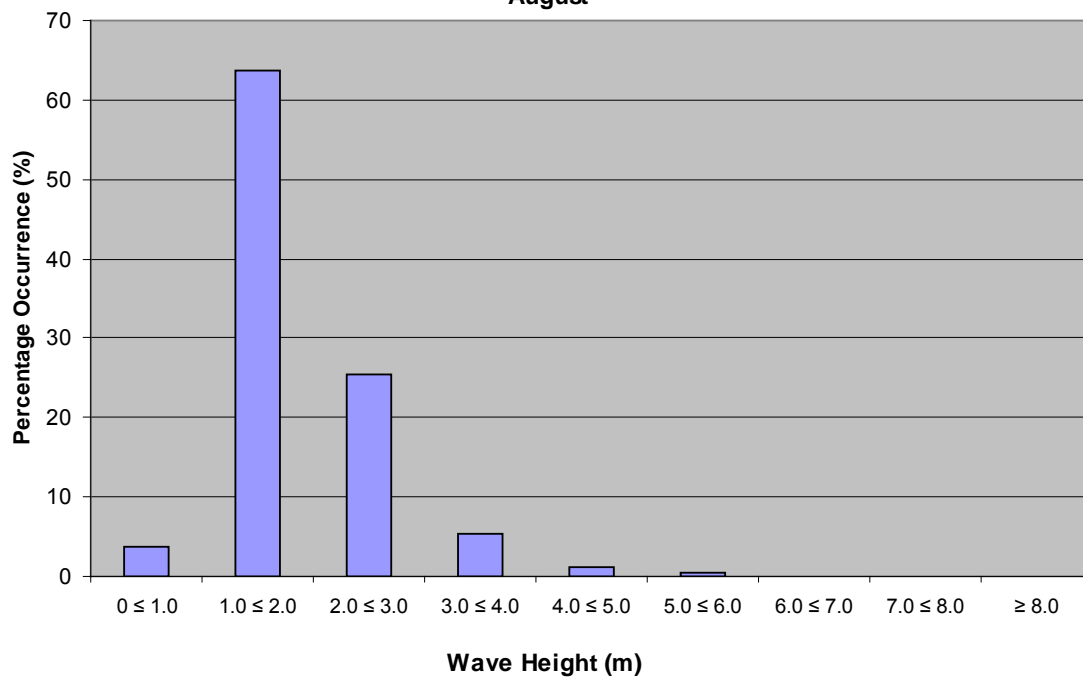
**Wave Height Percentage Occurrence
Grid Point 11423
July**



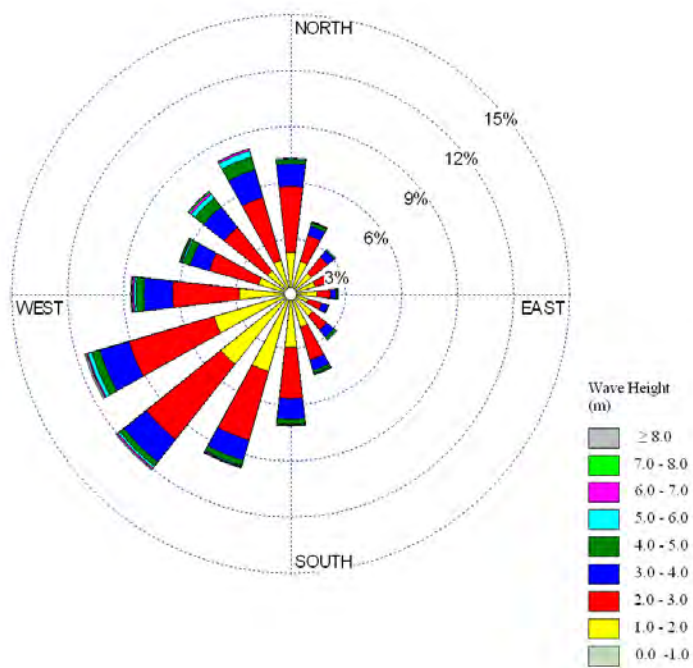
August



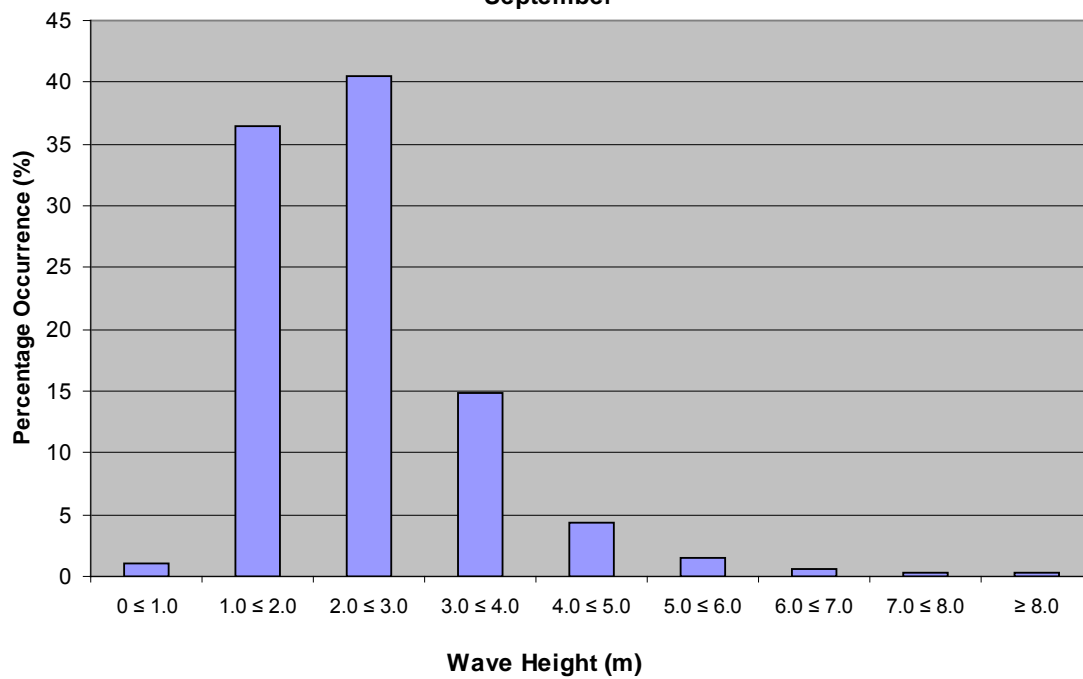
**Wave Height Percentage Occurrence
Grid Point 11423
August**



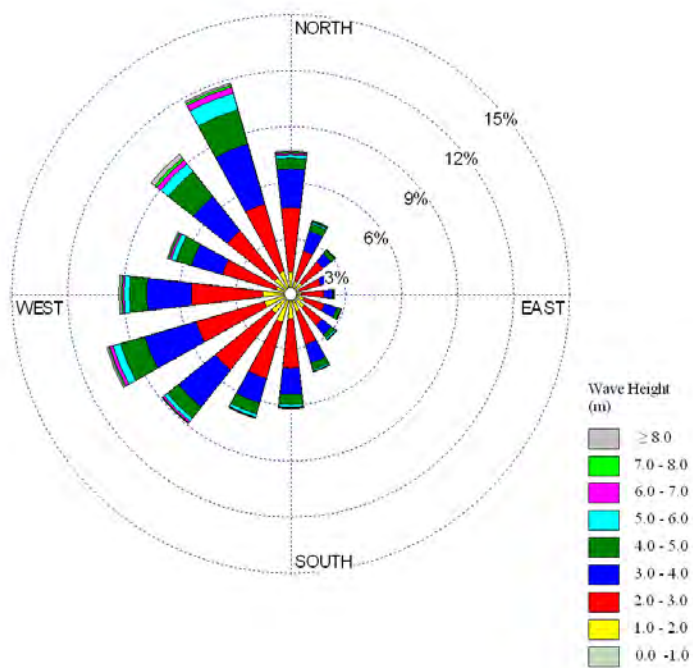
September



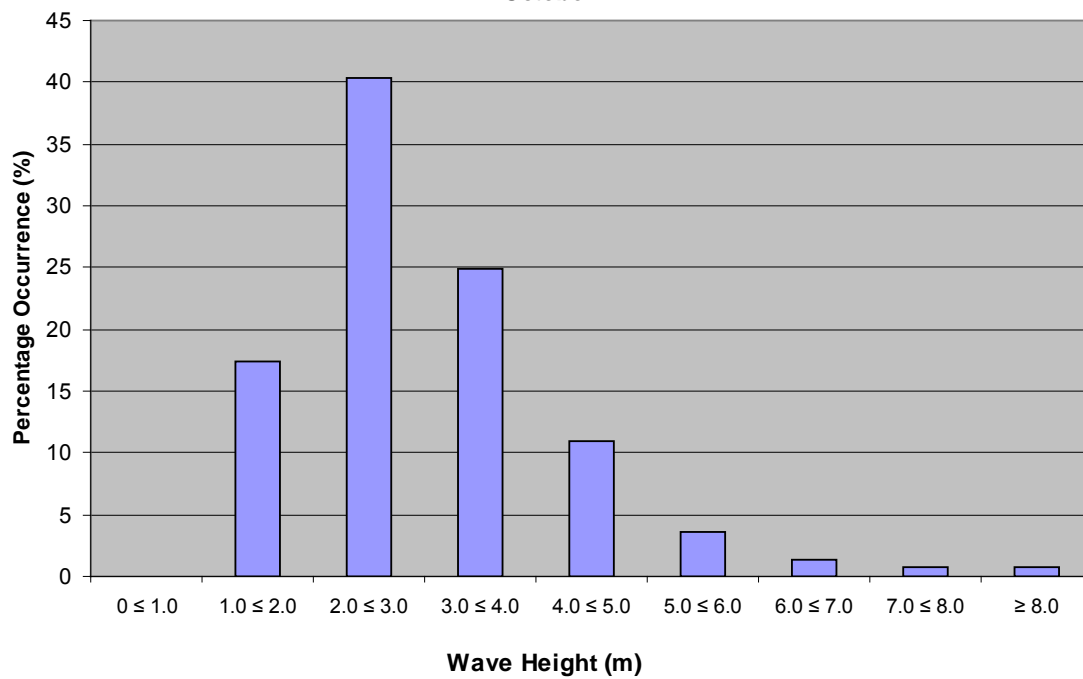
**Wave Height Percentage Occurrence
Grid Point 11423
September**



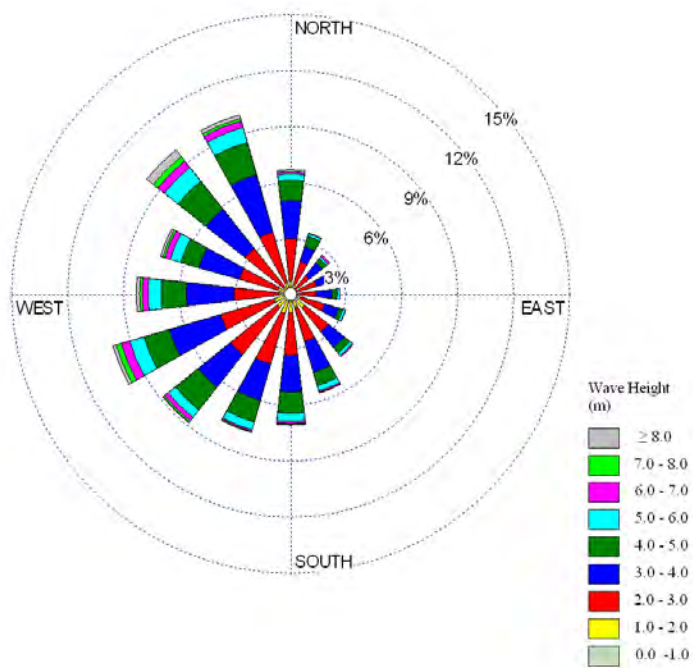
October



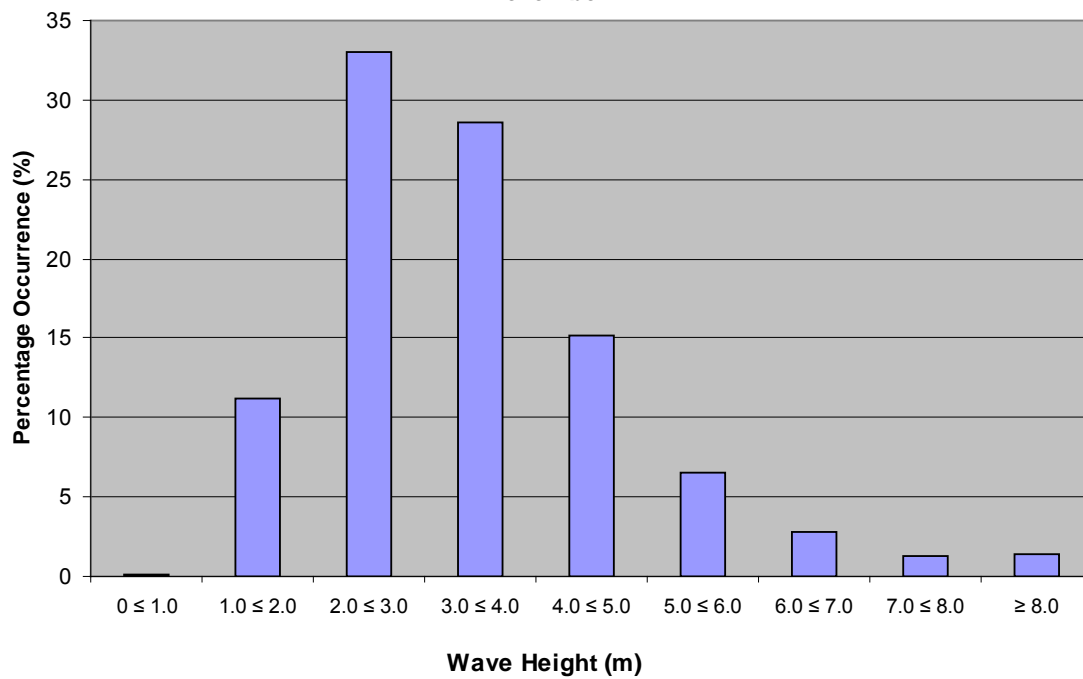
**Wave Height Percentage Occurrence
Grid Point 11423
October**



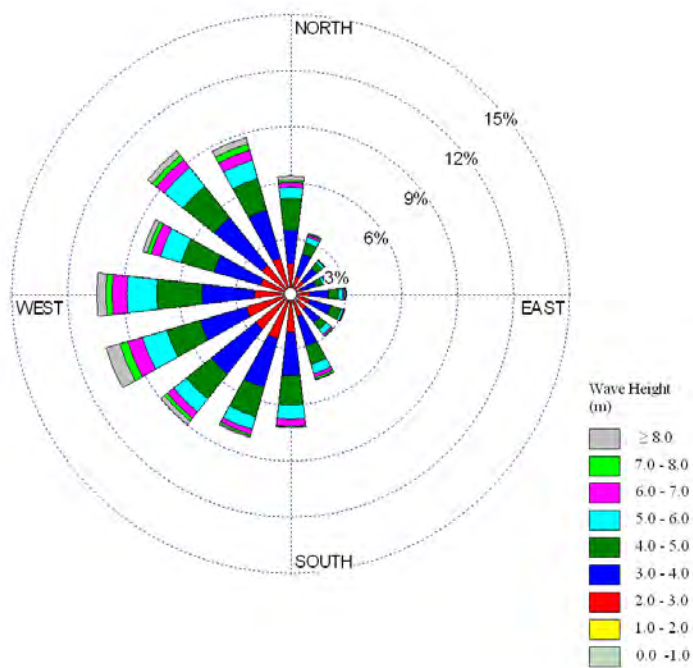
November



Wave Height Percentage Occurrence Grid Point 11423 November



December



**Wave Height Percentage Occurrence
Grid Point 11423
December**

